NPS-EC-93-022

NAVAL POSTGRADUATE SCHOOL
Monterey, California

THESIS

Low Altitude Near-the-Horizon Propagation:
A Comparison Between RPO and M-Layer

by

Chi-Wei Wu

December 1993

Prepared for: Program Executive Office, Theater Air Defense (D2)
2531 Jefferson Davis Highway
Arlington, VA 22242-5170

NAVAL POSTGRADUATE SCHOOL
Monterey, California, 93943

Rear Admiral T.A. Mercer
Superintendent

H. Shull
Provost

This thesis was prepared in conjunction with research sponsored in part by Program Executive Office, Theater Air Defense (D2) under NPS-EC-93-022.

Released by:

P.J. MARTO
Dean of Research

REPORT DOCUMENTATION PAGE

Form Approved
OMB No. 0704-0188

1. AGENCY USE ONLY *(Leave blank)*	2. REPORT DATE	3. REPORT TYPE AND DATES COVERED
	December 1993	Technical Report/Master's Thesis

4. TITLE AND SUBTITLE
Low Altitude Near the Horizon Propagation:
A Comparison Between RPO and M-Layer

5. FUNDING NUMBERS

6. AUTHOR(S)
Chi-Wei Wu

7. PERFORMING ORGANIZATION NAME(S) AND ADDRESS(ES)
Naval Postgraduate School

Monterey, CA 93943-5000

8. PERFORMING ORGANIZATION REPORT NUMBER
NPS-EC-93-022

9. SPONSORING/MONITORING AGENCY NAME(S) AND ADDRESS(ES)
Program Executive Office, Theater Air Defense (D-21)
Attn: Mr. George Hamilton
2531 Jefferson Davis Highway
Arlington, VA 22242-5170

10. SPONSORING/MONITORING AGENCY REPORT NUMBER

11. SUPPLEMENTARY NOTE
The views expressed in this thesis are those of the author and do not reflect the official policy or position of the Department of Defense or the United States Government.

12a. DISTRIBUTION/AVAILABILITY STATEMENT
Approved for public release;

Distribution is unlimited.

12b. DISTRIBUTION CODE

13. ABSTRACT *(Maximum 200 words)*

Predictions of propagation loss made by the computer programs Radio Physical Optics (RPO) Computer Software Configuration Item (CSCI) and M-Layer are compared. The results of the high frequency parabolic equation approximation, as formulated in RPO, agree almost always with those derived from the low frequency modal computation as formulated in M-Layer. But at low altitudes in the neighborhood of the radar horizon, deviations between RPO and M-Layer become significant for some cases. RPO appears not to be able to properly account for the effects of a high altitude surface-based duct at a short range. Since the discrepancies fall in regions of importance to naval operations, a definitive resolution is an urgent task to be undertaken in the immediate future.

14. SUBJECT TERMS	15. NUMBER OF PAGES
Propagetion loss, Radio Physical Optics CSCI, M-Layer, Parabolic Equation, Waveguide Mode, Evaporation Duct, Surface-Based Duct	140
	16. PRICE CODE

17. SECURITY CLASSIFICATION OF REPORT	18. SECURITY CLASSIFICATION OF THIS PAGE	19. SECURITY CLASSIFICATION OF ABSTRACT	20. LIMITATION OF ABSTRACT
UNCLASSIFIED	UNCLASSIFIED	UNCLASSIFIED	UL

NSN 7540-01-280-5500

Standard Form 298 (Rev. 2-89)
Prescribed by ANSI Std. Z39-18

Approved for public release; distribution is unlimited

LOW ALTITUDE NEAR THE HORIZON PROPAGATION: A COMPARISON BETWEEN RPO AND M-LAYER

by

Chi-Wei Wu
Lt., Republic of China Navy
B.S., Chung Cheng Institute of Technology, 1987

Submitted in partial fulfillment of the
requirement for the degree of

MASTER OF SCIENCE IN ELECTRICAL ENGINEERING

from the

NAVAL POSTGRADUATE SCHOOL

December 1993

Author: Wu, Chi-Wei

Chi-Wei Wu

Approved by: Hung-Mou Lee

Hung-Mou Lee, Thesis Advisor

Lawrence J. Ziomek

Lawrence J. Ziomek, Second Reader

Michael A. Morgan

Michael A. Morgan, Chairman
Department of Electrical and Computer Engineering

ABSTRACT

Predictions of propagation loss made by the computer programs Radio Physical Optics (RPO) Computer Software Configuration Item (CSCI) and M-Layer are compared. The results of the high frequency parabolic equation approximation, as formulated in RPO, agree almost always with those derived from the low frequency modal computation as formulated in M-Layer. But at low altitudes in the neighborhood of the radar horizon, deviations between RPO and M-Layer become significant for some cases. RPO appears not to be able to properly account for the effects of a high altitude surface-based duct at a short range. Since the discrepancies fall in regions of importance to naval operations, a definitive resolution is an urgent task to be undertaken in the immediate future.

TABLE OF CONTENTS

I. INTRODUCTION

A. THEORETICAL BACKGROUND

The importance of environmental effects on communication links and radar systems has been recognized for well over two decades. The proliferation of computer programs such as the Integrated Refraction Effects Prediction System (IREPS) [Ref. 1] and the Engineer's Refractive Effects Prediction System (EREPS) [Ref. 2] within the Navy for the prediction of propagation loss of radio waves, together with the general availability of computing power brought along by the personal computer (PC) revolution, has greatly increased the Navy's awareness of such effects.

EREPS essentially is a PC version of IREPS, with provisions for greater flexibility in setting input parameters. It employs a combination of different methodologies to deduce the propagation factor: ray-optics within line-of-sight; curve-fitting, together with frequency scaling based on the assumption that a single mode contributes to the complete field strength [Ref. 3], output from M-Layer [Ref. 4, 5] in the over-the-horizon region, and linear interpolation of the results from ray-optics and M-Layer in the region in between. Through such curve-fitting techniques, EREPS (and IREPS) gains speed at the expense of accuracy.

The M-Layer program, though time-consuming to run, provides results beyond the crude approximation of EREPS, especially in the penumbra region where hundreds of modes are required to give an accurate reading. As can be seen in Chapter III, M-Layer

works well at low altitudes, even in the illuminated region. The theory of M-Layer is formulated in terms of the excitation and propagation of electromagnetic waves in the earth-atmospheric waveguide. The earth, in fact, is treated as a flat, lossy, homogeneous half-space. Its curvature is compensated for by postulating the existence of a linearly increasing component of the index of refraction in the atmosphere, in addition to the slight natural variation of the index of refraction of real air. The rate of increase of the linear component is set to the inverse of the effective earth radius. This new index of refraction is called the modified index of refraction, and this method of simplifying the problem constitutes the earth-flattening approximation [Ref. 6]. Combined with the piecewise-linear approximation to the modified index of refraction, the eigenfunctions of the flattened earth-atmospheric waveguide are Airy functions of different variables over different regions of the atmosphere of linearly varying modified refractive indices. The waveguide modes are found numerically, which is the process taking up most of the computation time.

Recently, the RDT&E Division of the Naval Command, Control and Ocean Surveillance Center (NRaD), which previously produced IREPS, EREPS and M-Layer when it was known as Naval Ocean Systems Center (NOSC), came out with a Radio Physical Optic (RPO) program [Ref. 7]. It is structured in the same spirit as EREPS: different approximations are used over different regions of space. The part in EREPS which relies on curve-fitting of M-Layer predictions is replaced with direct computation based on the parabolic equation approximation (PE) [Ref. 8, 9]. This makes RPO far superior to EREPS. Computational expediency precludes extensive application of PE.

Instead, PE computations are launched at a range of 2.5 km, unless the incident ray to the earth gets near the diffraction limit first. A split-step, outward advancing scheme for solving the parabolic equation is utilized. At each step, a fast Fourier transform (FFT) is performed. The FFT size is set between 7 to 10 powers of 2, while the separation between FFT data points is limited to within 2 to 49 wavelengths. Hence, PE computations will never be done above a height of 50,176 wavelengths. At 10 GHz, this represents a height of no more than 1.50528 km. To avoid aliasing, the FFT coefficients computed from 3/4 of the height to the top of the region where the FFT is carried out are filtered with a factor which decreases from 1 to 3/4 following a sine-squared variation. Furthermore, the initial field strength at the range where PE computations start is weighted by a Gaussian factor which decays to -70 dB over the same altitudes. Thus, only the lowest 3/4 of the FFT results are actually used as PE solutions.

To fill the remainder of the space, RPO relies on ray-optics until the incident ray to the earth approaches the diffraction limit. Beyond this limit, PE results are utilized where they are available. This is called the PE region. Above the PE region, if the space is not covered by ray-optics, an extended optic (XO) region is defined. The PE solutions at the greatest height are treated as rays emanating from below, their interferences with the direct rays, if present, are taken as the fields in this region.

Even within the ray-optics region, RPO subdivides this region into flat-earth (FE) and ray-optics (RO) regions. The earth is considered as flat and all refraction effects are ignored in the FE region, which is limited to 2.5 km in range unless the antenna is elevated beyond 5°.

B. HIGH-FREQUENCY VERSUS LOW-FREQUENCY APPROXIMATION

Beyond regions where ray-optics is applicable, RPO relies on PE. The parabolic equation approximation to the Maxwell wave equations is developed under the optical assumption that the operating frequency is so high that a main direction of wave propagation in terms of a plane wave can be specified. Hence, only the variation of the "envelope" which modulates the magnitude and phase of the plane wave has to be considered, instead of the fast variation of the complete wave to the order of the wavelength. On the other hand, M-Layer has its theoretical basis in an eigenfunction expansion. This is an approach most suitable for low frequency applications because more and more modes will be needed as the size of the geometrical structure becomes large compared to the wavelength. Even though M-Layer removes the earth radius as the dominating length scale through the adoption of a flattened earth, the thickness of the overall atmospheric layers specified is still far greater than the wavelength in all applications. The comparison of the predictions of PE against M-Layer is one between two theories which approach a problem from two extremes. The fact that the results of the high frequency PE computations as formulated in RPO agree almost always with those derived from the low frequency modal computation as formulated in M-Layer represents a significant engineering achievement by NRaD. However, there are disagreements at low altitudes in the neighborhood of the radar horizon under some ducting conditions. These are regions of importance to naval operations. A definitive resolution of these discrepancies is an urgent task to be undertaken in the immediate future.

C. SCOPE OF THE WORK

In this thesis, the radiation of a vertically polarized transmitting antenna located at a height of 15 meters is investigated. Three modified refractive index profiles, with the first two given in Ref. 7, are utilized: a 300 m surface-based duct, a 14 m evaporation duct, and the combination of these two profiles with one sitting on top of the other. Three frequencies at 3 GHz, 6 GHZ and 12 GHz are chosen which give an approximate coverage of the radar bands. Since only low altitude, near the horizon propagation is of interest, propagation loss for altitudes up to 100 meters within the range of 15 to 110 km are evaluated by both RPO and M-Layer for comparison.

II. PROGRAM SETUP

A. TEST CONSIDERATIONS

Of interest to this thesis research are the propagation loss predictions made by the parabolic equation approximation method and by waveguide mode computations. The NPS version of M-Layer is a waveguide mode computation program which has been greatly enhanced in its accuracy and efficiency [Ref. 5] from its original incarnation assembled by NOSC [Ref. 4]. As explained in Chapter I, the RPO program, completed by NRaD and available to NPS only recently, includes several methods of computation applied to different regions of space. To ensure that only predictions made under the parabolic equation approximation are included in the comparison, the RPO FORTRAN source code [Ref. 7] is used. This source code consists of a set of subroutines. The output for each region comes from a distinct subroutine. By instructing every RPO subroutine which computes the propagation loss to associate a code number to its output, the predictions made with the parabolic equation approximation are easily identified.

The RPO FORTRAN source code comes without a main program. Nor does it contain input routines and files. Thus, the first task of this research was to write a main program for RPO which will call the relevant subroutines to compute the desired output. Next, data files had to be created to provide the program with refractive index profiles and other necessary parameters. An input subroutine had to be written to feed these data to the main program and the RPO subroutines. Furthermore, to ensure that both RPO and

M-Layer use the same environmental data and compatible input parameters, a new M-Layer input subroutine was created which replaces the subroutine of the same name in the NPS version of M-Layer. Finally, the output data are presented graphically using a plotting routine written in MATLAB, version 3. Specific considerations put into these subroutines are discussed in the following sections, with the RPO main program "RPOmain," the RPO input routine "RPOstdin," the substituting M-Layer input routine "MLstdin," listed respectively in Sections 1 through 4 of Appendix A.

B. RPO MAIN PROGRAM

In RPO, the parabolic equations are solved with the split-step algorithm. As a prerequisite, RPO has to estimate the electric field at an initial range. It then proceeds, at a pre-determined step size, toward the range where a propagation loss prediction is called for, computing the electric field at every step along the way. Hence the subroutines of RPO can be separated into two types: those providing other subroutines with initial values and defining their boundaries of application, and those handling the PE computation at each step. After the tedious but necessary bookkeeping of declaring global variables and setting up common blocks to pass along values, the main program first reads in data by calling the input subroutine "RPOstdin" and initializes the subroutines by calling "RPOini" before entering into a loop to step the computation through the desired range and write the propagation loss predictions within the selected region to an output file. A flow chart for the main program, RPOmain, is shown in Figure 1. A listing of the program is included in Appendix A.

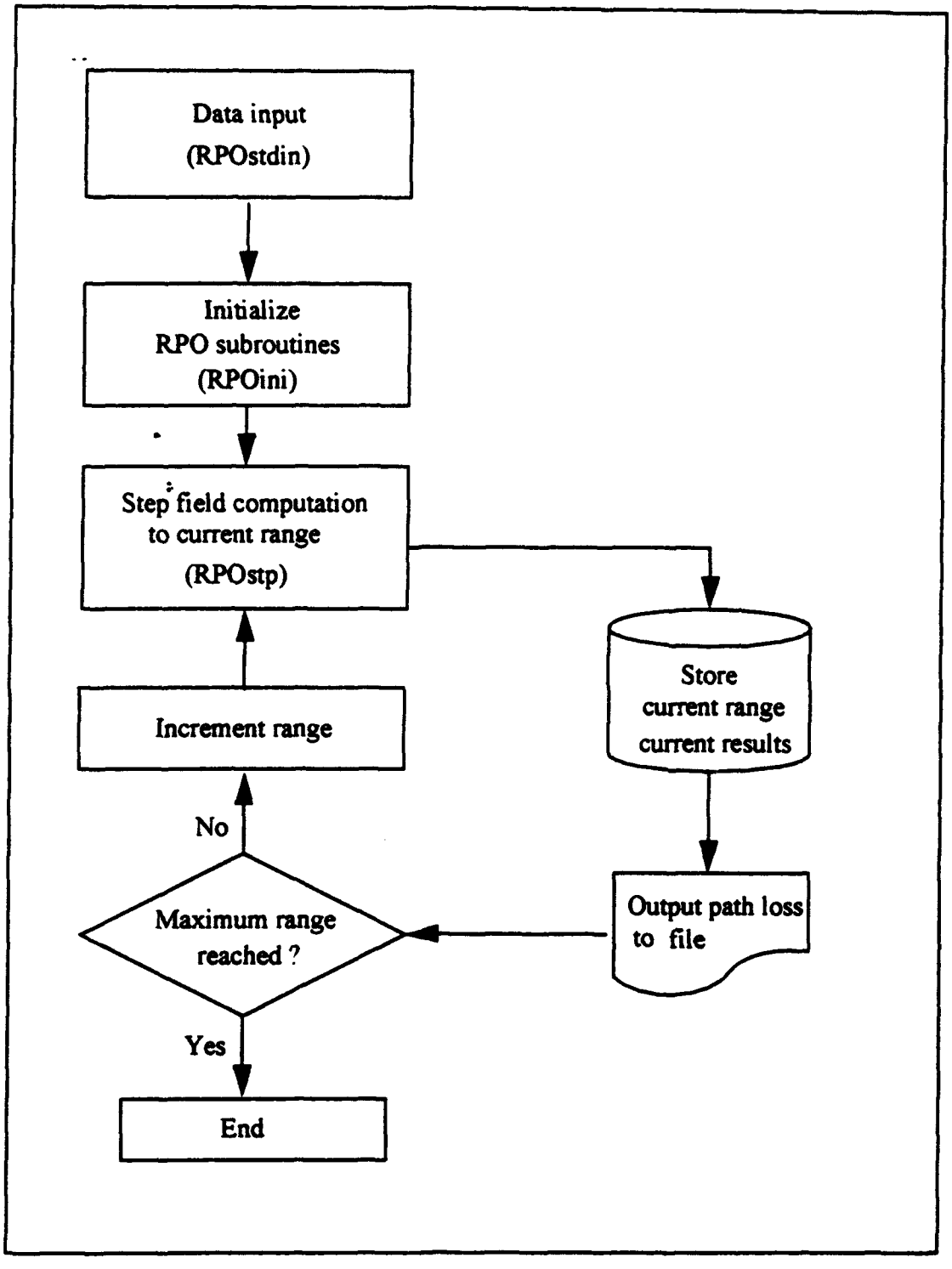

Figure 1. Program Flow of RPOmain

C. INPUT FILES AND SUBROUTINES

RPO and M-Layer have different capabilities and require different types of input. For example, RPO needs a presumed radiation pattern to set up its initial electric field to begin computation; it cannot compute electromagnetic (EM) radiation directly from a specified current distribution. On the other hand, M-Layer computes the radiation from a dipole source; it thus can not simulate antennas arbitrarily. RPO is able to handle multiple refractivity profiles at different ranges due to further approximations made in the theory beyond the reduction of the wave equation to a parabolic equation while M-Layer is restricted to deal with a single profile. Nevertheless, they use many parameters in common. Since the purpose of this work is to compare the predictions of these two programs, it is desirable to have them read in exactly the same files whenever possible. This is especially true for the refractivity profiles.

For this thesis, three ASCII files are set up: one contains the parameters common to both RPO and M-Layer, including the modified refractivity profile; another contains RPO specific parameters such as the antenna pattern; the third contains parameters used only by M-Layer such as the parameter *aloss*, which specifies the greatest range attenuation rate of the modes to be searched, in dB per kilometer. The parameters which are common to both RPO and M-Layer are listed in Table II.1. Those specific to RPO are listed in Table II.2. The M-Layer specific parameters are listed in Table II.3. Two batch files are written to combine automatically the two proper files for input into RPO and M-Layer respectively.

Table II.1. Input parameters common to RPO and M-Layer.

RPO	M-Layer	Description
nlevls	*nzlayr*	number of profile levels[a][b]
wind	*wind*	surface wind speed
fmhz	*fqmzin*	operating frequency
ipolar	*mpol*	antenna polarization[b][c]
ztran	*ztinit*	transmitter height
mlxout	*nx*	number of receiver ranges
xinit	*xinit*	initial range of the receiver
delx	*delx*	receiver range increment
nzout	*nzr*	number of receiver heights
zrinit	*zrinit*	initial height of the receiver
delzr	*delzr*	receiver height increment
zprof	*zi*	heights at which profile data are specified (an array)
capm	*zim*	profile data (modified index of refraction; an array)

(a) RPO: from 1 to *nlevls*; M-Layer: from 0 to *nzlayr*.

(b) follows M-Layer definition, adjust RPO during input.

(c) RPO: 1=horizontal; 2=vertical; M-Layer: 0=horizontal; 1=vertical.

Table II.2. RPO-specific input parameters.

RPO	Description	Remarks
nxout	number of output ranges computed	calculated by *Xmax/delx* where *Xmax=Xinit+delx*mlxout*
selx	minimum range to output data	
xprof	ranges at which index of refraction profiles are specified	set to 0.0
nprofs	number of profiles specified	set to 1
ipatrn	antenna pattern 1: omni-direction 2: sin(x)/x 3: Gaussian 4: cosecant-squared 5: height-finder 6: user defined	use 1 or 3 only
beamw	antenna elevation beamwidth	
elang	antenna elevation angle	set to 0.0
nfacs	number of height-finder data	set to 0 (not used)
iscatt	includes troposcatter 0: no 1: yes	set to 0 (not used)

Table II.3. M-Layer-specific parameters.

M-Layer	Description	Remarks
mfile	0: read input and compute eigenvalues 1: read eigenvalues as input	
delfq	frequency increment	set to 0.0 (not used)
nfreq	number of frequencies to be used	set to 1
aloss	maximum range attenuation rate in dB/km of modes to be found	set to 2.0 or 5.0
delzt	height increment of transmitter	set to 0.0 (not used)
nzt	number of transmitter heights	set to 1
refz	reference height at which *refm* and *refgab* are given	set to 0.0
refm	modified refractivity at the reference height	set to 339.0
refgab	modified gas absorption at the reference height	set to 0.0 (not used)

In RPO, special formulas for the dielectric constant and conductivity of sea water as a function of frequency are used. Sea surface roughness is also given in terms of a function of wind speed. To incorporate this into M-Layer, the input subroutine "MLstdin" for M-Layer is modified to carry out these computations using the same formulas before providing these parameters to the program, even though surface roughness is not considered in this comparison.

D. VALIDATION

Before proceeding with the comparison, a few RPO test cases are run using this newly written main program and the input subroutine. Specifically, the tests listed in Ref. 7 under the names LOBW (low beam width limit), SBDUCT (surface-based duct) and EDUCT (evaporation duct) are carried out. The tabulated results in Ref. 7 are reproduced exactly as long as the range increment *delx* and height increment *delz* are the same as those specified therein. Otherwise, variations of up to 4% are observed.

III. RESULTS

Propagation of waves through several refractivity profiles at many frequencies has been investigated. A clear trend has emerged which shows disagreement between the results from RPO and M-Layer at ranges near the horizon when surface based ducts are involved. In this thesis, results from three profiles are presented: a 300 m surface-based duct which is specified and used in Ref. 7 under the test name SBDUCT; a 14 meter evaporation duct which is also specified and used in Ref. 7, under the test name EDUCT; and a combination of these two ducts by merging the profile of the evaporation duct with that of the surface-based duct. The modified refractivity profile of the 300 m surface-based duct is given in Table III.1. The profile for the 14 m evaporation duct is given in Table III.2. The profile for the combination is given in Table III.3. For each of the three profiles, three frequencies at 3 GHz, 6 GHz and 12 GHz are selected. With the transmitter fixed at a height of 15 m, the propagation loss of up to 100 m at ranges of 15, 20, 30, 40, 50, 60, 70, 80, 90, 100 and 110 km is plotted. Since the results at different frequencies show similar features, only those at 6 GHz are included in this chapter. Those at 3 GHz and 12 GHz are collected in Appendices B through D.

Table III.1. A 300 m surface-based duct.

i	Z_i meters	M_i
0	0.000	339.0
1	250.0	368.5
2	300.0	319.0
3	1000.0	401.6

Table III.2. A 14 m evaporation duct.

i	Z_i meters	M_i
0	0.000	339.00
1	0.040	335.10
2	0.100	333.66
3	0.200	332.60
4	0.398	331.54
5	0.794	330.51
6	1.585	329.53
7	3.162	328.65
8	6.310	327.96
9	12.589	327.68
10	14.000	327.67
11	25.119	328.13
12	39.811	329.25
13	50.119	330.18
14	63.096	331.44
15	79.433	333.12
16	100.000	335.33
17	125.893	338.20
18	158.489	341.92
19	199.526	346.69
20	209.526	347.87

Table III.3. A 300 m surface-based duct over a 14 m evaporation duct.

i	Z_i meters	M_i
0	0.000	339.00
1	0.040	335.10
2	0.100	333.66
3	0.200	332.60
4	0.398	331.54
5	0.794	330.51
6	1.585	329.53
7	3.162	328.65
8	6.310	327.96
9	12.589	327.68
10	14.000	327.67
11	25.119	328.13
12	39.811	329.25
13	50.119	330.18
14	63.096	331.44
15	79.433	333.12
16	100.000	335.33
17	125.893	338.20
18	158.489	341.92
19	199.526	346.69
20	209.526	347.87
21	250.0	368.5
22	300.0	319.0
23	1000.0	401.6

For all the cases, the polarization is chosen to be vertical. The receiver height increment *delzr* is set at 0.5 m. The receiver range increment *delx* is set at 2500 m. For RPO computations, the maximum height *zmax* is set at 100 m; the maximum range *xmax* is set at 115 km. The Gaussian beam pattern with a beamwidth of 5° is chosen for the antenna. Within the altitudes and ranges considered, there is no perceivable difference when the omni-directional pattern is used instead. For M-Layer computation, the parameter *aloss* is set to 2 dB/km. In all the figures, results from M-Layer are drawn as a solid line. Results from RPO are marked with asterisks if they are in the PE region and with dots if they are in the RO region. For easy reference, the height of the transmitter horizon at each distance, based on the four-thirds effective earth radius, is indicated with a horizontal line drawn across the figure on which it is present. It starts to appear in the figure for the 20 km range. Figures beyond 50 km lie below the horizon completely and this horizontal line cannot be seen.

In what follows, results of RPO and M-Layer computations at 6 GHz are presented. Their analysis and discussions are given in Chapter IV.

A. 300 METER SURFACE-BASED DUCT

Figures 2 through 12 show the propagation loss at various ranges from 15 through 110 km when a 300 m surface-based duct is present. This is the profile in which most significant deviations between RPO and M-Layer are observed, especially at 50 and 60 km ranges. Even at 40 km, the two differ by 10 to 30 dB at low altitudes. On the other hand, the two agree well within line-of-sight and deep shadow regions.

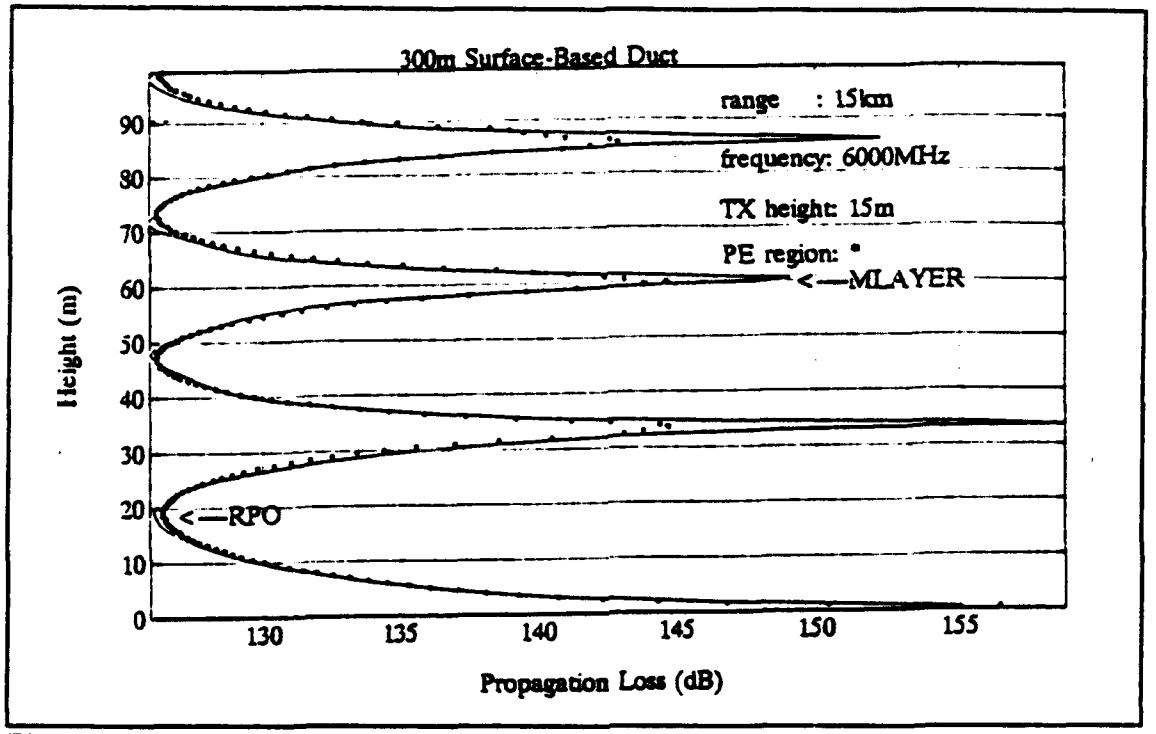

Figure 2. Propagation loss at 15 km.

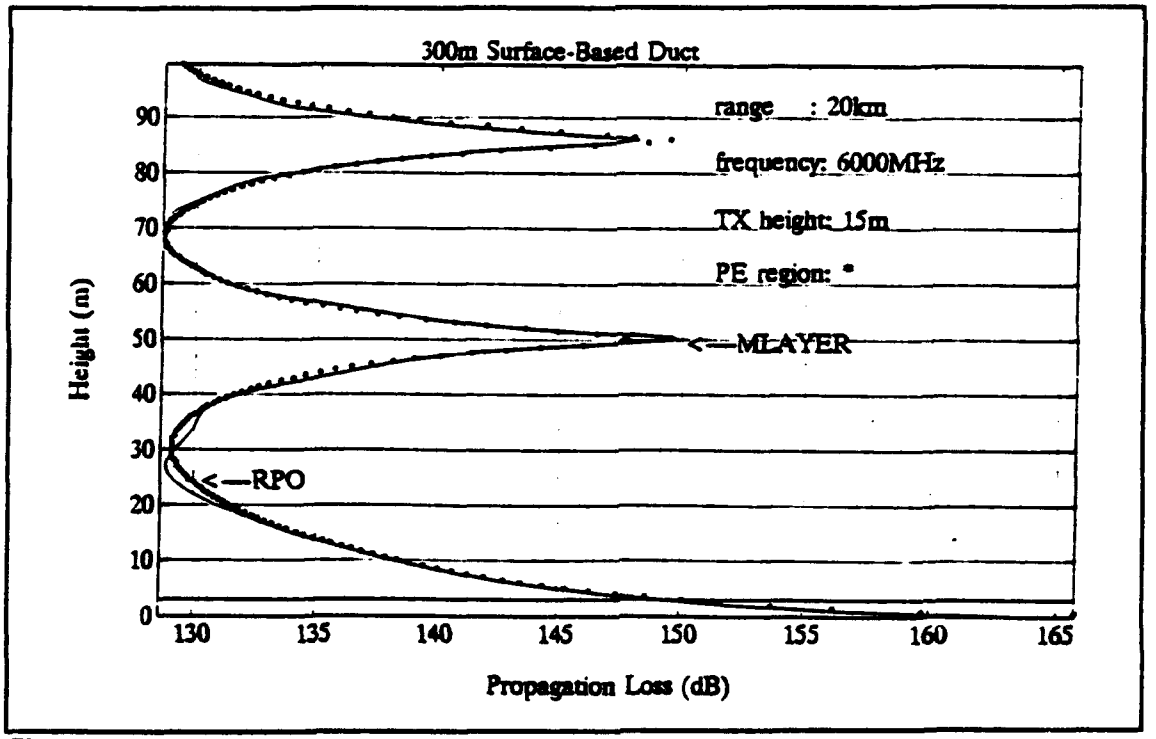

Figure 3. Propagation loss at 20 km.

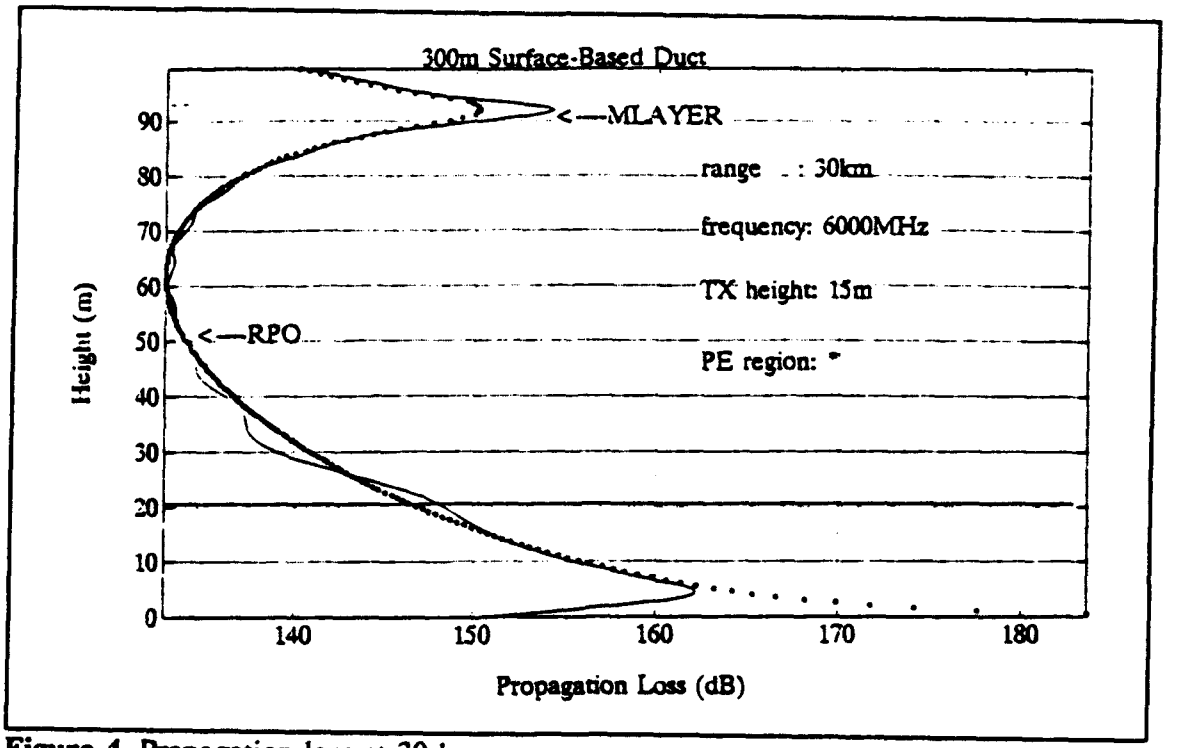

Figure 4. Propagation loss at 30 km.

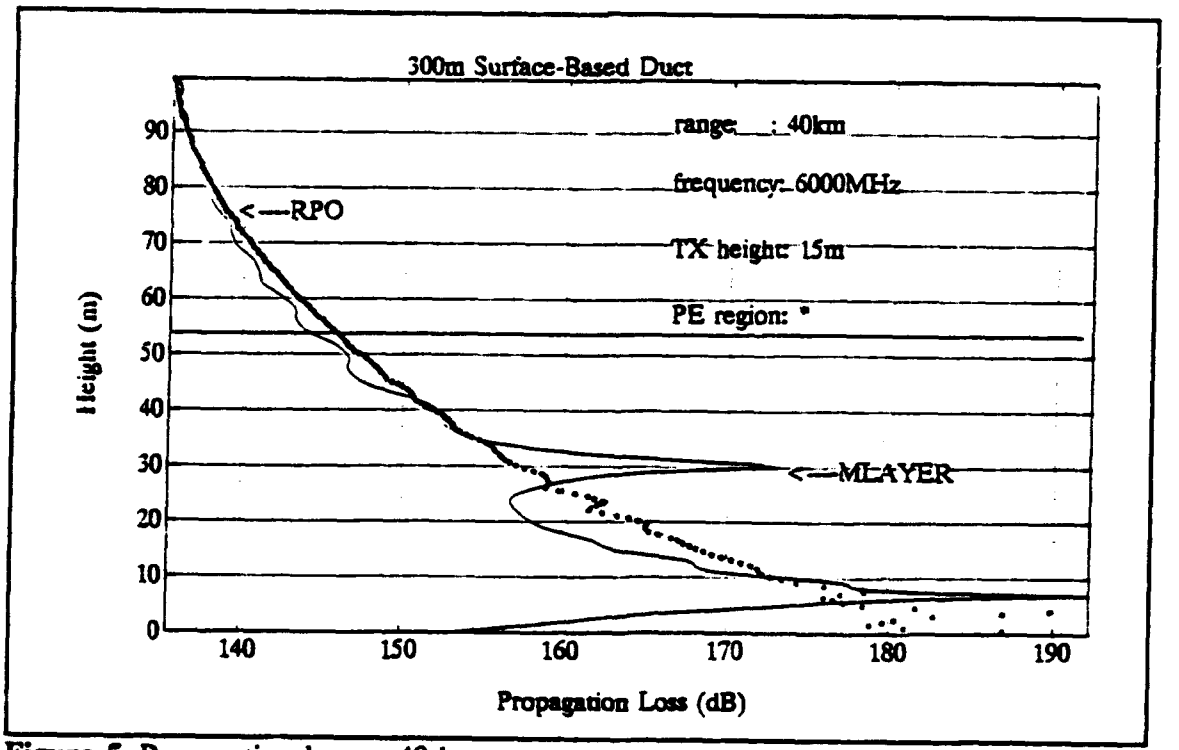

Figure 5. Propagation loss at 40 km.

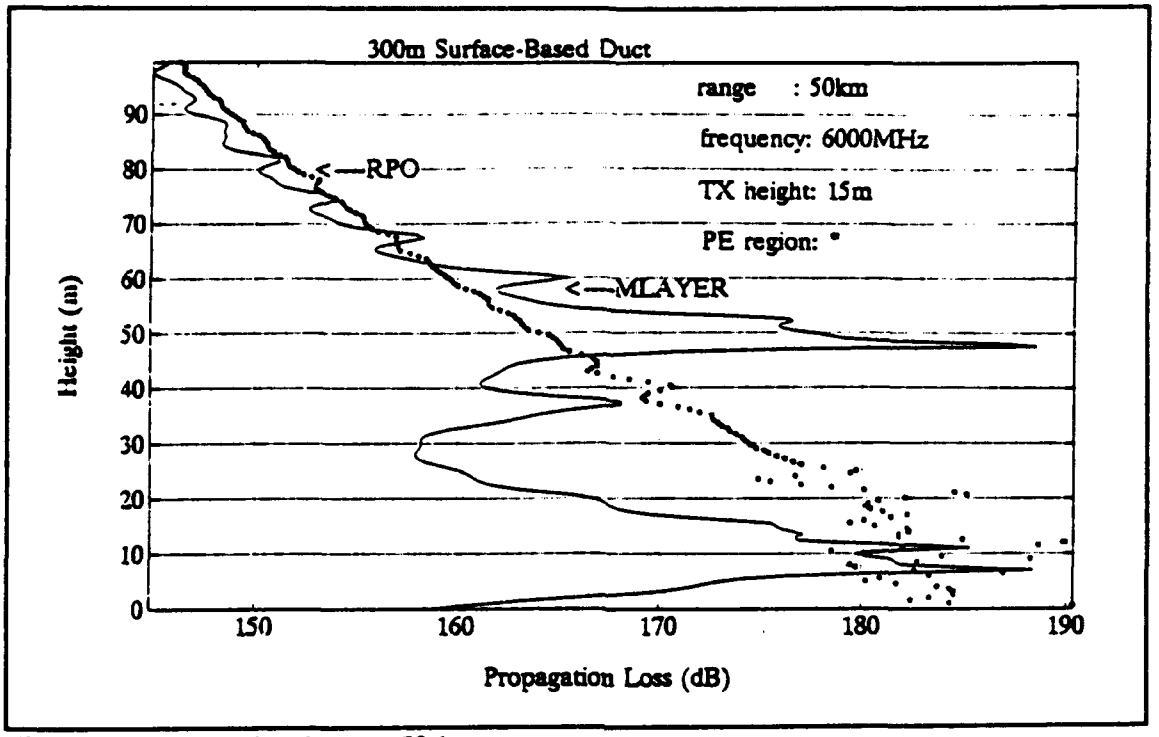

Figure 6. Propagation loss at 50 km.

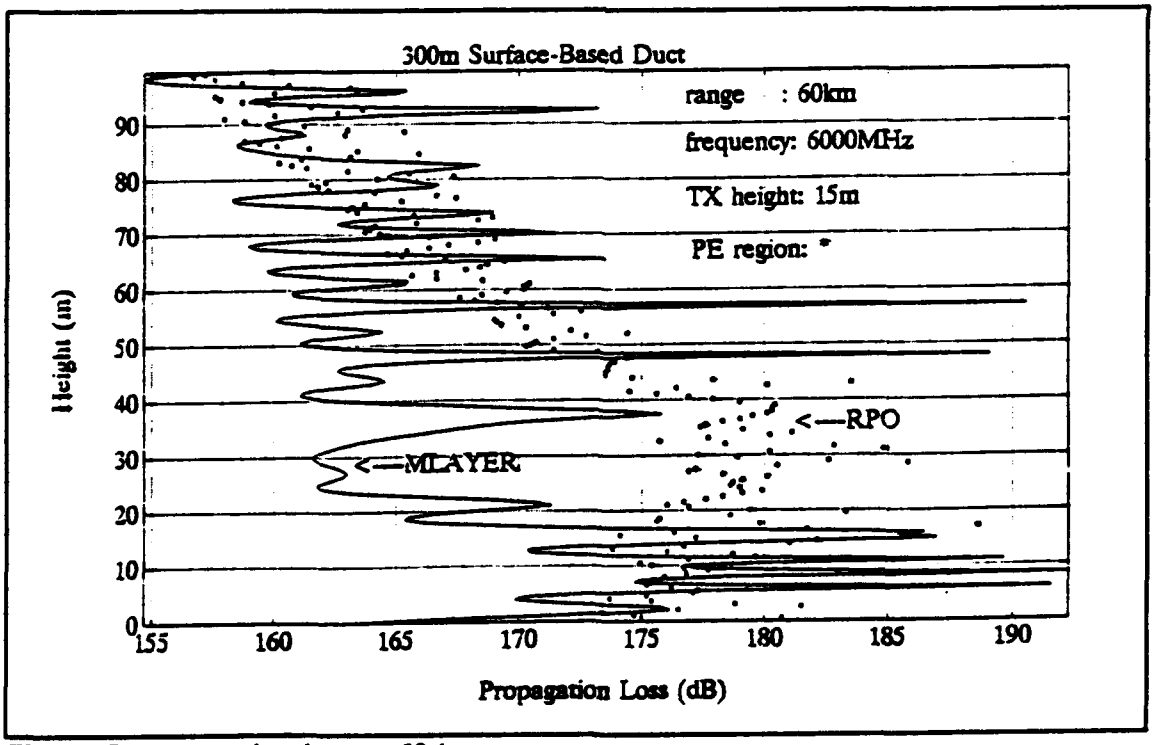

Figure 7. Propagation loss at 60 km.

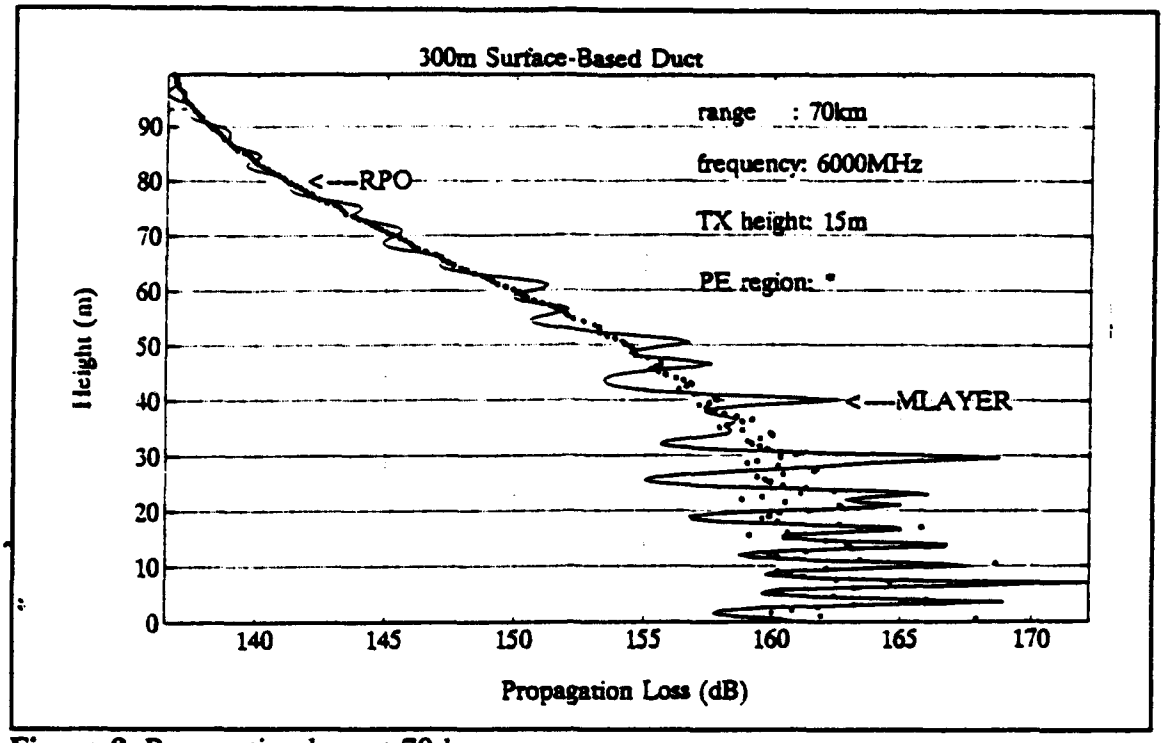

Figure 8. Propagation loss at 70 km.

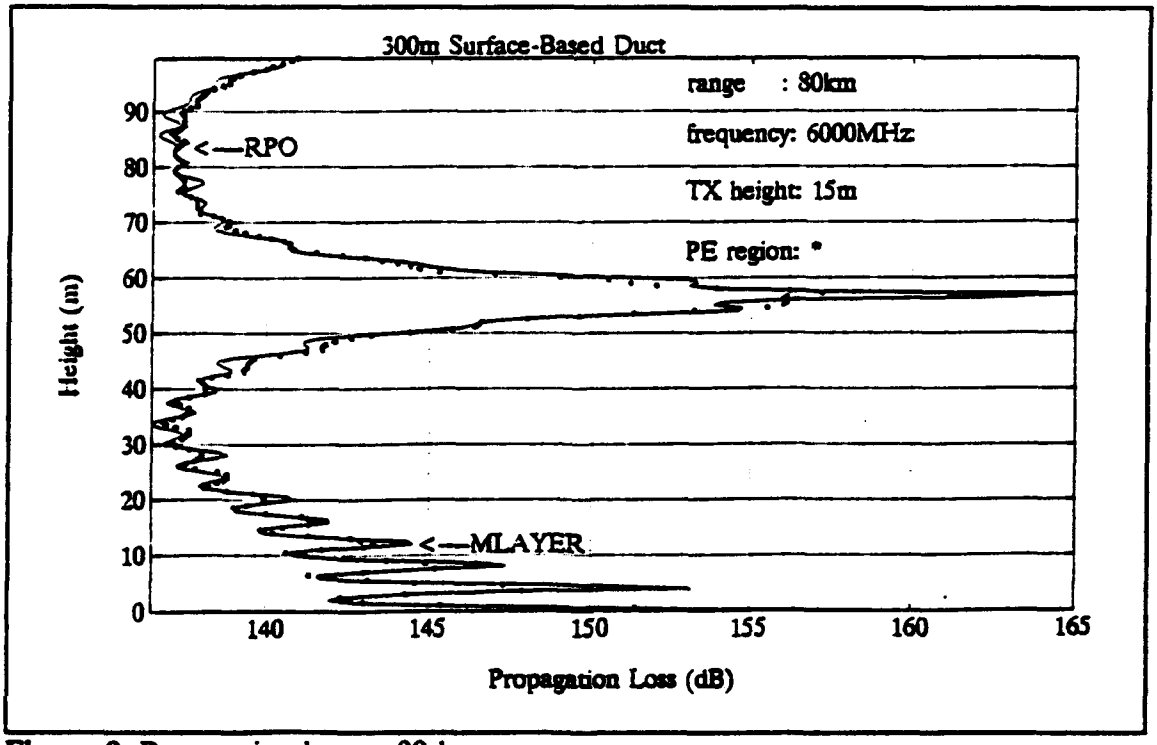

Figure 9. Propagation loss at 80 km.

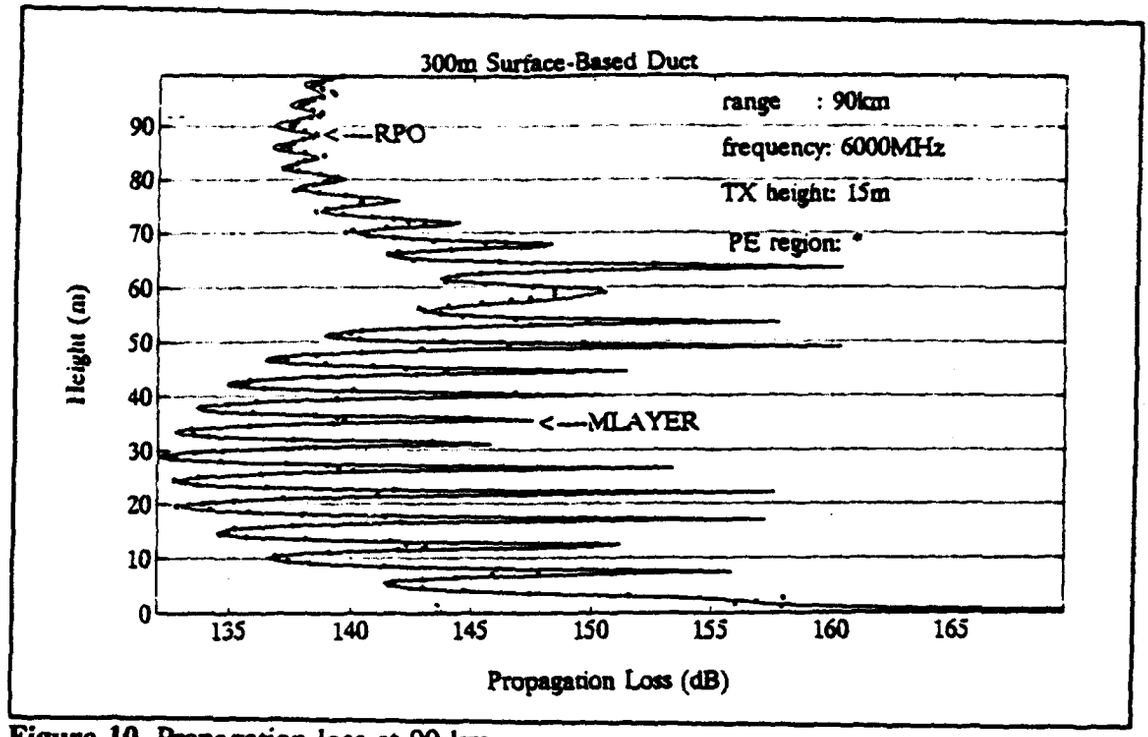

Figure 10. Propagation loss at 90 km.

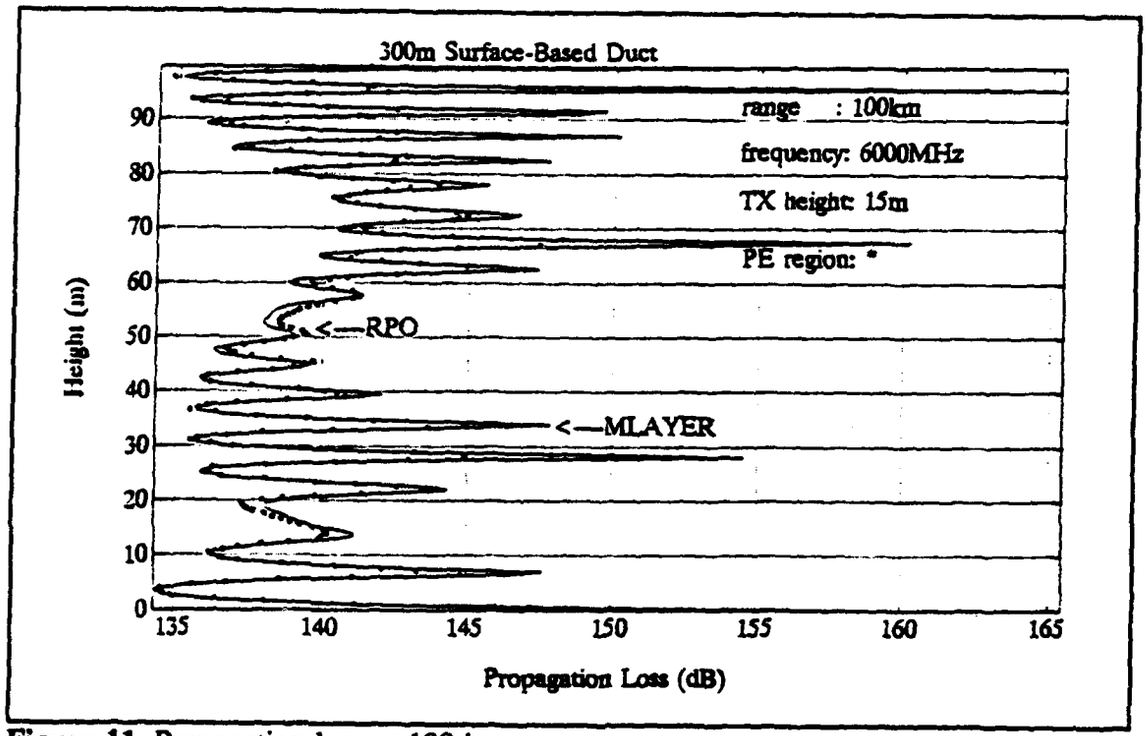

Figure 11. Propagation loss at 100 km.

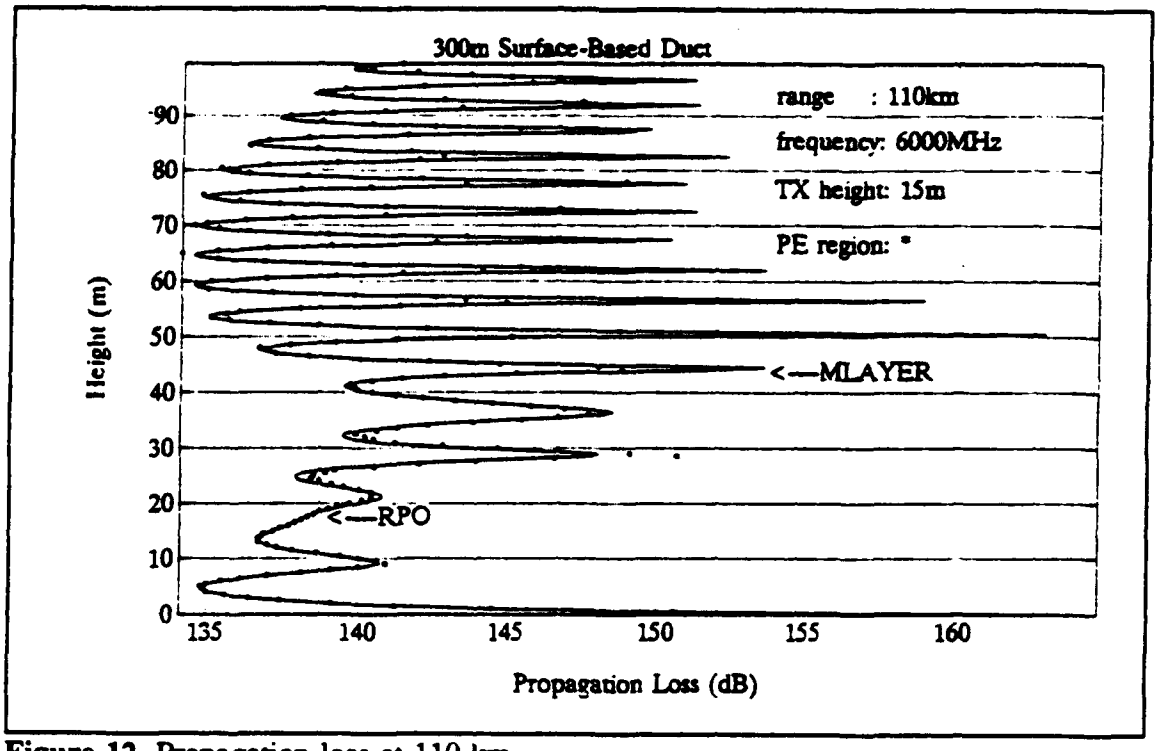

Figure 12. Propagation loss at 110 km.

B. 14 METER EVAPORATION DUCT

Figures 13 through 23 show the propagation loss in the presence of a 14 m evaporation duct. RPO and M-Layer agree well over the entire range. From the figures in Appendix C , it can be seen that this is true for all the frequencies investigated, with only a less than 1.5 dB difference around where the loss is maximum for the 12 GHz case in the over-the-horizon region.

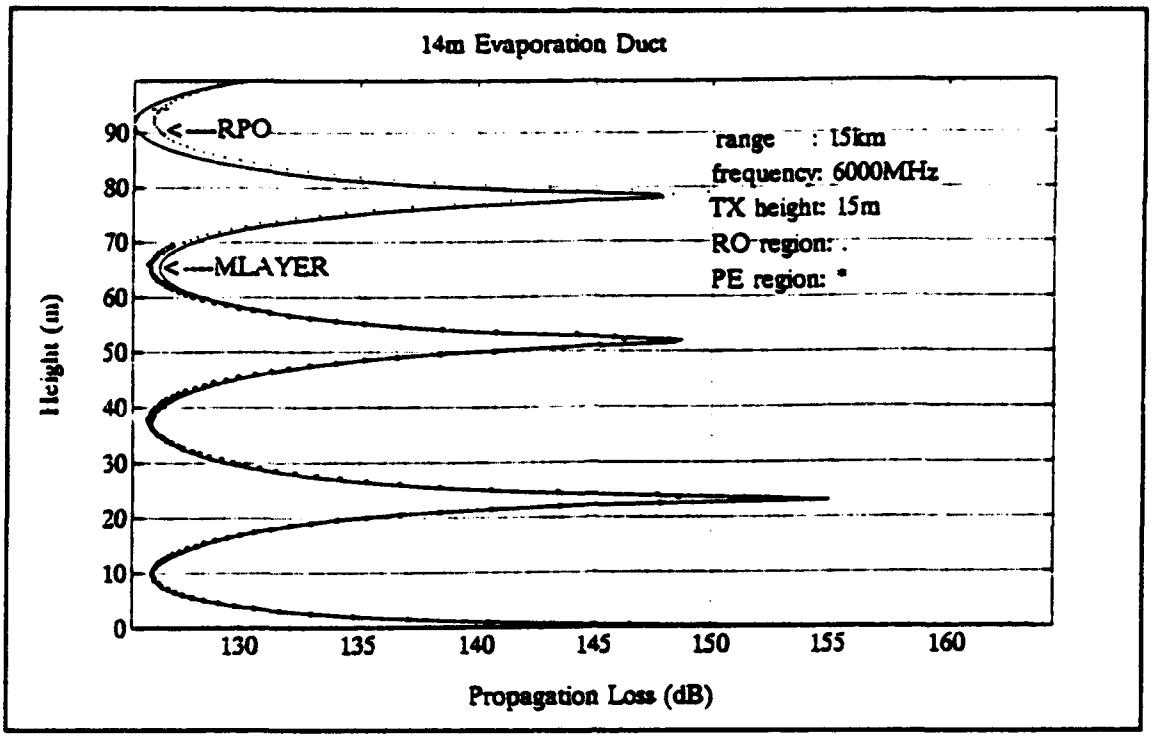

Figure 13. Propagation loss at 15 km.

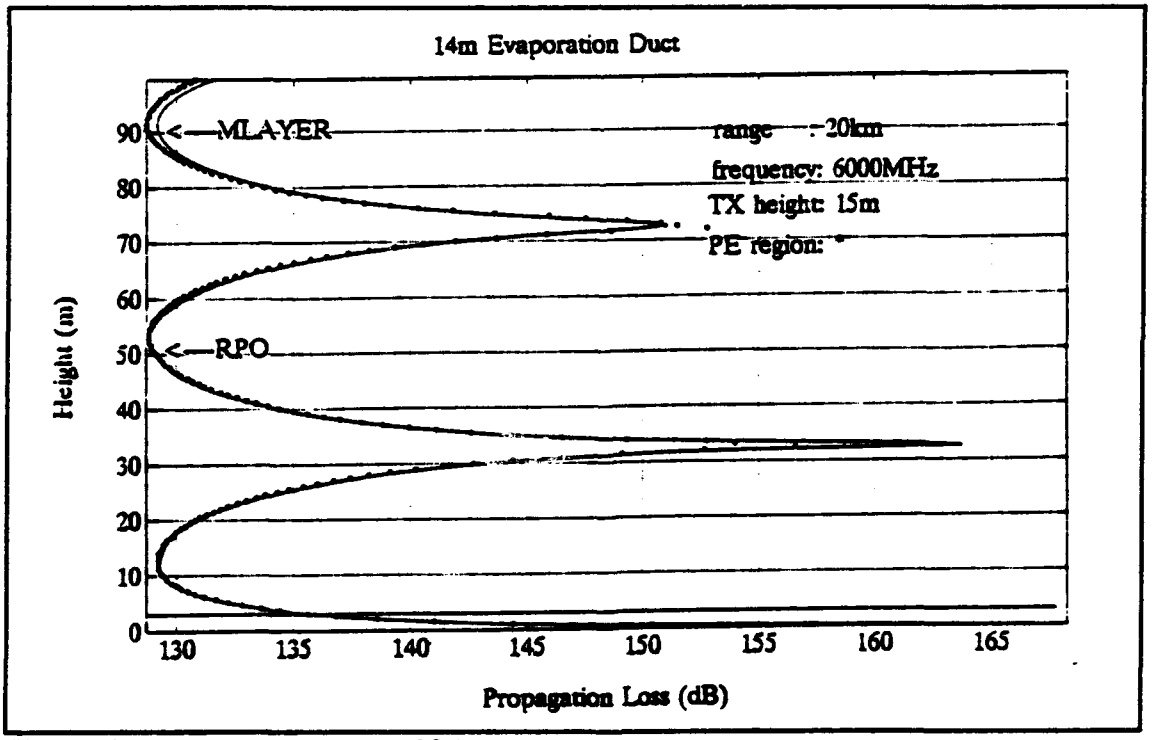

Figure 14. Propagation loss at 20 km.

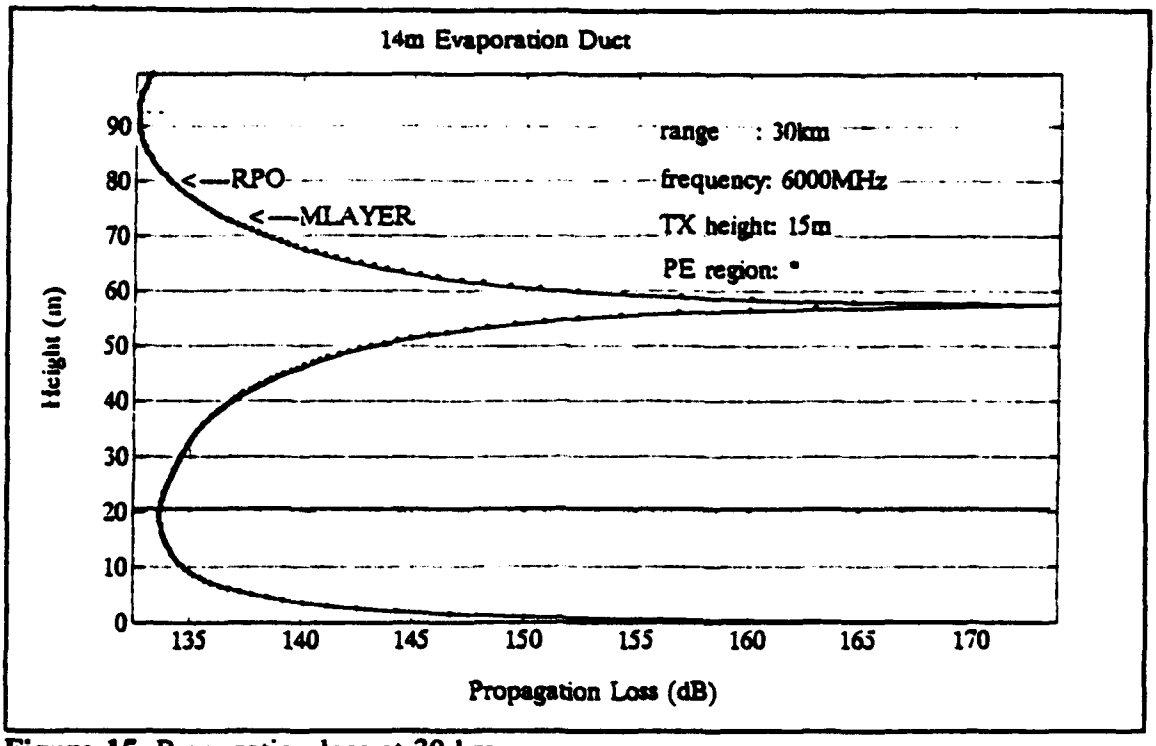

Figure 15. Propagation loss at 30 km.

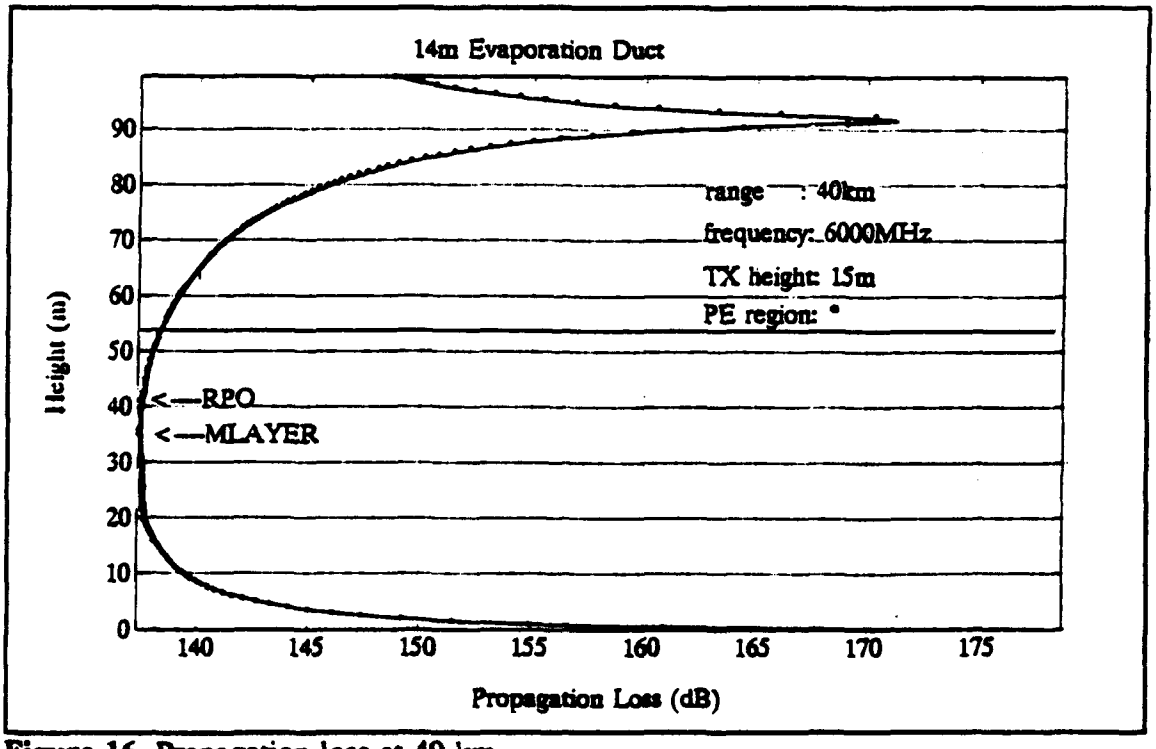

Figure 16. Propagation loss at 40 km.

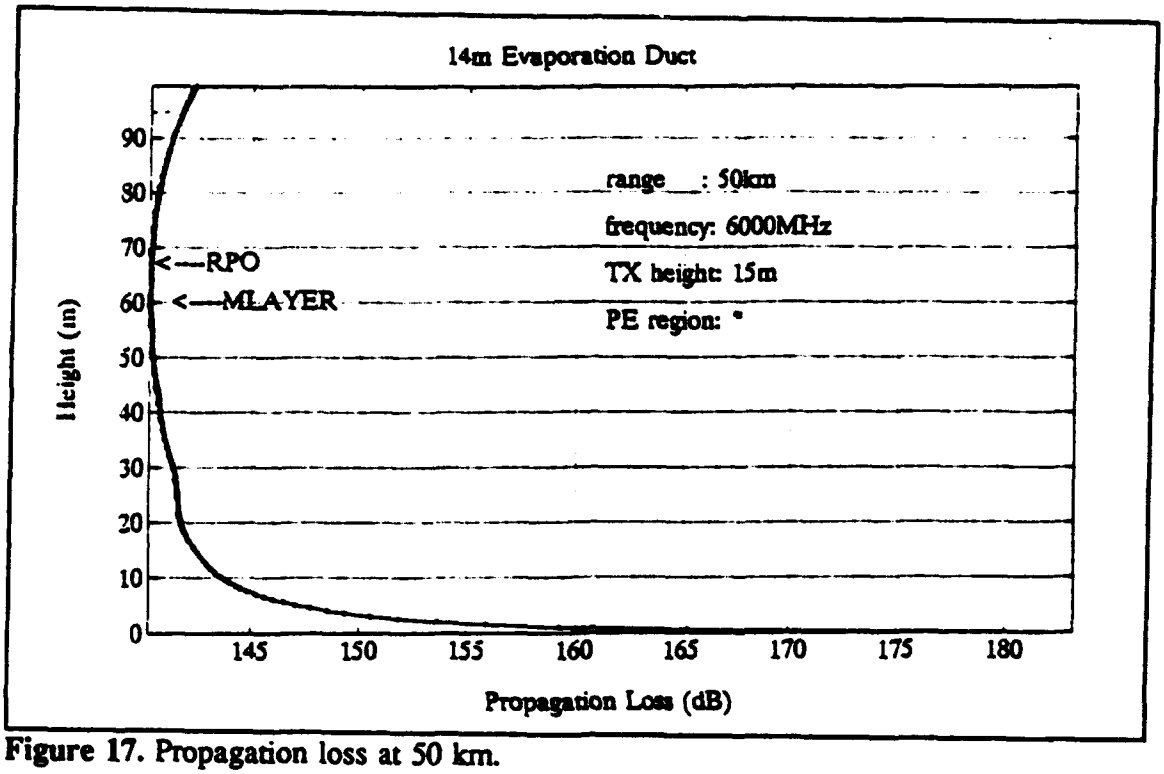

Figure 17. Propagation loss at 50 km.

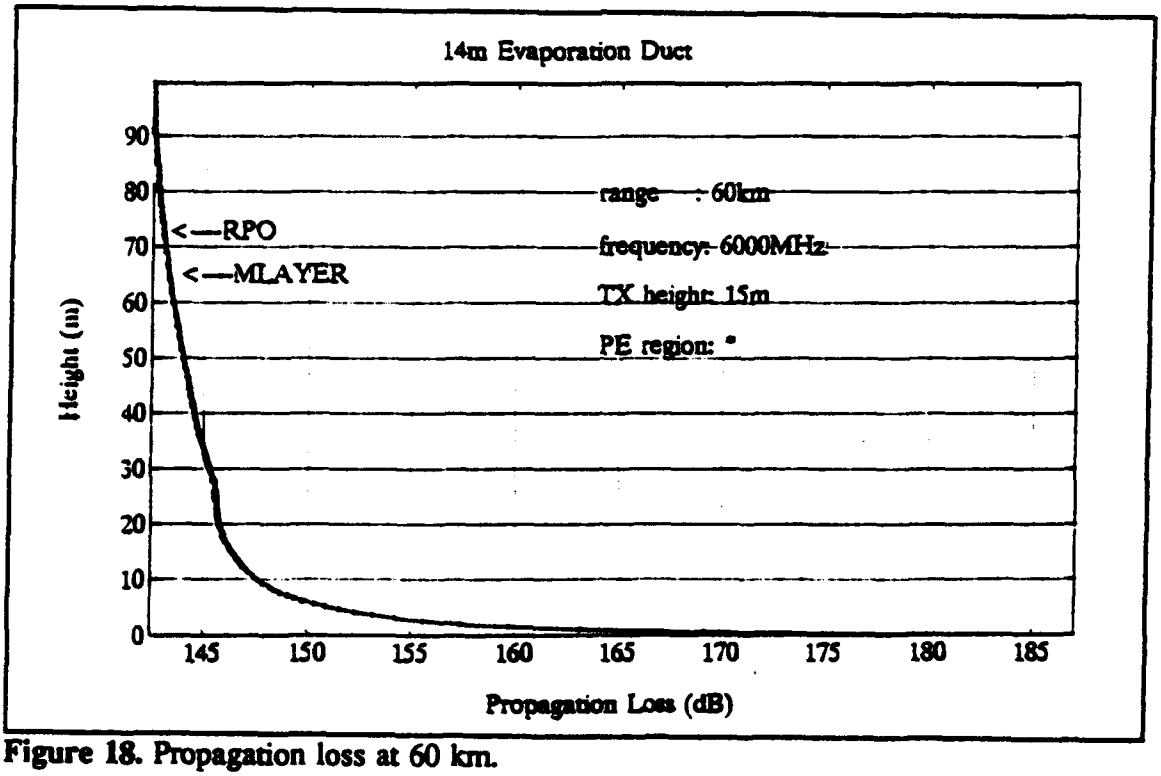

Figure 18. Propagation loss at 60 km.

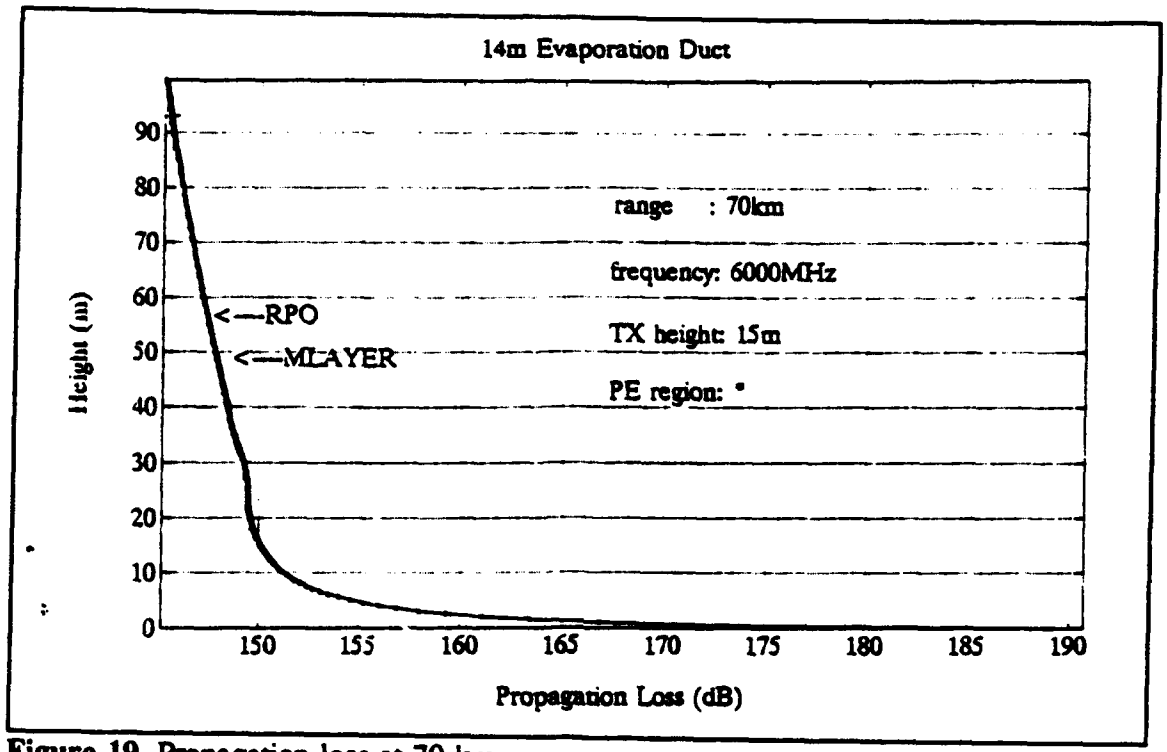

Figure 19. Propagation loss at 70 km.

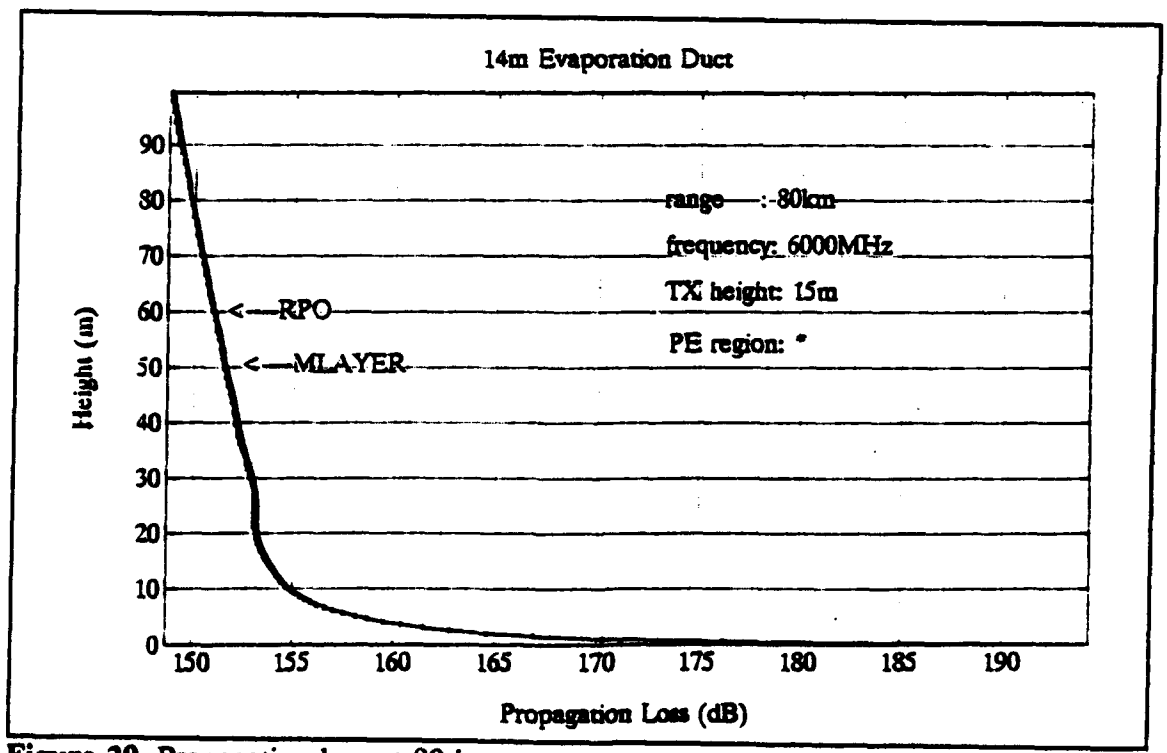

Figure 20. Propagation loss at 80 km.

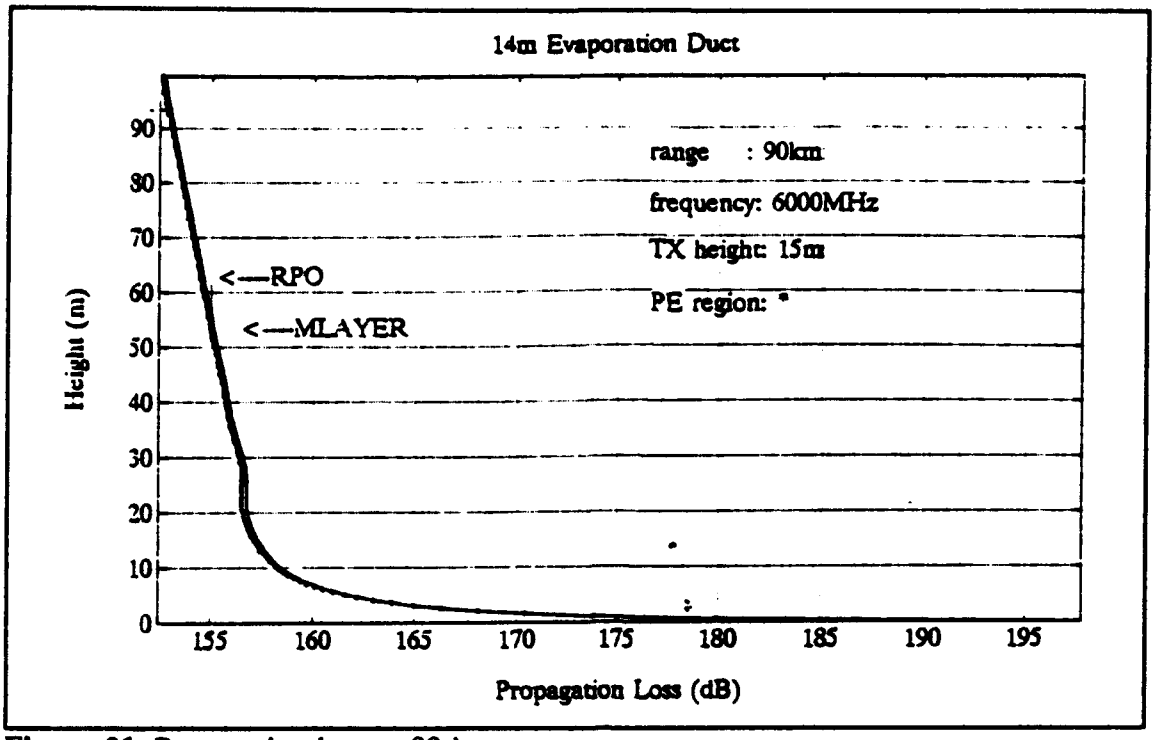

Figure 21. Propagation loss at 90 km.

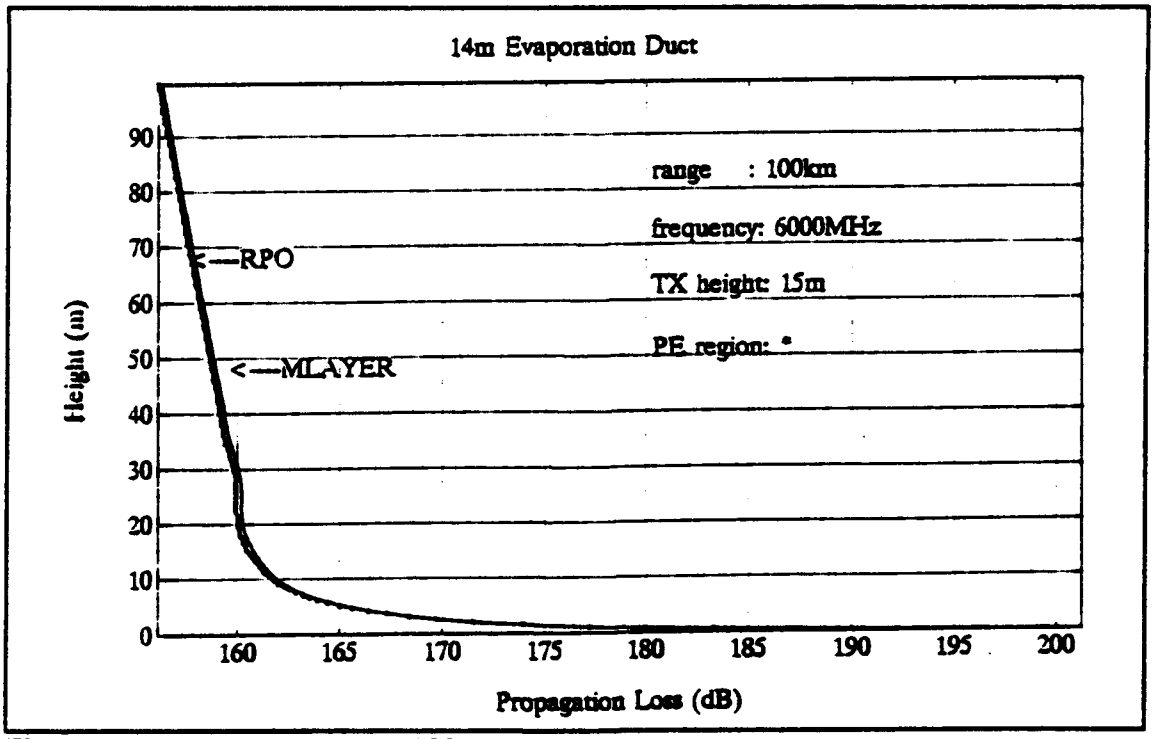

Figure 22. Propagation loss at 100 km.

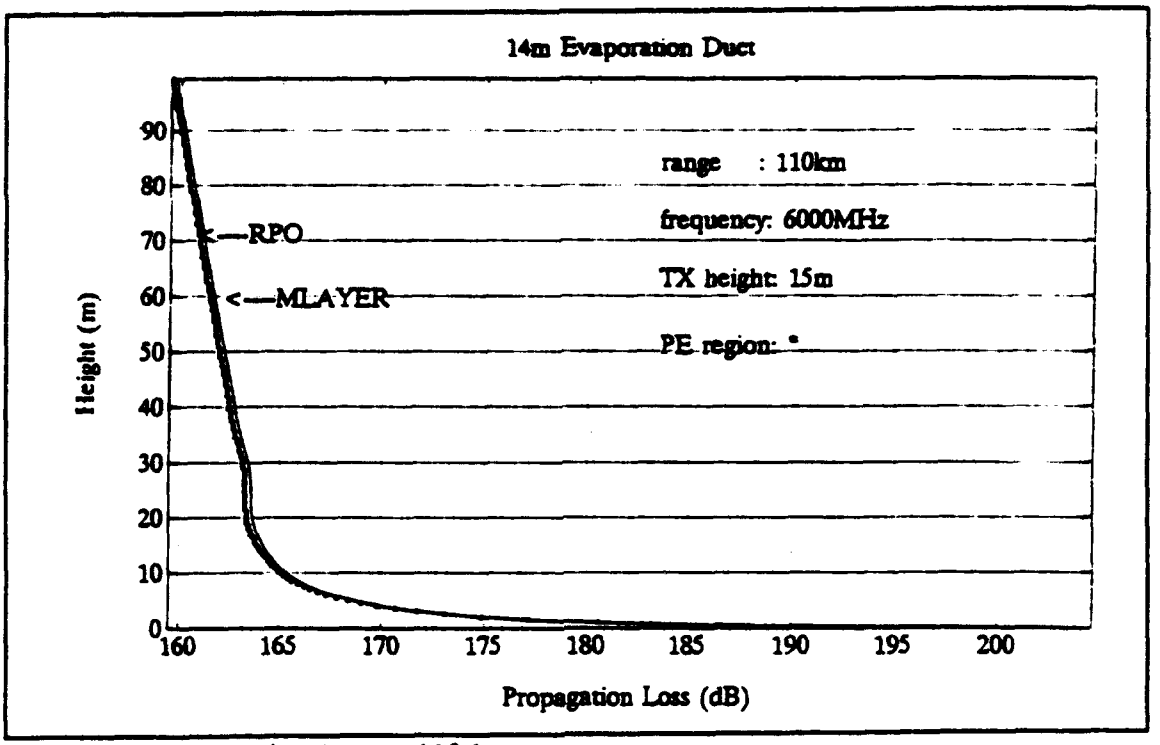

Figure 23. Propagation loss at 110 km.

C. SURFACE-BASED DUCT OVER EVAPORATION DUCT

The agreement in one case and the disagreement in another between RPO and M-Layer prompted an investigation into a combined profile consisting of these two ducts. Figures 24 through 34 show the propagation loss under such a refractivity profile. At 6 GHz, RPO and M-Layer agree well over the entire range except between 50 and 60 km when M-Layer displays an increase in field strength toward the surface over the lowest few meters while RPO continues to decrease. This leads to more than 10 dB deviations in propagation loss at these ranges. At 12 GHz, the two programs agree even better when M-Layer does not show the increase toward surface level within the last few meters. At 3 GHz, this difference is more pronounced. Below 10 to 20 m, this divergence starts to appear and leads to deviations in propagation loss of up to 40 dB.

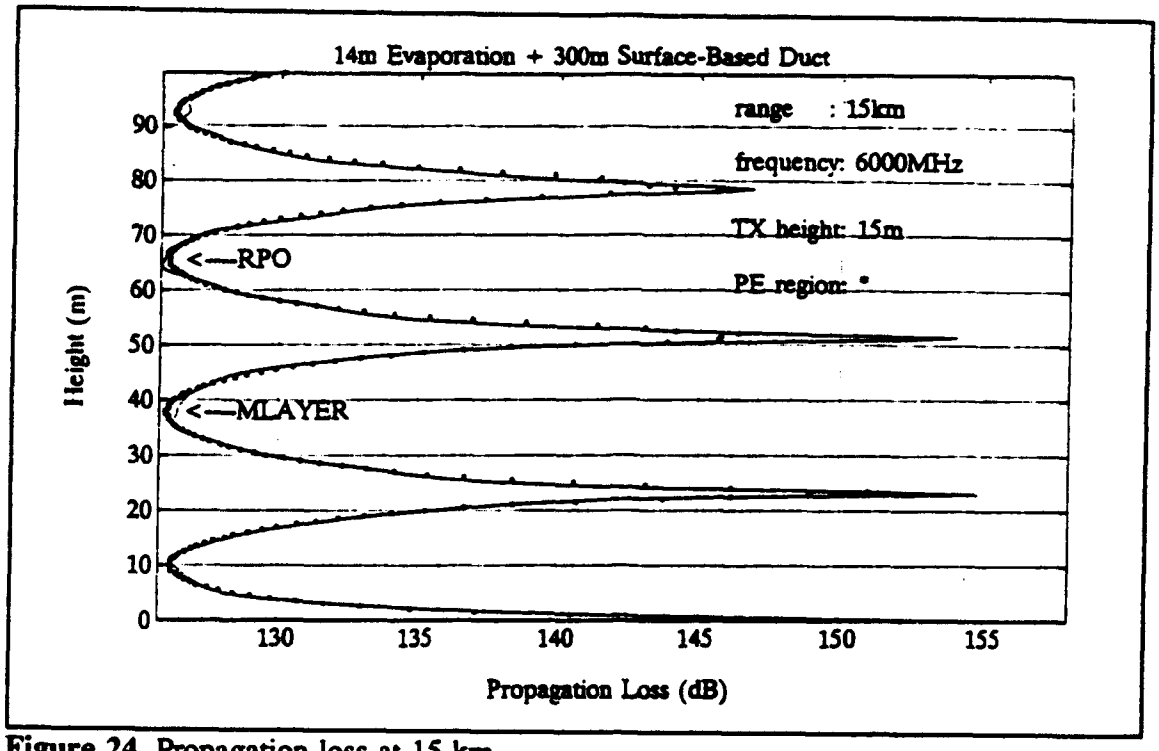

Figure 24. Propagation loss at 15 km.

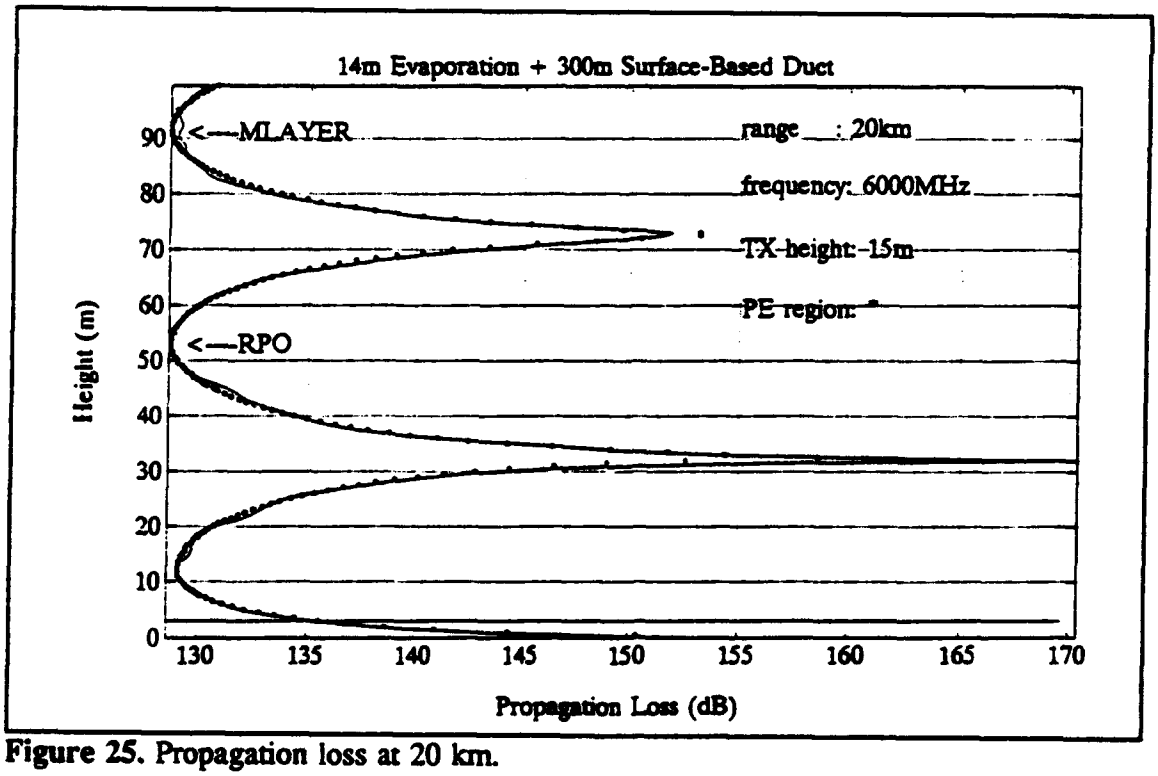

Figure 25. Propagation loss at 20 km.

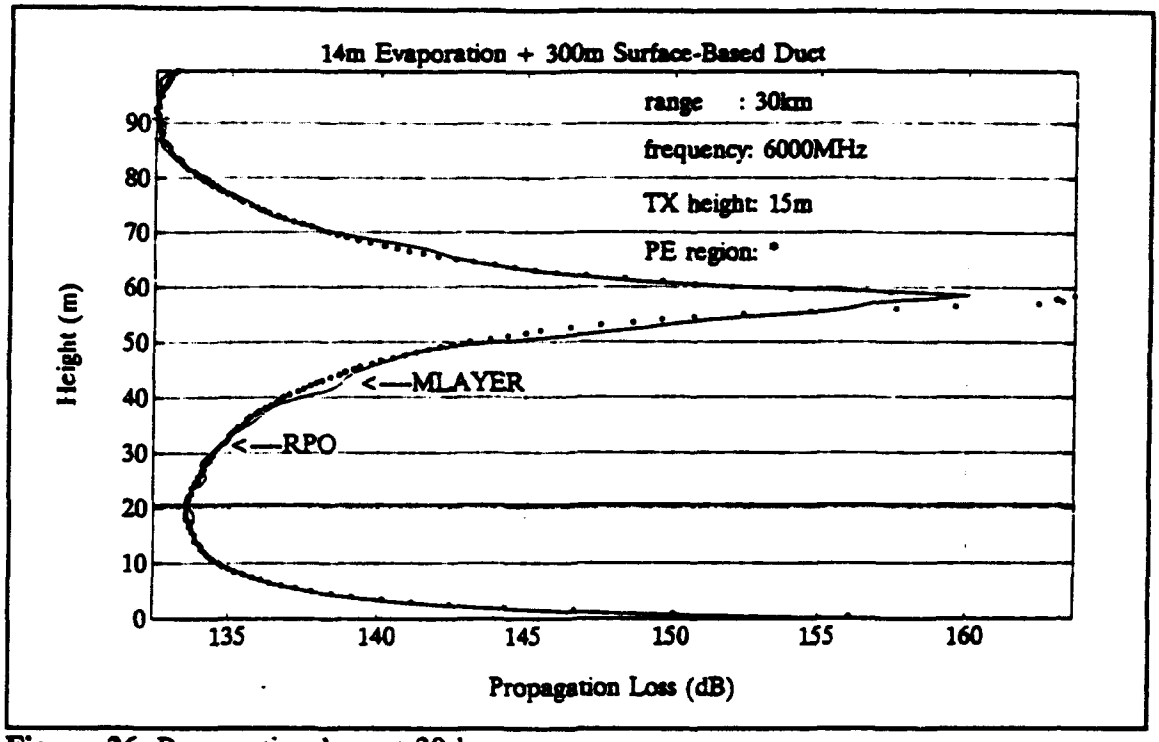

Figure 26. Propagation loss at 30 km.

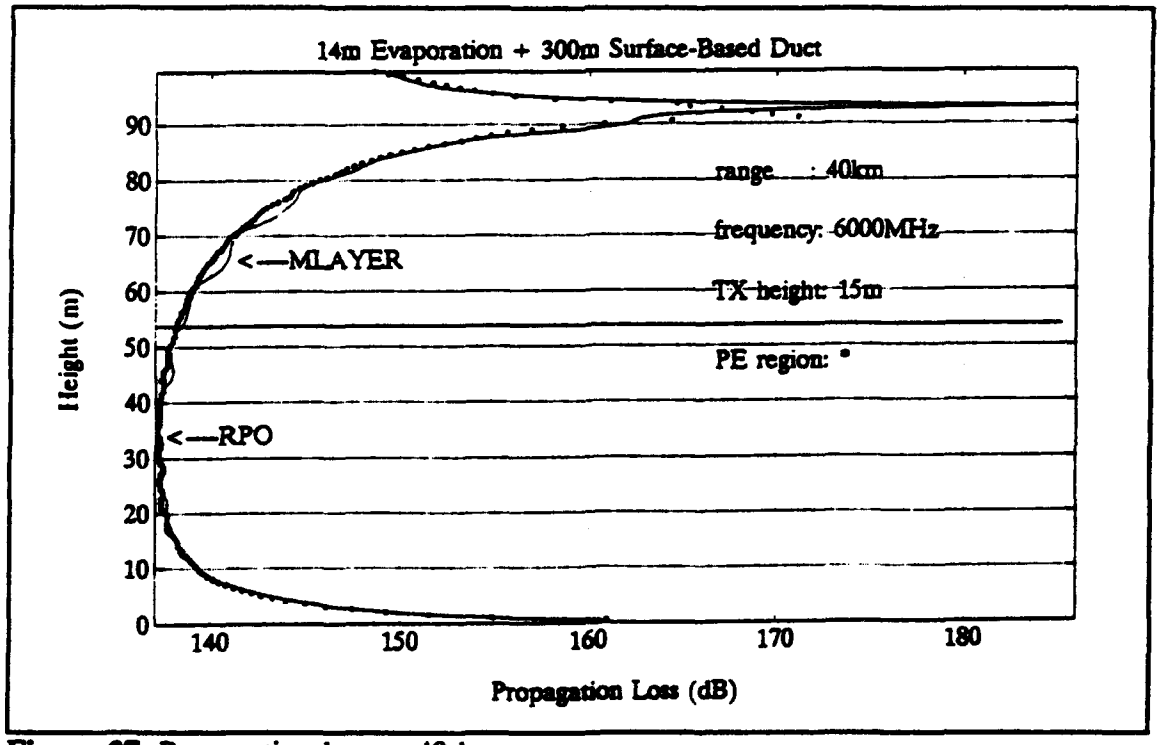

Figure 27. Propagation loss at 40 km.

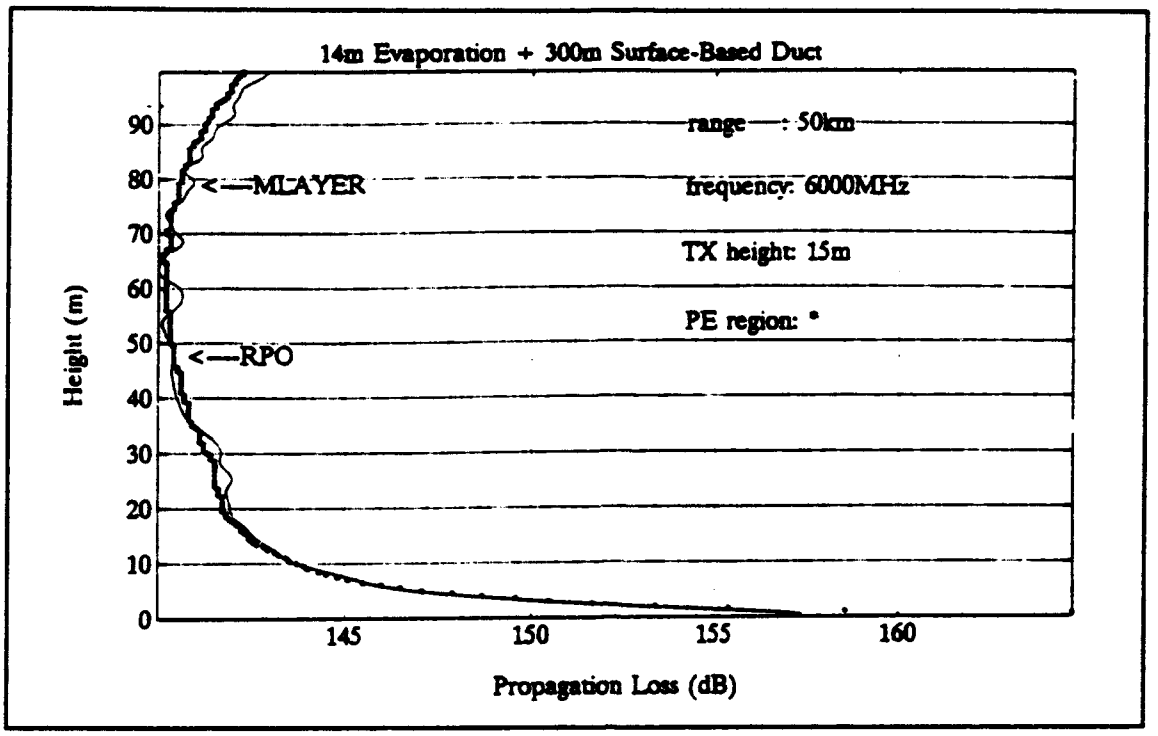

Figure 28. Propagation loss at 50 km.

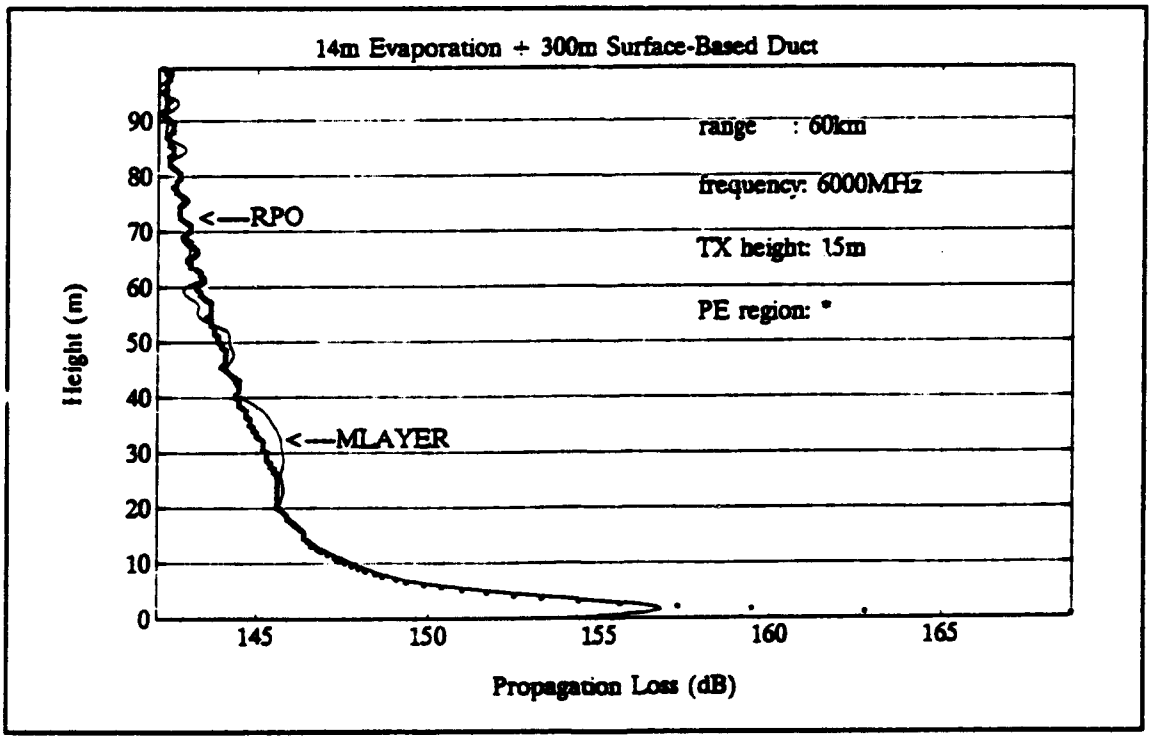

Figure 29. Propagation loss at 60 km.

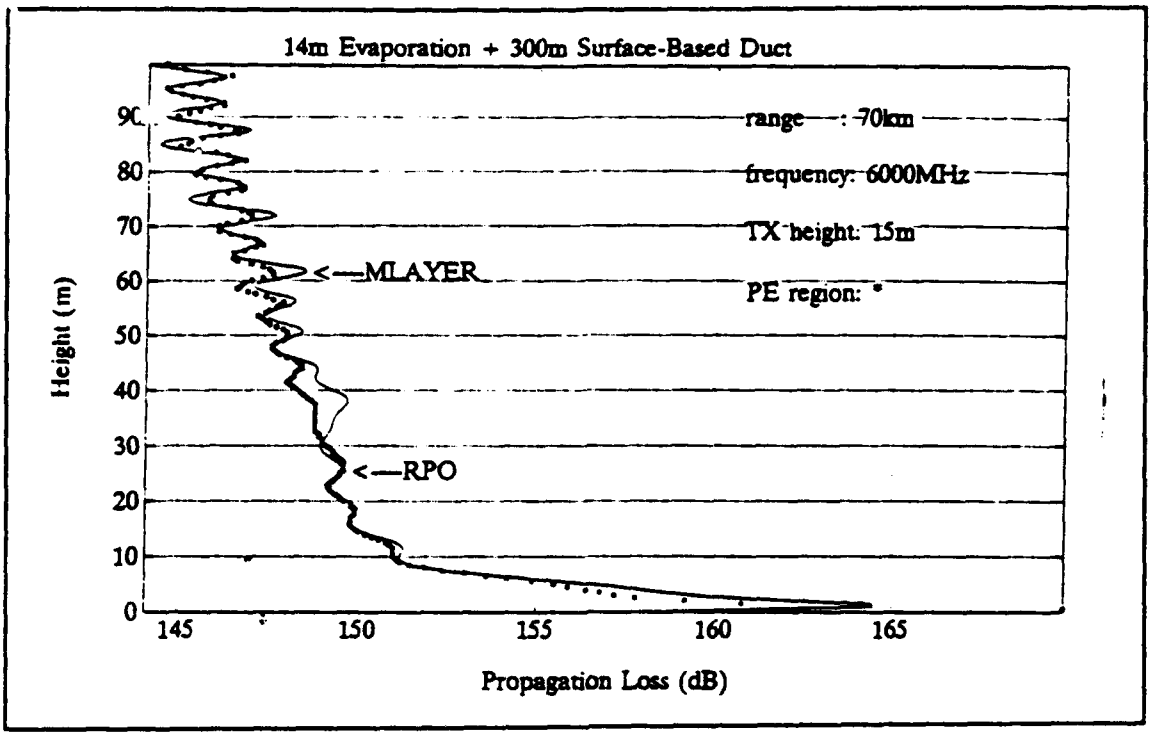

Figure 30. Propagation loss at 70 km.

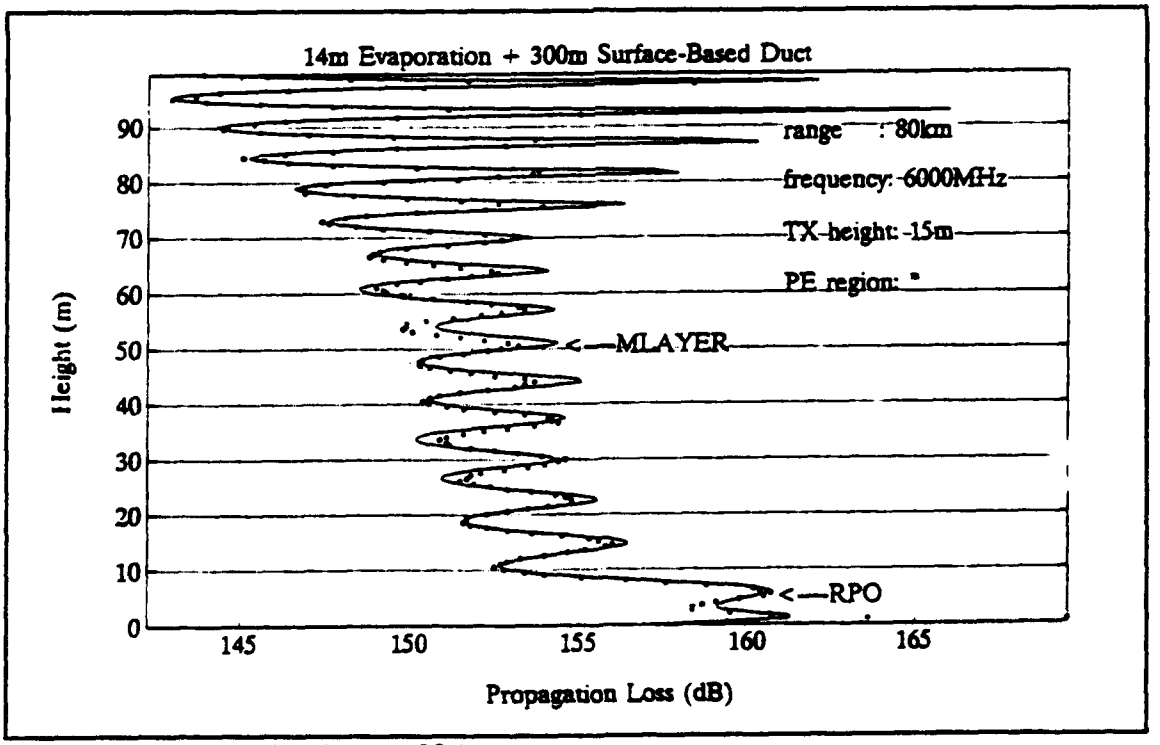

Figure 31. Propagation loss at 80 km.

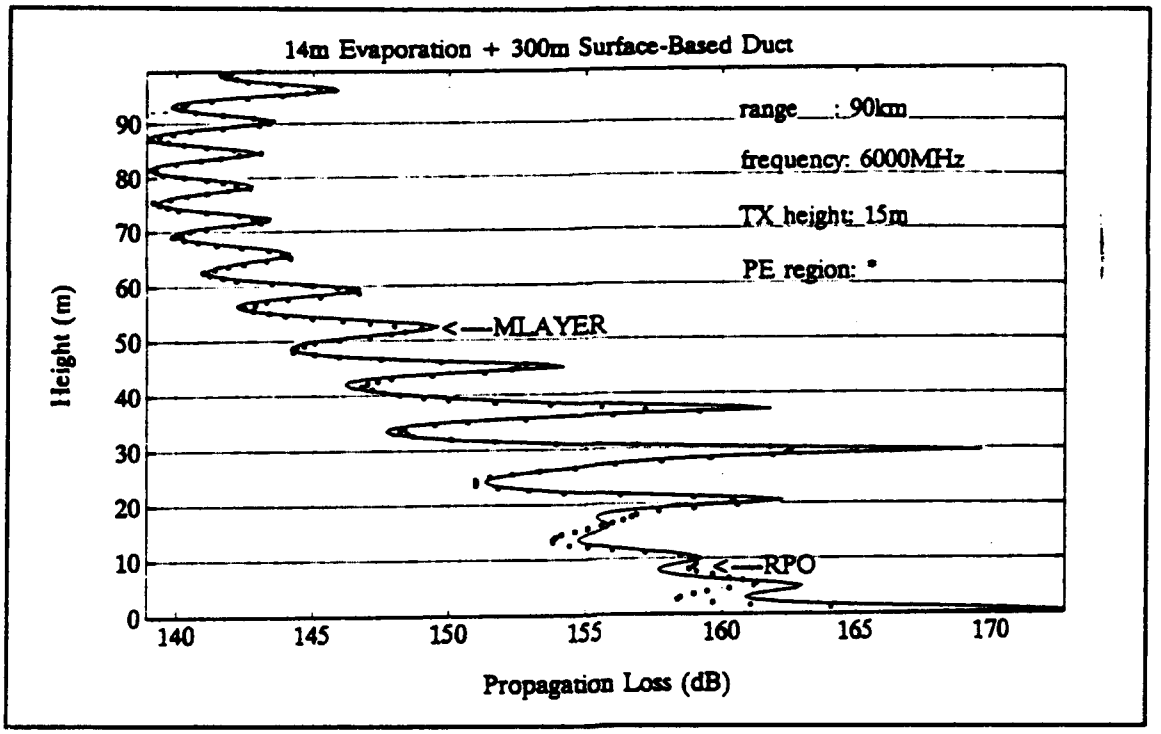

Figure 32. Propagation loss at 90 km.

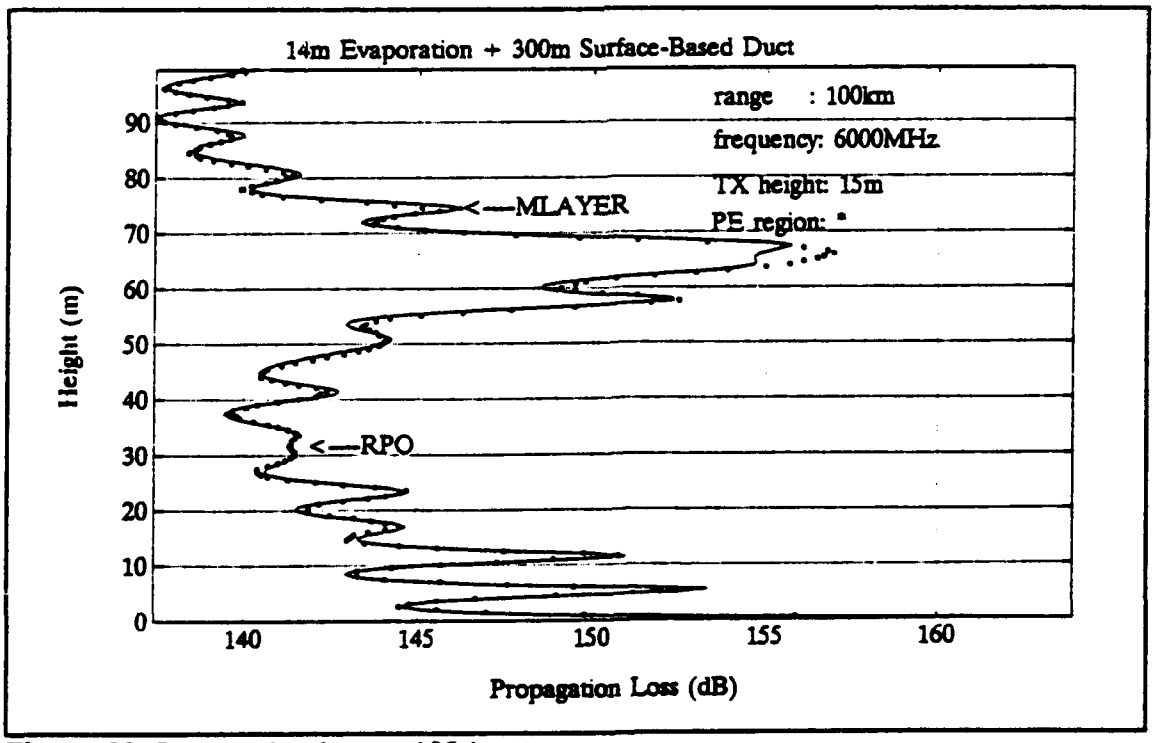

Figure 33. Propagation loss at 100 km.

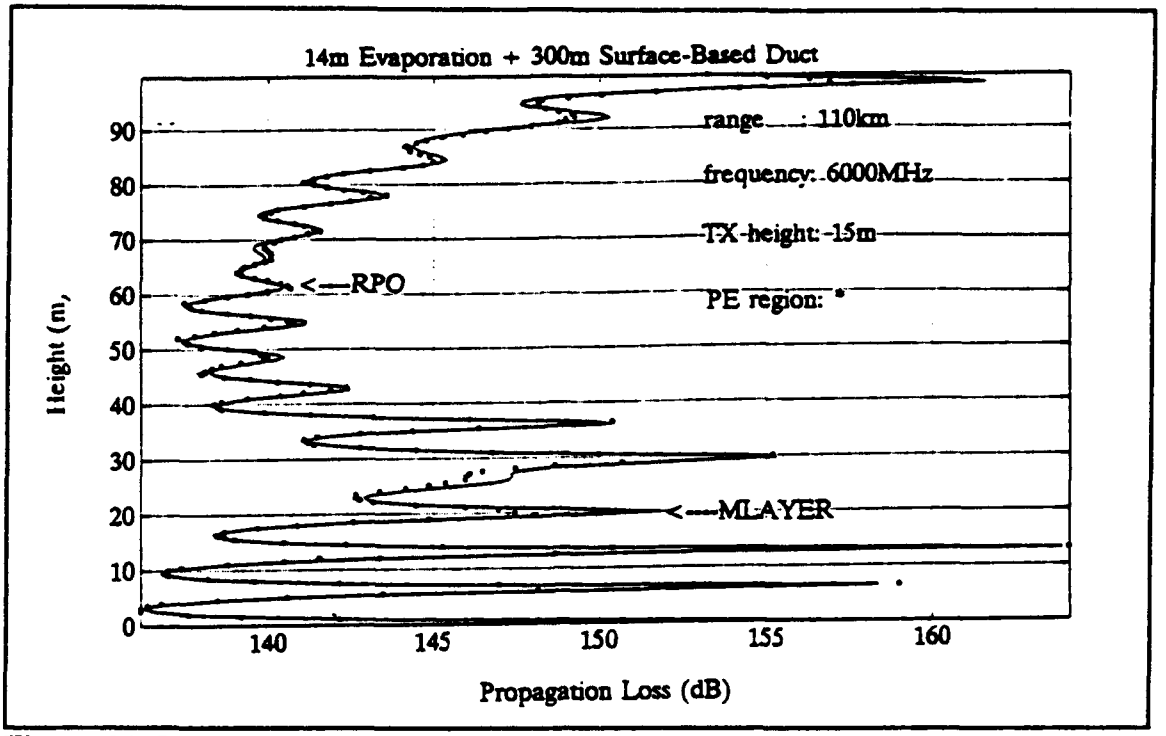

Figure 34. Propagation loss at 110 km.

IV. ANALYSIS AND CONCLUSIONS

A. ANALYSIS

Since RPO is a high frequency approximation while M-Layer is based on a low frequency technique, and the vertical extent within which the index of refraction of the atmosphere is specified is much larger than the wavelength under consideration, RPO is expected to be more accurate at short ranges. The fact that M-Layer matches the results of ray-optics computations in Fig. 13 at 15 km from the transmitter for heights over 90 m above ground confirms the reliability of M-Layer. RPO and M-Layer agree well also in the region far beyond the radar horizon. What happens then over the region in-between when a 300 m surface-based duct is present?

The physics of the situation is revealed if the earth-flattening approximation as prescribed in Ref. 6 is re-examined. In fact, both RPO and M-Layer are treating the propagation problem as one involving only a flat "earth" surface. The waves are traveling in a flat, layered dielectric waveguide. There is no blockage of rays due to the earth to create a shadow; instead, the rays are bent away from the "shadow" region by the linearly increasing component of the modified refractivity. The ducting structure bends the wave back towards the surface. Properly implemented, these two programs should provide identical predictions over ranges of common validity.

Above a flat surface, the concept of interference between a direct ray and a reflected ray, even though bent by the atmosphere, remains valid. The bending shifts the locations

of constructive and destructive interferences, but their separations are less affected. From Figs. 2 and 13, it is clear that at 15 km, the separations between two neighboring nulls above ground are about 28 m, independent of the particular environment and close to a free-space, parallel-ray estimate of 25 m. The separations of nulls are expected to increase as the range is increased. This is observed in Figs. 13 through 23 for the propagation in the presence of the 14 m evaporation duct. But when the 300 m surface-based duct is present, both RPO and M-Layer predict, for ranges greater than 90 km, similar field strength variations which oscillate much faster than those observed within the line-of-sight region. It is clear that this is a phenomenon due to the presence of the surface-based duct. In terms of high frequency ray-optics terminology, this fast oscillation is due to additional rays which are bent back by the duct. In terms of waveguide mode theory, it is due to the propagation of waves in many modes established in the surface-based duct, each at a distinct phase velocity, thus interfering severely.

The deviations between RPO and M-Layer at ranges from 30 through 70 km which show up in Figs. 4 to 12 can now be explained. RPO fails to fully take into account the effects of a high surface-based duct. This argument is further supported by investigating the effects of lowering the duct height. At all frequencies, the fast oscillation characteristic of the presence of a surface based duct sets in at a shorter range with a lower duct height. Agreement between RPO and M-Layer gets better as the duct height is lowered. These can be observed from the results presented in Appendix E for propagation in a 150 m surface-based duct and in Appendix F for propagation in a 100 m duct.

B. CONCLUSIONS

At low altitudes in the neighborhood of the radar horizon, deviations between RPO and M-Layer can be significant. RPO appears not to be able to properly include the effects of a high surface-based duct at a short range. It is recommended that parabolic equation computations should start at a closer range than currently prescribed in RPO. The altitude at which the filtering of field strength starts should always be much higher than the duct height.

APPENDIX A: PROGRAM SOURCE CODES

This Appendix contains listings of the RPO main program RPOmain, the RPO input subroutine RPOstdin, the M-Layer input subroutine MLstdin and the MATLAB M-file RPOMLA.M for plotting the propagation loss computed with RPO and M-Layer.

1. Subroutine RPOmain

```
      program  RPOmain
c
c PURPOSE: Main program for RPO.
c
c
c input:
c   Argument List: None
c  Common: fmhz, ztran, ipolar, ipatrn, beamw, elang, hfang, hffac, nfacs
c          capm, zprof, nprofs, nlevls, xprof, wind
c         iscatt, maxlev, maxnx, nxout, maxnz, nzout, maxpro, xmax, zmax
c
c
c output:
c   Argument list: None
c   Common: losscb, srng
c
c
c subroutines calling RPOmain: None.
c subroutines called by RPOmain: rpostdin, rpoini, rpostp,
c
c
c common block
c       /system/
c       fmhz   : EM system frequency
c       ztran  : antenna height
c       ipolar: antenna polarization
c       ipatrn: antenna pattern
c       beamw  : antenna vertical beam width
c       elang  : antenna elevation angle
c       hfang  : height-finder angles array in degrees (0. to 99)
c       hffac  : height-finder power reduction factor array (0. to 1.0 )
c      nfacs  : number of power reduction angles/factors for user-defined
c               height-finder radar
c
c       /enviro/
c       capm   : (*) profile modified refractivity array
c       zprof  : (*) profile heights in meters (.GE. 0.)
c       nprofs: number of profile levels
c       nlevls: number of refractivity profile levels (1 to maxlev)
c       xprof  : (*) range to each profile in meter (.GE. 0.)
c       wind   : wind speed at range zero in meter/sec (.GE. 0.)
c
```

```
c       /init/
c       iscatt: flag to include troposcatter
c       maxlev: maximum number of profile level above zero height
c       maxnx : maximum number of output range points
c       nxout : number of output range points (1 to maxnx)
c       maxnz : maximum number of output height points
c       nzout : number of output height points (1 to maxnz)
c       maxpro: maximun number of profiles beyond zero range
c       xmax  : maximum range for output in meter
c       zmax  : maximum height for output in meter
c Declares the types of parameters
      character*8 filein

      integer*4 ipolar, ipatrn, nfacs, nprofs, nlevls, iscatt,
     +          nxout, nzout, maxlev, maxnx, maxnz, maxpro

      integer*2 losscb, srng

      real      fmhz, ztran, beamw, elang, hfang, hffac,
     +          xprof, wind, capm, zprof, xmax, zmax

c The following include file contains a PARAMETER statement to
c define maximun array sizes maxpro, maxlev, maxnz

      INCLUDE 'RPOSIZE.INC'

c
c     The following PARAMETER statement defines maximum array
c     dimensions used throughout RPO.  Generally, these constants
c     will have to be changed for each implementation of RPO.
c     GLOSSARY:
c       maxlev: maximum number of profile levels above zero height.
c       maxnx : maximum number of output range points.
c       maxnz : maximum number of output height points.
c       maxpro: maximum number of profiles beyond zero range.
c
      PARAMETER (maxnx = 440, maxnz = 280, maxlev = 50, maxpro =32)
c
      dimension losscb(maxnz),srng(maxnz)

      COMMON /system/ fmhz, ztran, ipolar, ipatrn, beamw, elang,
     +                hfang(10), hffac(10), nfacs
      COMMON /enviro/ nlevls, nprofs, wind, zprof(0:maxlev, 0:maxpro),
     +                capm(0:maxlev, 0:maxpro), xprof(0:maxpro)
      COMMON /init/ iscatt, nxout, nzout, xmax, zmax
      COMMON /misc/ jminFE, nx, xstep, zstep, wl, rk, fterm, pi
      COMMON /inout/ filein, selx, mlxout


c read data from input files
      write (*,*) 'Begin with rpostdin'
      call rpostdin

c initialize RPO
      write (*,*) 'Begin with rpoini'
      call rpoini(nsteps)


c call rpostp to compute propagation loss
c and write the result to a file on disk
```

```
      open(16,file=filein//'.out')
      do i=1, nxout
         call rpostp(x,losscb,srng)
         xkm=x*.001
         write(*,*) 'Begin with rpostp',i,xkm
         if (x.ge.selx) then
            do j=1,nzout
               write (16,1102) xkm, j*zstep, .1*losscb(j), srng(j)
            end do
         end if
      end do
 1102 format(f9.2, 6x, f6.1, 5x, f6.2, 5x, i2)
      end
```

2. Subroutine RPOstdin

```
c*************************************************************************
c Subroutine RPOstdin reads in data from a file concocted from two     *
c files: one contains parameters specific to RPO, the other contains   *
c and parameters used by both RPO and M-Layer, including the modified *
c refractivity, the transmitter height, and the output points.         *
c*************************************************************************

      subroutine RPOstdin

c The following include file contains a PARAMETER statement to
c define maximun array sizes maxpro, maxlev
      INCLUDE 'RPOSIZE.INC'
c
c     The following PARAMETER statement defines maximum array
c     dimensions used throughout RPO.  Generally, these constants
c     will have to be changed for each implementation of RPO.
c     GLOSSARY:
c       maxlev: maximum number of profile levels above zero height.
c       maxnx : maximum number of output range points.
c       maxnz : maximum number of output height points.
c       maxpro: maximum number of profiles beyond zero range.
c
      PARAMETER (maxnx = 440, maxnz = 280, maxlev = 50, maxpro =32)
c
      character*8 filein, fileb

      COMMON /system/ fmhz, ztran, ipolar, ipatrn, beamw, elang,
     +                hfang(10), hffac(10), nfacs
      COMMON /enviro/ nlevls, nprofs, wind, zprof(0:maxlev, 0:maxpro),
     +                capm(0:maxlev, 0:maxpro), xprof(0:maxpro)
      COMMON /init/ iscatt, nxout, nzout, xmax, zmax
      COMMON /inout/ filein, selx, mlxout

c-----read the RPO parameter---------
      read(*,'(a)') filein
      read(*,*)  nxout
      read(*,*)  selx
      read(*,*)  xprof(0)
      read(*,*)  nprofs

c RPO starts its array index with 0. It adopts Microsoft BASIC
```

```
c convention in its coding of this FORTRAN program. In the documentation
c and the input file, "nprofs" is the total number of profiles. Thus
c "nprofs" as the array index as used in RPO has to be adjusted by
c substracting "nprofs" by 1.
      nprofs=nprofs-1
      read(*,*)  ipatrn
      read(*,*)  beamw

c For omnidirectional pattern, the parameter "beamw" is ignored in the
c program. On the other hand, the upper limit for "beamw" is 45 degrees.
      if (ipatrn.eq.1) then
         beamw=45.0
      end if
      read(*,*)  elang
      read(*,*)  nfacs
      read(*,*)  iscatt

c---- read parameters common to RPO and M-Layer -----
      read(*,'(a)')  fileb
      read(*,*)  nlevls
      read(*,*)  wind
      read(*,*)  fmhz
      read(*,*)  ipolar
c The definition of ipolar in RPO is 1 plus that in M-LAYER.
      ipolar=ipolar+1
      read(*,*)  ztran
      read(*,*)  nzout
      read(*,*)  delzr
      read(*,*)  zrinit
      zmax=nzout*delzr+zrinit
      read(*,*)  mlxout
      read(*,*)  delx
      read(*,*)  xinit
      delx=delx*1000
      xinit=xinit*1000
      xmax=mlxout*delx+xinit
      do i=0,nlevls
        read(*,*)  zprof(i,0)
        read(*,*)  capm(i,0)
        capm(i,0)=capm(i,0)+339.0
      end do
      open(17,file=filein//'.in')
      write(17,*)'---- parameters common to RPO and M-Layer ----'
      write(17,*)filein, '       :RPO file'
      write(17,*)nlevls, '      :nlevls (count from 0)'
      write(17,190)wind
 190  format(f15.2, '   :wind')
      write(17,192)fmhz
 192  format(f15.2, '   :fmhz')
      write(17,*)ipolar-1, '      :ipolar (0:horizontal  1:vertical )'
      write(17,194)ztran
 194  format(f15.2, '   :ztran')
      write(17,*)nzout,  '      :nzout'
      write(17,201)delzr
 201  format(f15.2, '   :delzr')
      write(17,202)zrinit
 202  format(f15.2, '   :zrinit')
      write(17,*)mlxout ,'      :mlxout (max number of range output) '
      write(17,203)delx
 203  format(f15.2, '   :delx')
```

```
      write(17,204)xinit
 204  format(f15.2, '  :xinit ')
      write(17,*)'----------  RPO parameters  ------------'
      write(17,205)zmax
 205  format(f15.2, '  :zmax (nzout*delzr,calculated by program)' )
      write(17,206)xmax
 206  format(f15.2, '  :xmax (xinit+delx*mlxout,calculated by program)')
      write(17,*)nxout,'     :nxout (xmax / delx, read from input) '
      write(17,207)selx
 207  format(f15.2, '  :selx (selected range x >= selx )')
      write(17,208)xprof(0)
 208  format(f15.2, '  :xprof')
      write(17,*)nprofs+1, '     :nprofs'
      write(17,*)ipatrn, '     :ipatrn'
      write(17,209)beamw
 209  format(f15.2, '  :beamw')
      write(17,210)elang
 210  format(f15.2, '  :elang')
      write(17,*) '           N/A  :hfang (not used)'
      write(17,*) '           N/A  :hffac (not used)'
      write(17,*)nfacs,  '     :nfacs'
      write(17,*)iscatt, '     :iscatt'
      write(17,*)'---- M-profile ---- value on surface: 339.0 -----'

      do i=0,nlevls
        write(17,211)zprof(i,0)
 211    format(f15.2, '  :zprof')
        write(17,212)capm(i,0)
 212    format(f15.2, '  :capm ')
      end do
      return
      end
```

3. Subroutine MLstdin

```
c*************************************************************************
c Subroutine MLstdin reads data from a file concocted from two files:  *
c one contains parameters specific to M-Layer, the other contains      *
c parameters used by both RPO and M-Layer, including the modified      *
c refractivity, the transmitter height, and the output points.         *
c*************************************************************************

      subroutine MLstdin
c
c   MLstdin is the revised input program of M-Layer, NPS version, to
c   read in data files. The common block /inpt9/ has been removed from
c   all subroutines.
c
      implicit real*8 (a-h,o-z)
      complex*16 qeigen
      integer iflgab,mpol,nzt,nzr,nx,nzlayr,nrmode,mfile,i
      character*40 filein, fileb
c
c   use include file for parameters of
c              mxlayr  max # layers
c              mxmode  max # modes
c
      include 'mlaparm.inc'
```

```
c
c
c       include file to define the
c               maximum # of layers (mxlayr)
c        ..     maximum # of modes  (mxmode)
c
        parameter (mxlayr=35 )
        parameter (mxmode=390)
      dimension zi(mxlayr+1),zim(mxlayr+1),zigab(mxlayr+1),
     $          qeigen(mxmode)
c
      common /inpt0/filein,mfile,fqmzin,mpol,aloss,dielcg,sigmag,
     +              ztinit,delzt,nzt,zrinit,delzr,nzr,xinit,delx,nx,
     +              refz,refm,refgab,zim,zigab
     +       /inpt1/nzlayr
     +       /inpt2/zi
     +       /inpt4/rmsbht
     +       /modes/nrmode,qeigen
c
c
c   read M-LAYER specific parameters
      read(*,'(a)') filein
      read(*,*) mfile
      read(*,*) delfq
      read(*,*) nfreq
      read(*,*) aloss
      read(*,*) iflgab
      read(*,*) delzt
      read(*,*) nzt
      read(*,*) zref
      read(*,*) refz
      read(*,*) refm
      read(*,*) refgab
c   read parameters common to RPO and M-Layer
      read(*,'(a)') fileb
      read(*,*) nzlayr
      read(*,*) wind
      read(*,*) fqmzin
      read(*,*) mpol
      read(*,*) ztinit
      read(*,*) nzr
      read(*,*) delzr
      read(*,*) zrinit
      read(*,*) nx
      read(*,*) delx
      read(*,*) xinit

c
c   The profile must contain at least three levels. The M gradients
c   in adjacent layers must not be equal.
c
      do i=1,nzlayr+1
         read(*,*) zi(i)
         read(*,*) zim(i)
      end do

      if (mfile.ne.0) then
c   mfile<>0 indicates input file contains eigenvalues
         read(*,*)nrmode
         do i=1,nrmode
```

```
            read(*,*) qeigen(i)
          end do
        endif

c   Calculate the root mean square bump height of sea surface.
c
        rmsbht=0.00514*wind**2
c
c   Calculate the dielectric constant and conductivity of sea water.

        if (fqmzin .LE. 1500.) then
          dielcg= 80.
          sigma = 4.3
        else if (fqmzin .LE. 3000.) then
          dielcg= 80. - .00733 * (fqmzin-1500.)
          sigma = 4.3 + .00148 * (fqmzin-1500.)
        else if (fqmzin .LE. 10000.) then
          dielcg= 69. - .00243 * (fqmzin-3000.)
          sigma = 6.52 + .001314 * (fqmzin-3000.)
        else
          dielcg= 51.99
          sigma = 15.718
        end if

c-----write input data to a file on the disk-----

        open(27,file=filein//'.in')
        write(27,*) '------ parameters common to RPO and M-Layer ------'
        write(27,' (2(A13))')filein, ':ML  file'
        write(27,*)nzlayr, '      :nzlayr'
        write(27,190)wind
 190    format(f15.2, '   :wind')
        write(27,192)fqmzin
 192    format(f15.2, '   :fqmzin')
        write(27,*)mpol, '      :mpol  (0:horizontal  1:vertical )'
        write(27,194)ztinit
 194    format(f15.2, '   :ztinit')
        write(27,*)nzr,  '      :nzr'
        write(27,201)delzr
 201    format(f15.2, '   :delzr')
        write(27,202)zrinit
 202    format(f15.2, '   :zrinit')
        write(27,*)nx,   '      :nx'
        write(27,203)delx
 203    format(f15.2, '   :delx in km')
        write(27,204)xinit
 204    format(f15.2, '   :xinit in km')
        write(27,*) '--------- M-Layer specific parameters -----------'
        write(27,*) mfile,'      :mfile=0:read input and compute e.v.'
        write(27,205)delfq
 205    format(f15.2, '   :delfq')
        write(27,*)nfreq,'      :nfreq'
        write(27,207)aloss
 207    format(f15.2, '   :aloss')
        write(27,*)iflgab,'      :iflgab'
        write(27,208)delzt
 208    format(f15.2, '   :delzt')
        write(27,*)nzt, '      :nzt'
        write(27,209)zref
 209    format(f15.2, '   :zref')
```

```
      write(27,210)refz
 210  format(f15.2, '  :refz')
      write(27,211)refm
 211  format(f15.2, '  :refm')
      write(27,212) refgab
 212  format(f15.2, '  :refgab')
      write(27,*)'------ M-profile ---------'
      do i=1,nzlayr+1
         write(27,214) zi(i),i
 214     format(f15.2, '  :zi(' ,I2, ')' )
         write(27,215) zim(i),i
 215     format(f15.2, '  :zim(' ,I2, ')' )
      end do
      return
      end
```

4. MATLAB Plotting M-file

```
% file name:'RPOMLA.M
  clg
  clear
  fno=input(' input the no. of test file: ','s');
% delete the old .met file
  xdel=['delete rl', fno, '.met'];
  eval(xdel);
% load the data
  t1=['load d:\matlab\wu\dat\','rpo', fno, '.dat']
  t2=['load d:\matlab\wu\dat\','ml', fno, '.dat'];
  eval(t1);
  eval(t2);
% read the data
  rpfr=['rpo', fno];
  mlfr=['ml', fno];
  r1=[rpfr,'(:,1)']; r2=[rpfr,'(:,2)'];
     r3=[rpfr,'(:,3)']; r4=[rpfr,'(:,4)'];
  m1=[mlfr,'(:,1)']; m2=[mlfr,'(:,3)']; m3=[mlfr,'(:,6)'];
  rpox=eval(r1); rpoz=eval(r2); rpos=eval(r3); rpor=eval(r4);
  mlx=eval(m1); mlz=eval(m2); mls=eval(m3);

% set up initial conditoin for while loop
  an=1;
  prof=input('The name for profile: ','s');
  frq=input('The frequency (in MHz): ');
  anh=input('The antenna height (m): ');

% loop for range increment
  while an>0
      xrg= input(' The x range ' );
% calculate the receiver antenna height of horizontal distance
      ae=6371000;
      anh2=  ( xrg*1000-sqrt(2*ae*anh) )^2 /(2*ae);
      k1=1; k2=1; k3=1; k4=1; p=1;
% x1, x2... is used to decide which region should be plotted in plot.
      x1=0; x2=0; x3=0; x4=0;

% find the index of rpo loss for x range equal to xrg
      tmpxrg=xrg+.05;
      xindex=find( (rpox>=xrg) & (rpox<=tmpxrg) );
```

```
      stri=xindex(1); endi=xindex( length(xindex) );

% find the min. and max. of rpo loss for x range equal to xrg
      xrpomin=min(rpos(xindex));
      xrpomax=max(rpos(xindex));

% get rpo loss, receiver height, according to the method of computation
% (fe, ro, xo & pe)
      for i=stri:endi
            if rpor(i)==1
               rpz1(k1)= rpoz(i); rps1(k1)= rpos(i); rpr1(k1)= rpor(i);
               k1=k1+1;
               x1=1;
            end
            if rpor(i)==2
               rpz2(k2)= rpoz(i); rps2(k2)= rpos(i);
               k2=k2+1;
               x2=2;
            end
            if rpor(i)==3
               rpz3(k3)= rpoz(i); rps3(k3)= rpos(i);
               k3=k3+1;
               x3=3;
            end
            if rpor(i)==4
               rpz4(k4)= rpoz(i); rps4(k4)= rpos(i);
               k4=k4+1;
               x4=4;
            end
      end

% find the index of mlayer loss for the x range equal to xrg
      xindex=find( (mlx>=xrg) & (mlx<=tmpxrg) );
      stri=xindex(1); endi=xindex( length(xindex) );

% find the min. and max. of ml loss for x range is equal to xrg
      xmlmin=min(mls(xindex));
      xmlmax=max(mls(xindex));

% get the data which satisfy x=xrng
      for i=stri:endi
            mx(p)= mlx(i); mz(p)= mlz(i); ms(p)= mls(i);
            p=p+1;
      end

% set the axis of plot
      maxz=max(mz);
      maxx=max(xmlmax,xrpomax);
      minx=min(xmlmin,xrpomin);
      axis( [ minx  maxx  0  maxz ] )
      plot(ms,mz,'-g')
      hold on

% plot the horizontal line
      hrs=[];hrz=[];
      hrs=minx:1:maxx;
      for i=1:length(hrs)
          hrz(i)=anh2;
      end
      plot(hrs,hrz)
```

```
% plot rpo
      if x1==1
         plot(rps1,rpz1,'+b')
      end
      if x2==2
         plot(rps2,rpz2,'.w')
      end
      if x3==3
         plot( rps3,rpz3,'xb')
      end
      if x4==4
         plot( rps4,rpz4,'*r')
      end
      xlabel(' Propagation Loss (dB) ');
      ylabel(' Height (m) ');
      gtext([num2str(prof)]);
      gtext(['<----RPO']);
      gtext(['<----MLAYER']);
      gtext(['range     : ',num2str(xrg),'km']);
      gtext(['frequency: ',num2str(frq),'MHz']);
      gtext(['TX height: ',num2str(anh),'m']);
      if x1==1
        gtext(['FE region: +'])
      end
      if x2==2
        gtext(['RO region: .'])
      end
      if x3==3
        gtext(['XO region: x'])
      end
      if x4==4
        gtext(['PE region: *'])
      end
      grid
      pause
      csav=input(' save the plot ? (y/n) ','s');
      if (csav=='y')|(csav=='Y')
         t3=['meta ', 'rl',fno];
         eval(t3);
      end
      ans=input(' enter  N  to Exit ','s');
      if (ans=='N')|( ans=='n')
         an=0;
      end
      clear mz ms;
      clear rps1 rps2 rps3 rps4
      clear rpz1 rpz2 rpz3 rpz4
      clg
      hold off
 end
```

APPENDIX B: PROPAGATION LOSS UNDER THE INFLUENCE OF A 300 M SURFACE-BASED DUCT

This Appendix displays the propagation loss computed by RPO and M-Layer under the influence of a 300 m surface-based duct at 3 GHz and 12 GHz at ranges of 15, 20, 30, 40, 50, 60, 70, 80, 90, 100 and 110 km.

1. Propagation loss at 3 GHz

Figures B.1 through B.11 displays the propagation loss at 3 GHz computed by RPO and M-Layer.

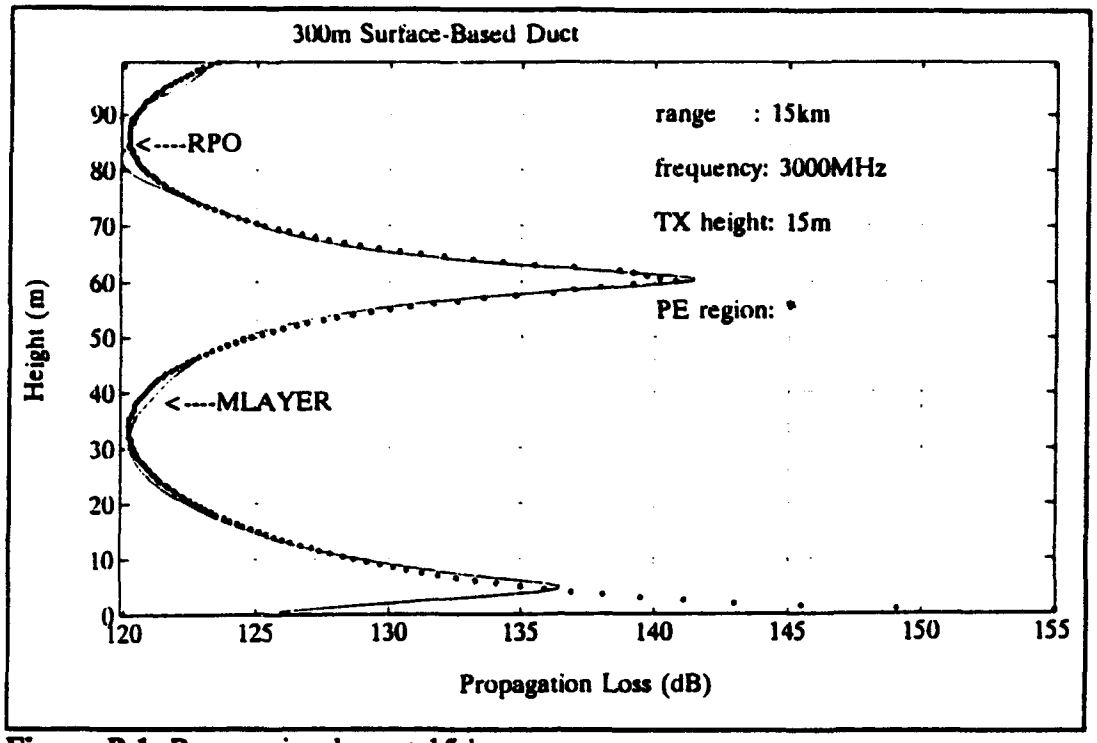

Figure B.1. Propagation loss at 15 km.

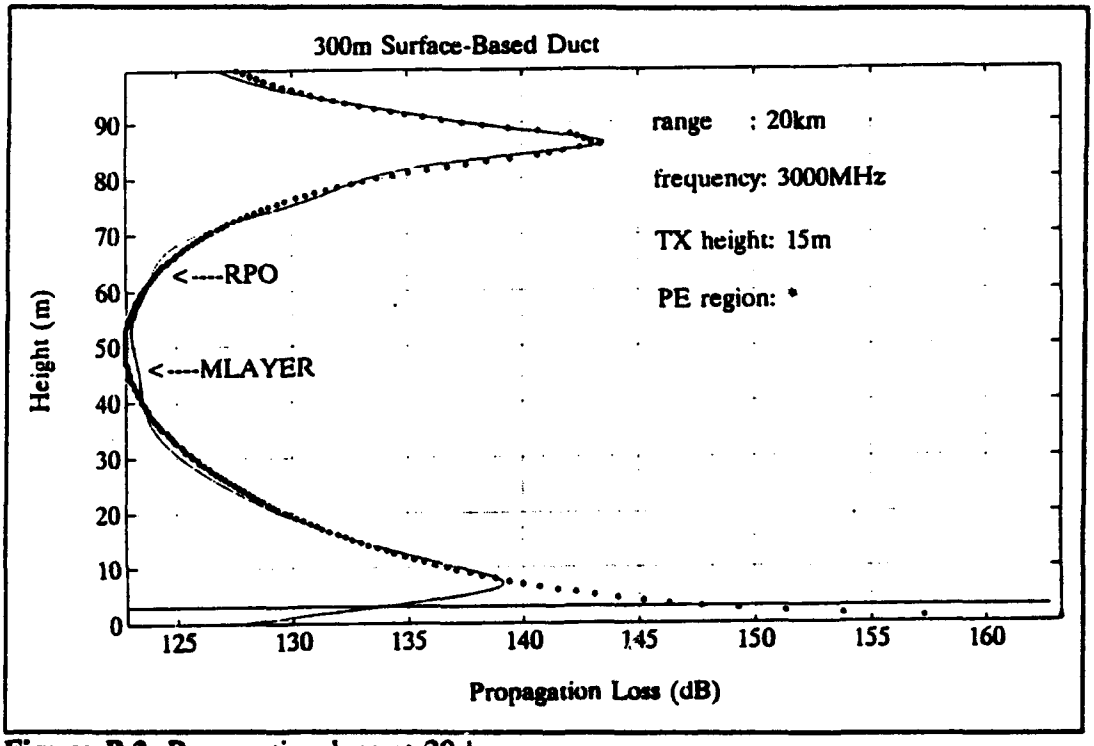

Figure B.2. Propagation loss at 20 km.

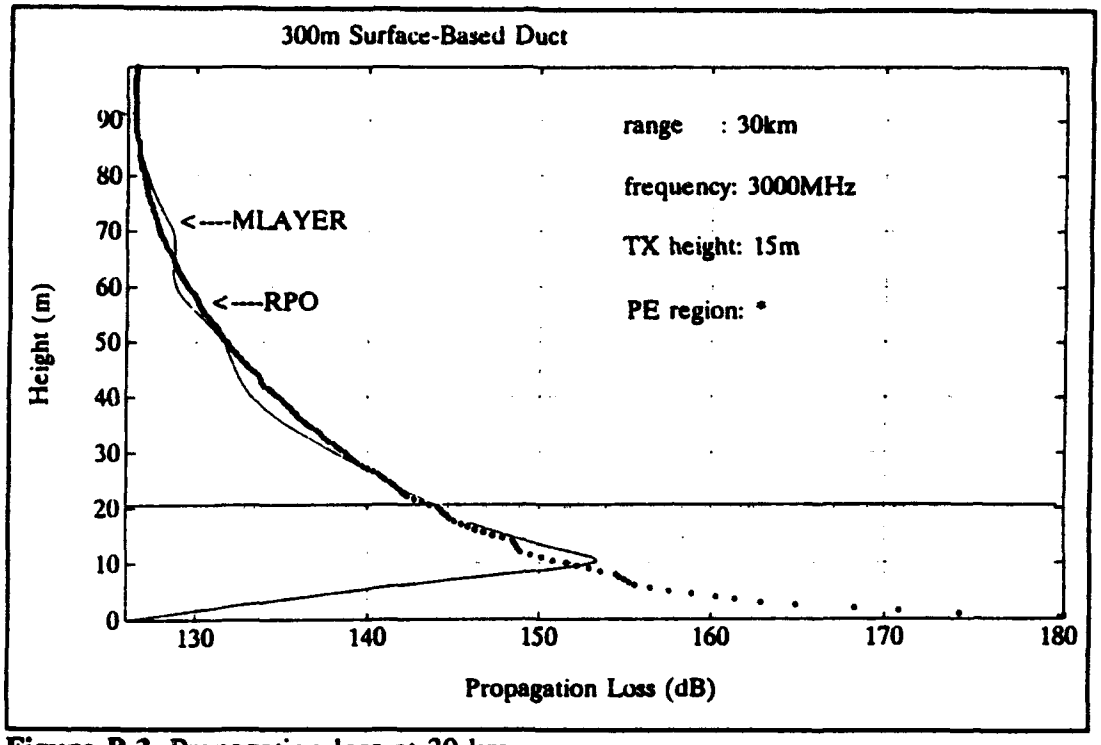

Figure B.3. Propagation loss at 30 km.

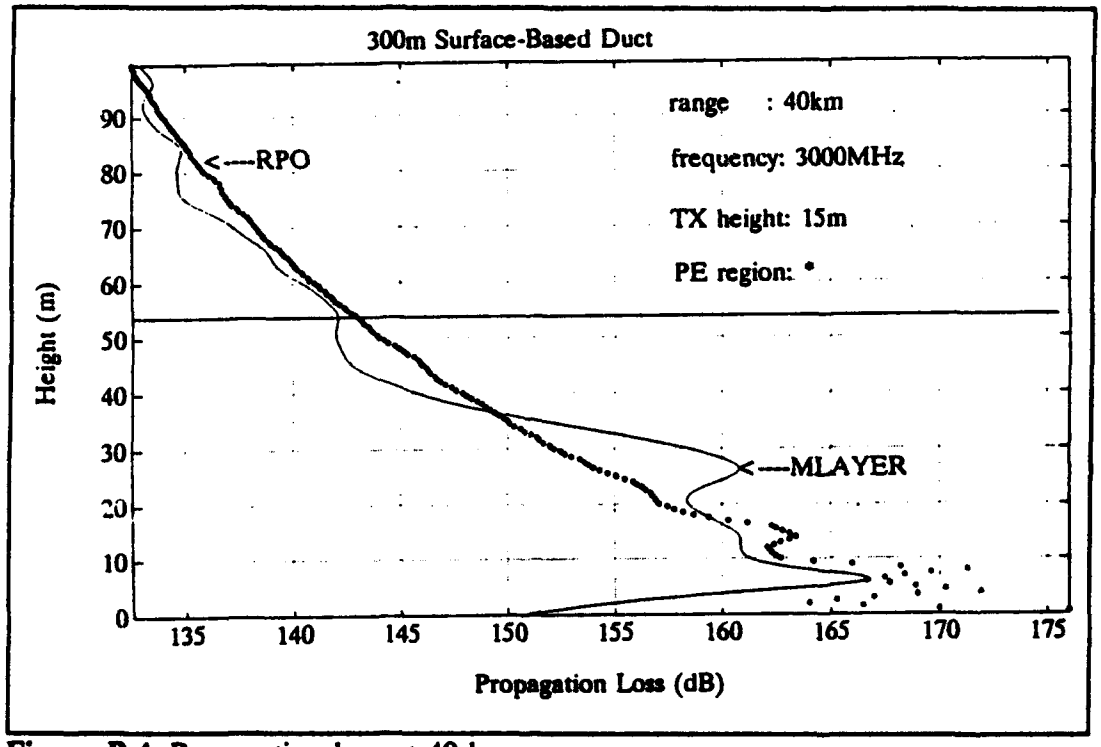

Figure B.4. Propagation loss at 40 km.

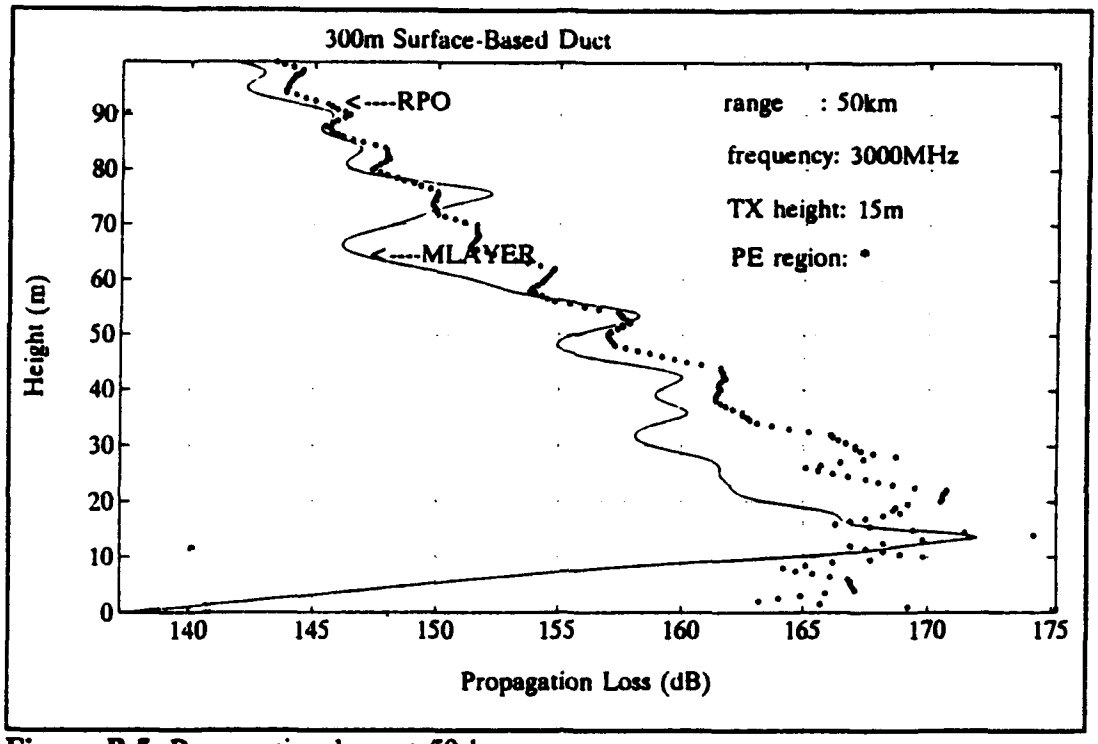

Figure B.5. Propagation loss at 50 km.

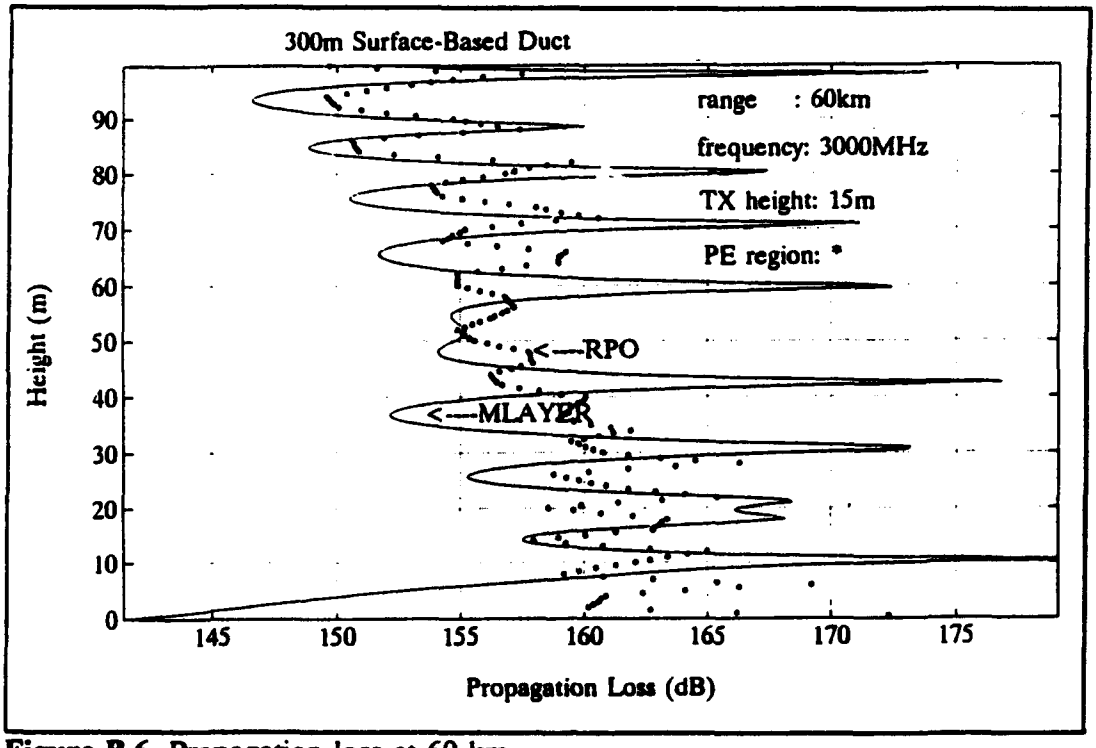

Figure B.6. Propagation loss at 60 km.

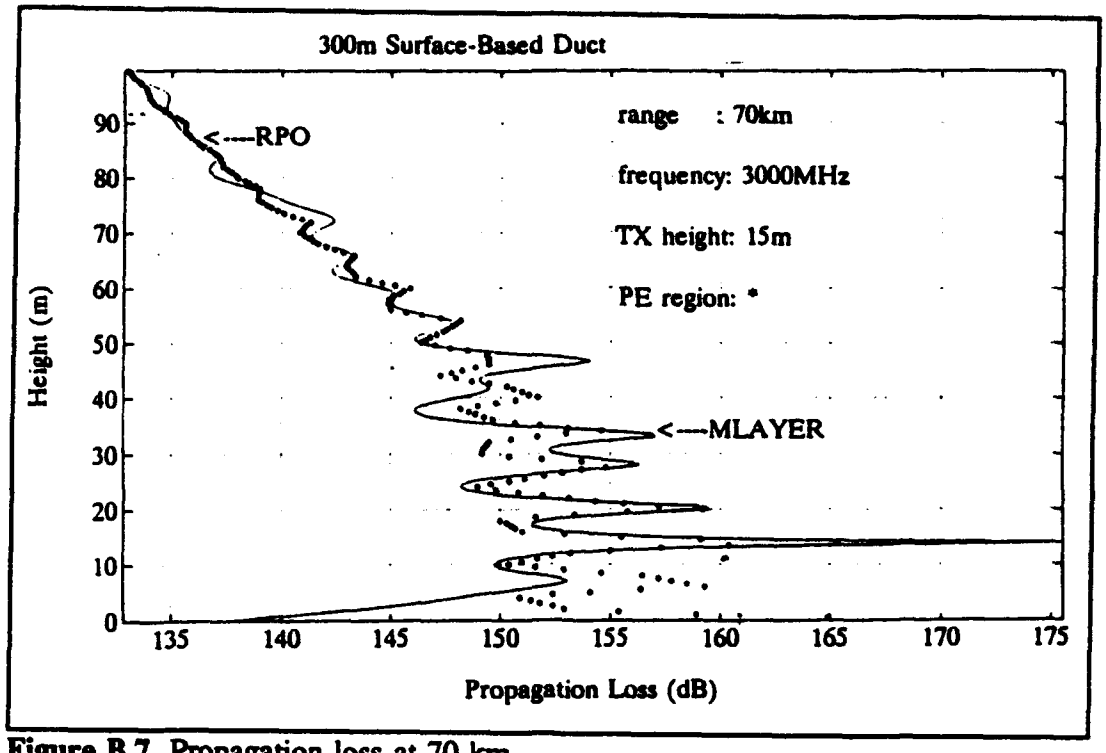

Figure B.7. Propagation loss at 70 km.

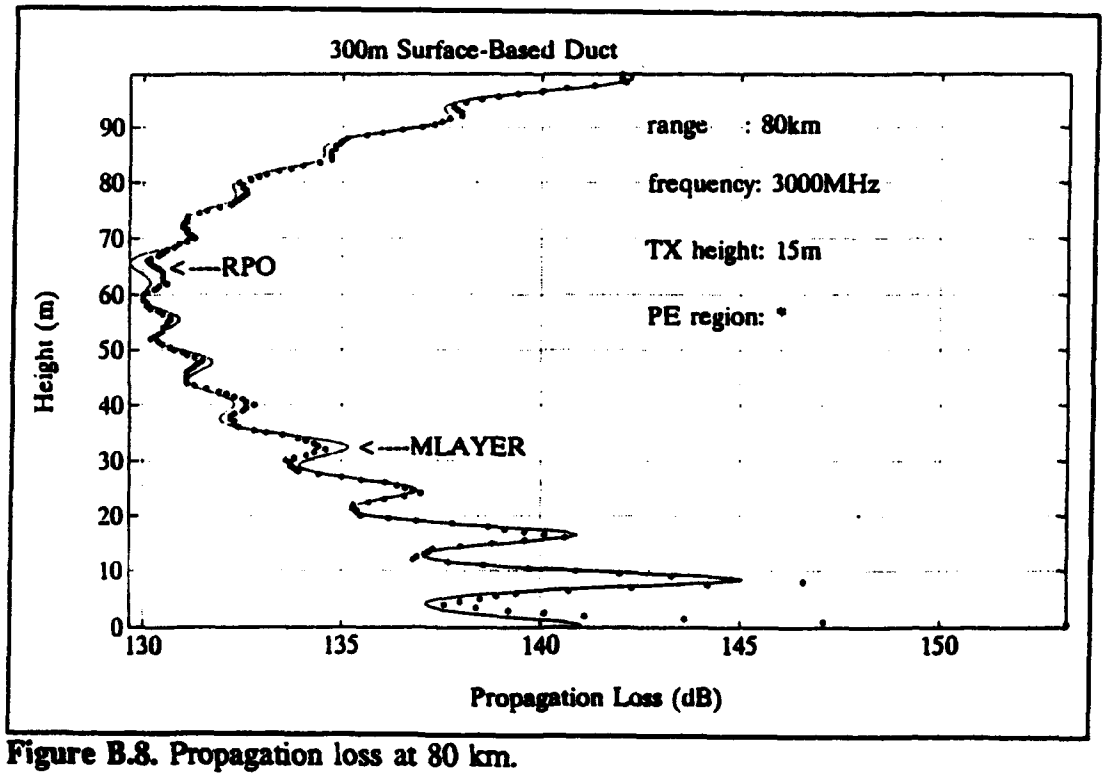

Figure B.8. Propagation loss at 80 km.

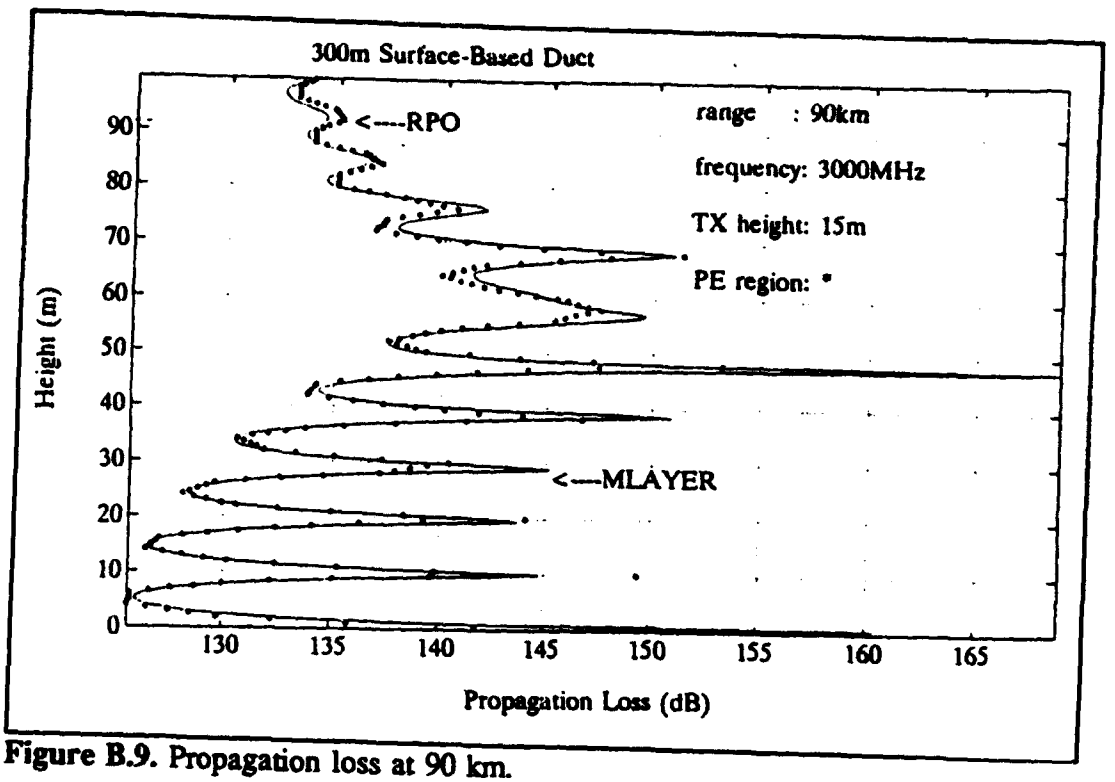

Figure B.9. Propagation loss at 90 km.

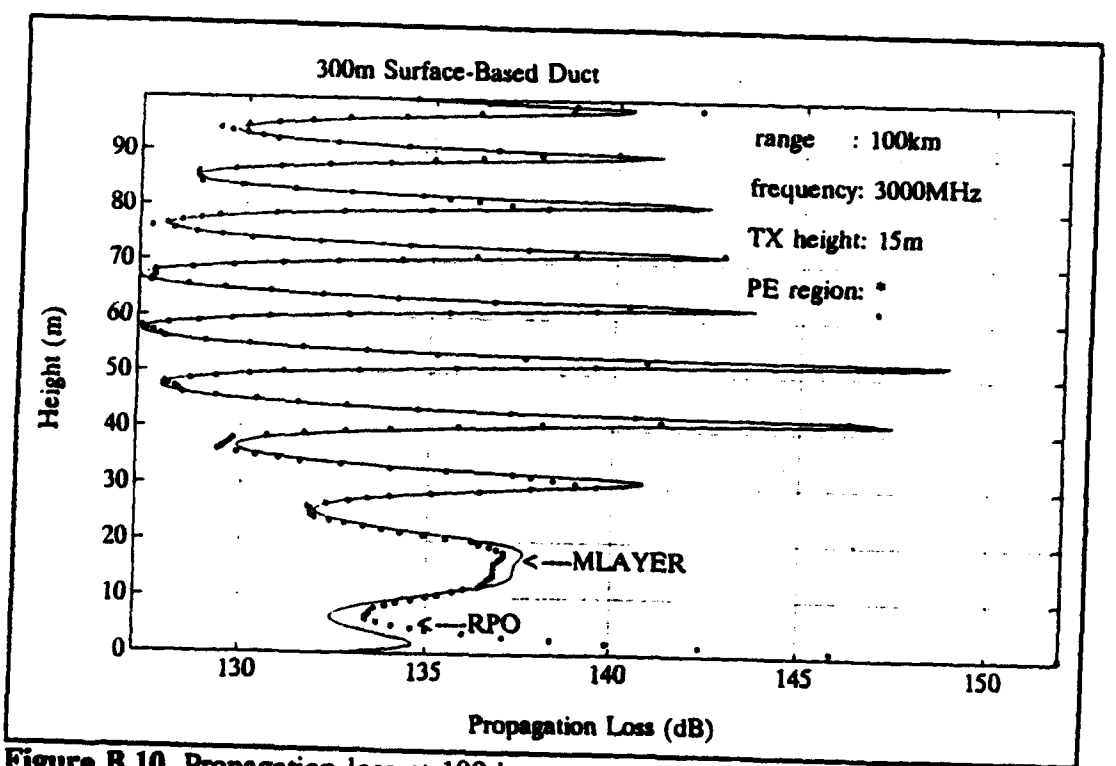

Figure B.10. Propagation loss at 100 km.

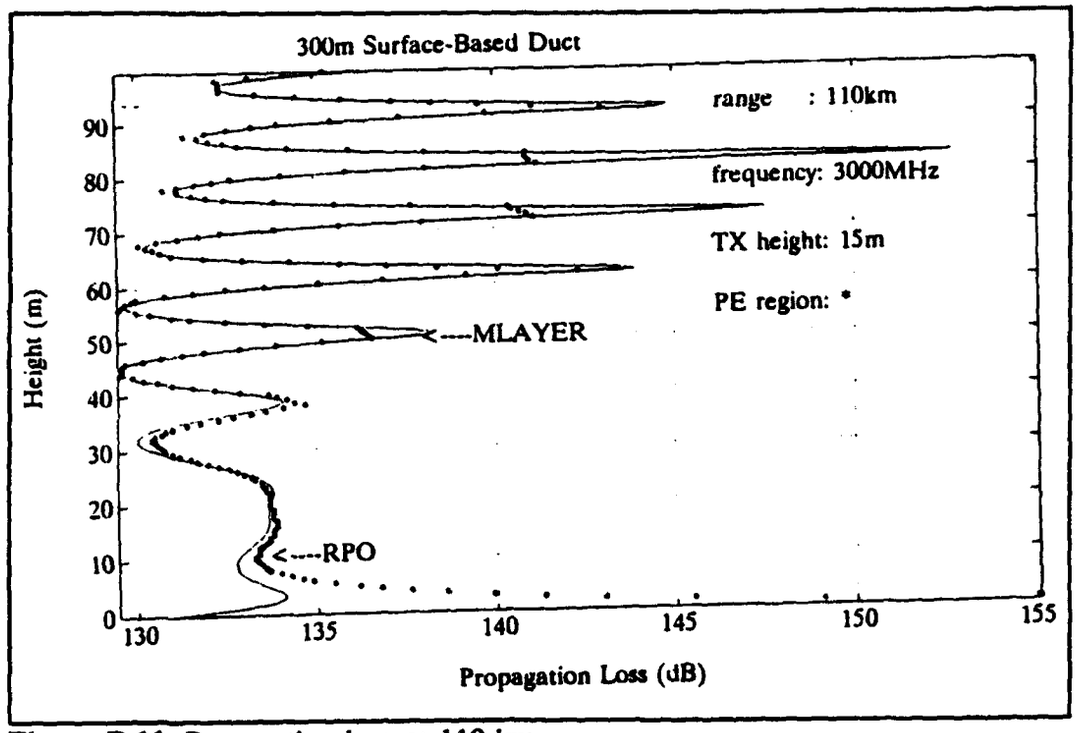

Figure B.11. Propagation loss at 110 km.

2. Propagation loss at 12 GHz

Figures B.12 through B.22 displays the propagation loss at 12 GHz computed by RPO and M-Layer.

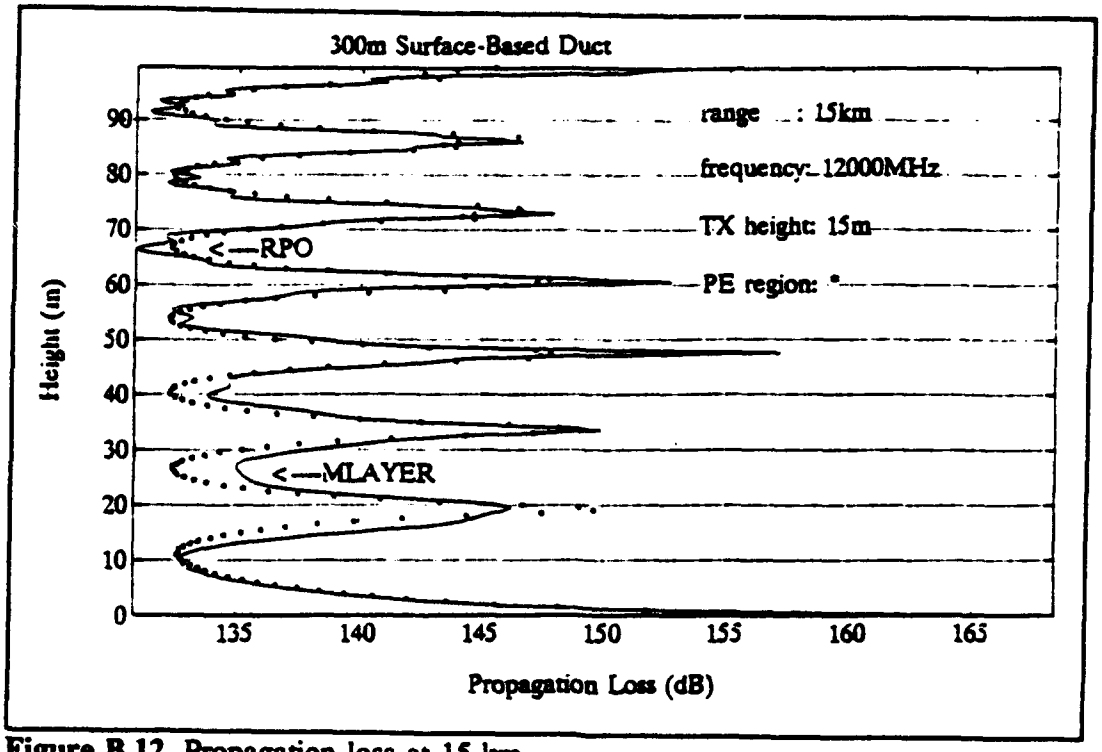

Figure B.12. Propagation loss at 15 km.

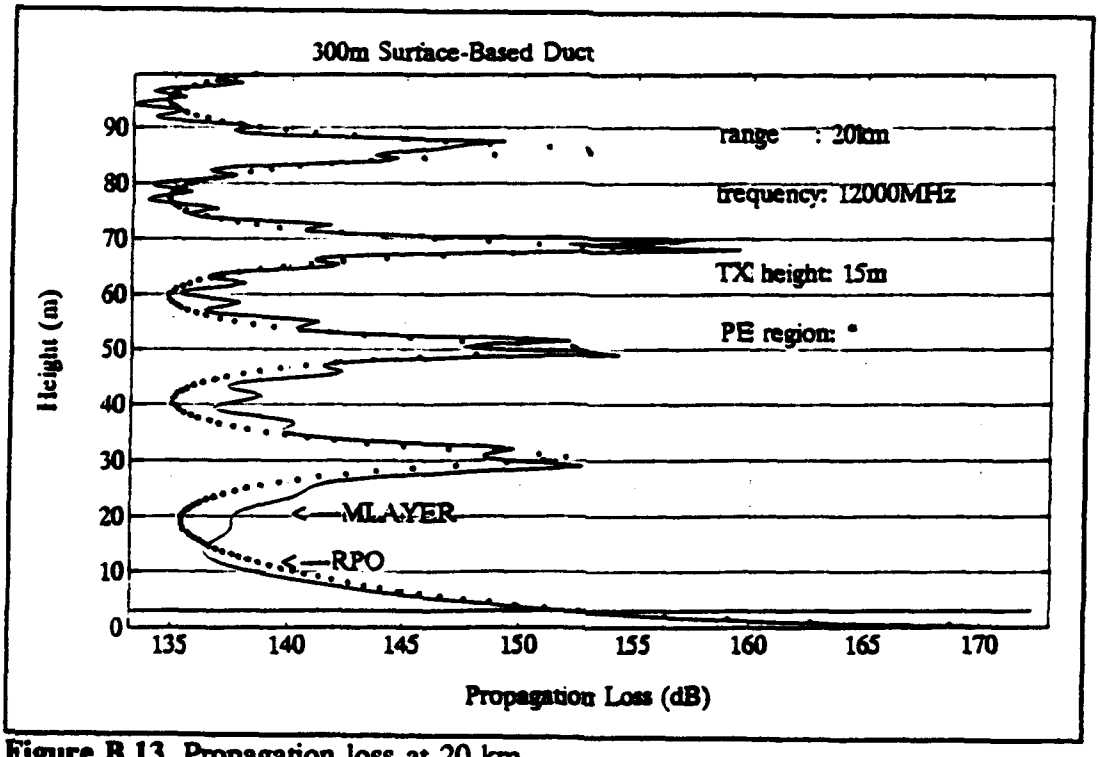

Figure B.13. Propagation loss at 20 km.

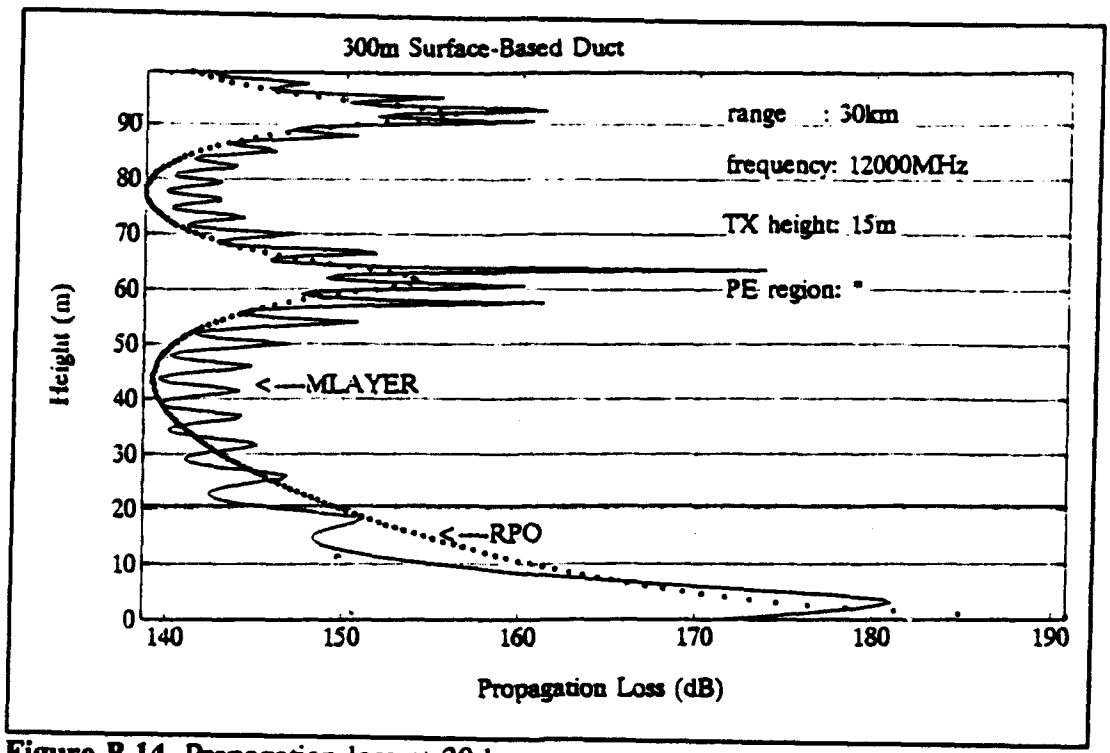

Figure B.14. Propagation loss at 30 km.

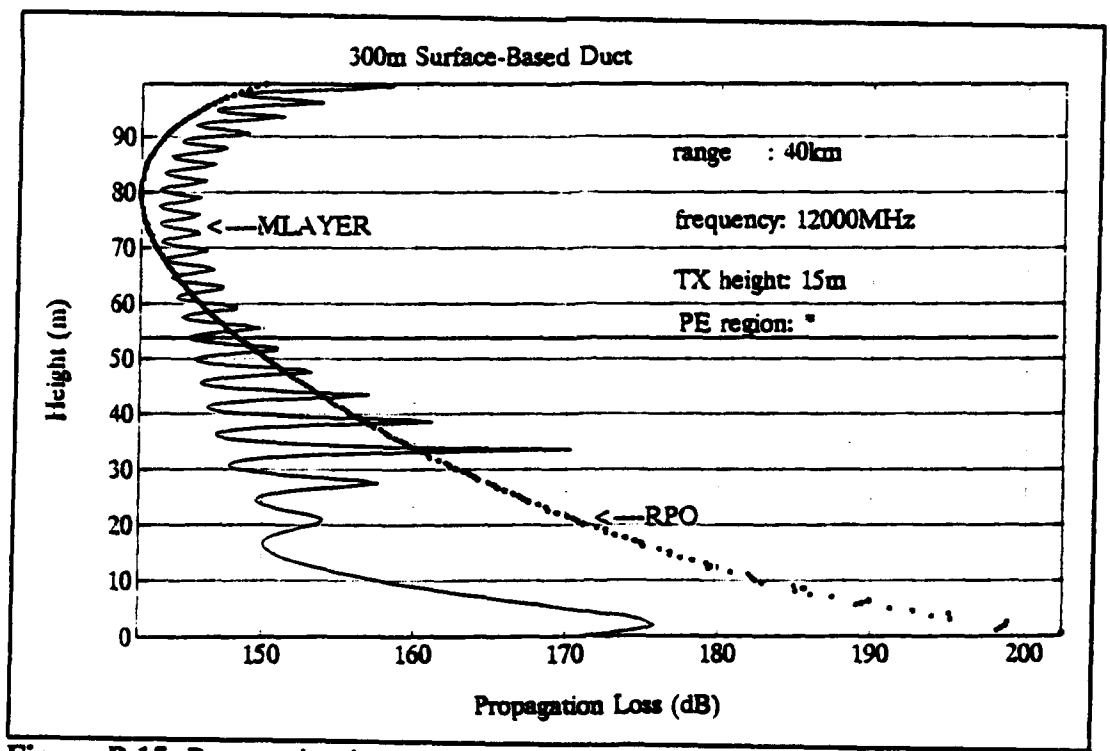

Figure B.15. Propagation loss at 40 km.

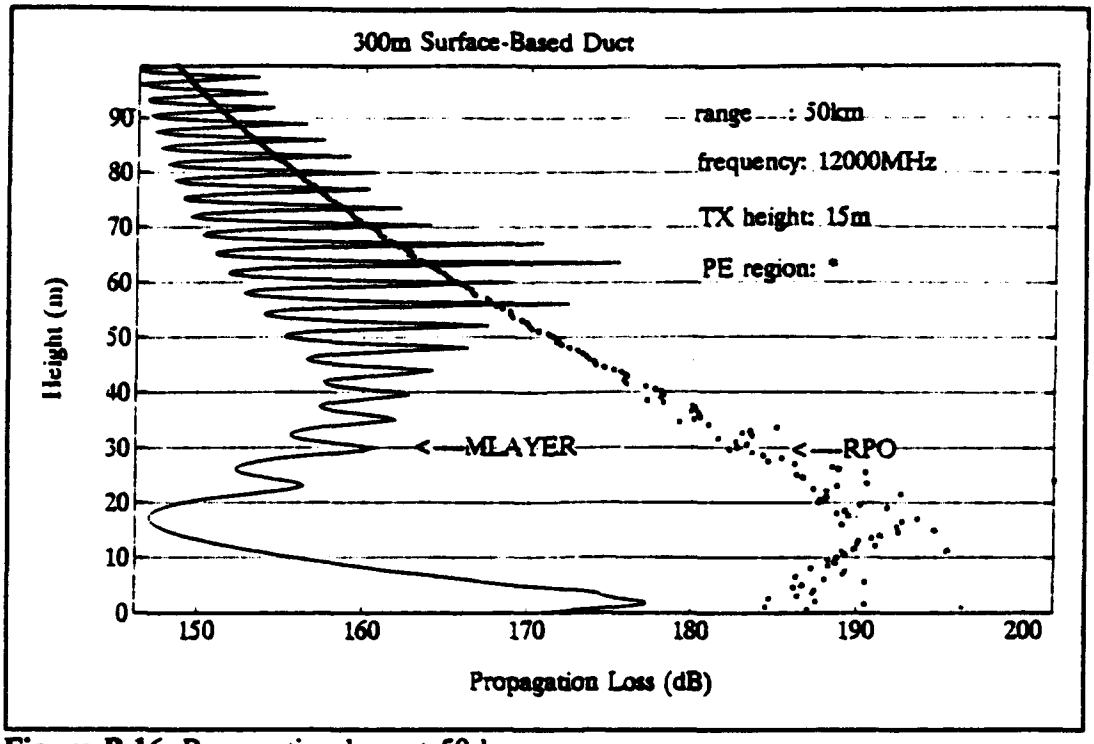

Figure B.16. Propagation loss at 50 km.

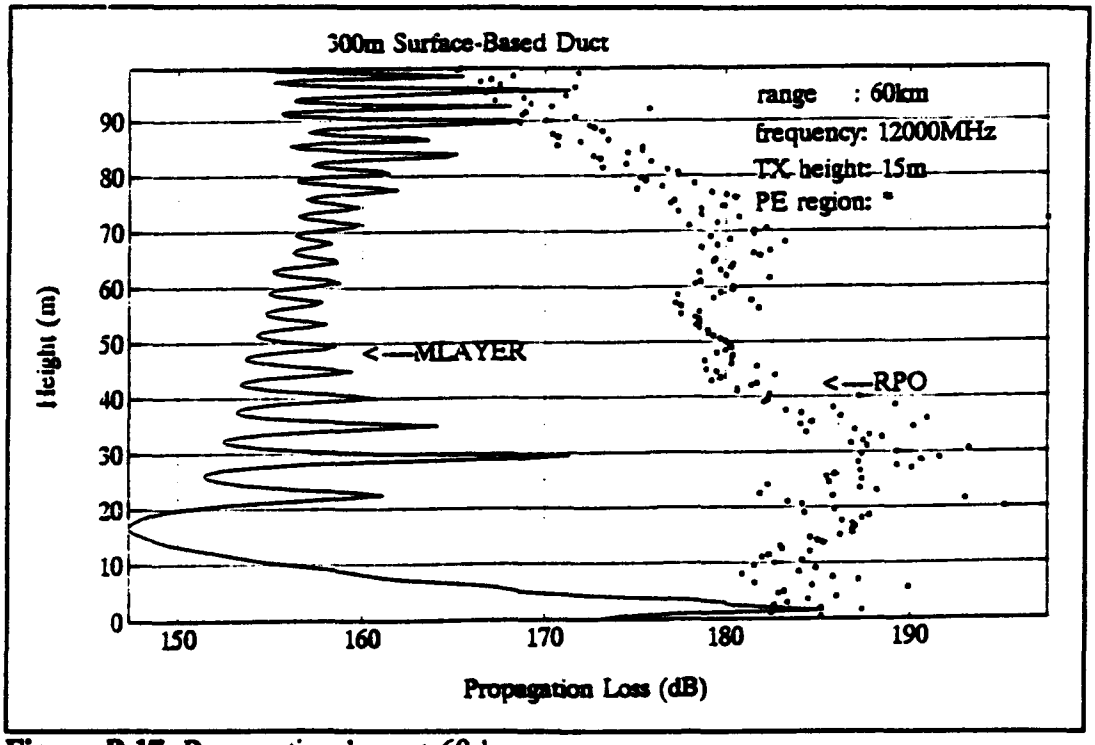

Figure B.17. Propagation loss at 60 km.

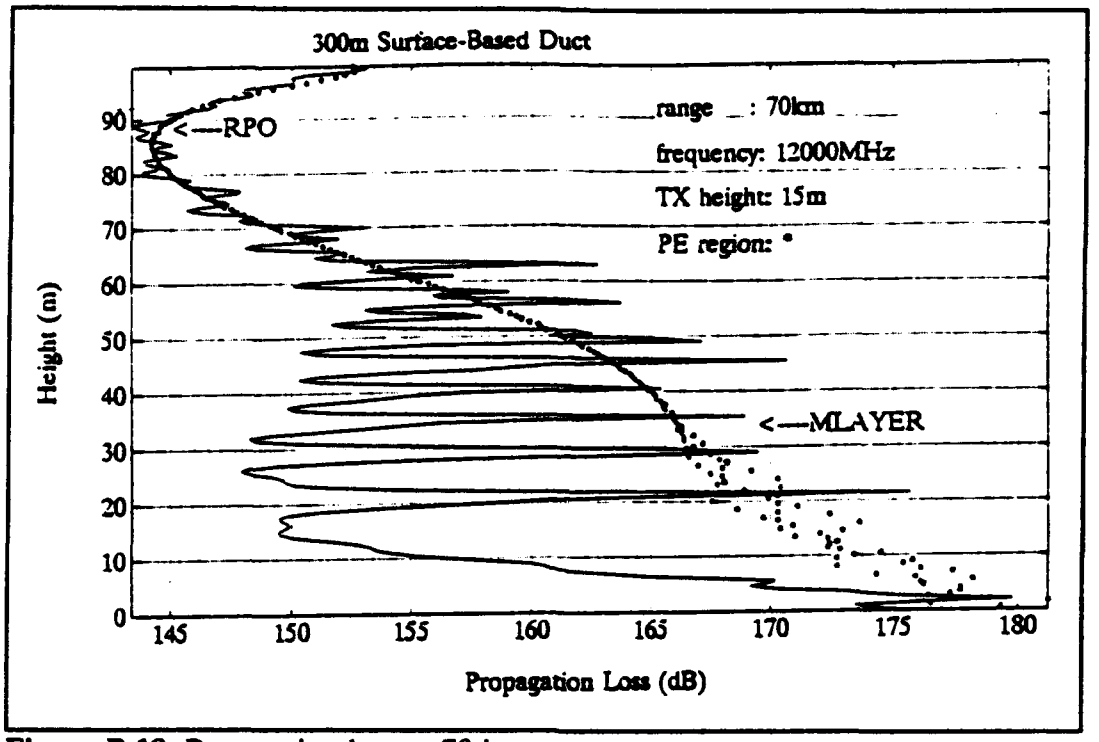

Figure B.18. Propagation loss at 70 km.

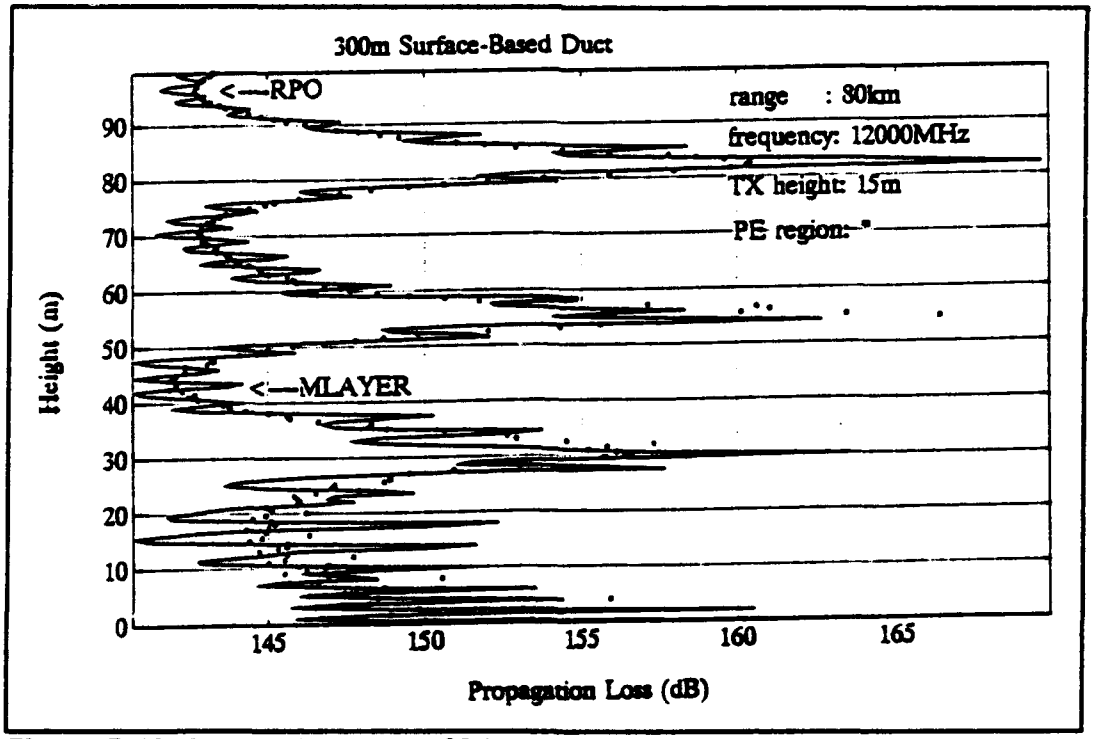

Figure B.19. Propagation loss at 80 km.

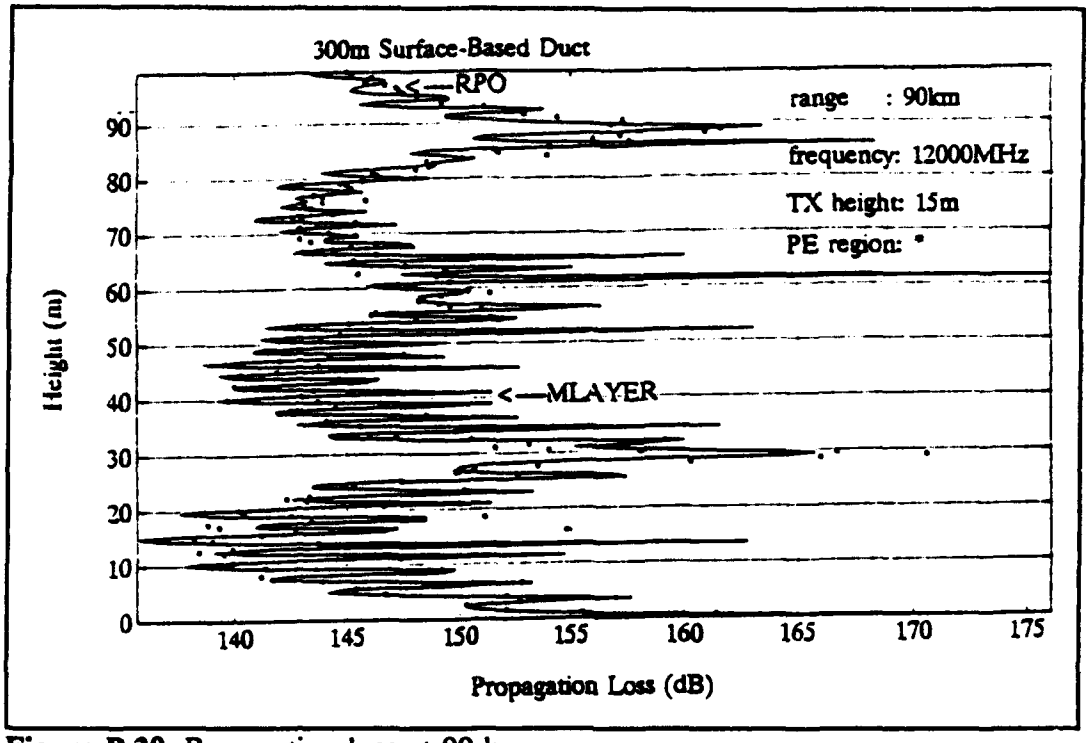

Figure B.20. Propagation loss at 90 km.

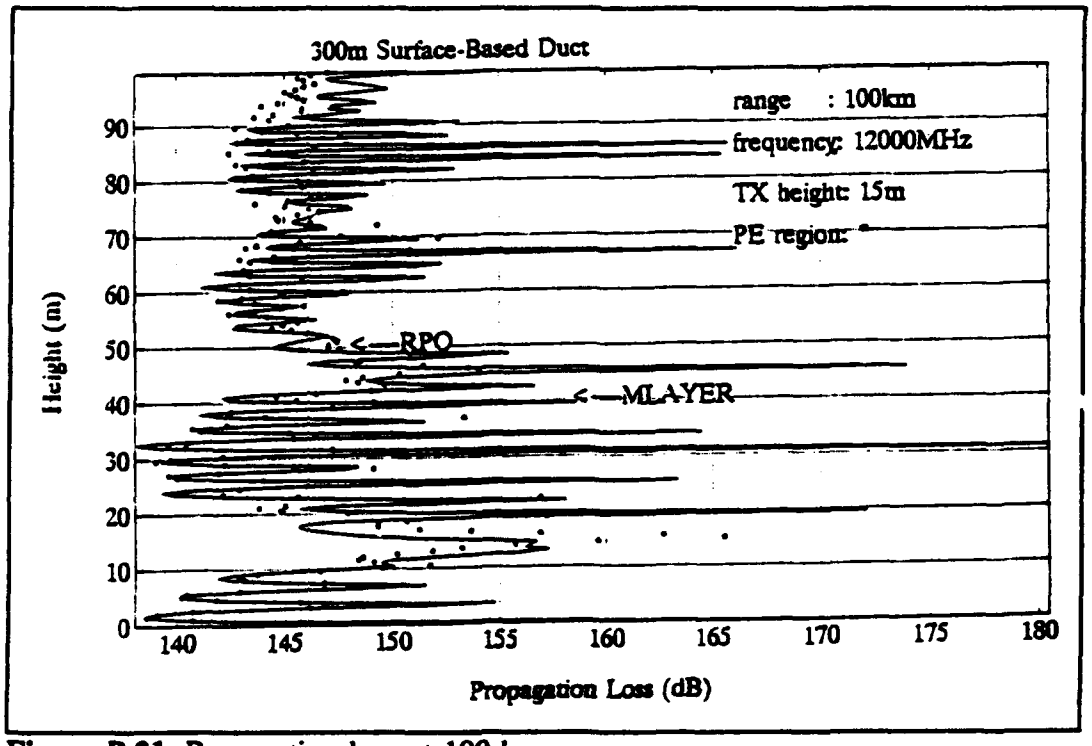

Figure B.21. Propagation loss at 100 km.

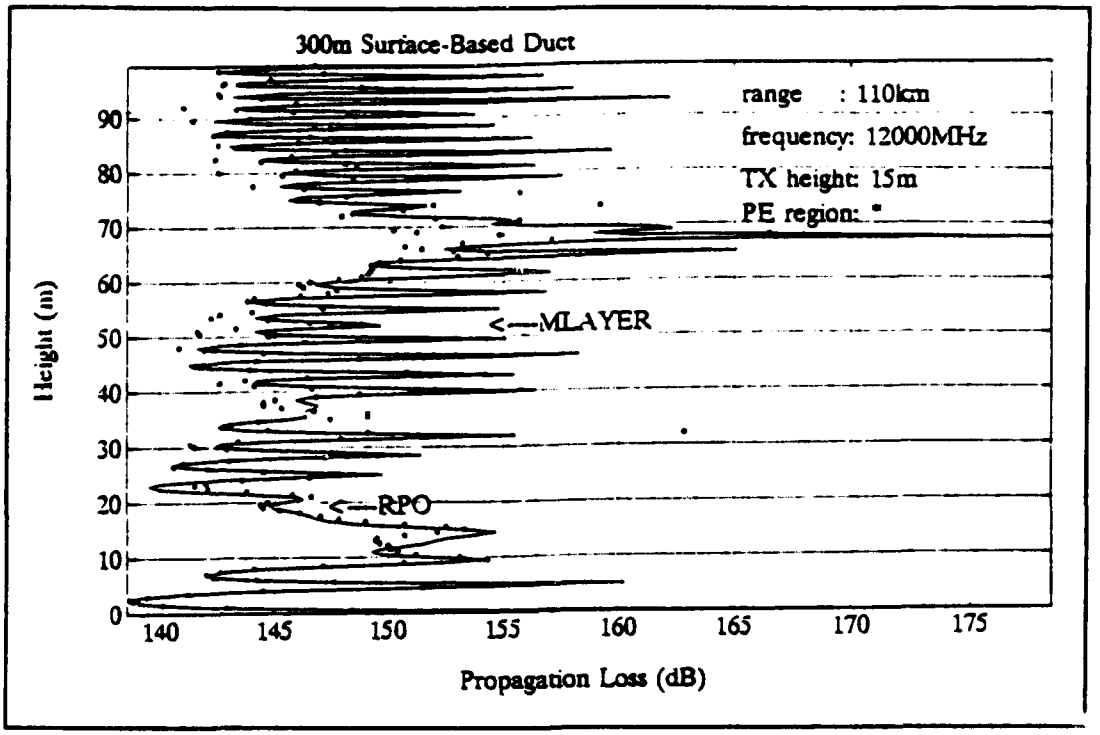

Figure B.22. Propagation loss at 110 km.

APPENDIX C: PROPAGATION LOSS UNDER THE INFLUENCE OF A 14 M EVAPORATION DUCT

This Appendix displays the propagation loss computed by RPO and M-Layer under the influence of a 14 m evaporation duct at 3 GHz and 12 GHz at ranges of 15, 20, 30, 40, 50, 60, 70, 80, 90, 100 and 110 km.

1. Propagation loss at 3 GHz

Figures C.1 through C.11 displays the propagation loss at 3 GHz computed by RPO and M-Layer.

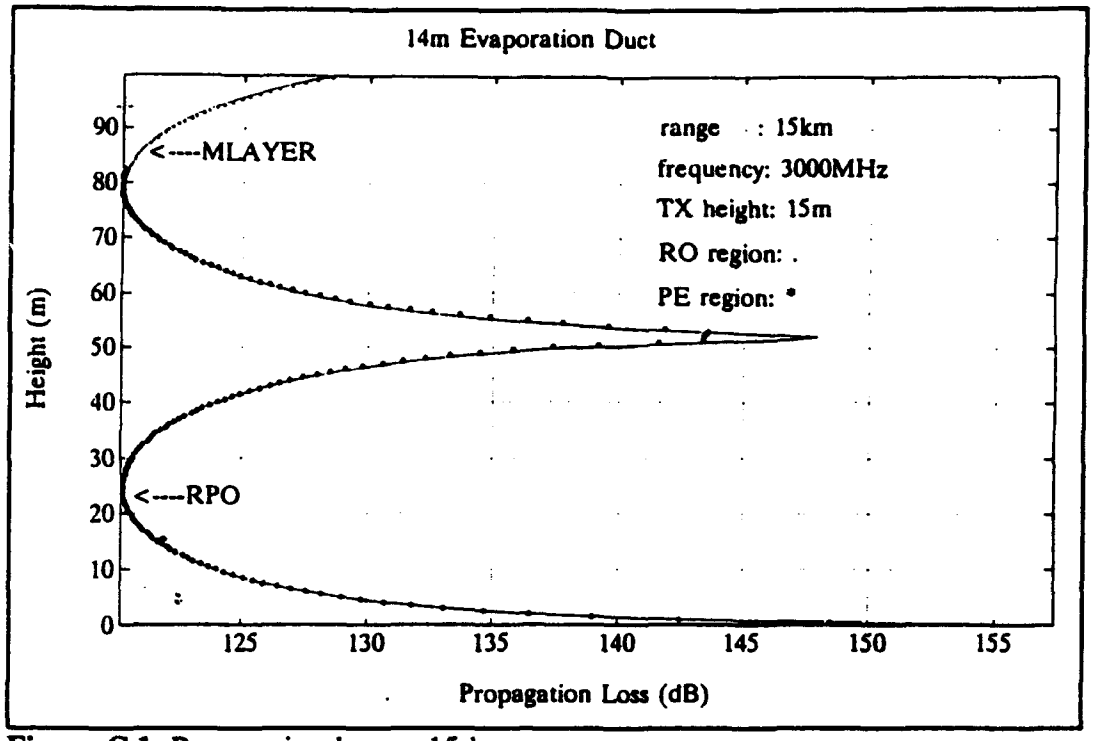

Figure C.1. Propagation loss at 15 km.

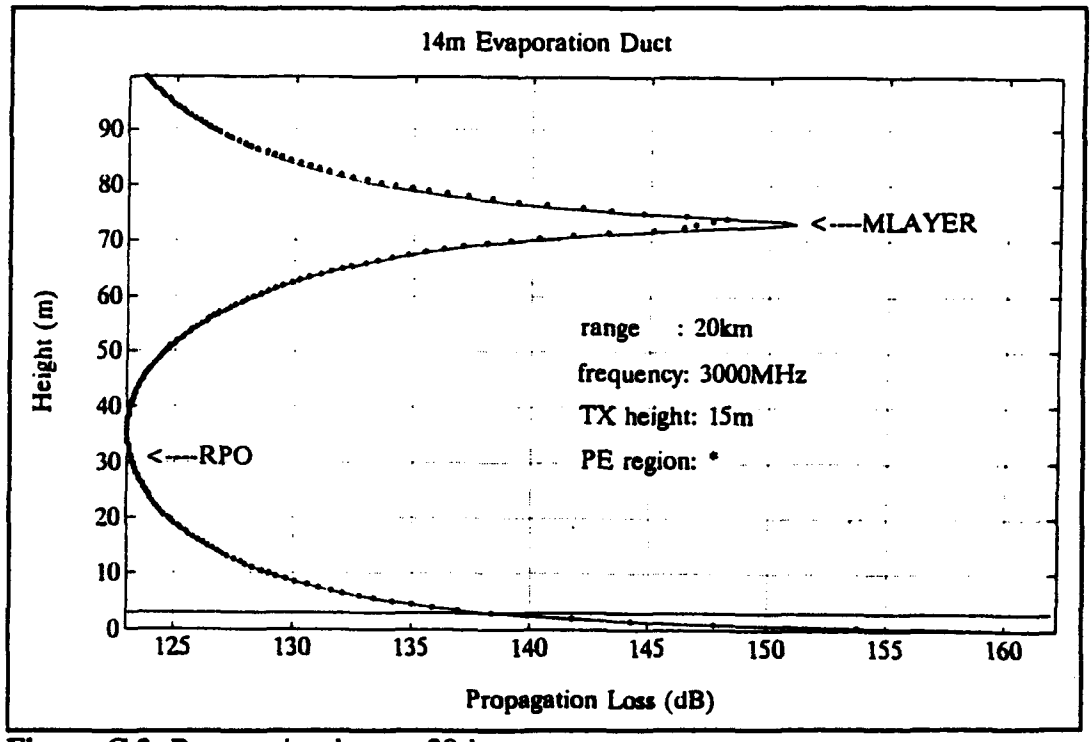

Figure C.2. Propagation loss at 20 km.

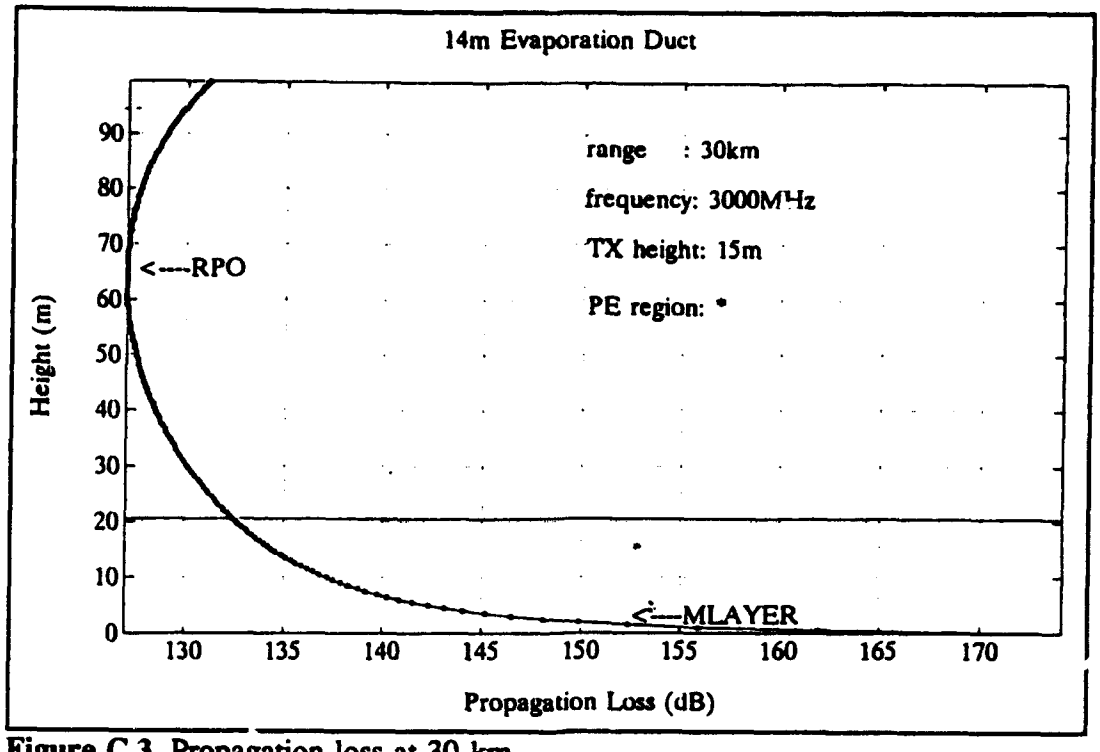

Figure C.3. Propagation loss at 30 km.

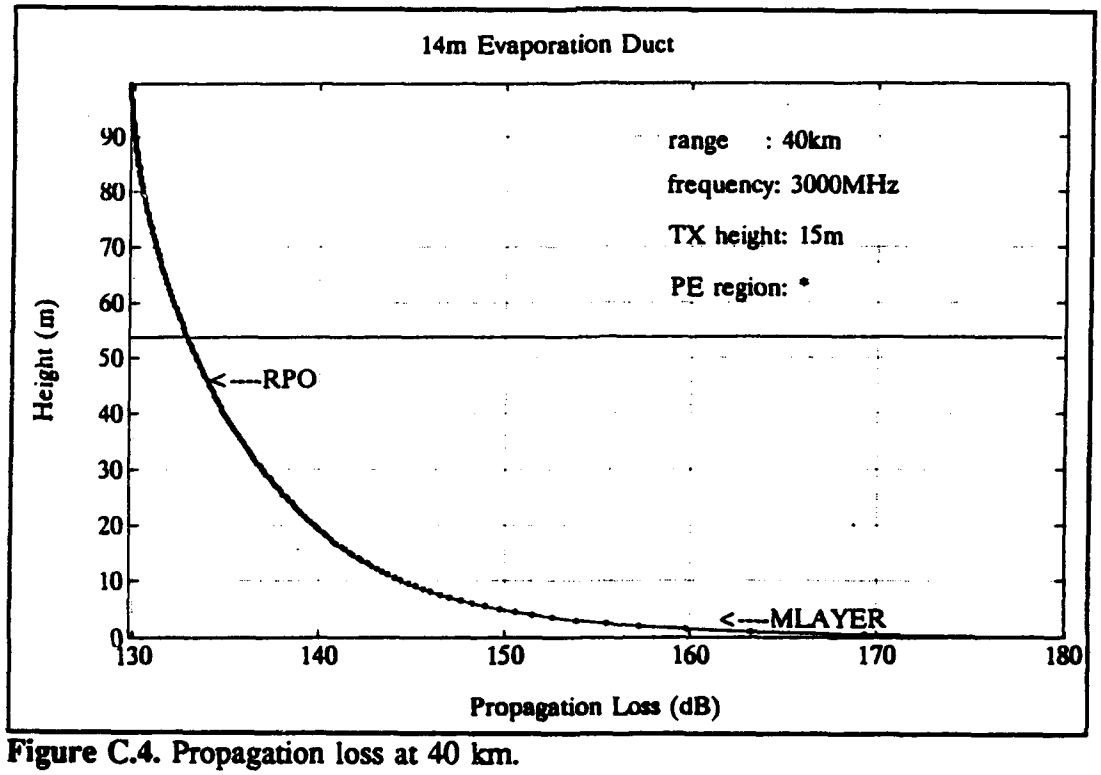

Figure C.4. Propagation loss at 40 km.

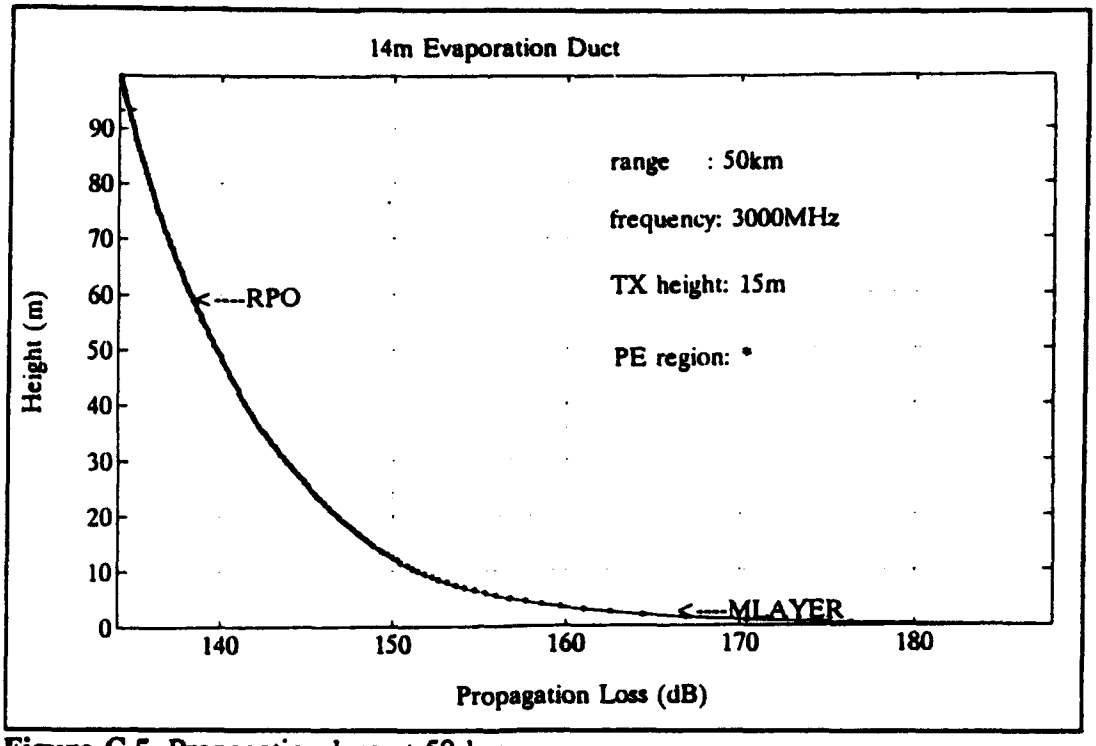

Figure C.5. Propagation loss at 50 km.

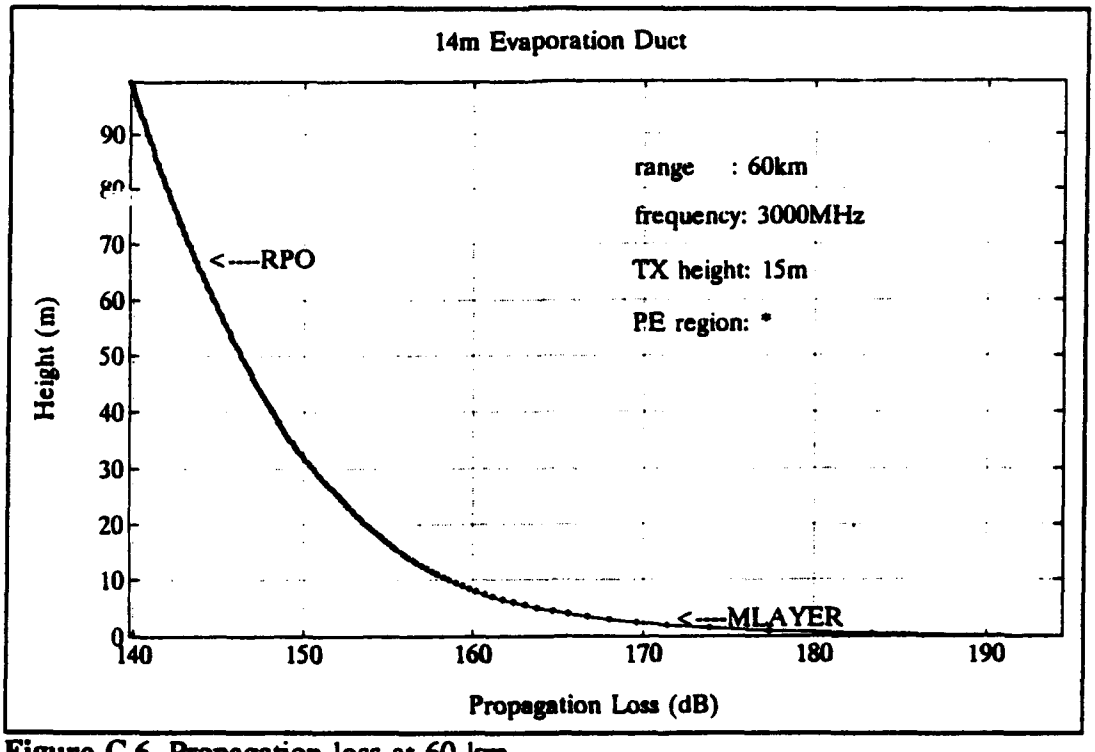

Figure C.6. Propagation loss at 60 km.

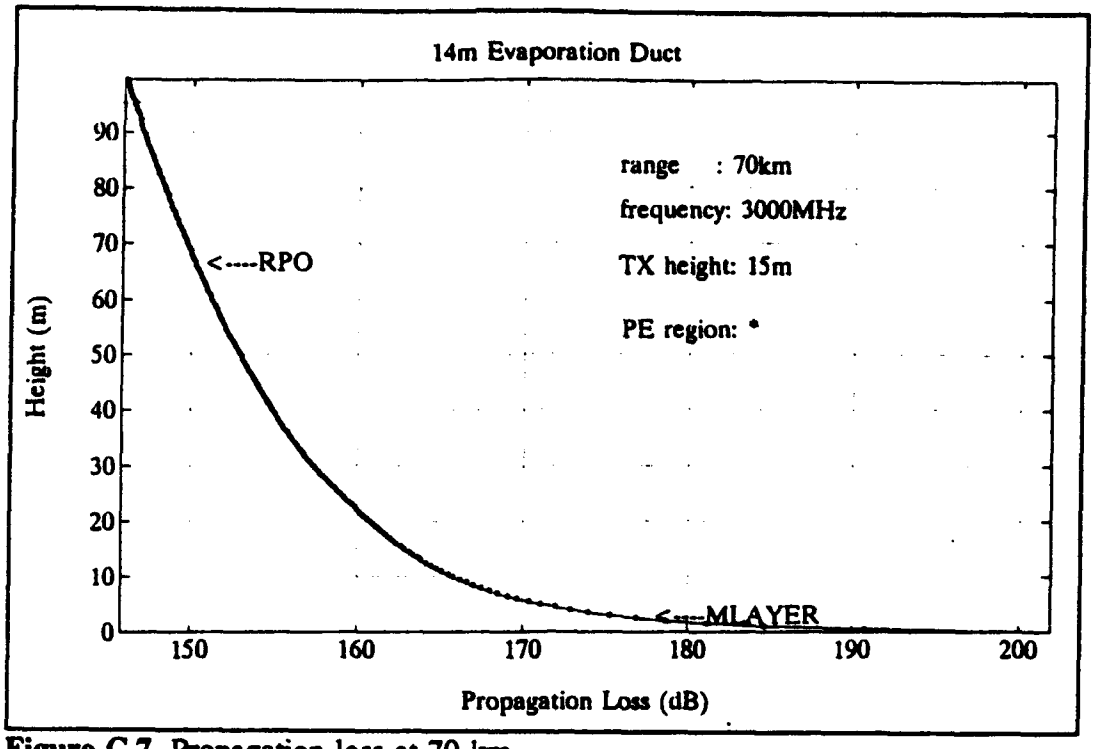

Figure C.7. Propagation loss at 70 km.

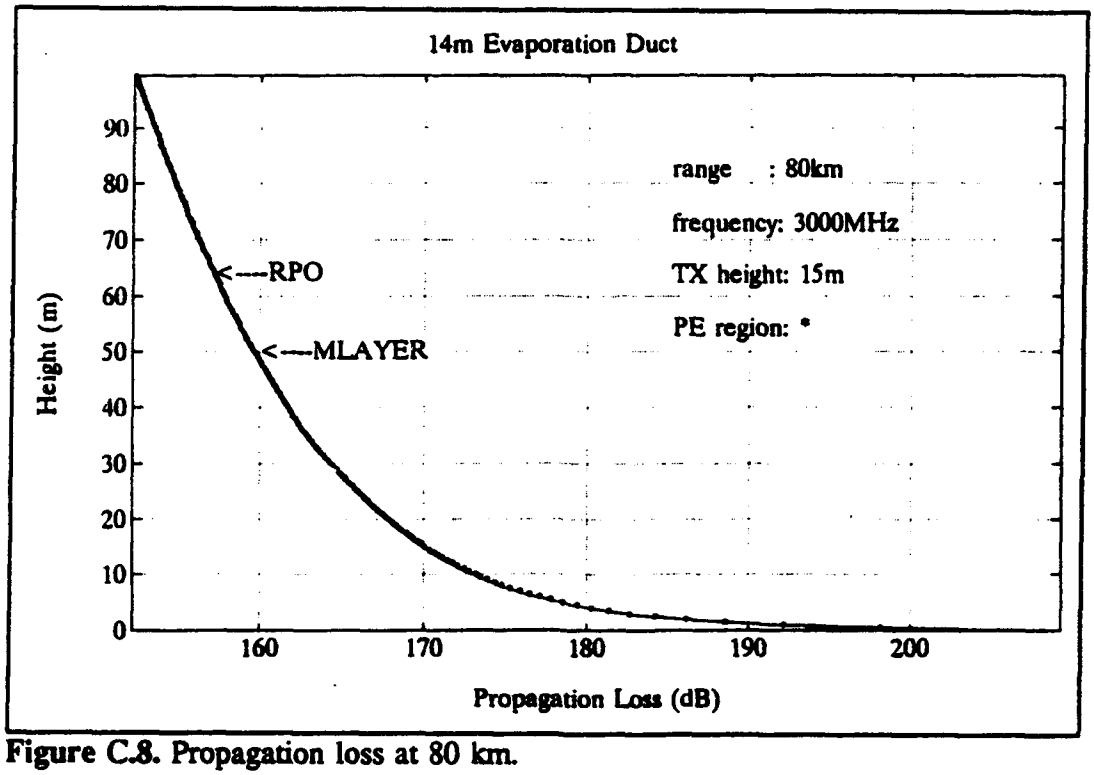

Figure C.8. Propagation loss at 80 km.

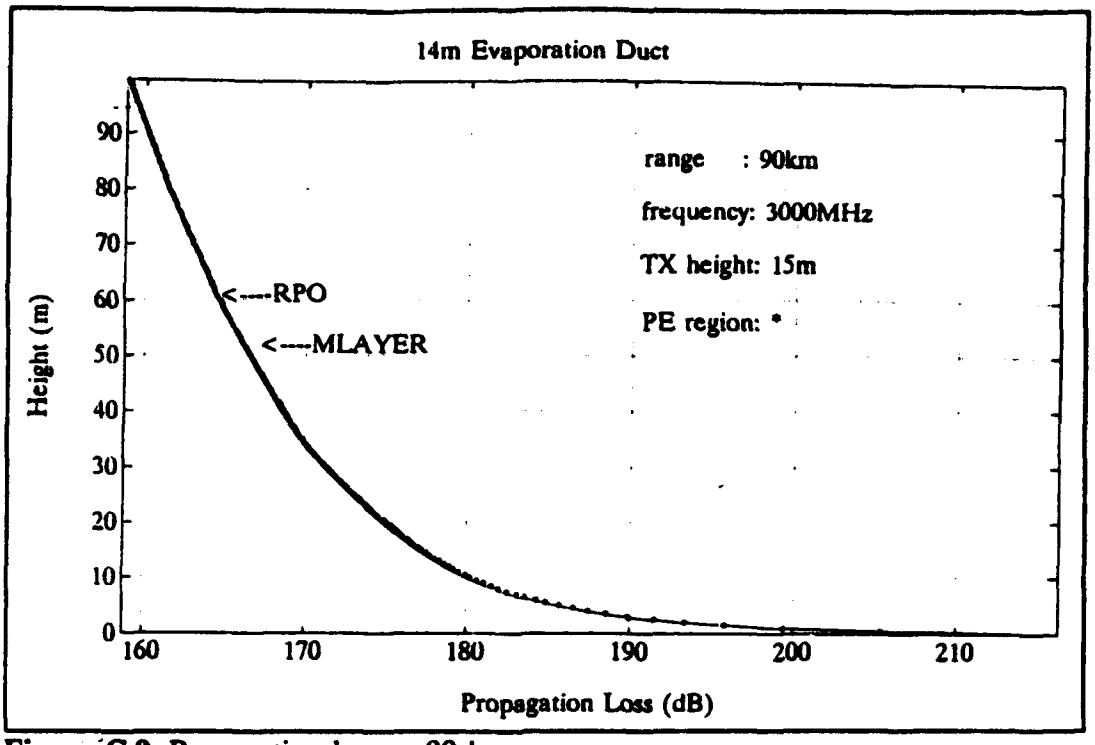

Figure C.9. Propagation loss at 90 km.

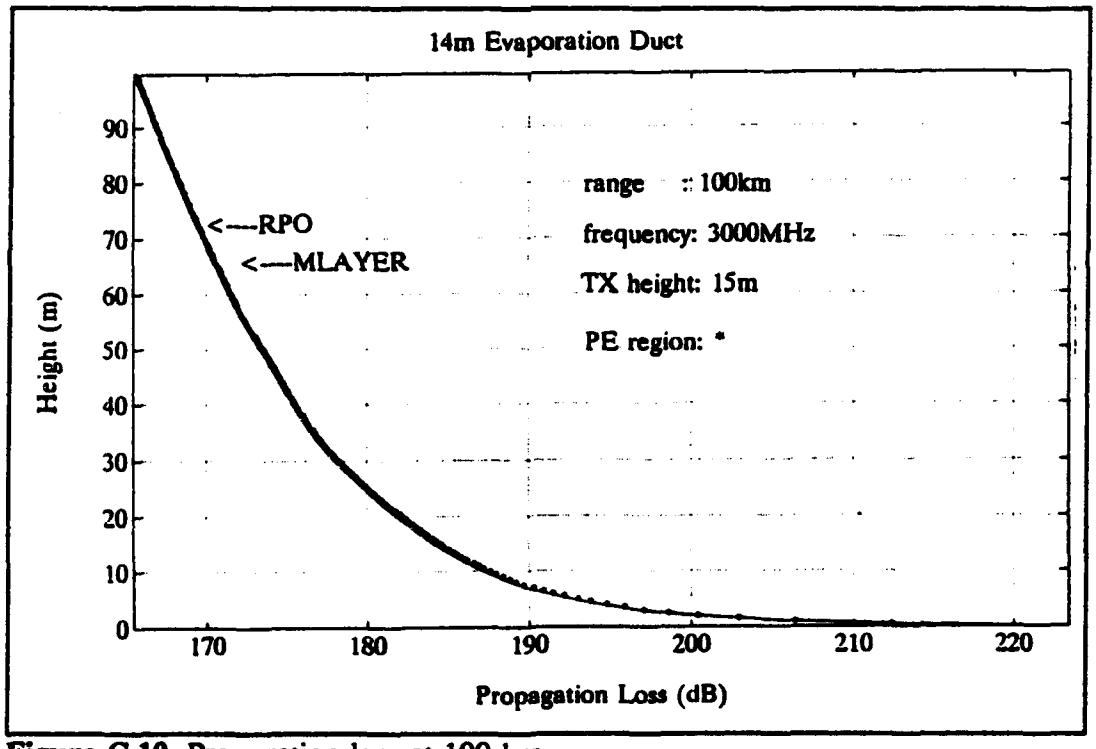

Figure C.10. Propagation loss at 100 km.

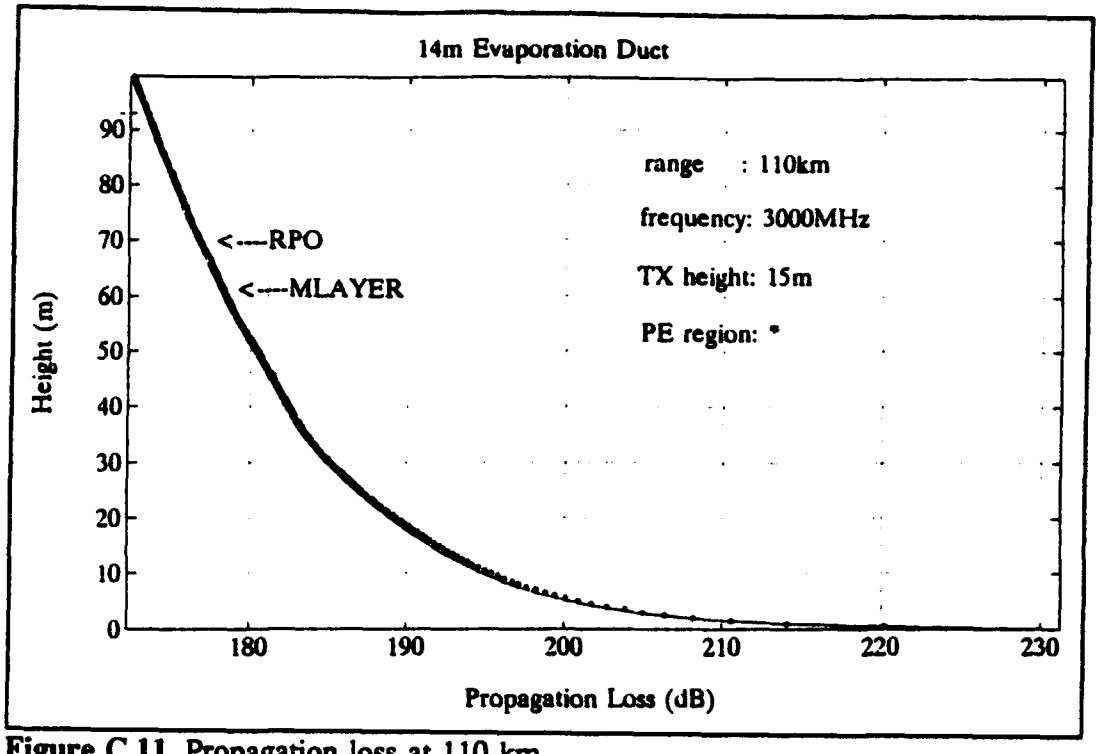

Figure C.11. Propagation loss at 110 km.

2. Propagation loss at 12 GHz

Figures C.12 through C.22 displays the propagation loss at 12 GHz computed by RPO and M-Layer.

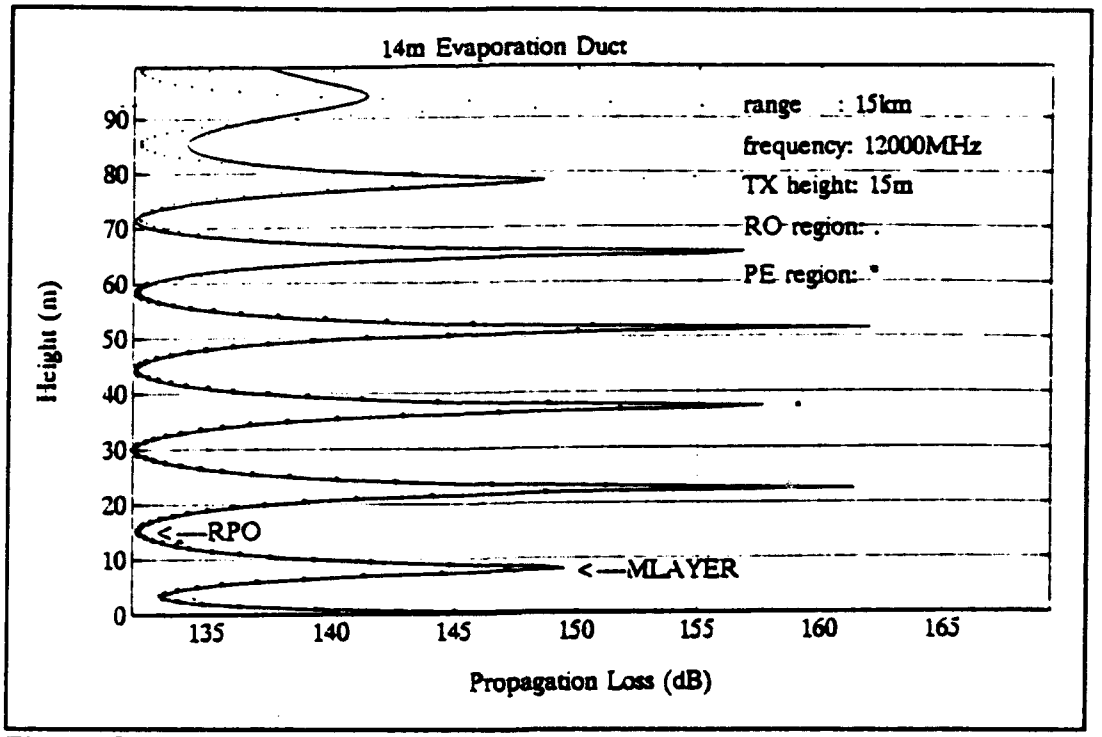

Figure C.12. Propagation loss at 15 km.

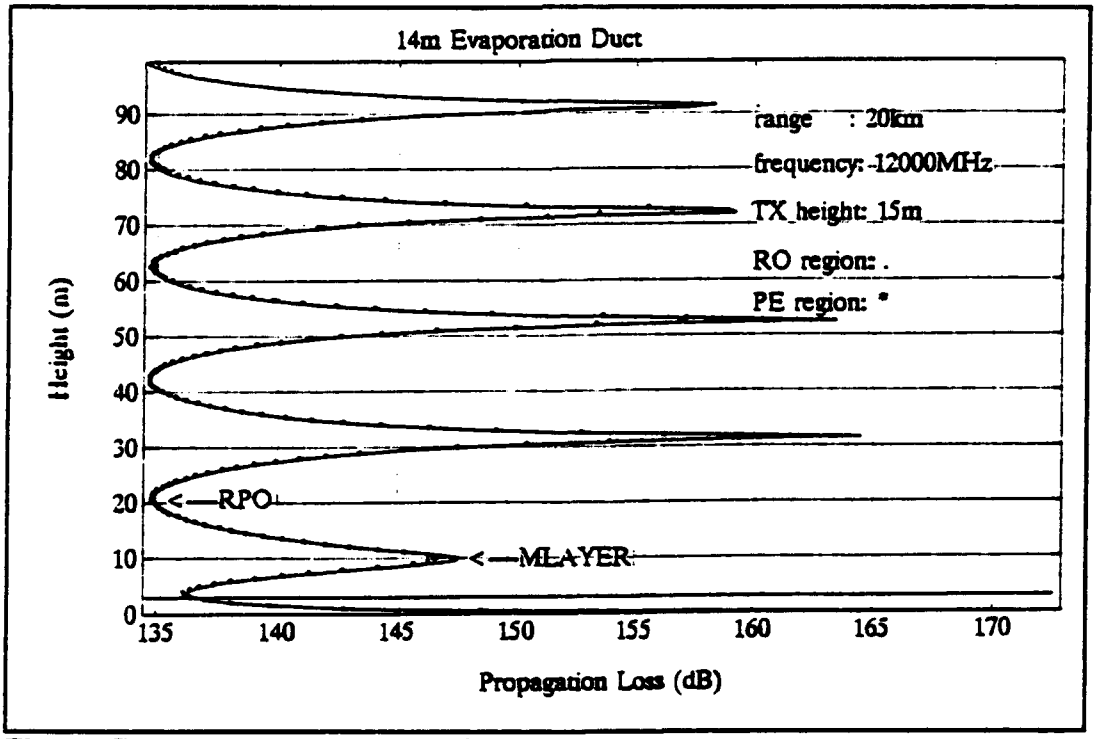

Figure C.13. Propagation loss at 20 km.

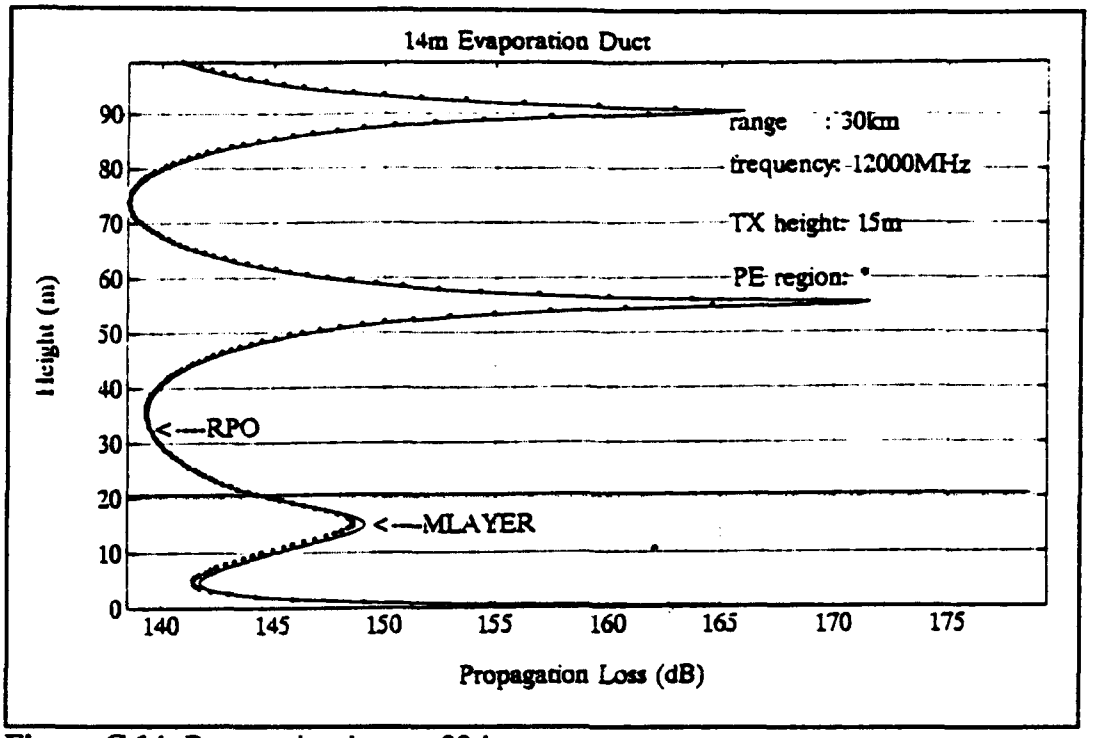

Figure C.14. Propagation loss at 30 km.

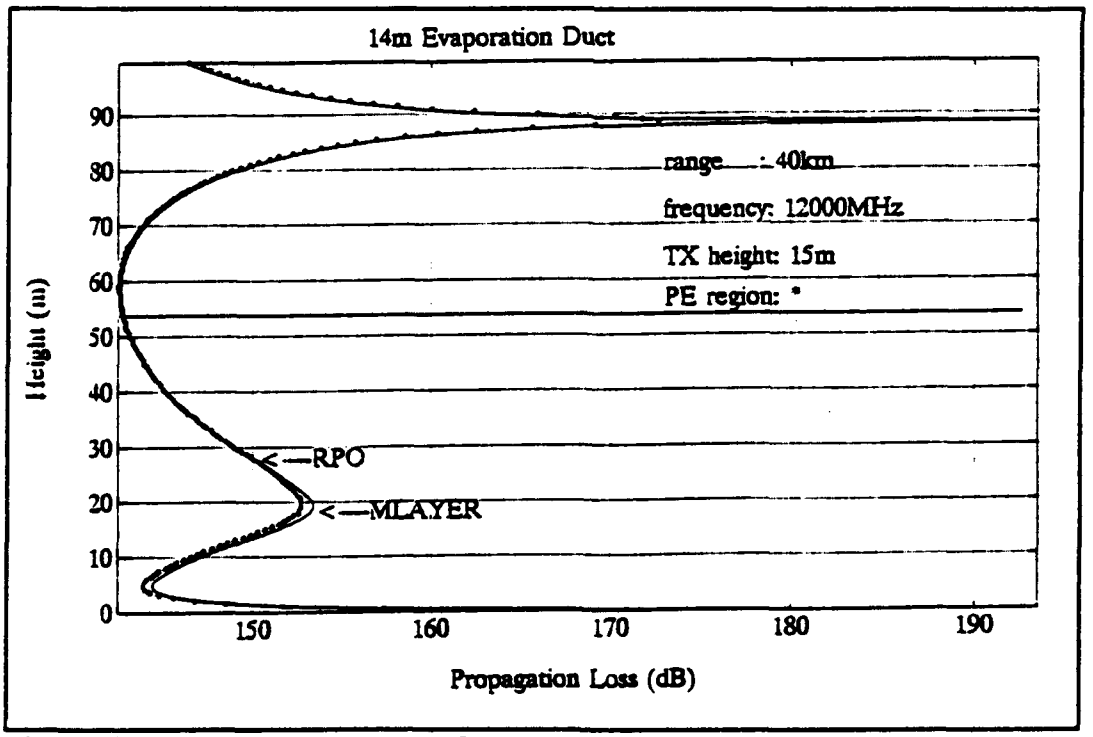

Figure C.15. Propagation loss at 40 km.

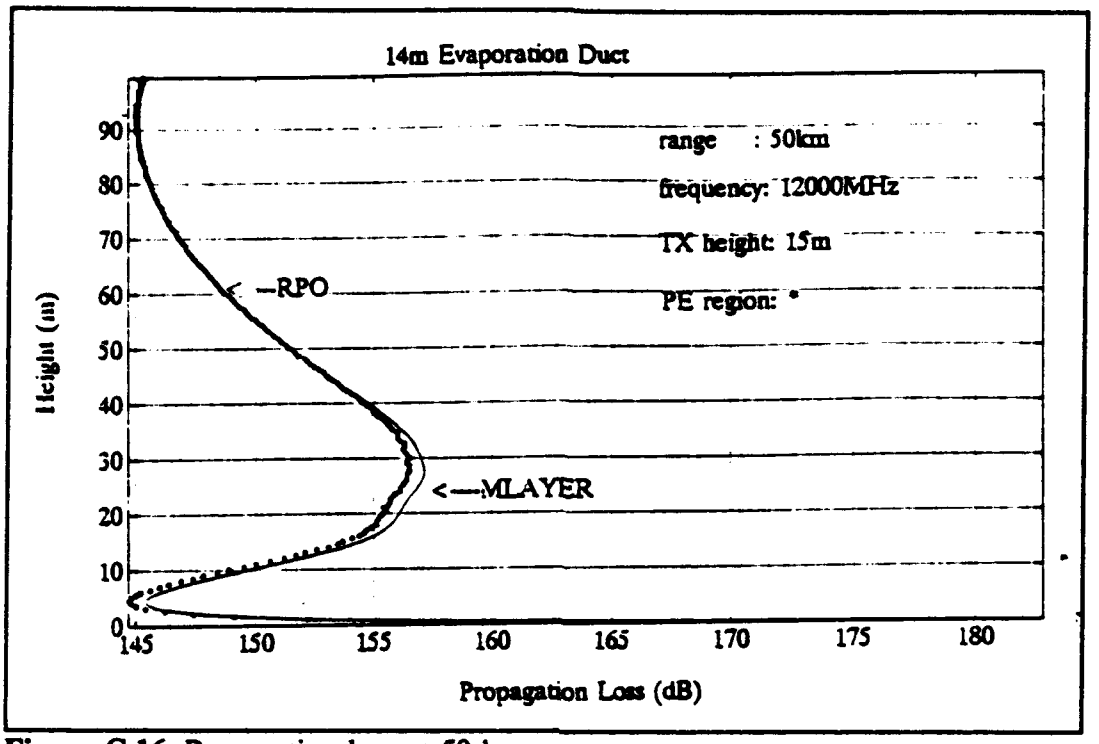

Figure C.16. Propagation loss at 50 km.

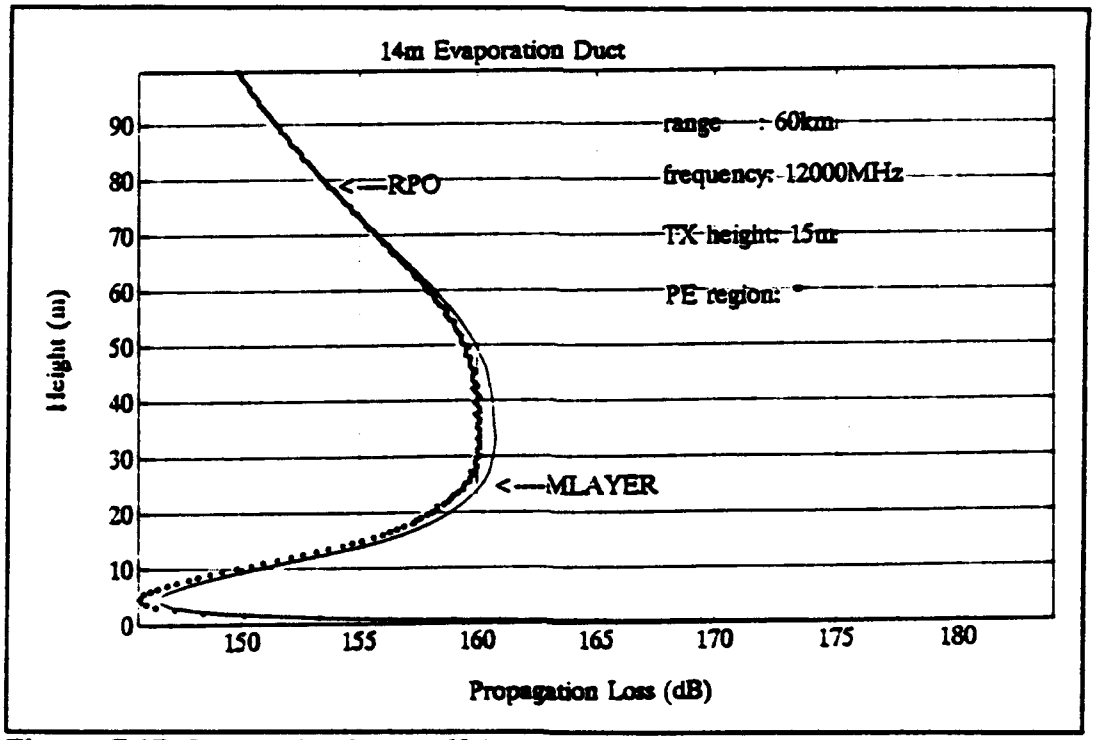

Figure C.17. Propagation loss at 60 km.

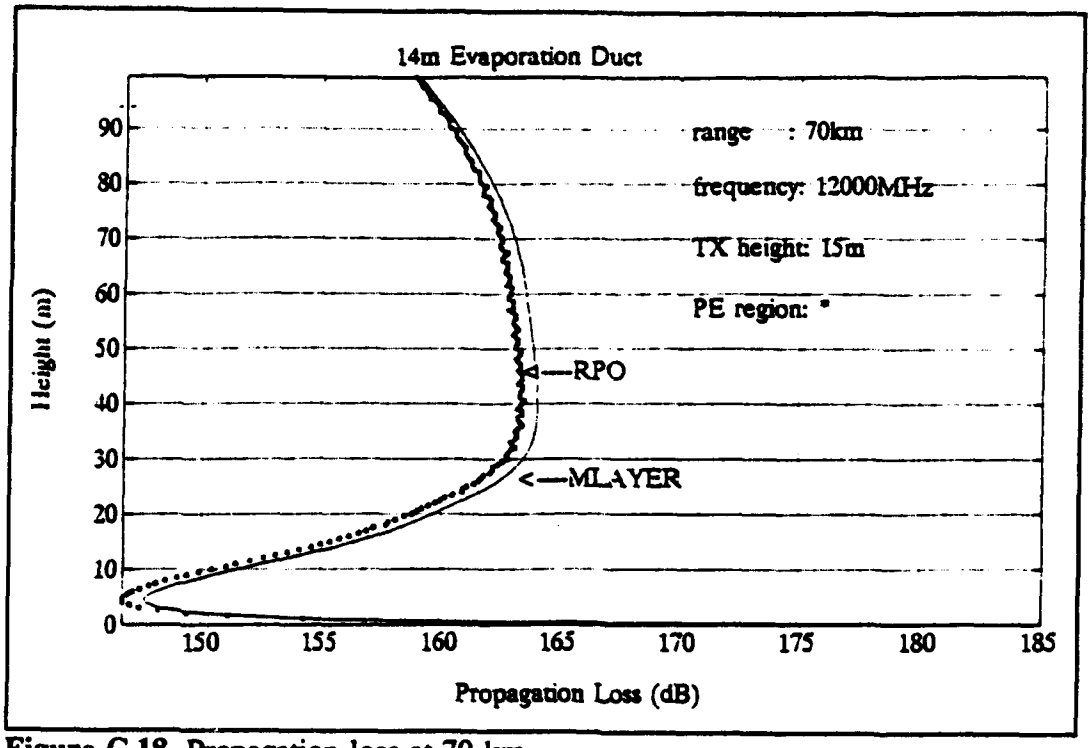

Figure C.18. Propagation loss at 70 km.

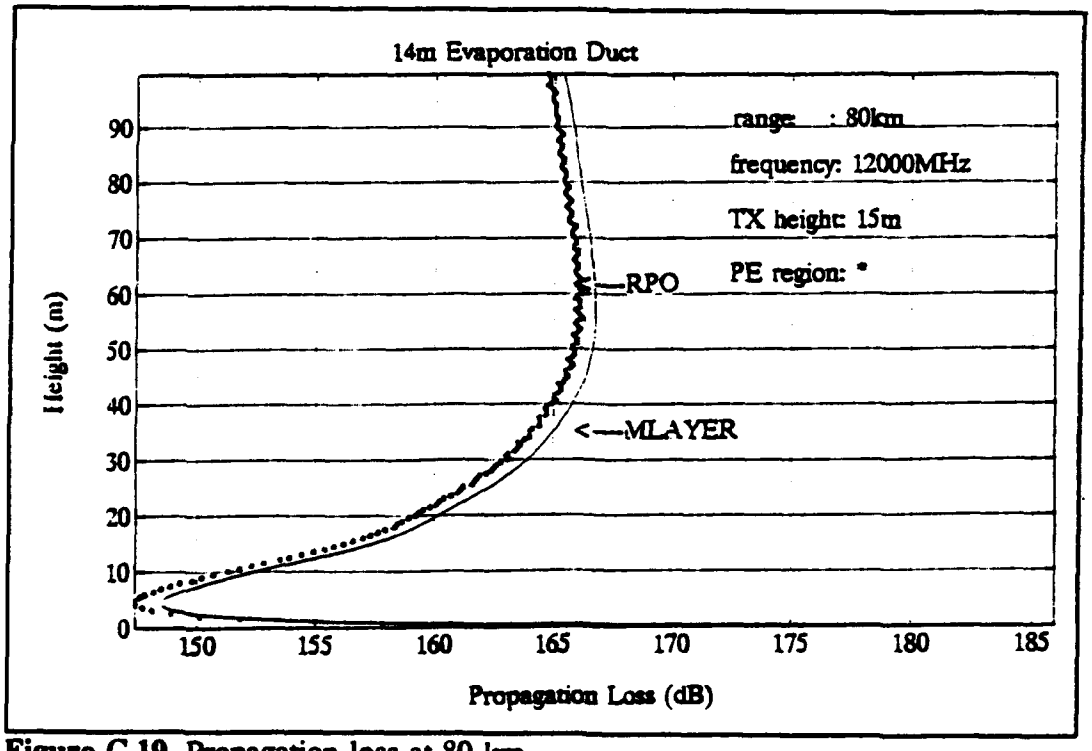

Figure C.19. Propagation loss at 80 km.

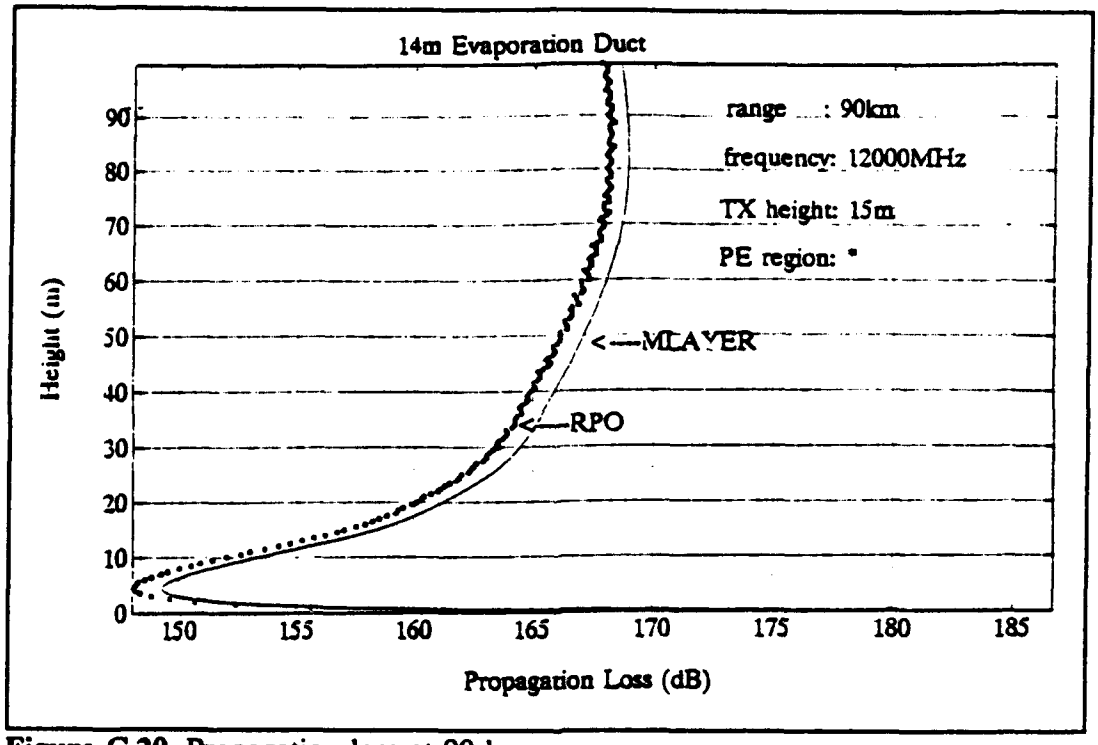

Figure C.20. Propagation loss at 90 km.

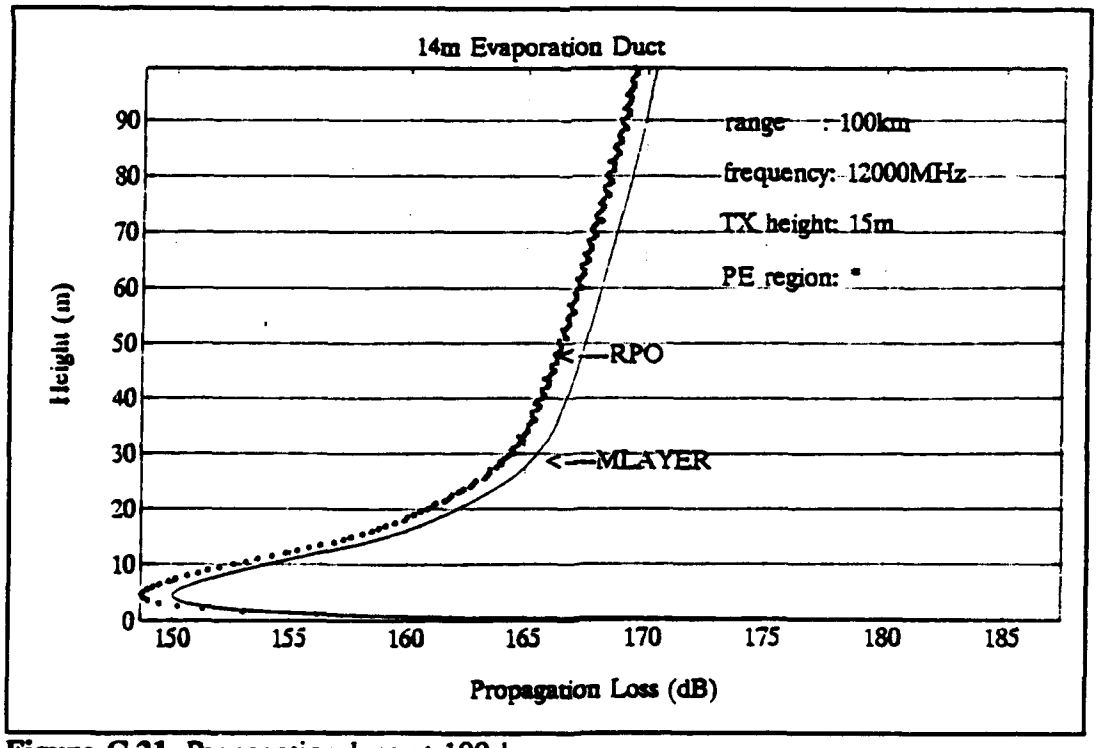

Figure C.21. Propagation loss at 100 km.

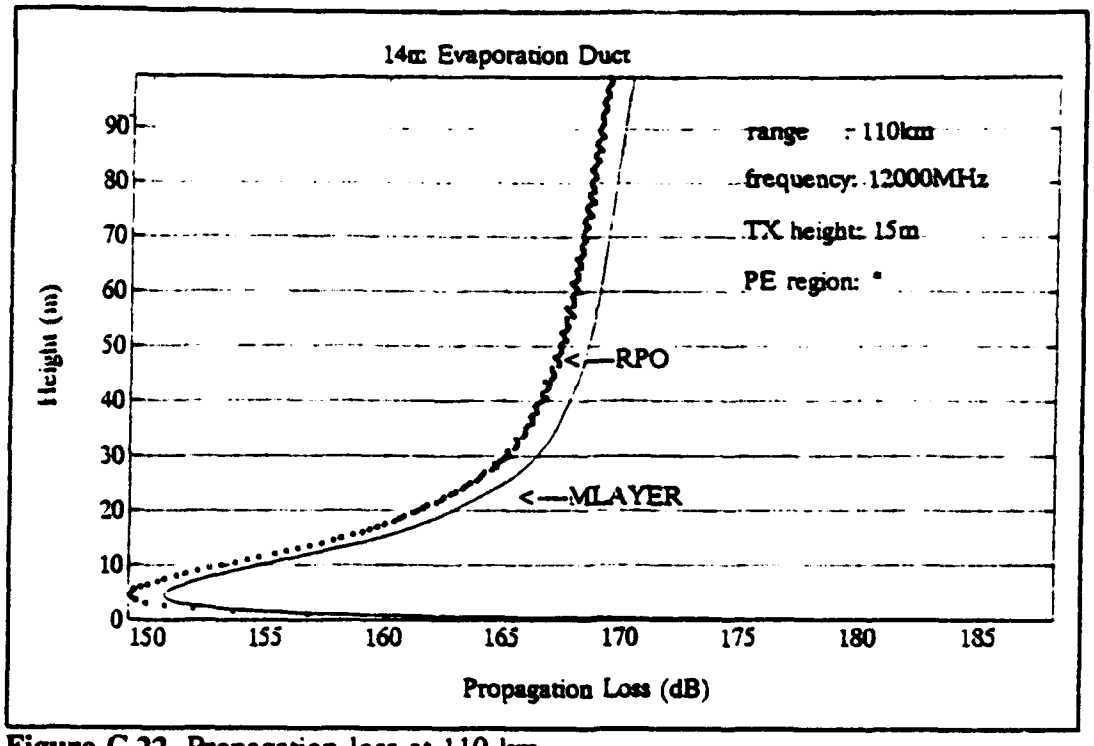

Figure C.22. Propagation loss at 110 km.

APPENDIX D: PROPAGATION LOSS UNDER THE INFLUENCE OF A 300 M SURFACE-BASED DUCT OVER A 14 M EVAPORATION DUCT

This Appendix displays the propagation loss computed by RPO and M-Layer under the influence of a 300 m surface-based duct over a 14 m evaporation duct at 3 GHz and 12 GHz at ranges of 15, 20, 30, 40, 50, 60, 70, 80, 90, 100 and 110 km.

1. Propagation loss at 3 GHz

Figures D.1 through D.11 displays the propagation loss at 3 GHz computed by RPO and M-Layer.

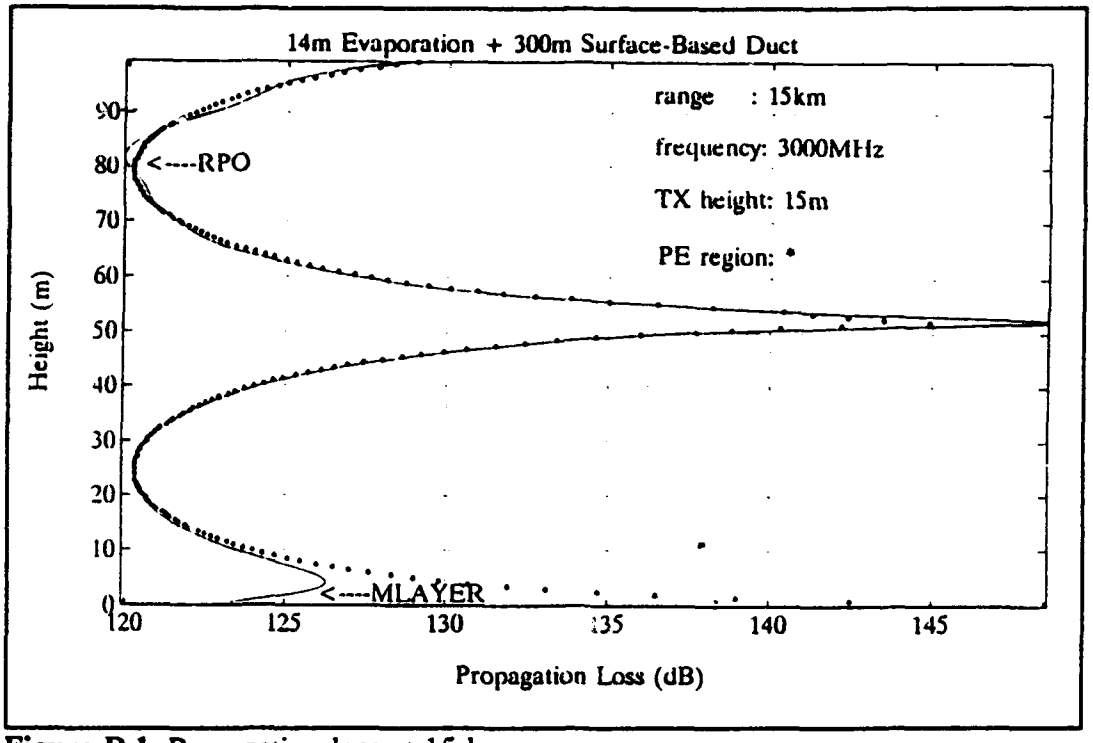

Figure D.1. Propagation loss at 15 km.

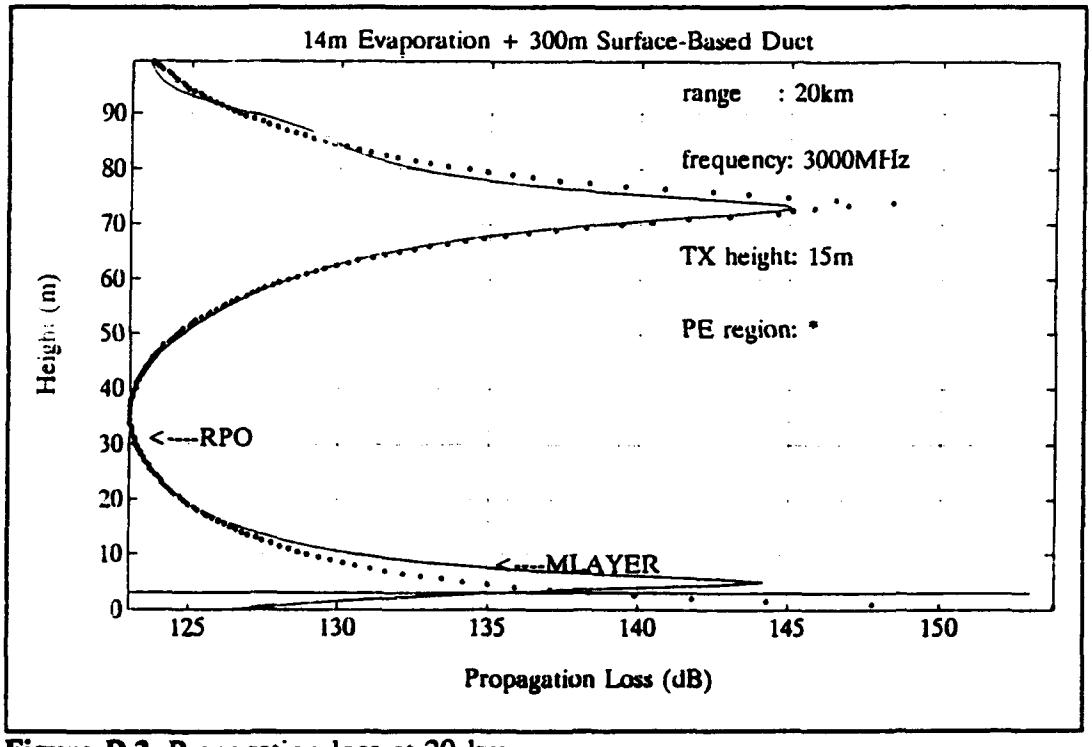

Figure D.2. Propagation loss at 20 km.

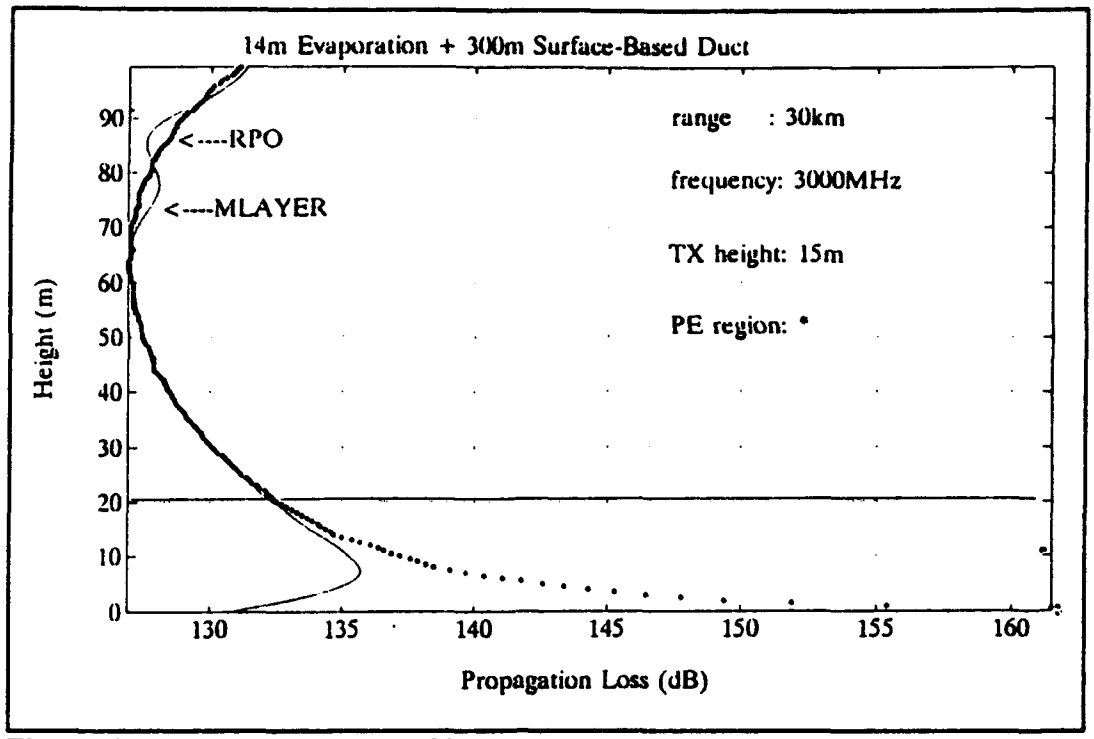

Figure D.3. Propagation loss at 30 km.

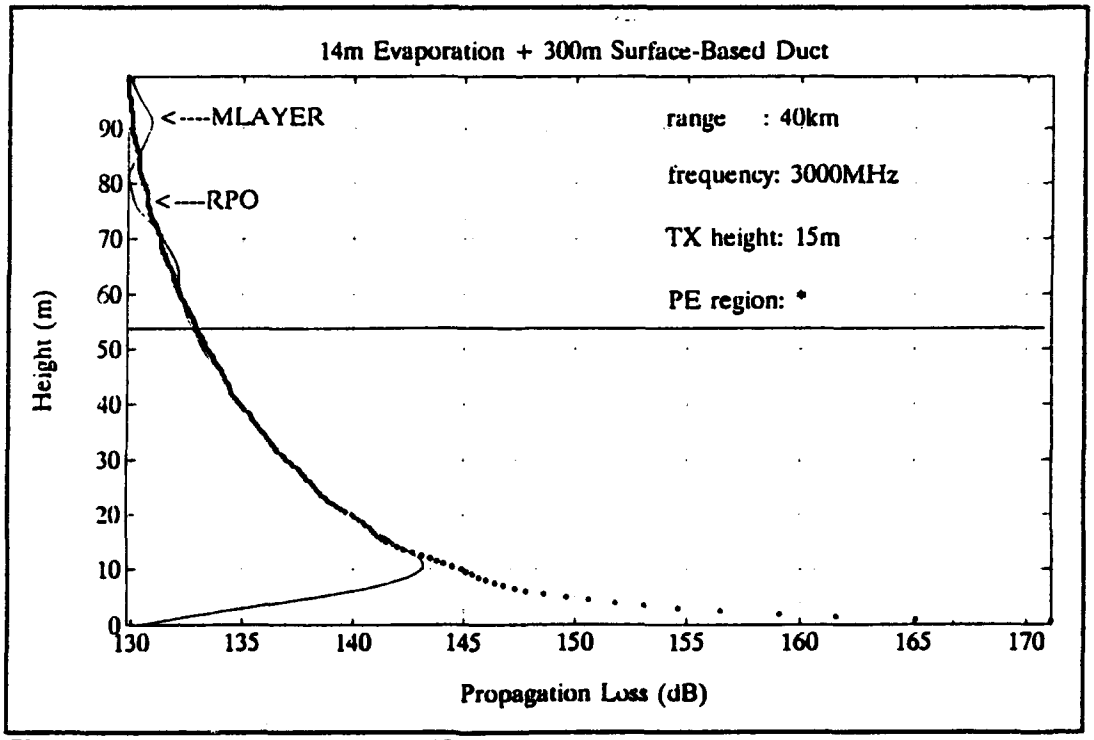

Figure D.4. Propagation loss at 40 km.

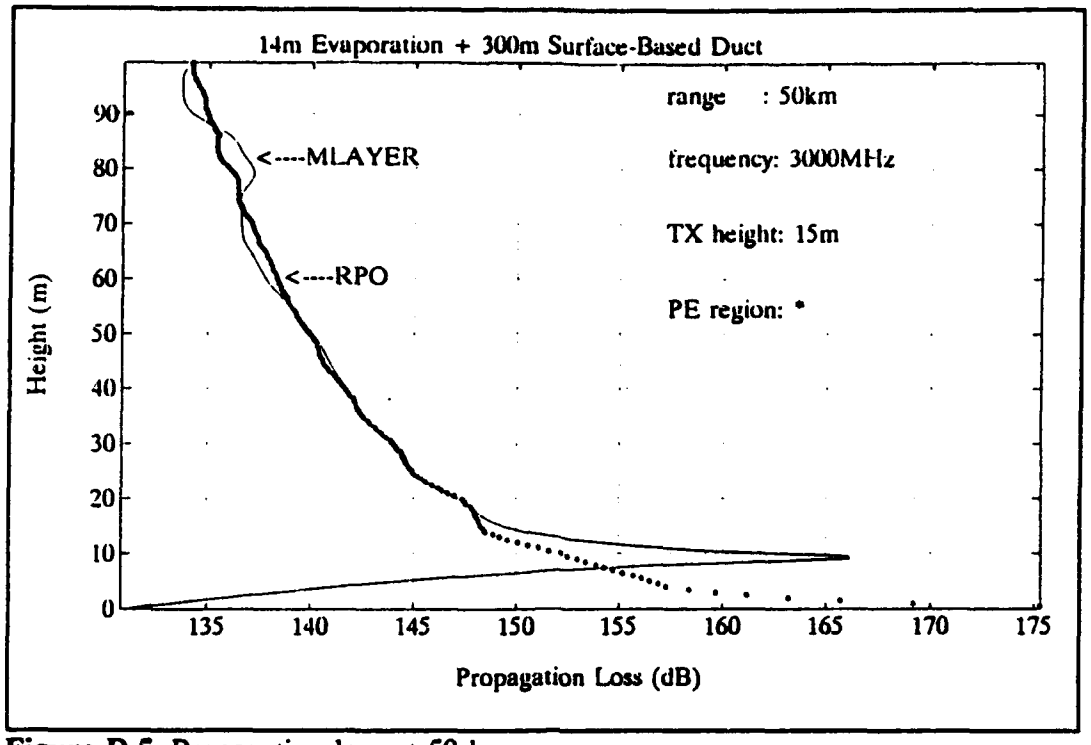

Figure D.5. Propagation loss at 50 km.

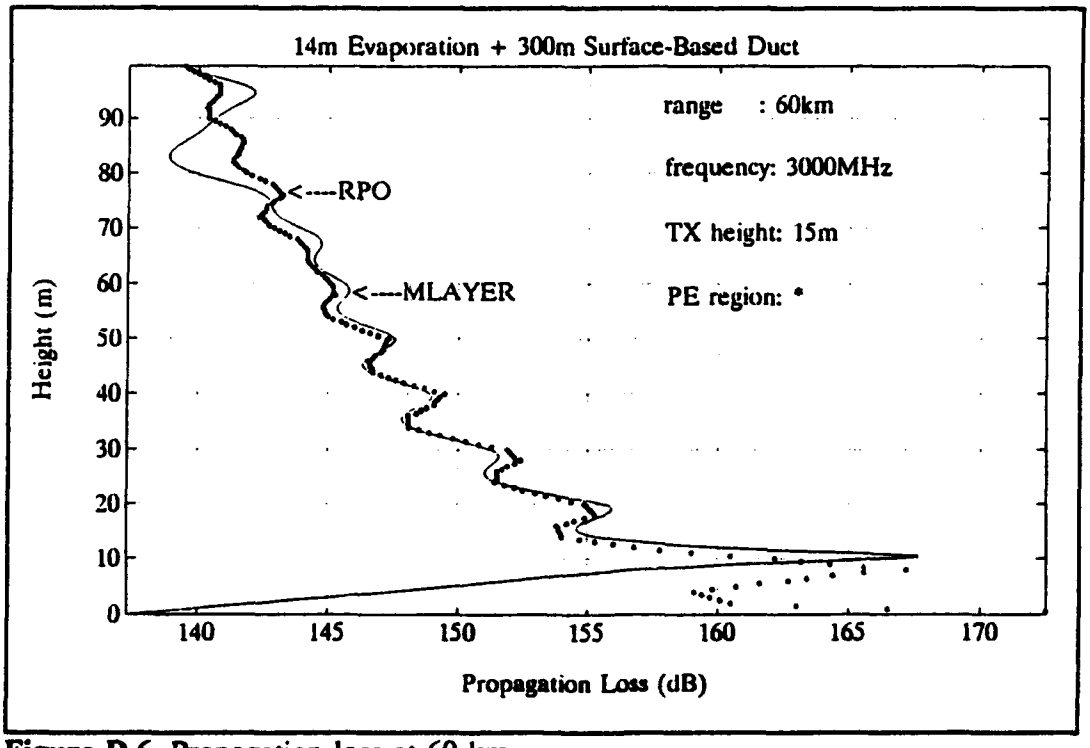

Figure D.6. Propagation loss at 60 km.

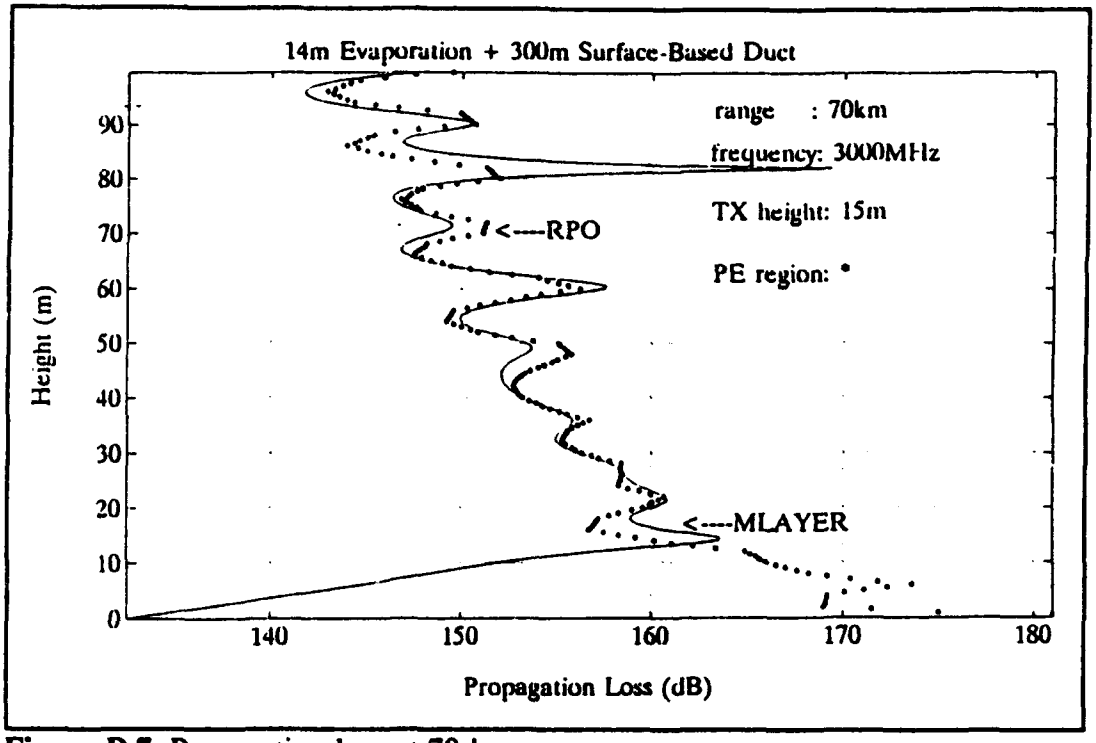

Figure D.7. Propagation loss at 70 km.

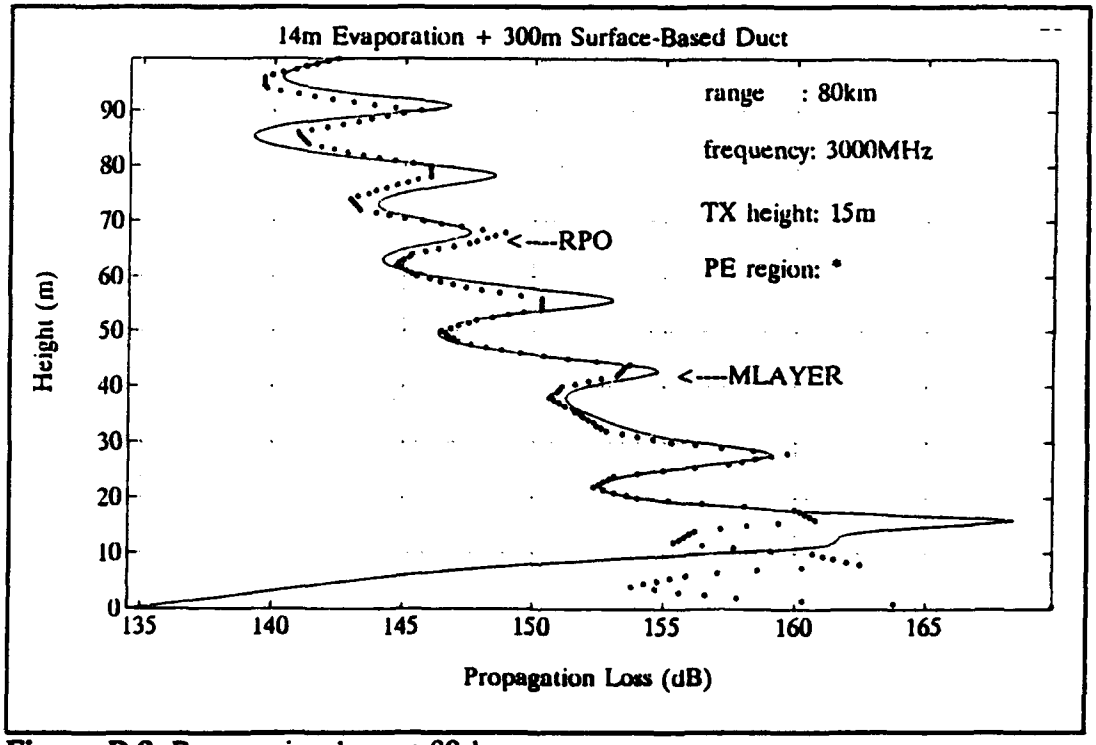

Figure D.8. Propagation loss at 80 km.

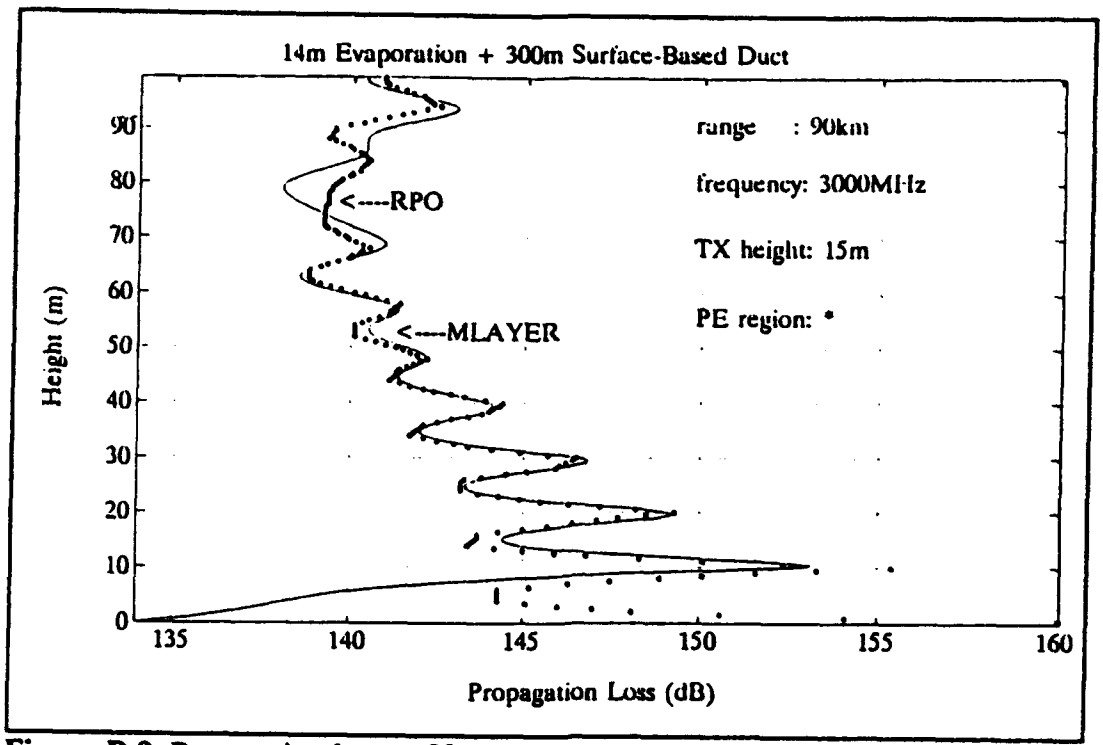

Figure D.9. Propagation loss at 90 km.

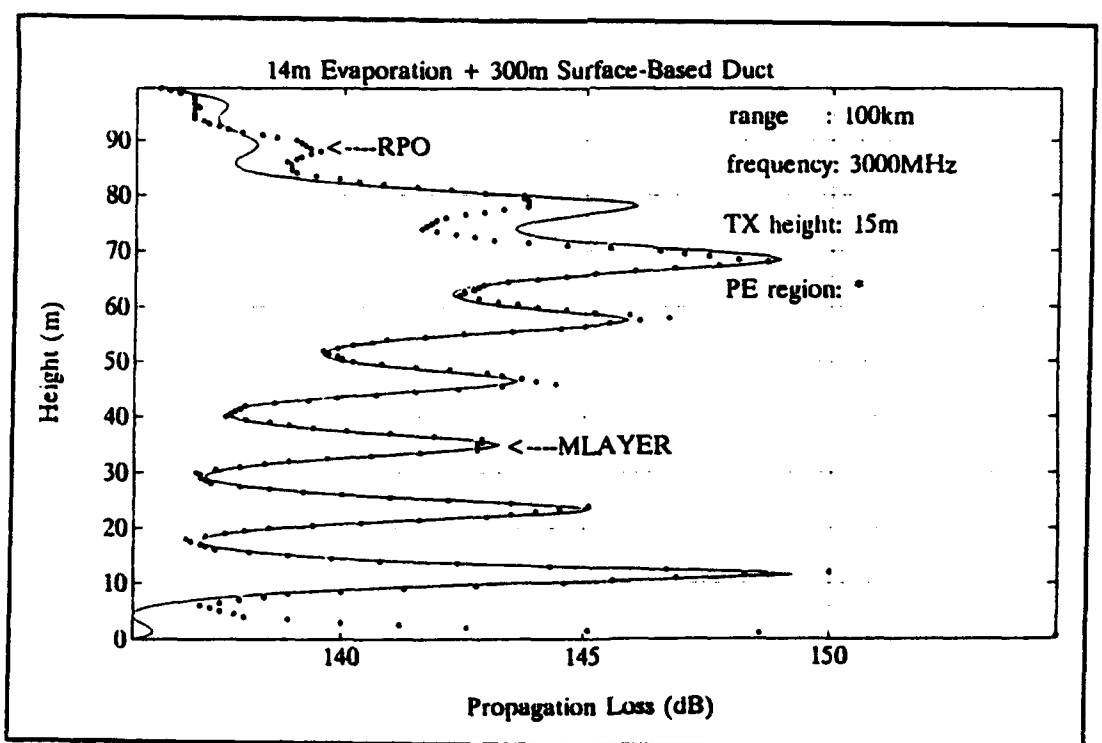

Figure D.10. Propagation loss at 100 km.

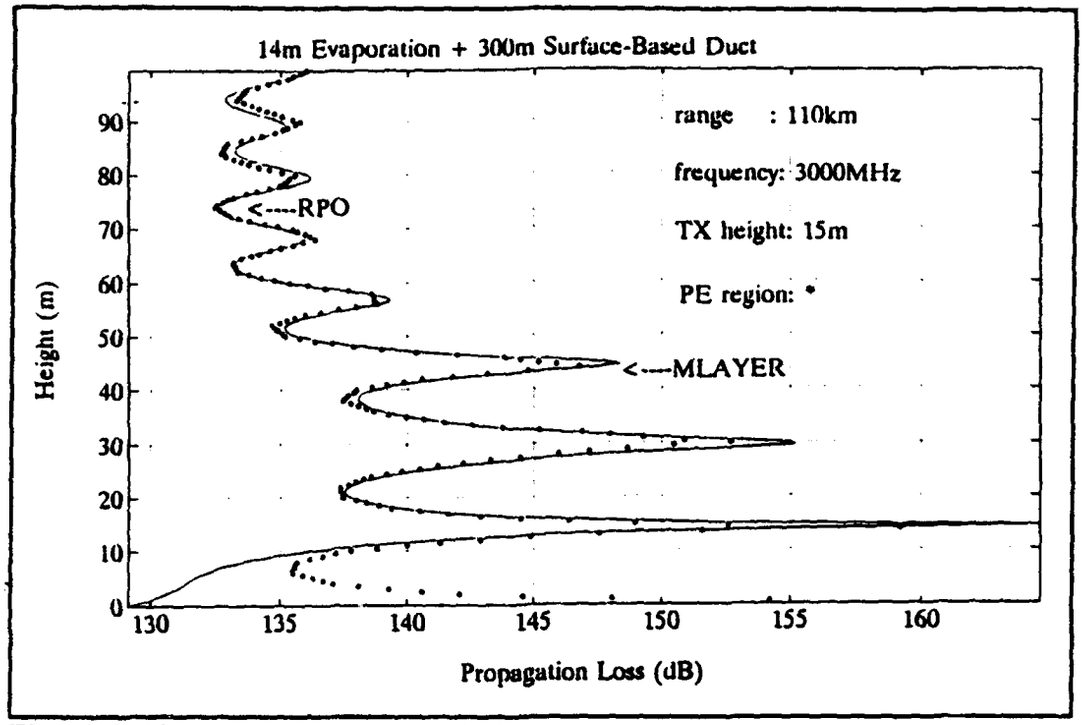

Figure D.11. Propagation loss at 110 km.

2. Propagation loss at 12 GHz

Figures D.12 through D.22 displays the propagation loss at 12 GHz computed by RPO and M-Layer.

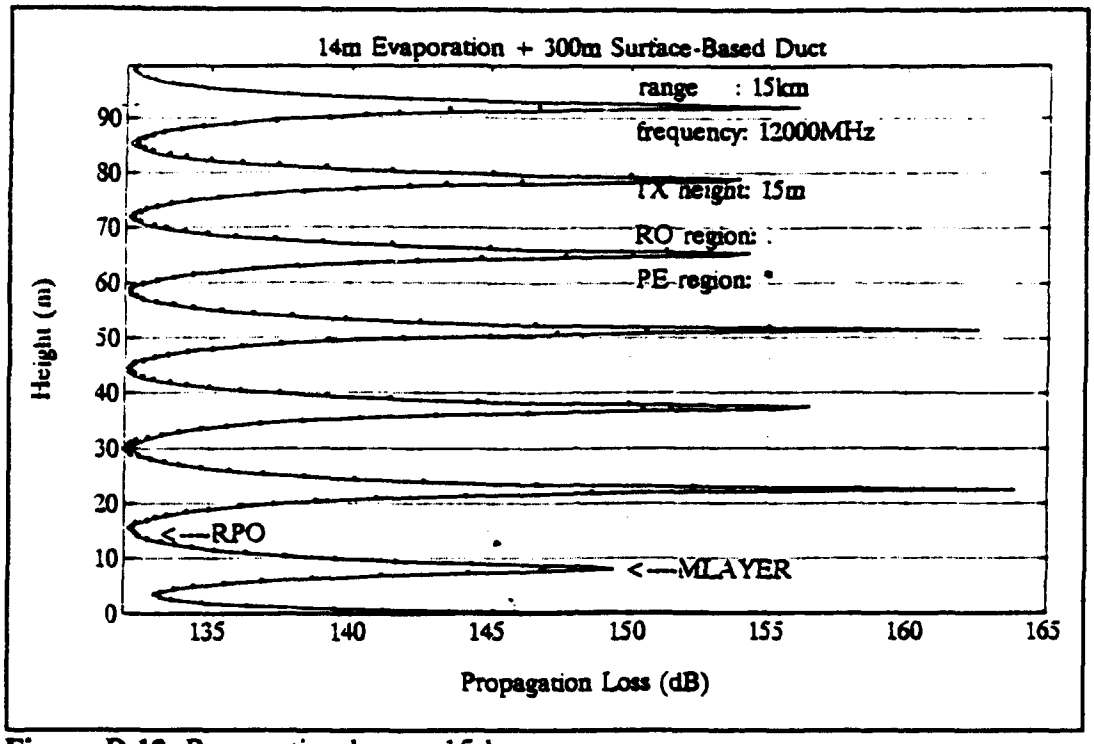

Figure D.12. Propagation loss at 15 km.

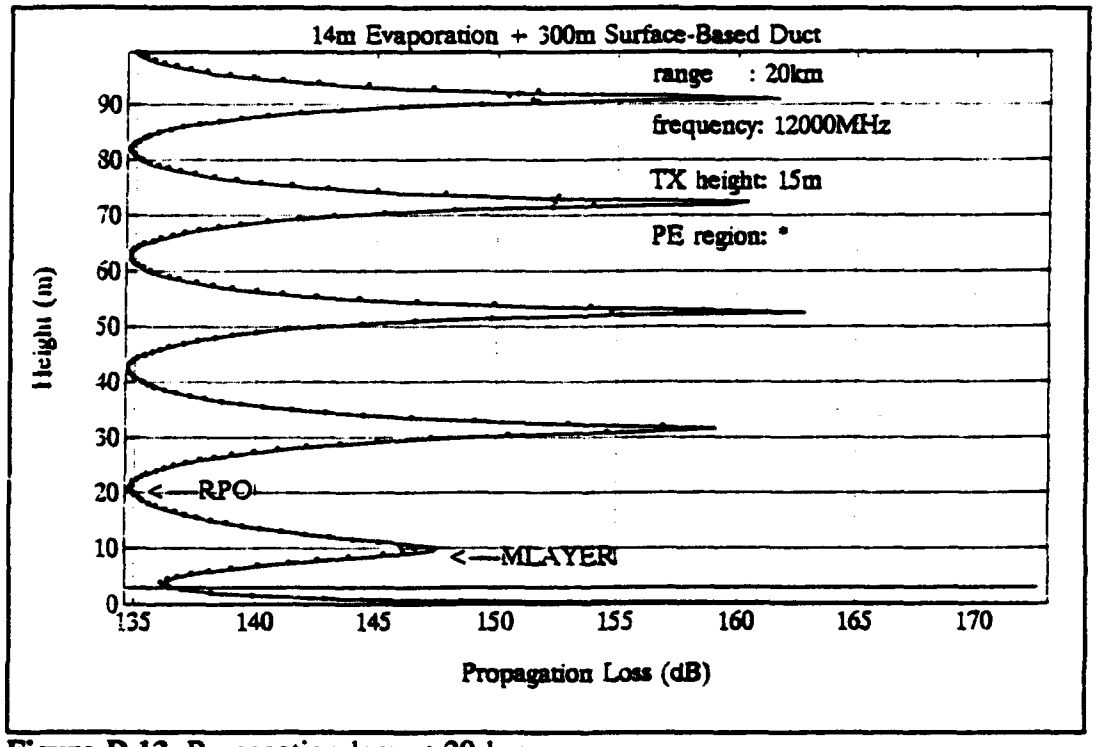

Figure D.13. Propagation loss at 20 km.

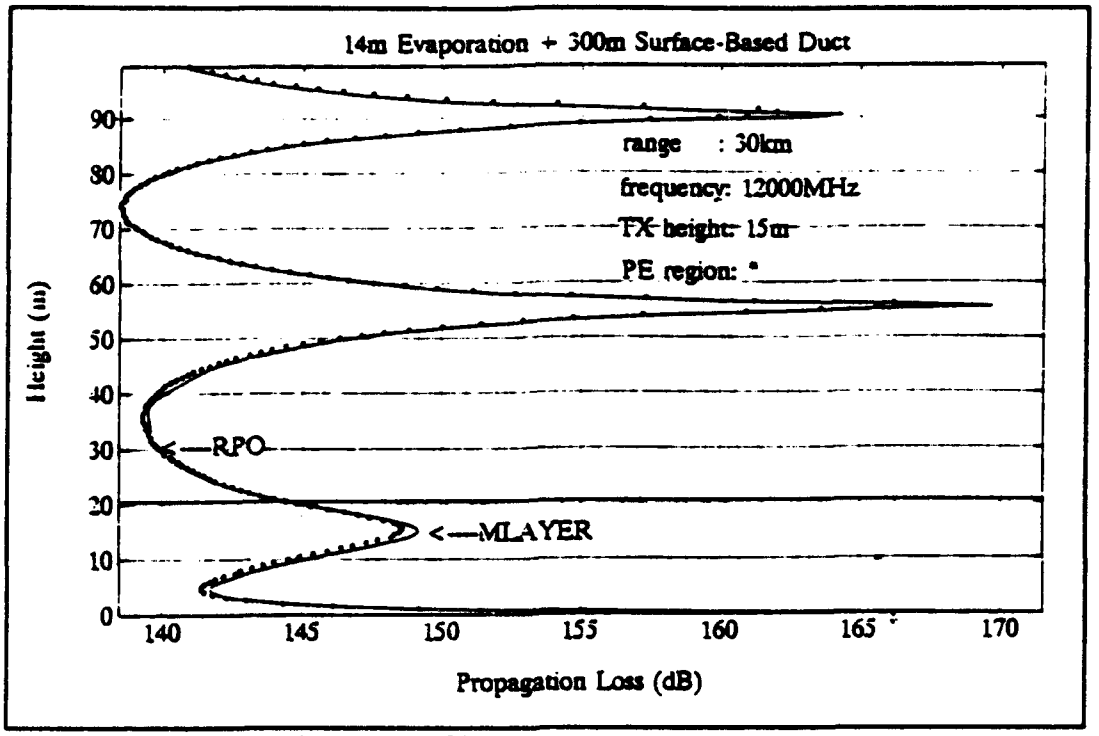

Figure D.14. Propagation loss at 30 km.

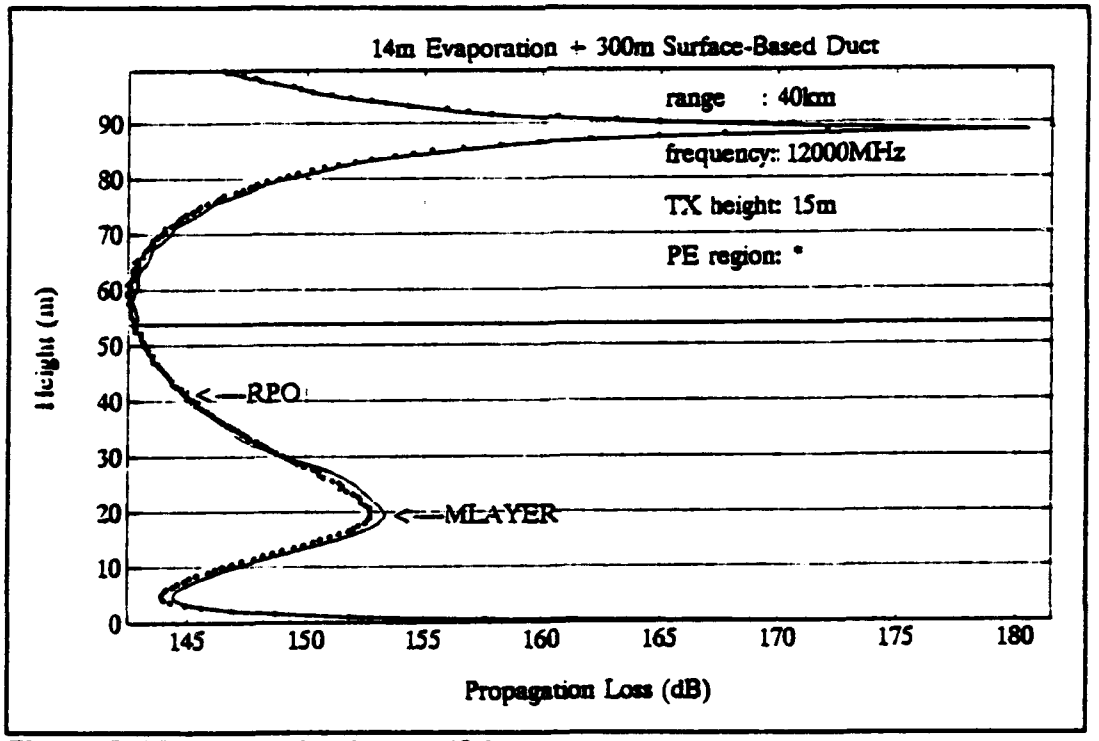

Figure D.15. Propagation loss at 40 km.

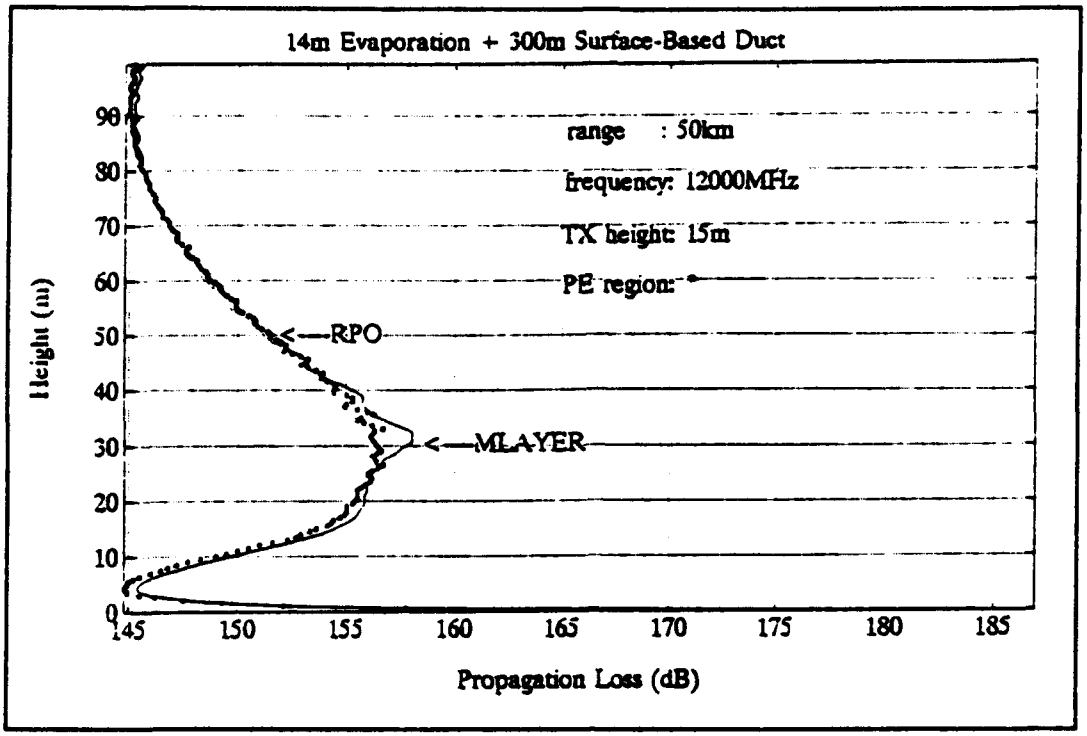

Figure D.16. Propagation loss at 50 km.

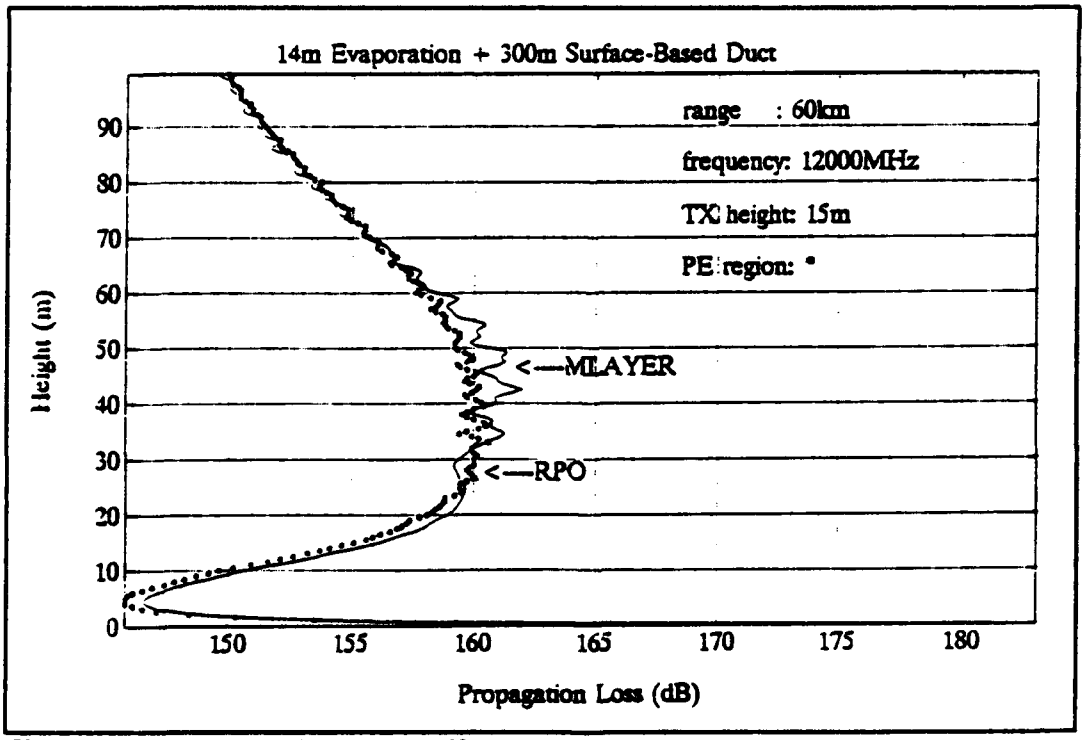

Figure D.17. Propagation loss at 60 km.

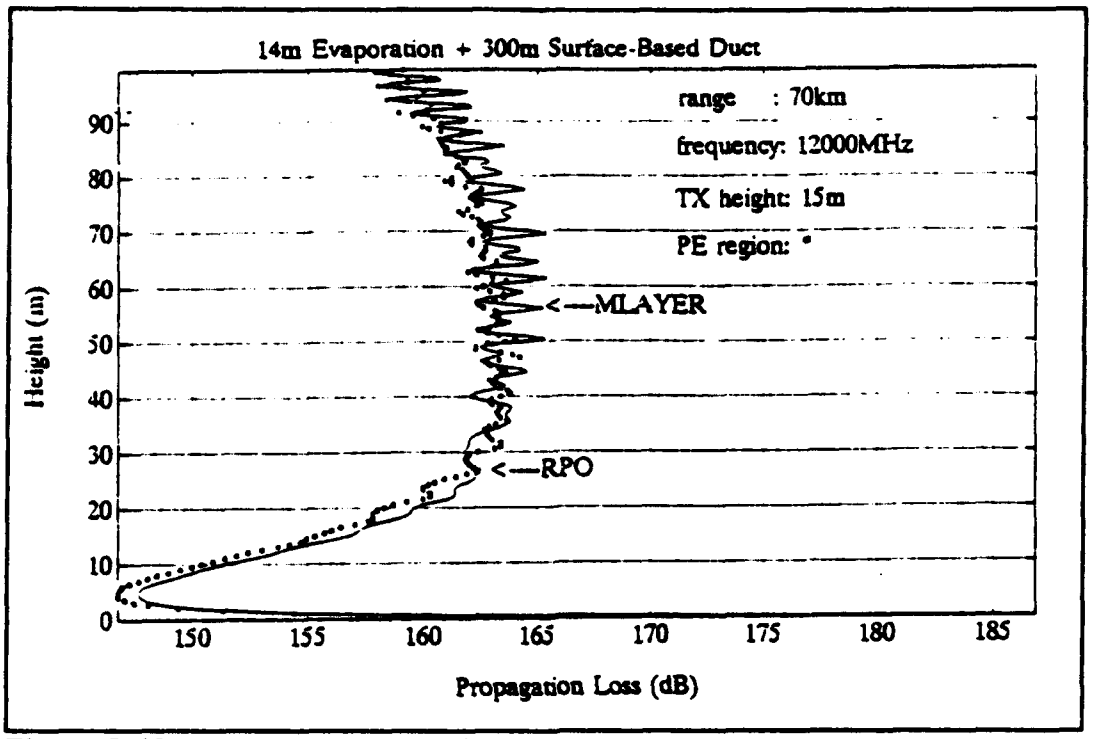

Figure D.18. Propagation loss at 70 km.

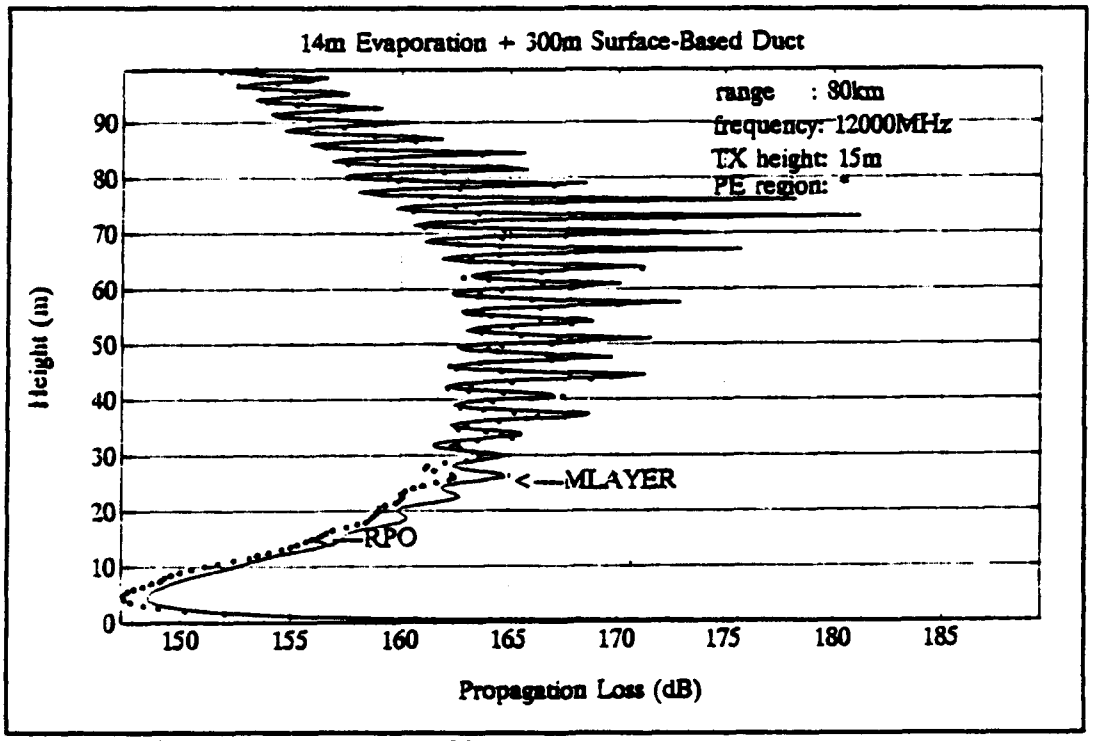

Figure D.19. Propagation loss at 80 km.

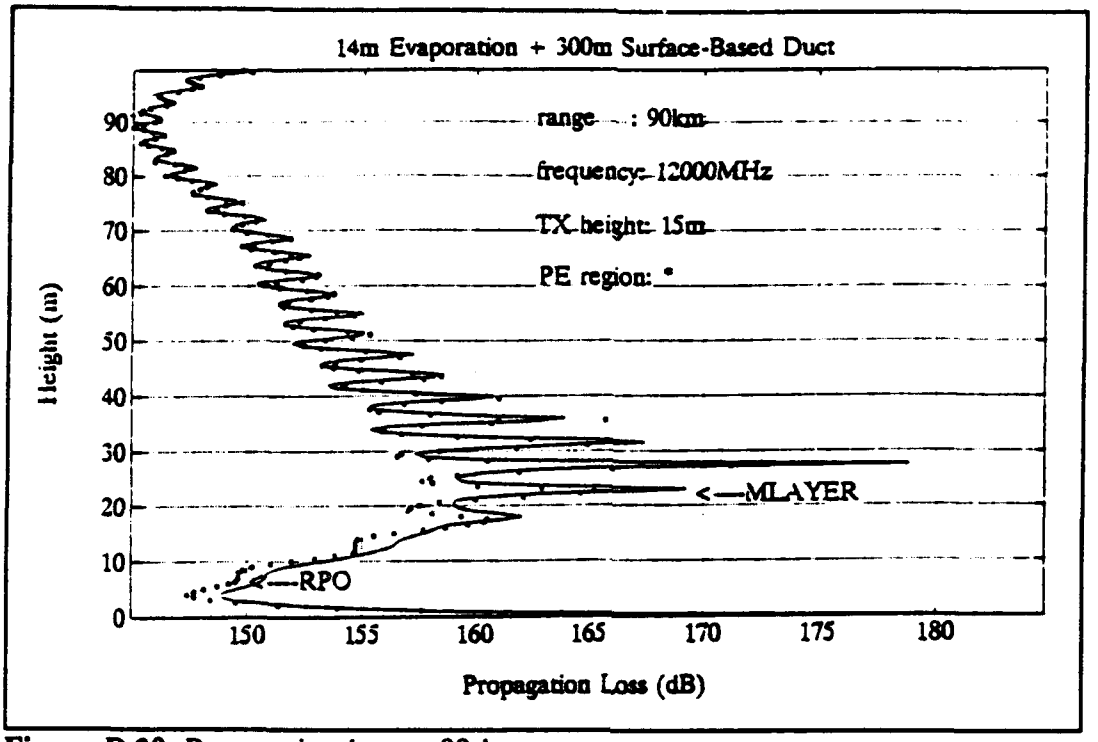

Figure D.20. Propagation loss at 90 km.

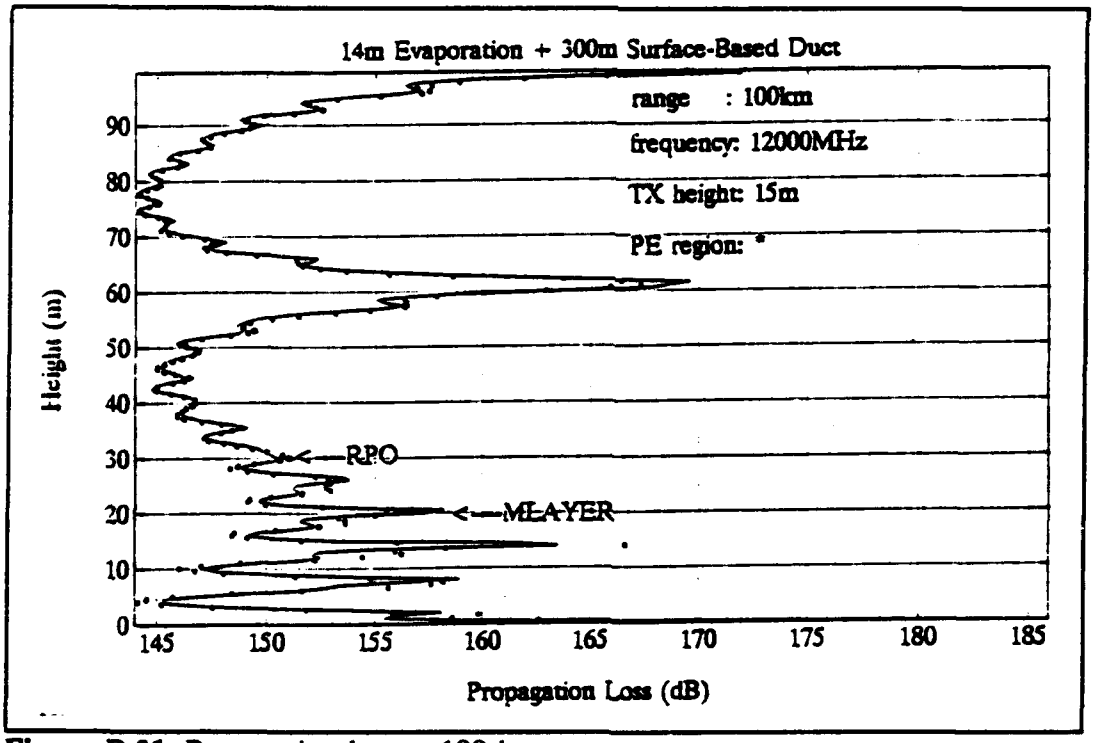

Figure D.21. Propagation loss at 100 km.

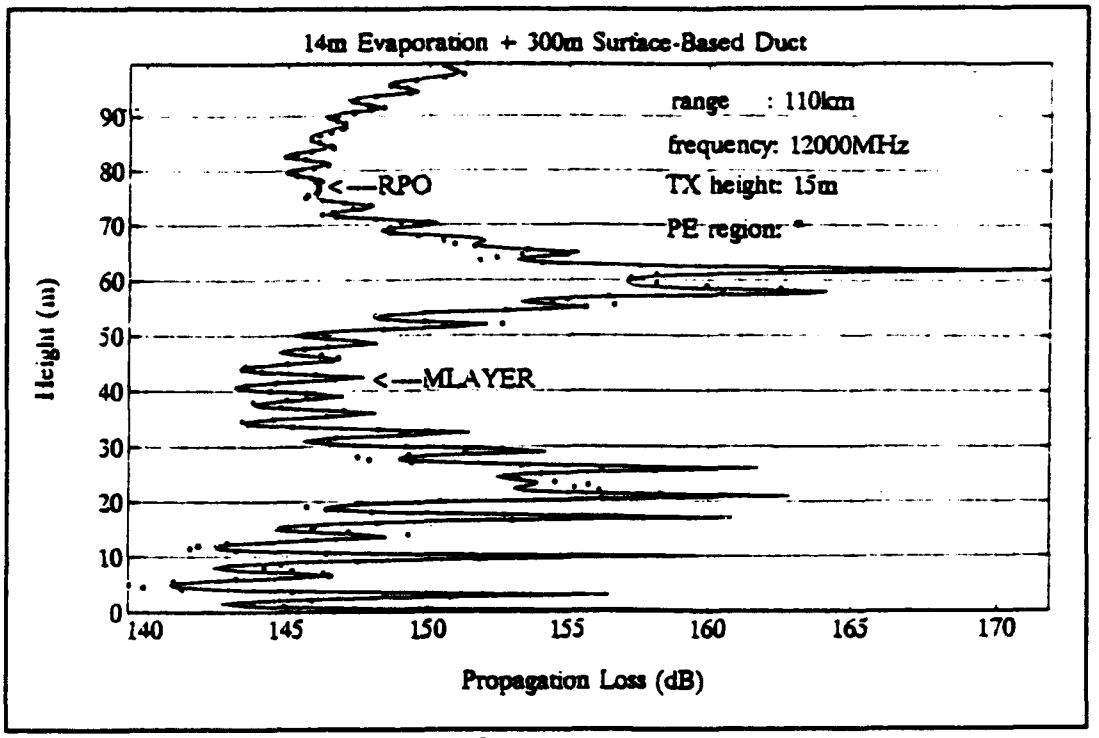

Figure D.22. Propagation loss at 110 km.

APPENDIX E: PROPAGATION LOSS UNDER THE INFLUENCE OF A 150 M SURFACE-BASED DUCT

This Appendix displays the propagation loss computed by RPO and M-Layer under the influence of a 150 m surface-based duct at 3 GHz, 6 GHz and 12 GHz at ranges of 15, 20, 25, 30, 35, 40, 50, 60, 70, 80, 90, 100 and 110 km. The modified refractivity profile is given in Table E.1.

Table E.1. A 150 m surface-based duct.

i	Z_i meters	M_i
0	0.0	339.0
1	100.0	350.8
2	150.0	301.3
3	1,000	401.6

1. Propagation loss at 3 GHz

Figures E.1 through E.13 displays the propagation loss at 3 GHz computed by RPO and M-Layer.

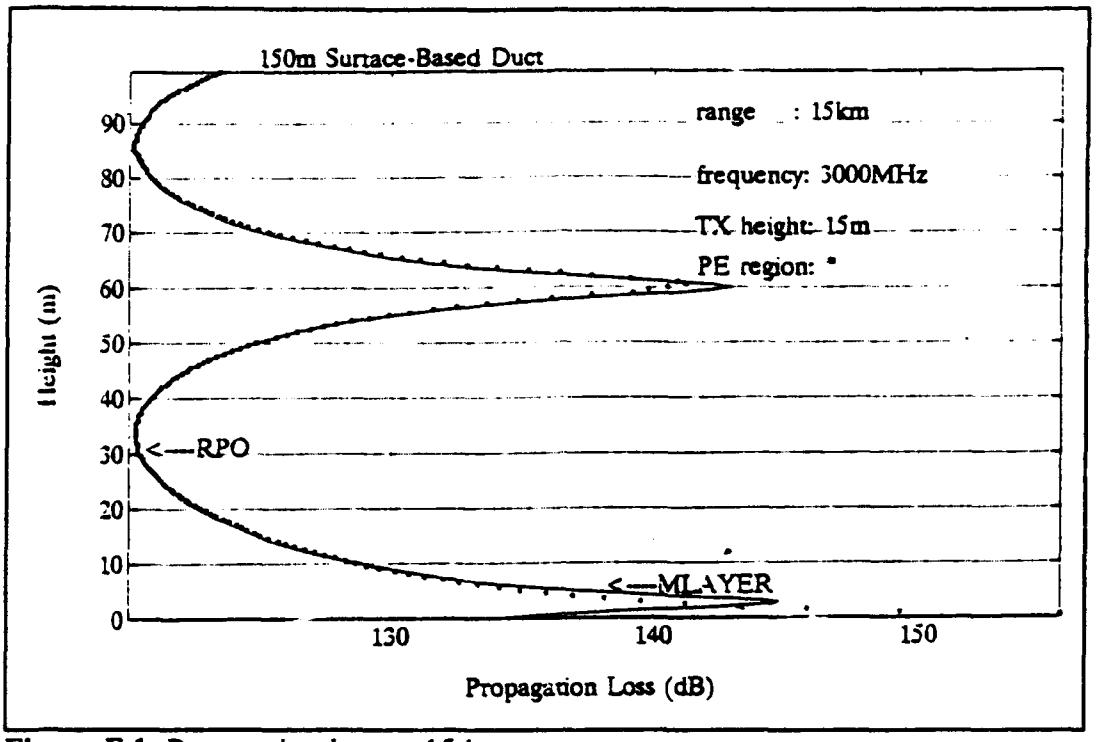

Figure E.1. Propagation loss at 15 km.

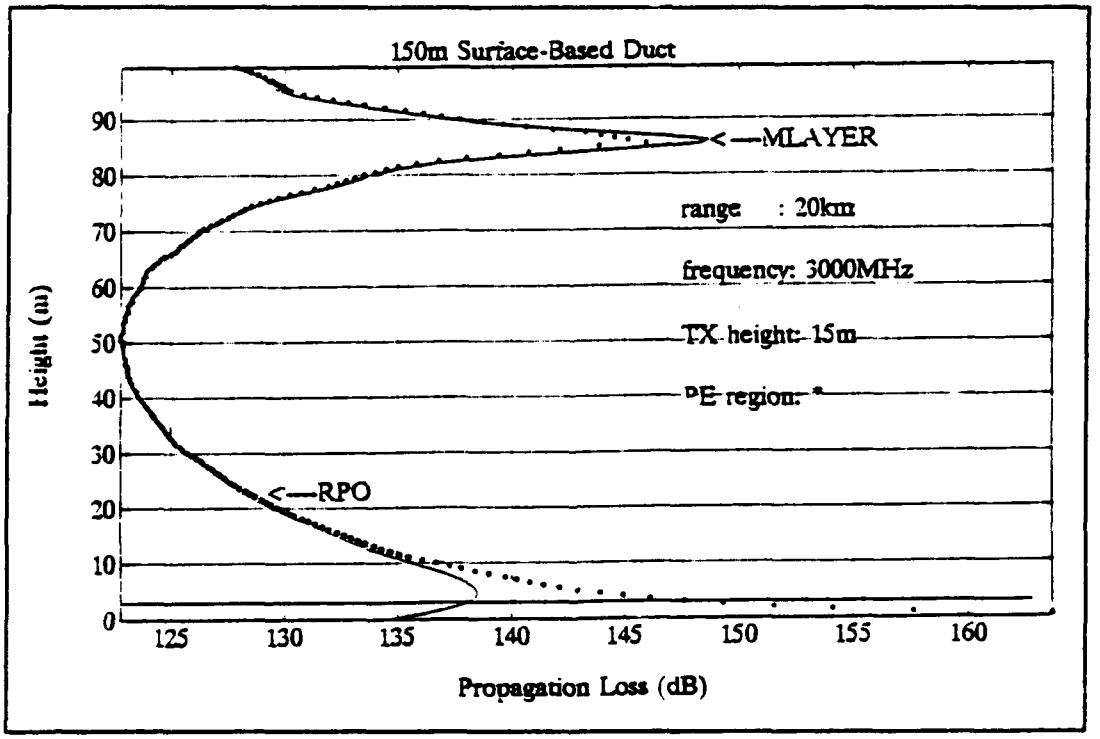

Figure E.2. Propagation loss at 20 km.

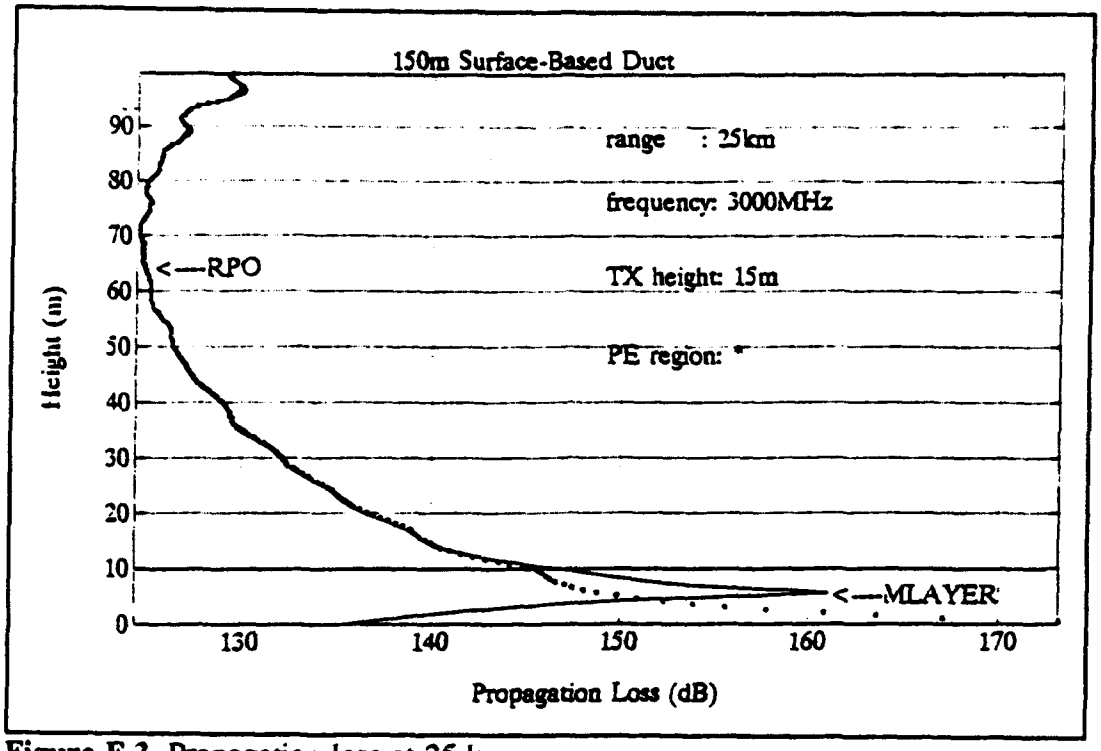

Figure E.3. Propagation loss at 25 km.

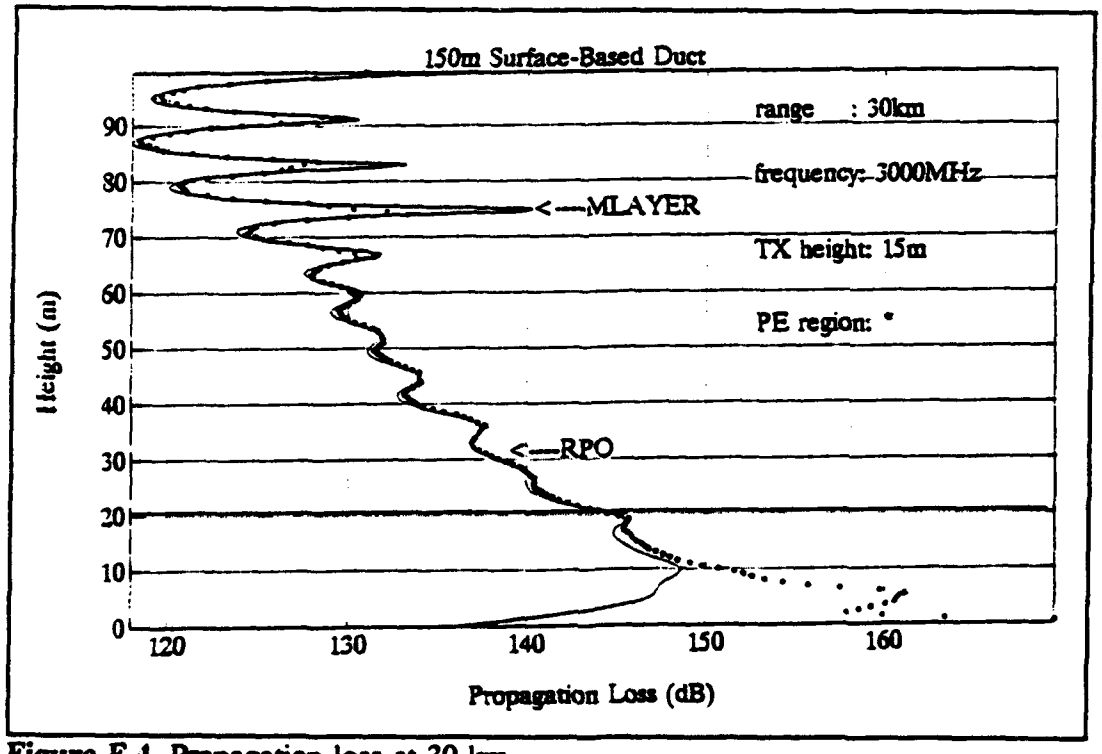

Figure E.4. Propagation loss at 30 km.

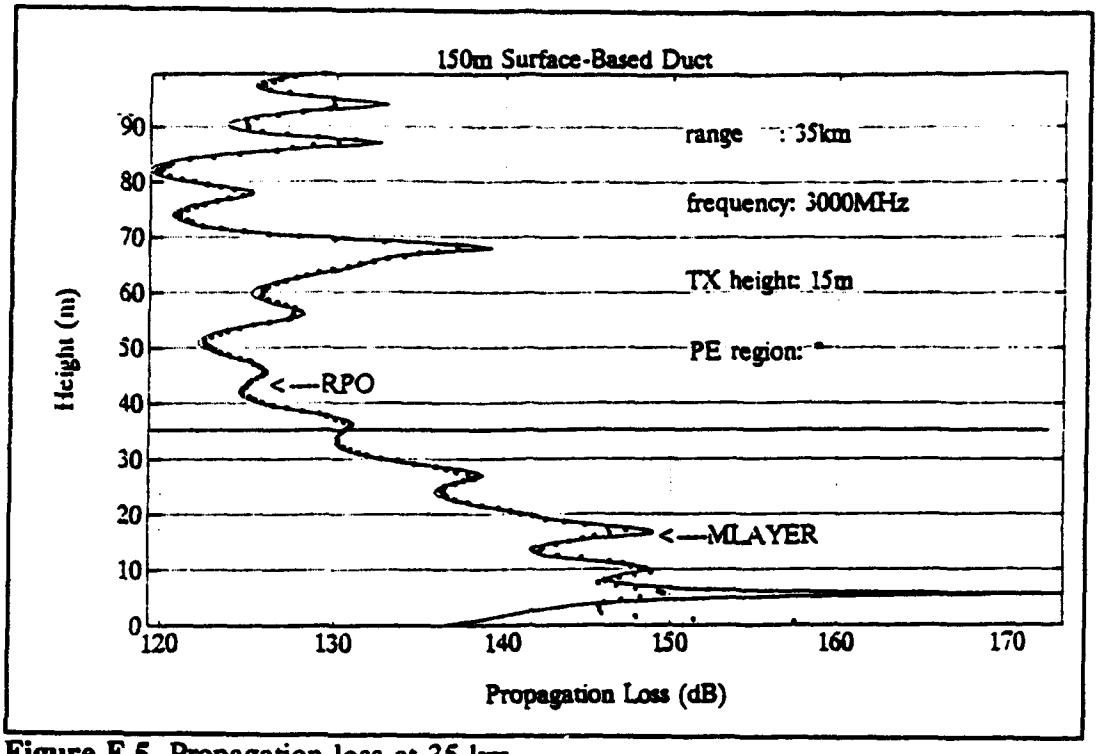

Figure E.5. Propagation loss at 35 km.

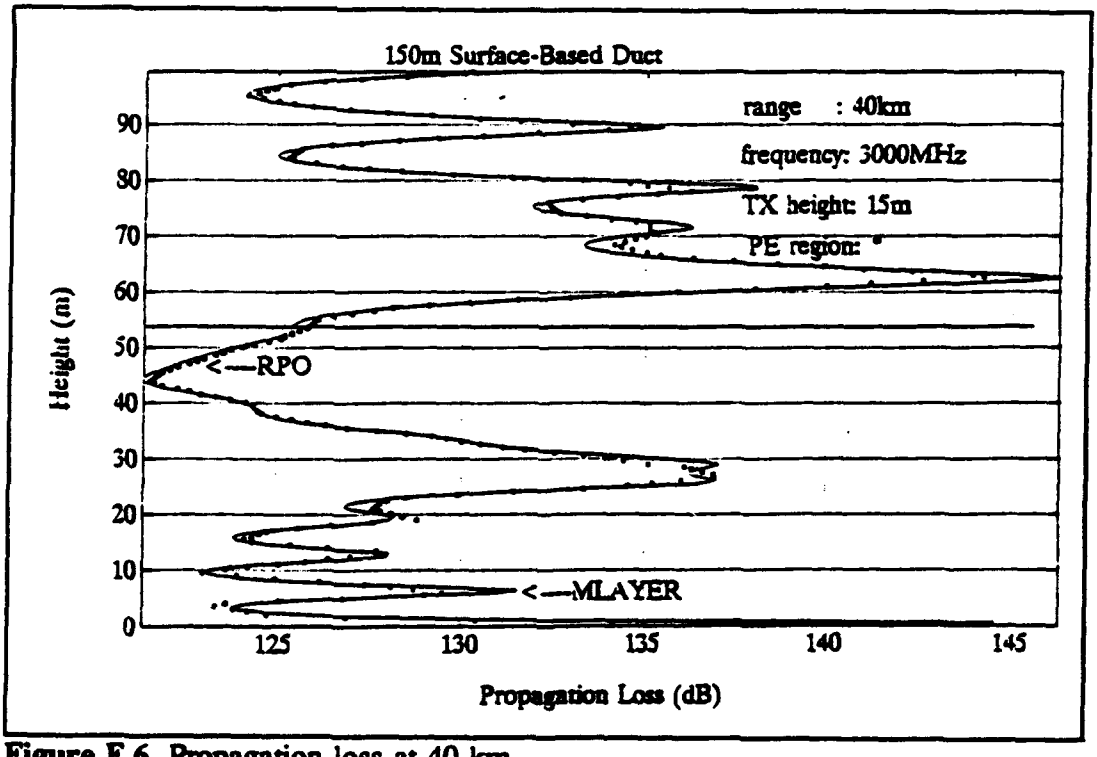

Figure E.6. Propagation loss at 40 km.

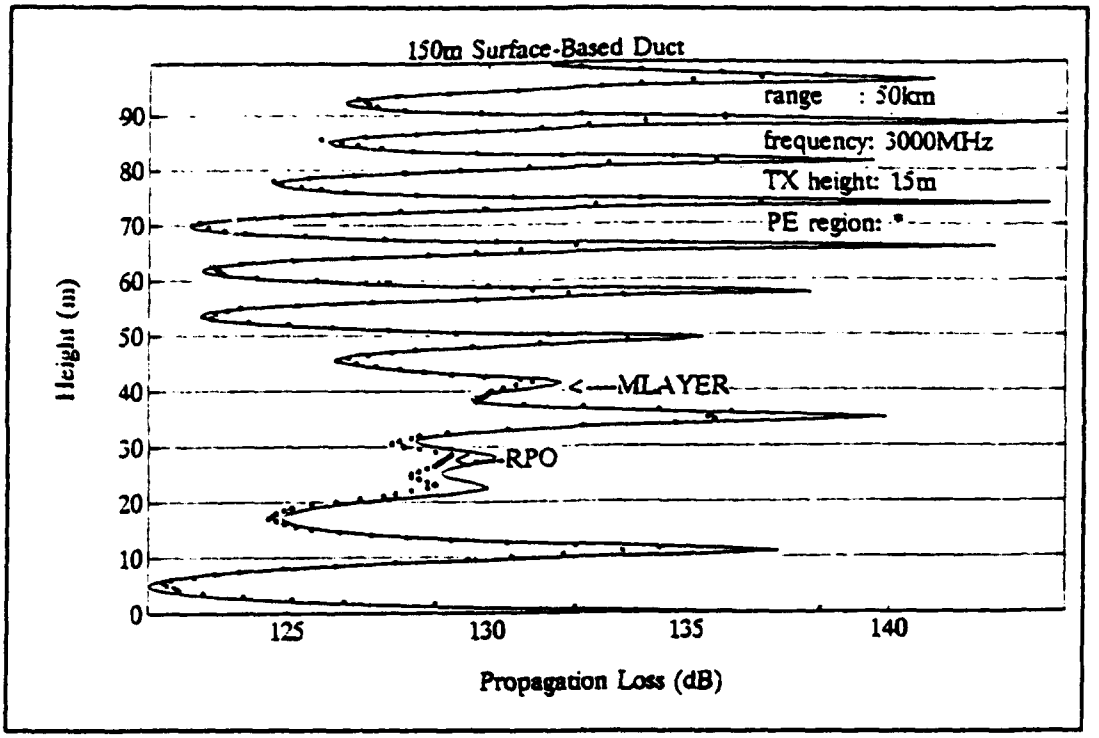

Figure E.7. Propagation loss at 50 km.

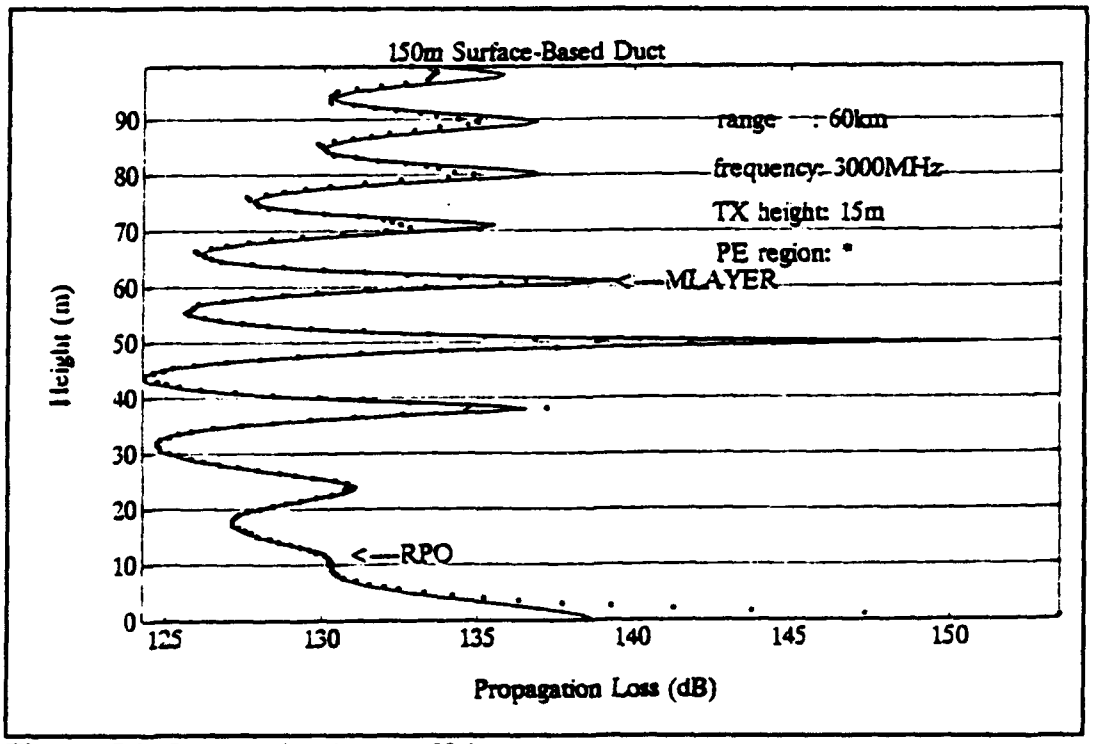

Figure E.8. Propagation loss at 60 km.

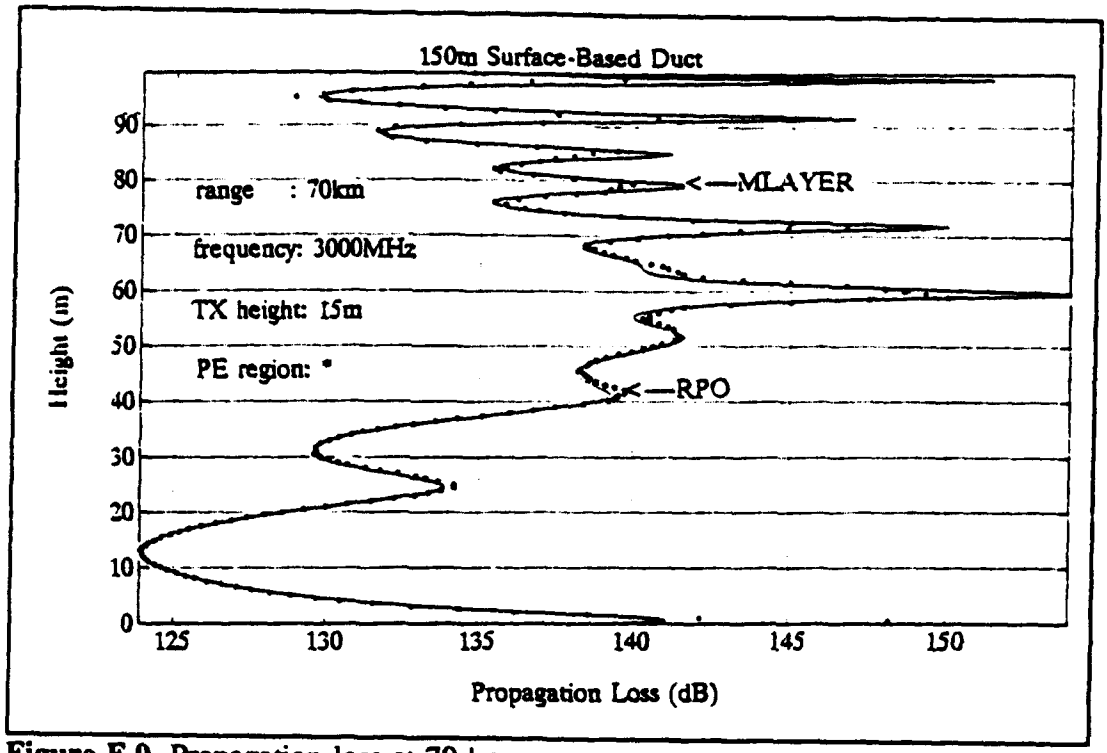

Figure E.9. Propagation loss at 70 km.

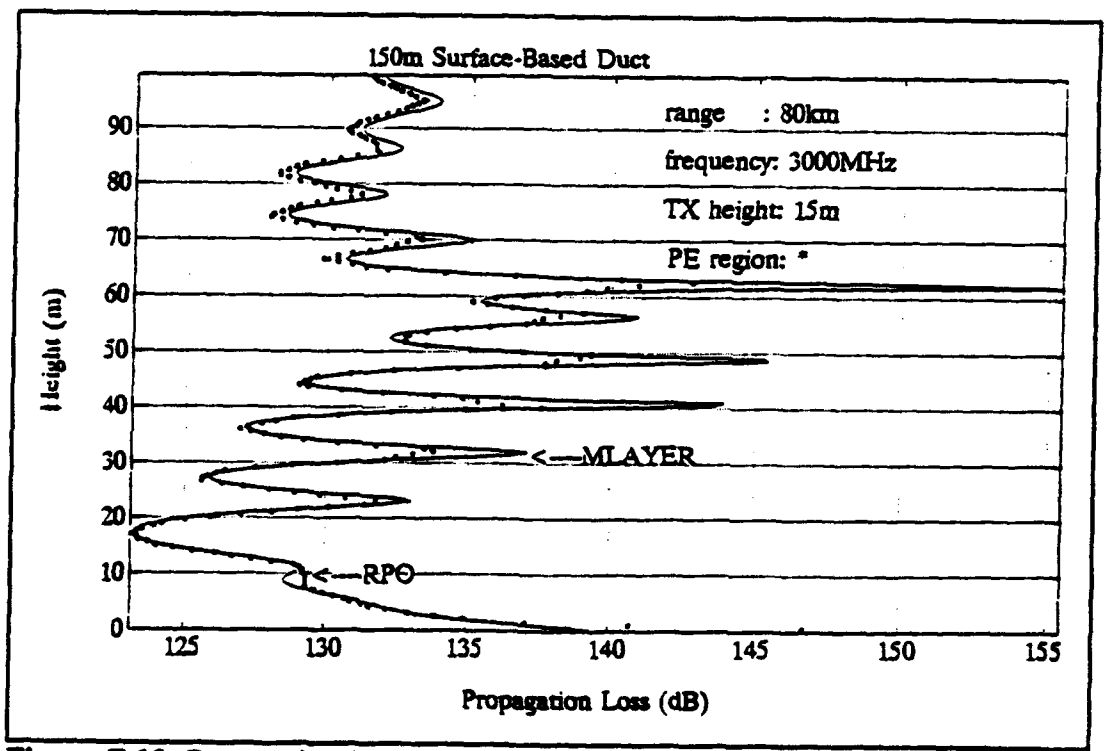

Figure E.10. Propagation loss at 80 km.

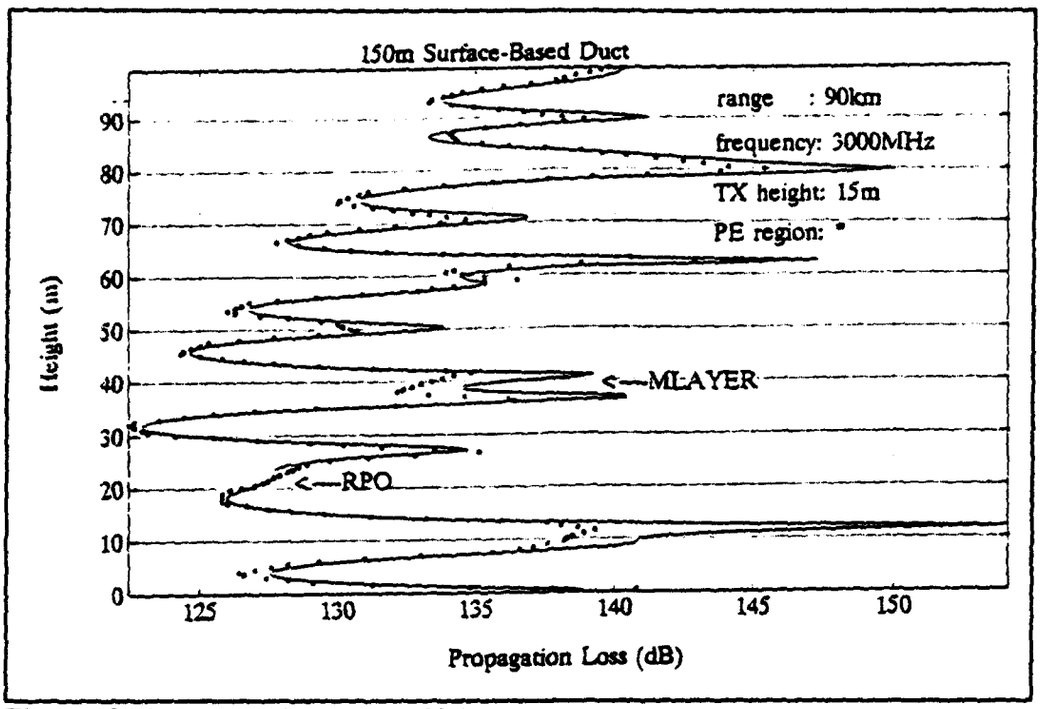

Figure E.11. Propagation loss at 90 km.

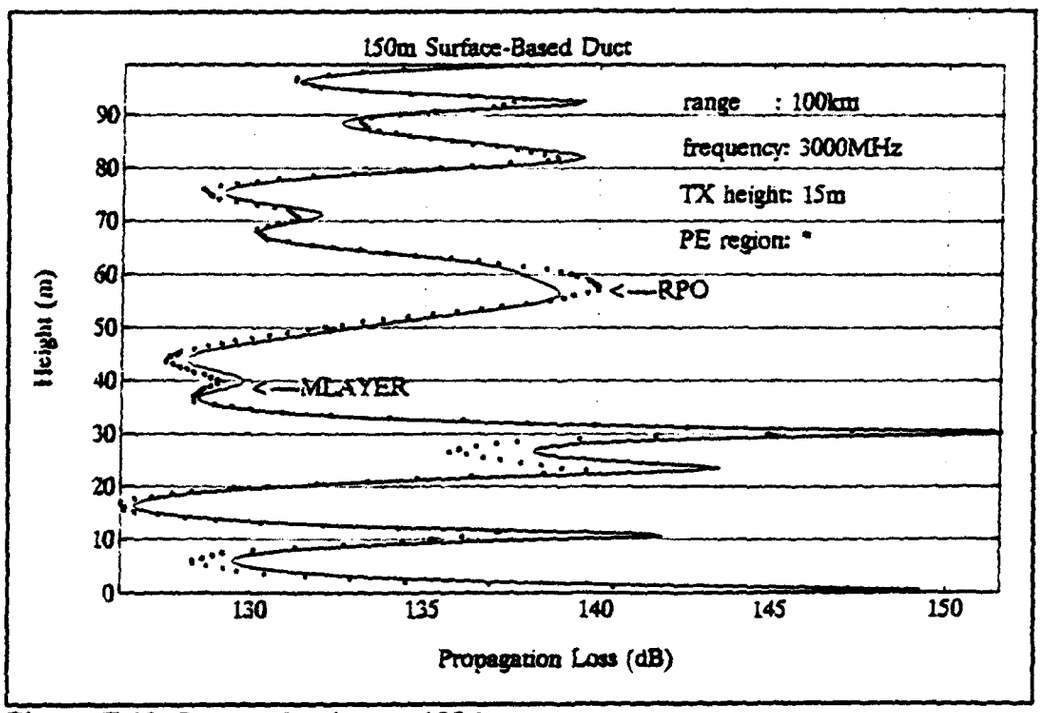

Figure E.12. Propagation loss at 100 km.

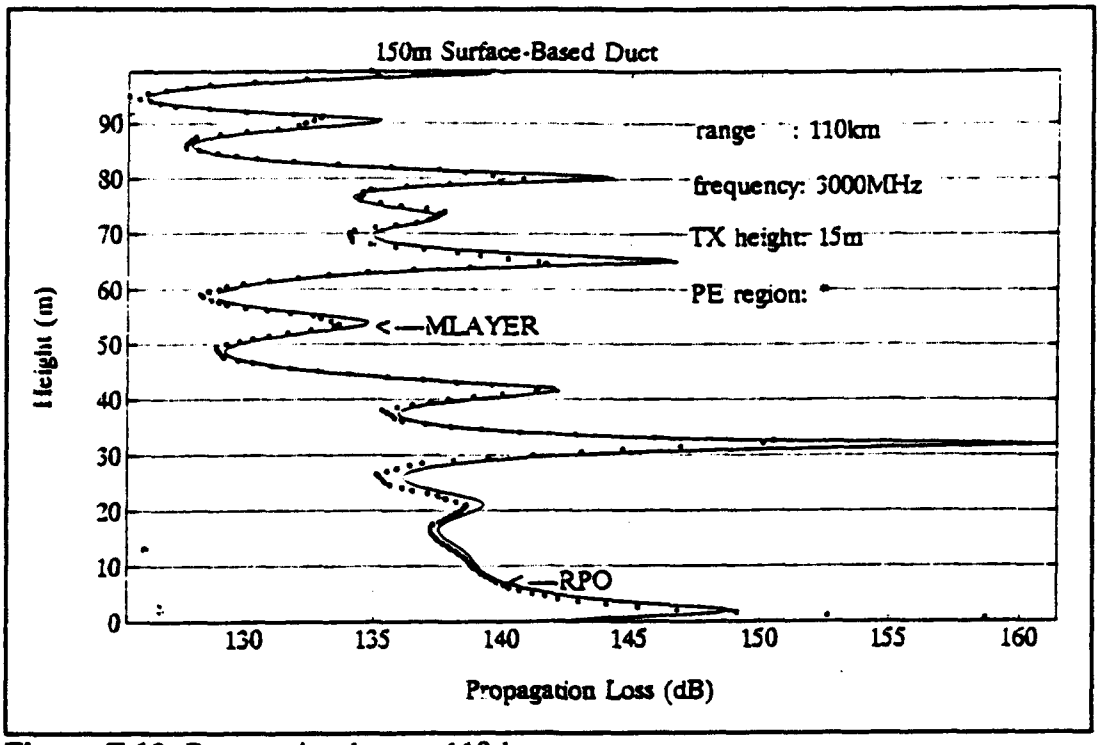

Figure E.13. Propagation loss at 110 km.

2. Propagation loss at 6 GHz

Figures E.14 through E.26 displays the propagation loss at 6 GHz computed by RPO and M-Layer.

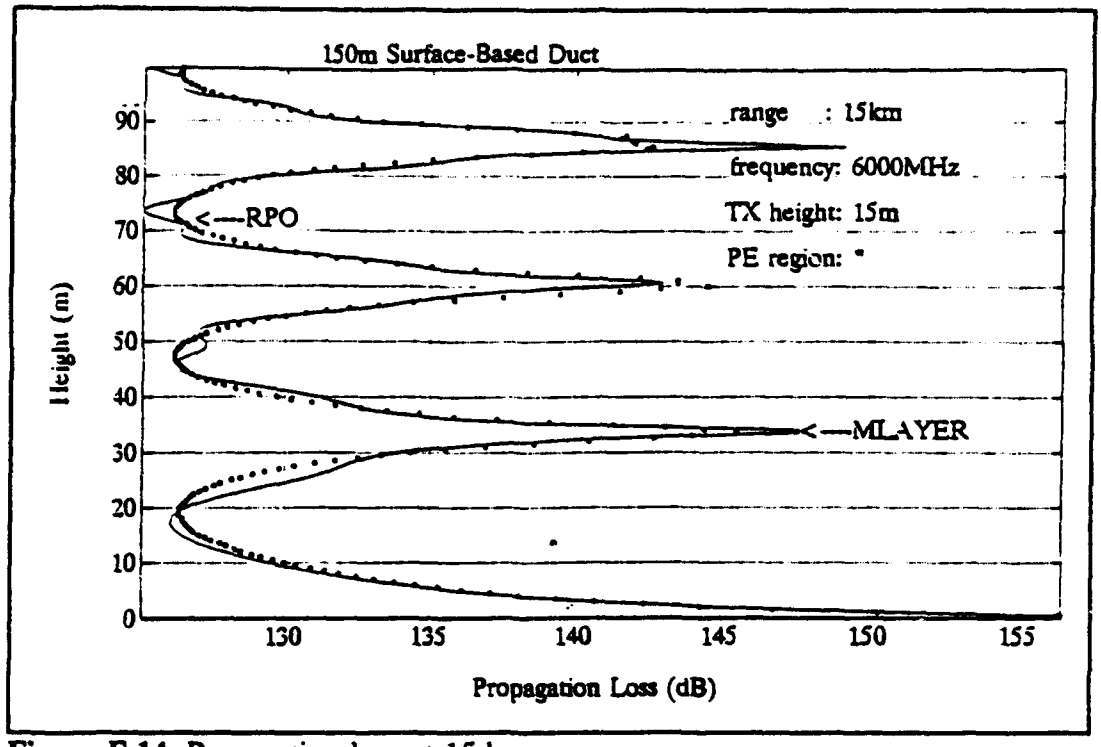

Figure E.14. Propagation loss at 15 km.

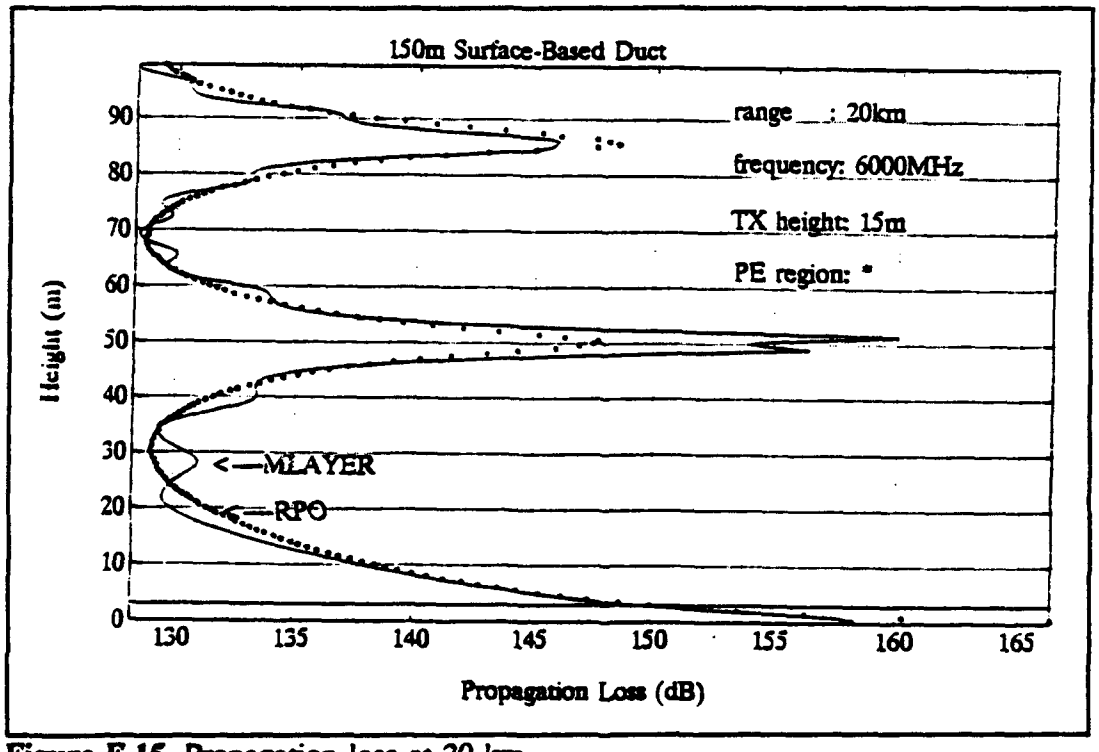

Figure E.15. Propagation loss at 20 km.

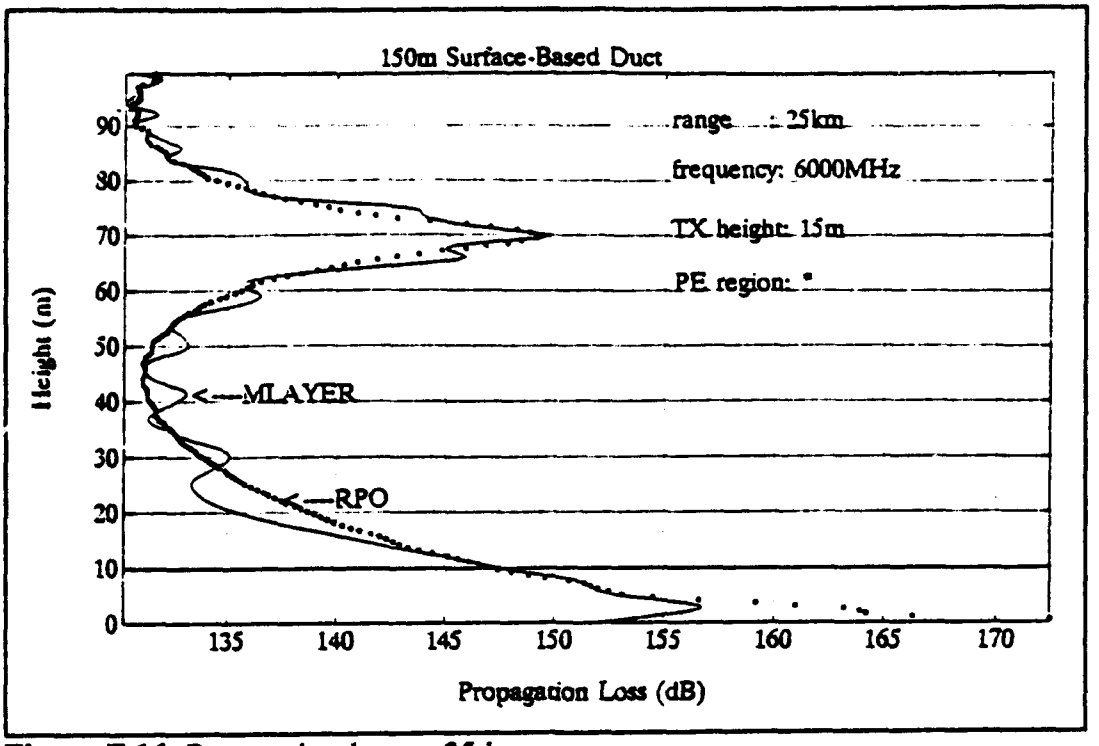

Figure E.16. Propagation loss at 25 km.

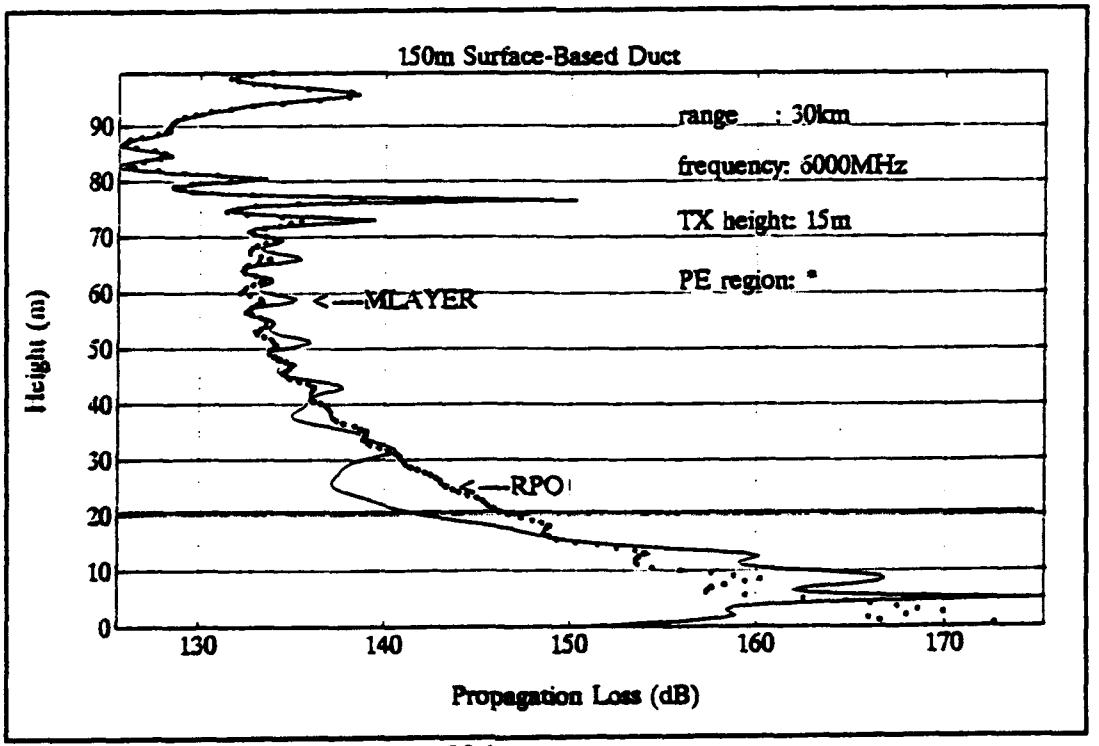

Figure E.17. Propagation loss at 30 km.

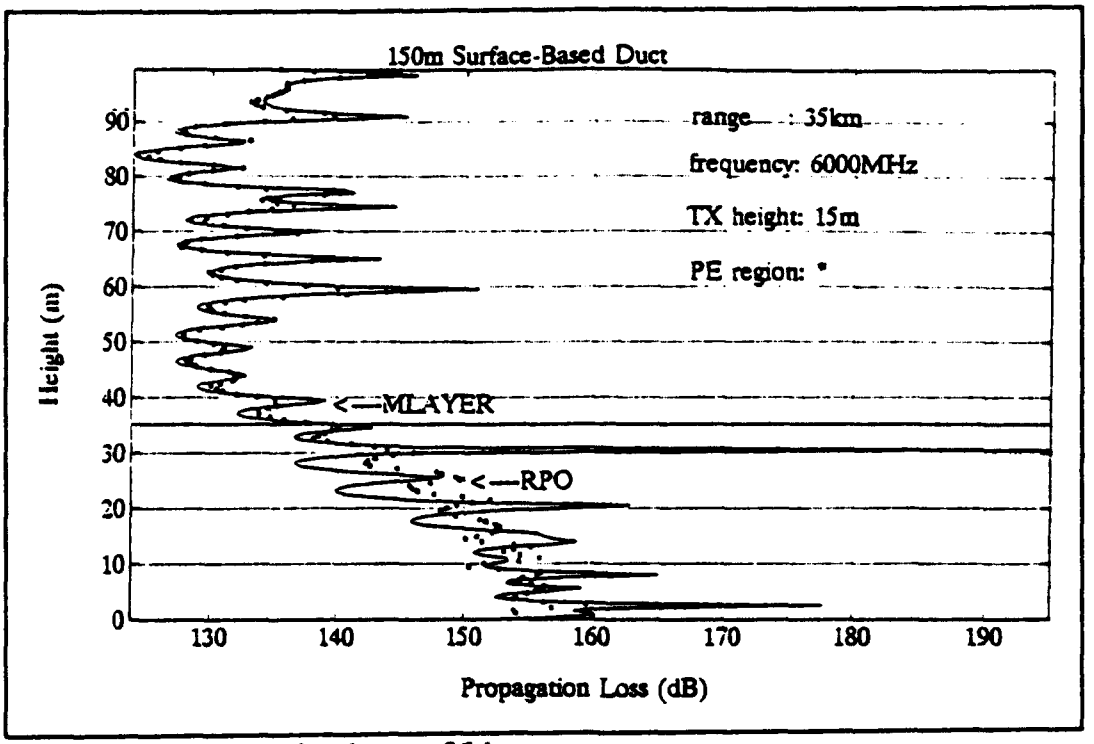

Figure E.18. Propagation loss at 35 km.

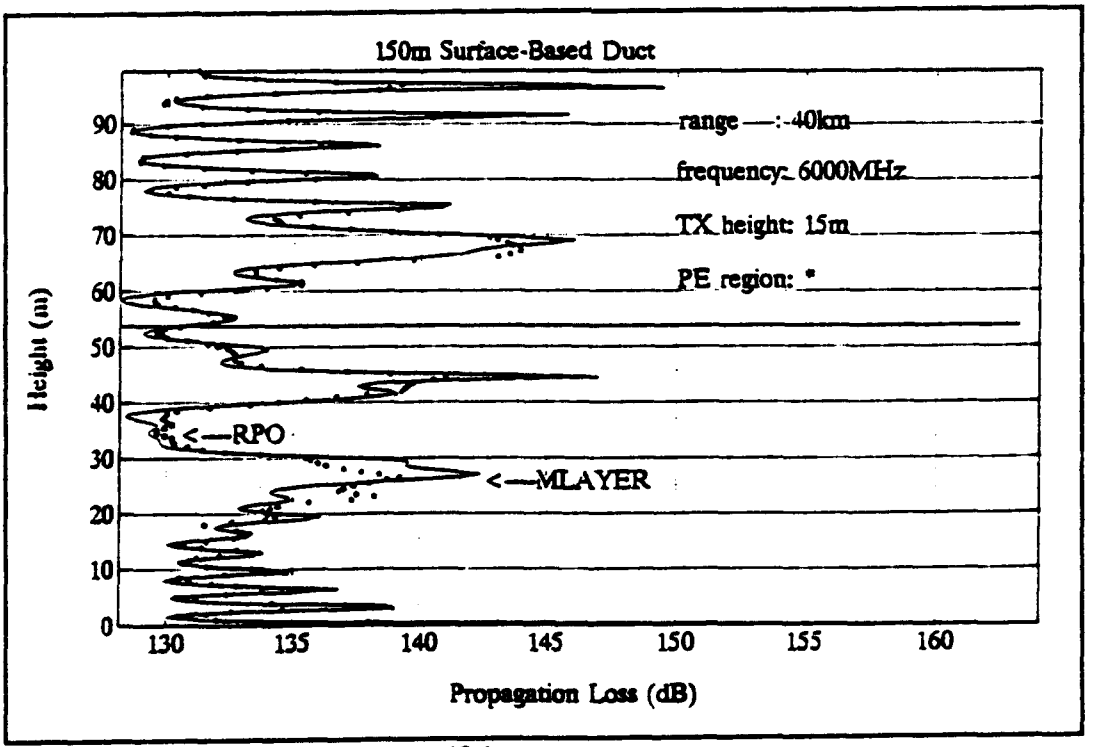

Figure E.19. Propagation loss at 40 km.

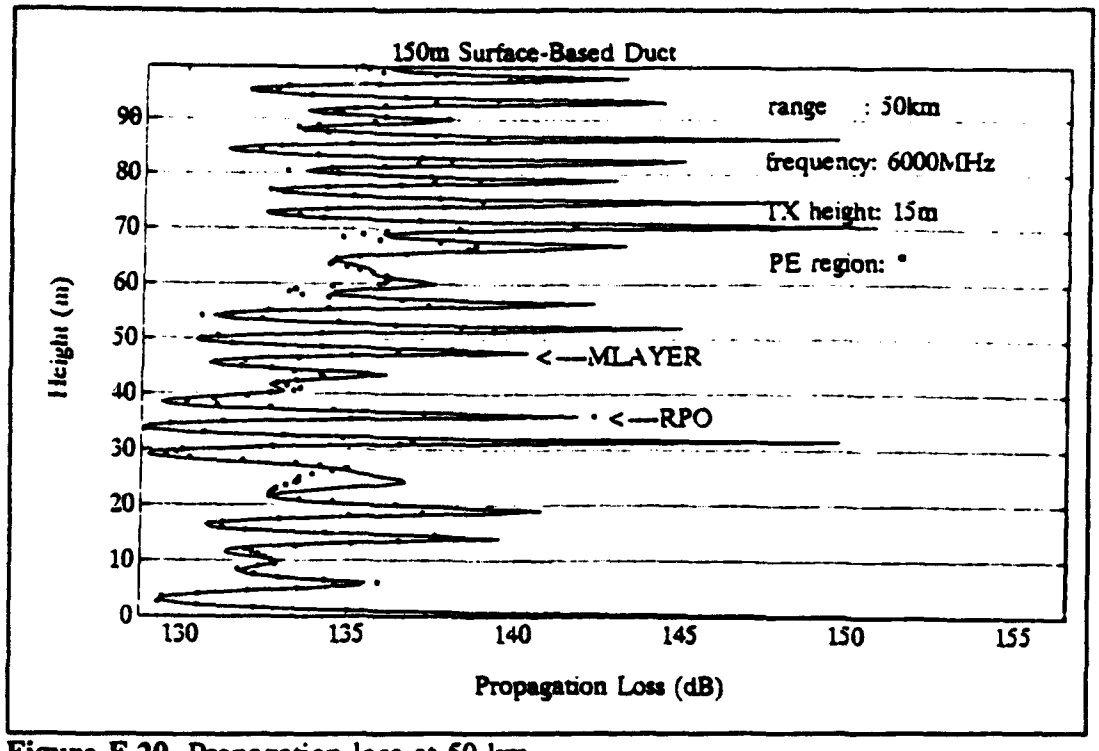

Figure E.20. Propagation loss at 50 km.

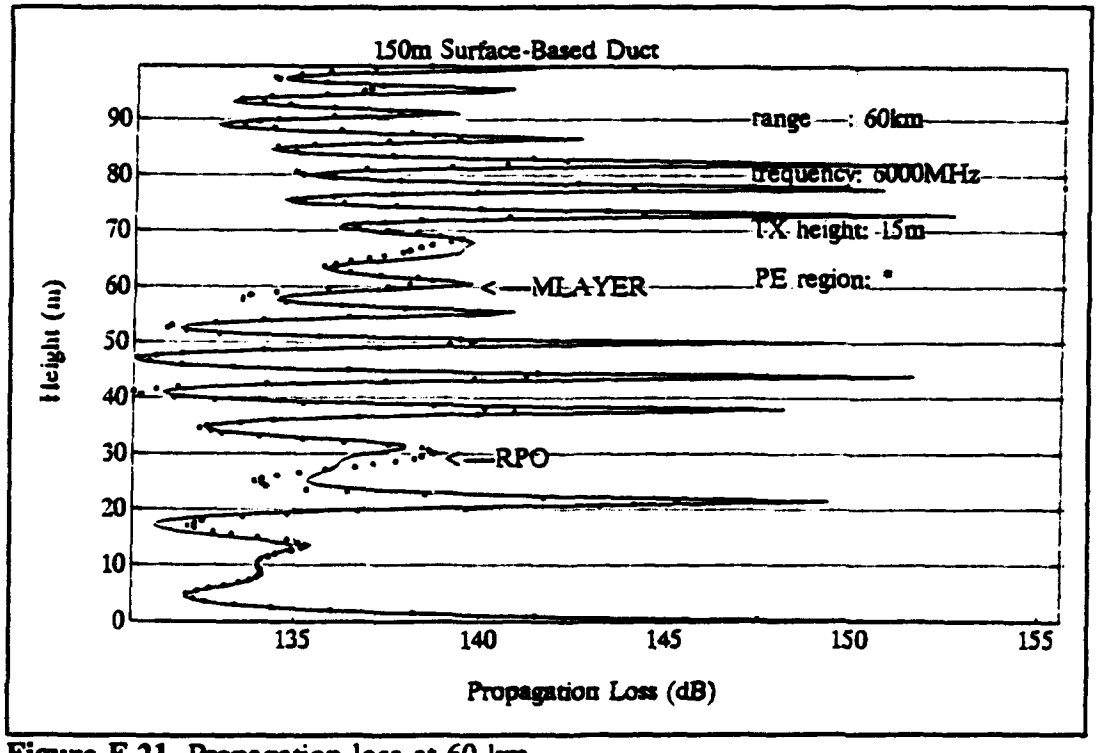

Figure E.21. Propagation loss at 60 km.

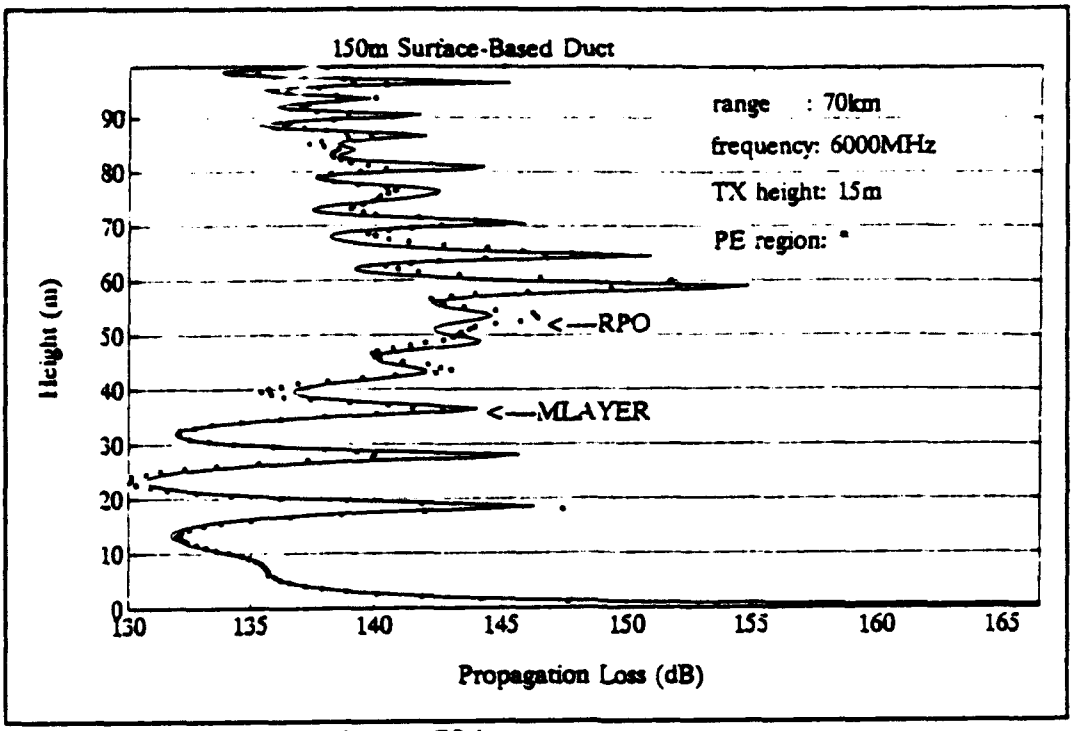

Figure E.22. Propagation loss at 70 km.

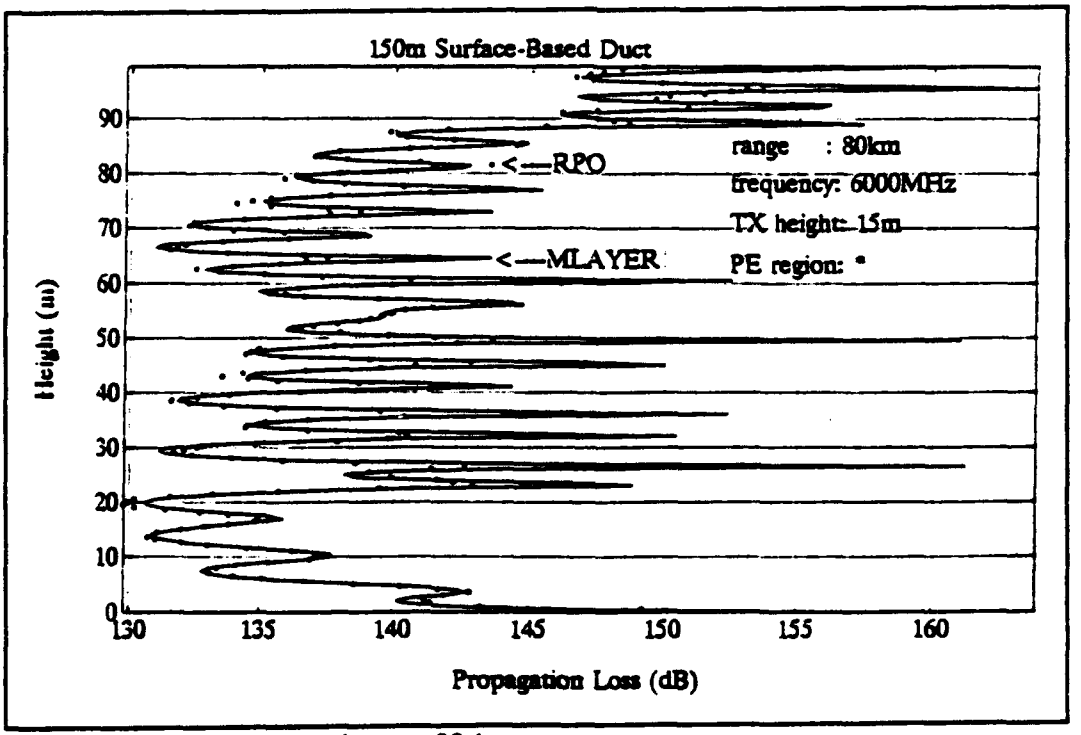

Figure E.23. Propagation loss at 80 km.

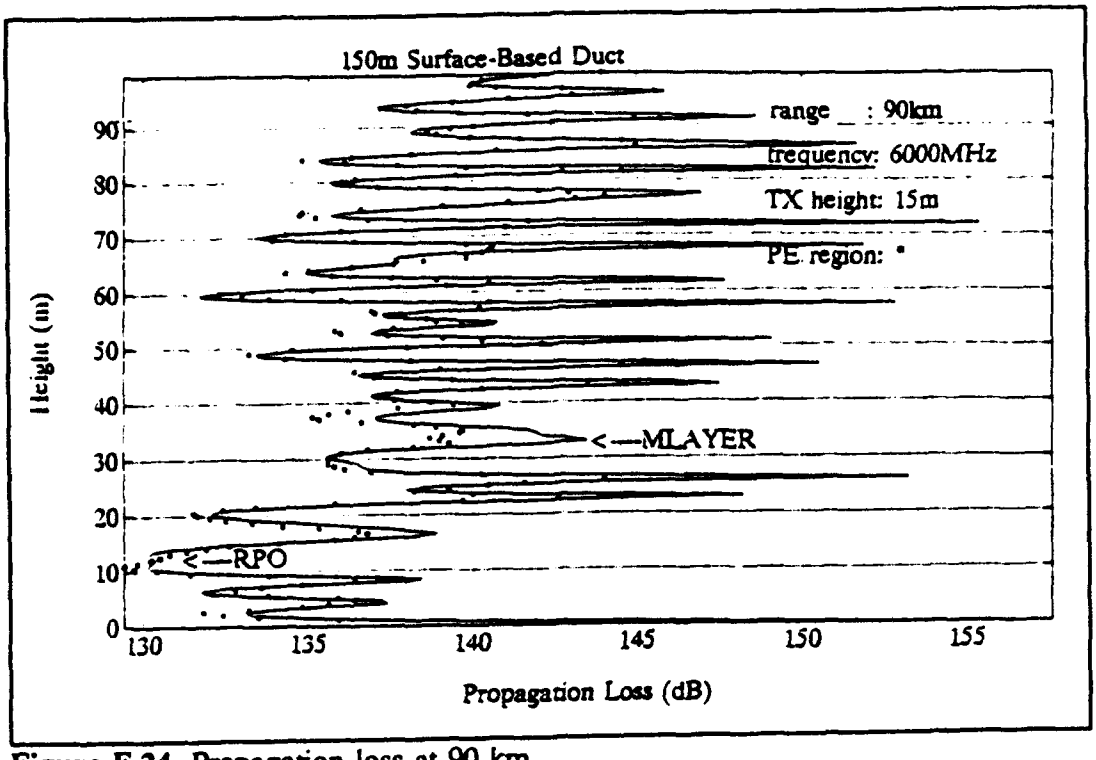

Figure E.24. Propagation loss at 90 km.

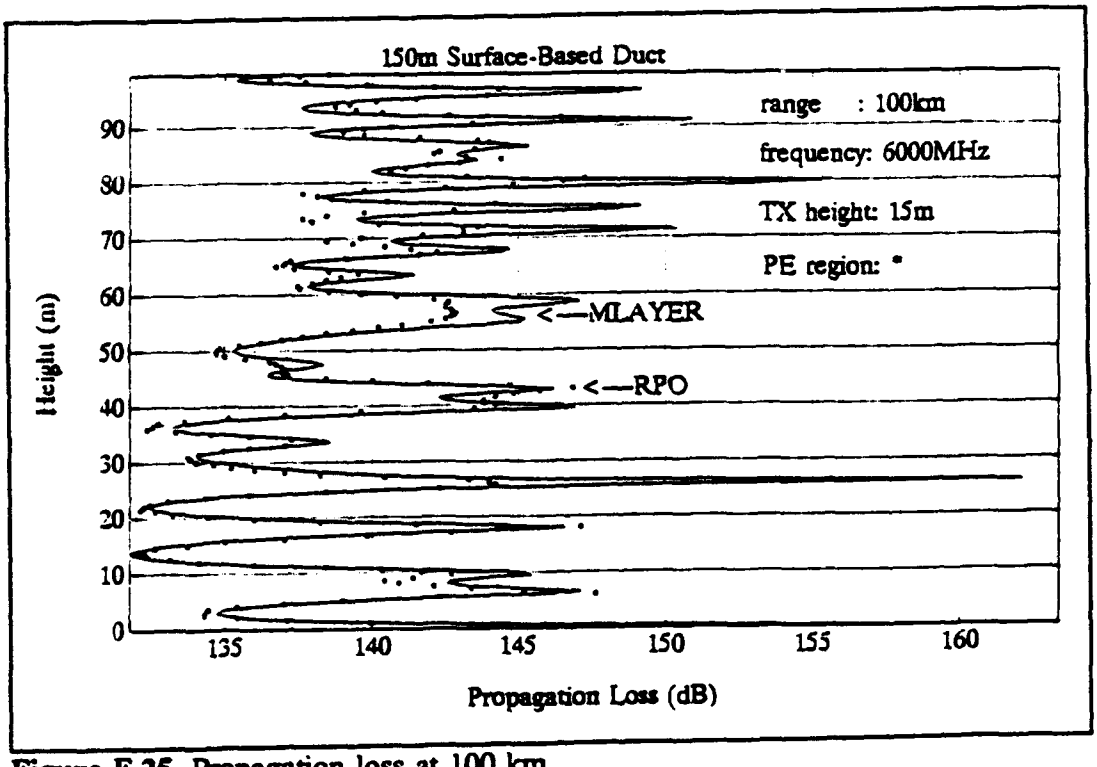

Figure E.25. Propagation loss at 100 km.

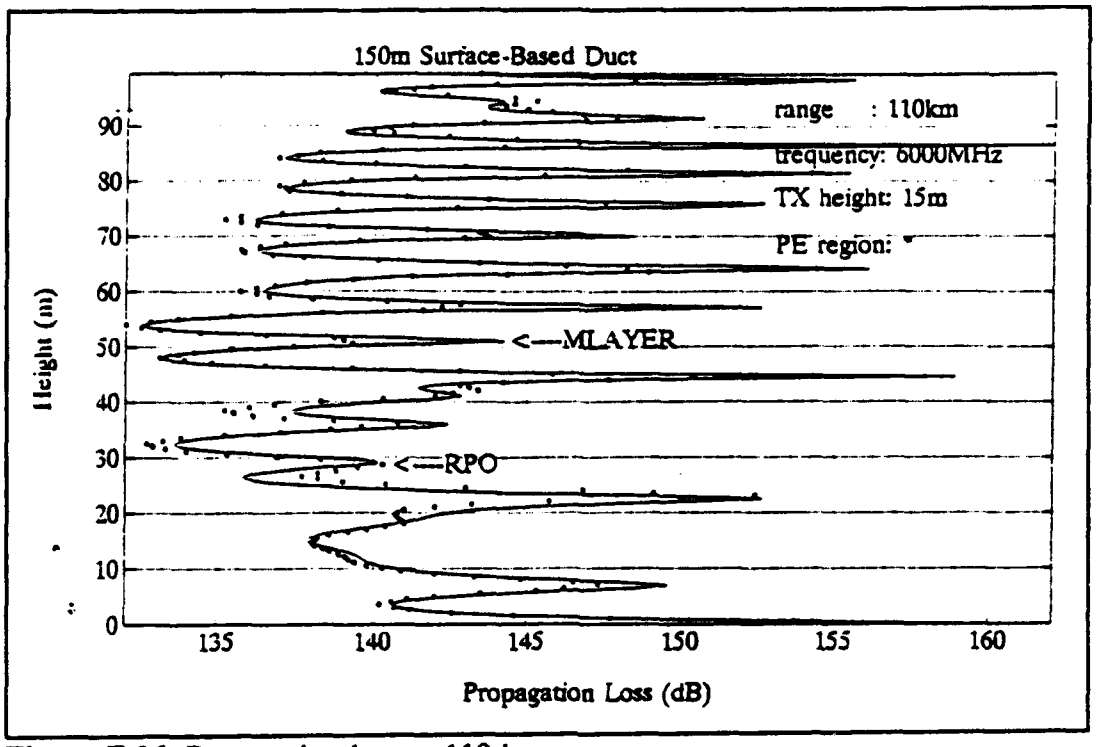

Figure E.26. Propagation loss at 110 km.

3. Propagation loss at 12 GHz

Figures E.27 through E.39 displays the propagation loss at 12 GHz computed by RPO and M-Layer.

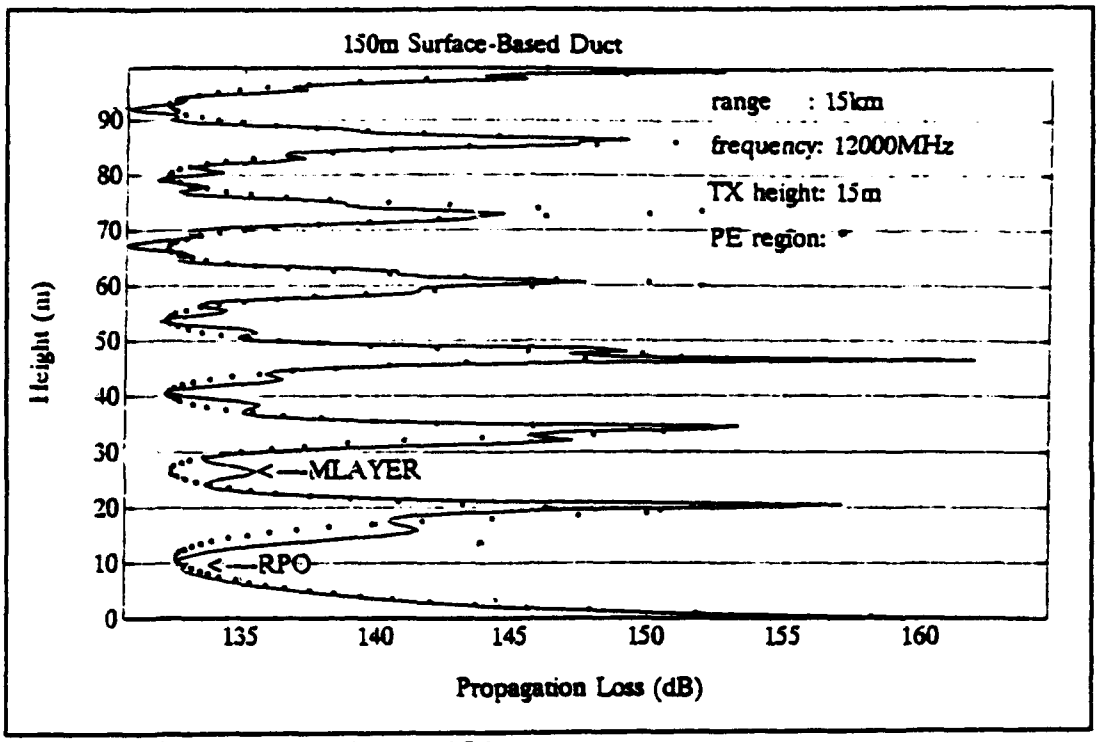

Figure E.27. Propagation loss at 15 km.

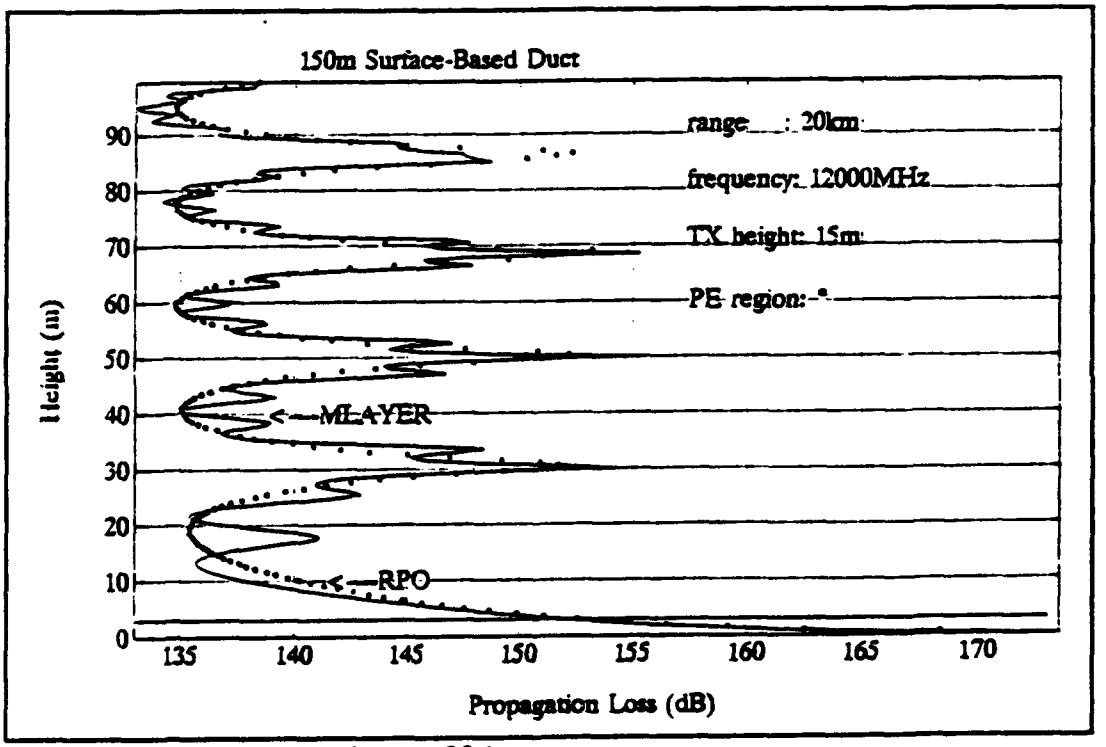

Figure E.28. Propagation loss at 20 km.

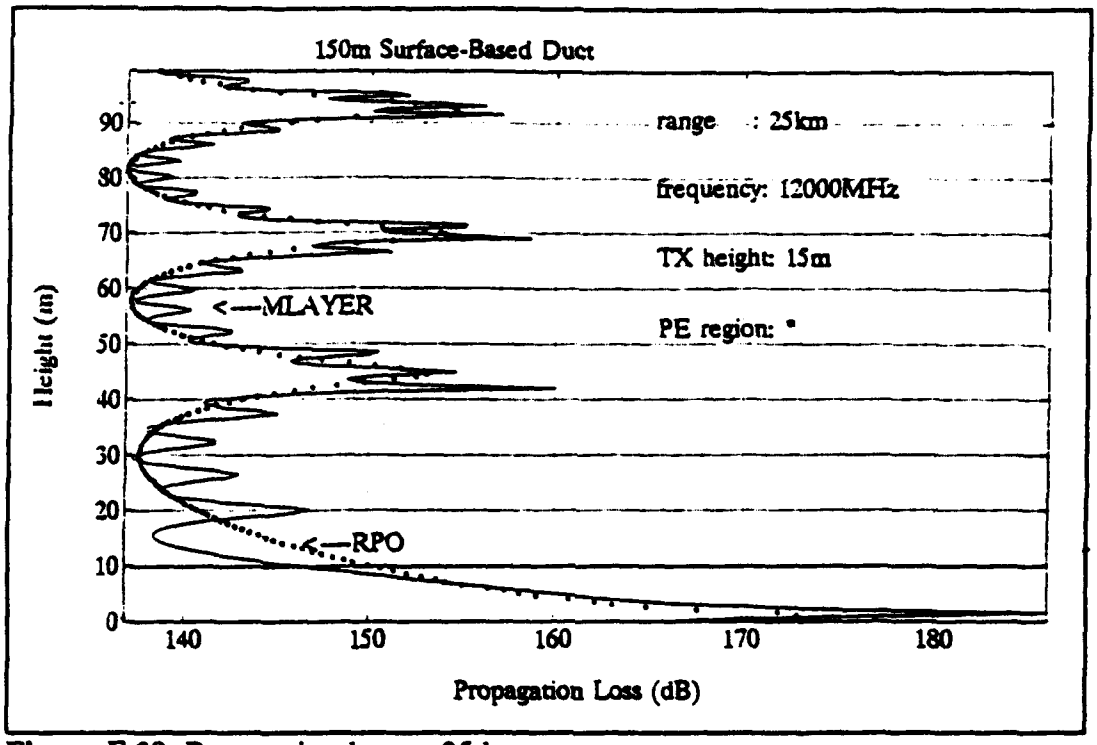

Figure E.29. Propagation loss at 25 km.

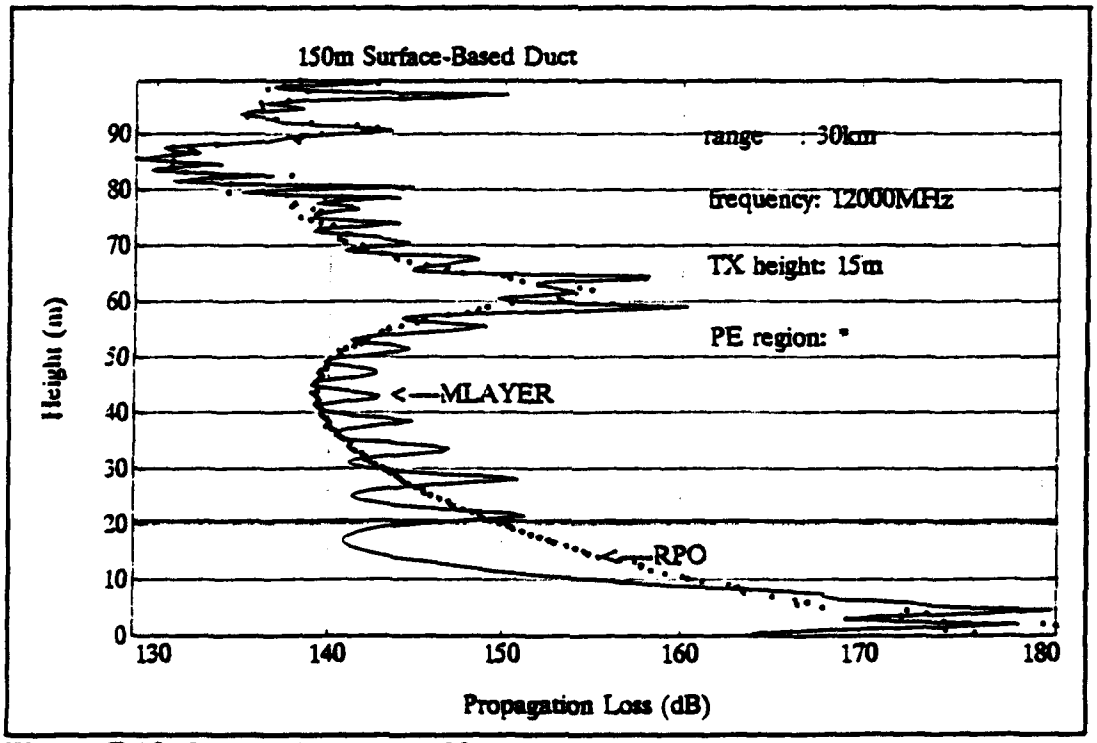

Figure E.30. Propagation loss at 30 km.

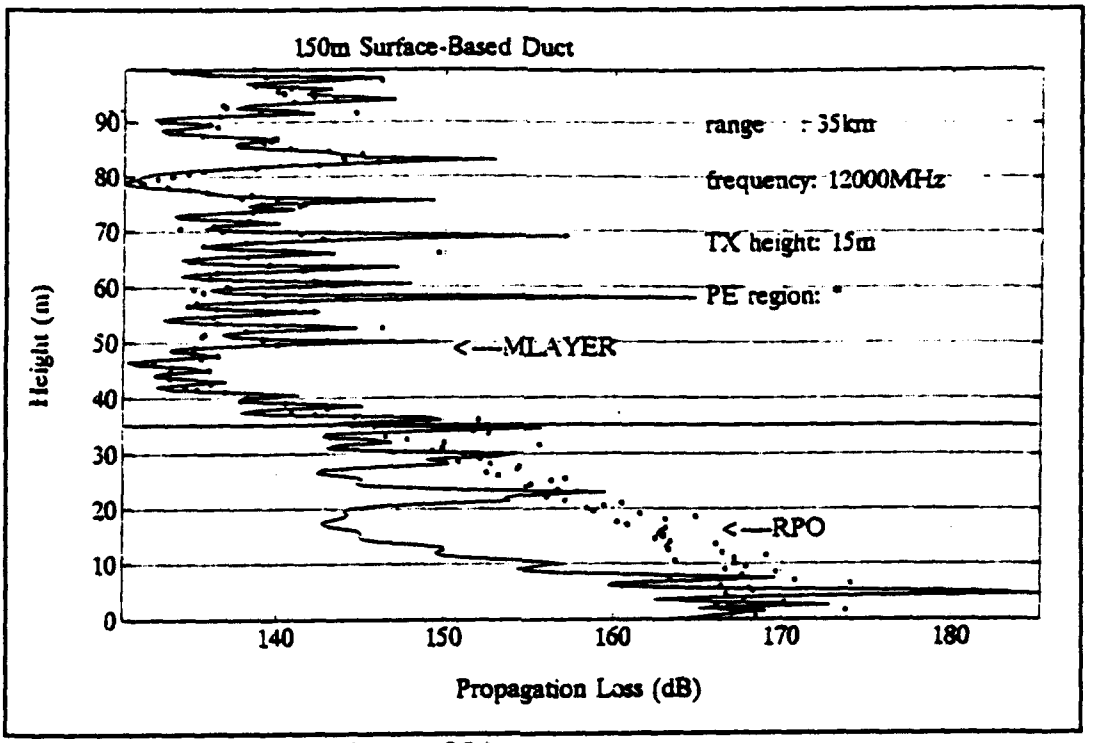

Figure E.31. Propagation loss at 35 km.

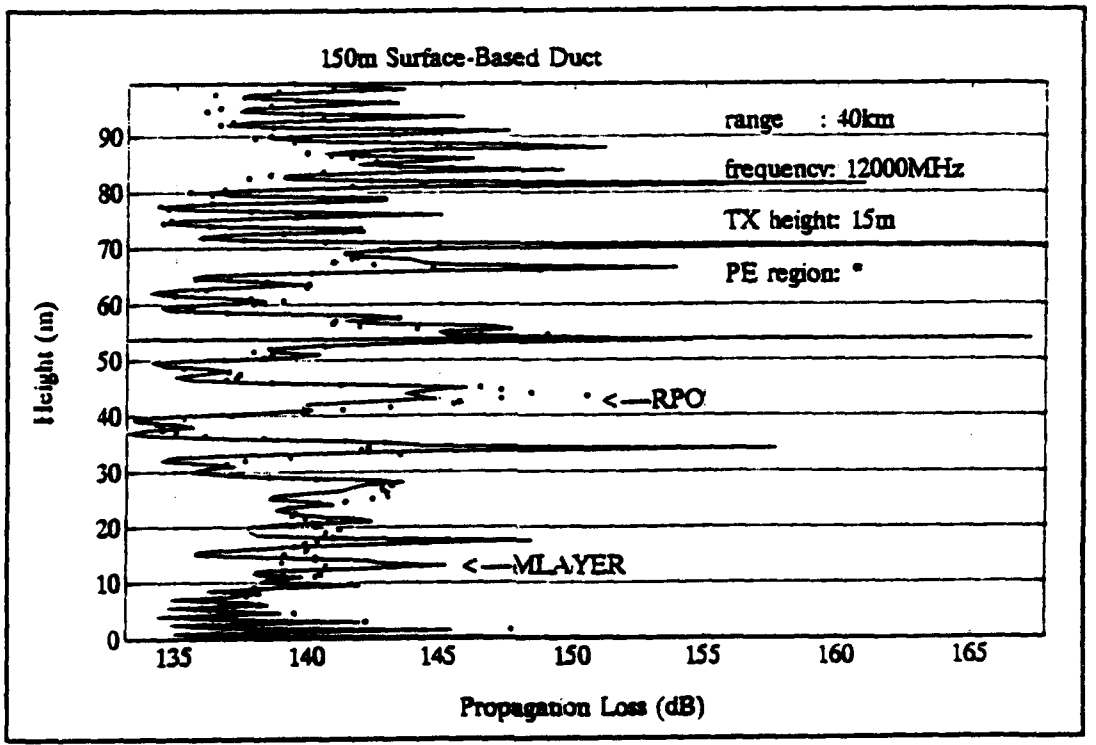

Figure E.32. Propagation loss at 40 km.

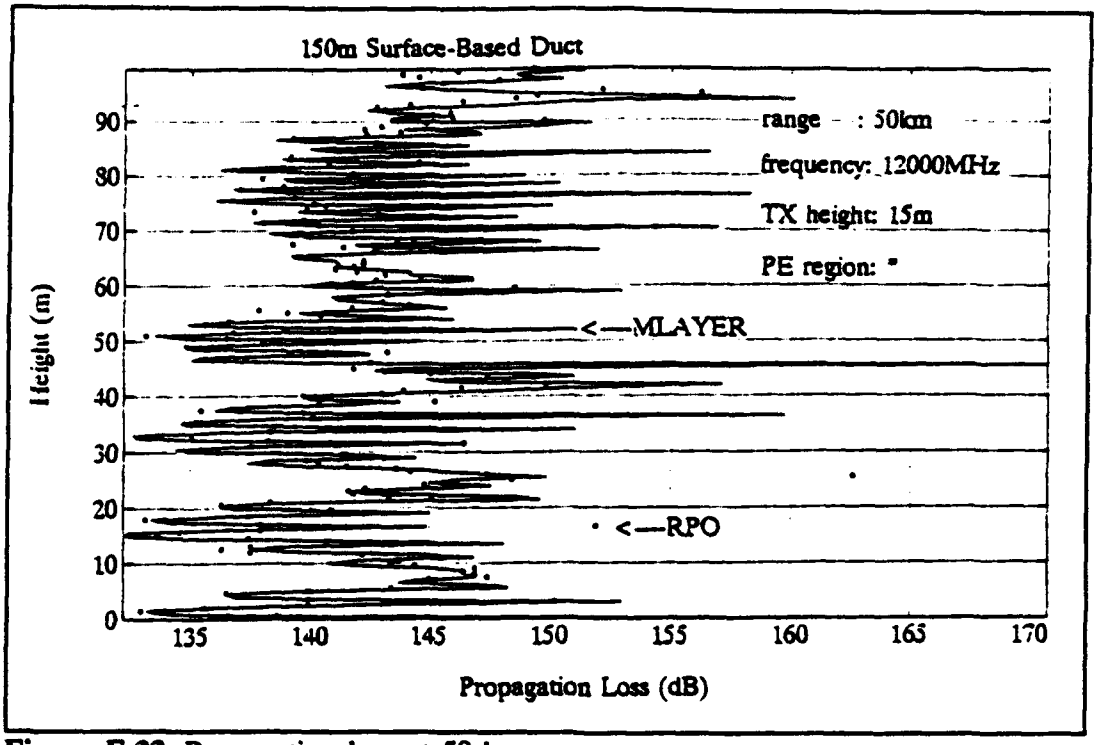

Figure E.33. Propagation loss at 50 km.

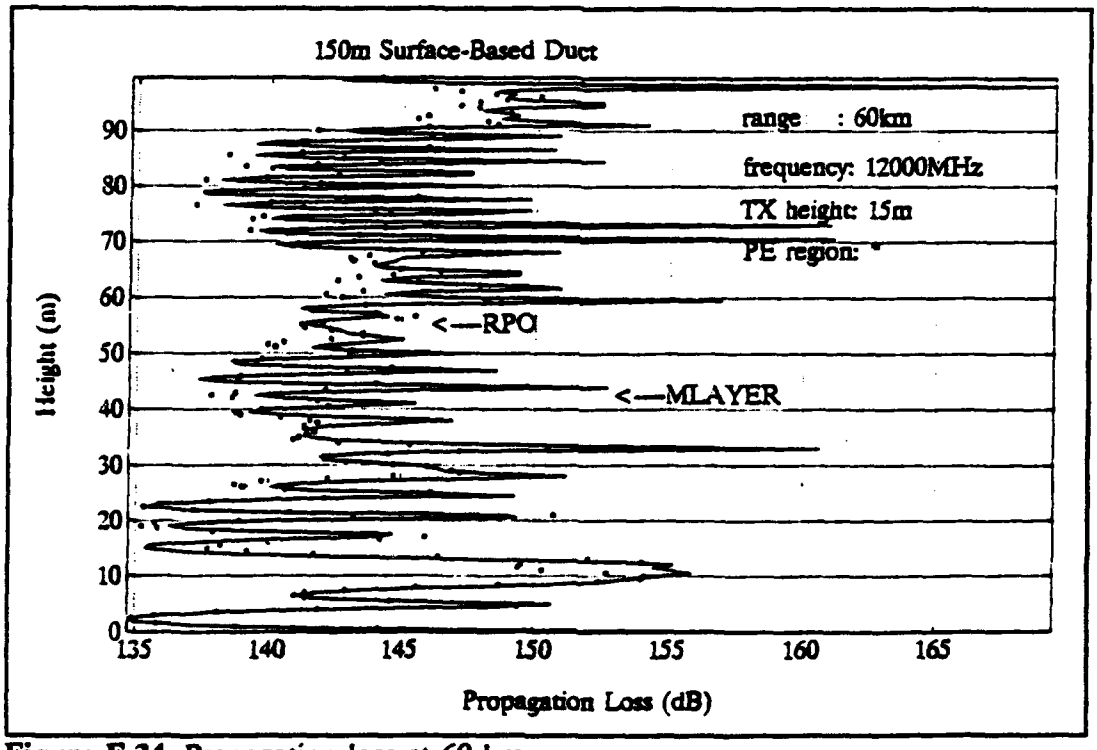

Figure E.34. Propagation loss at 60 km.

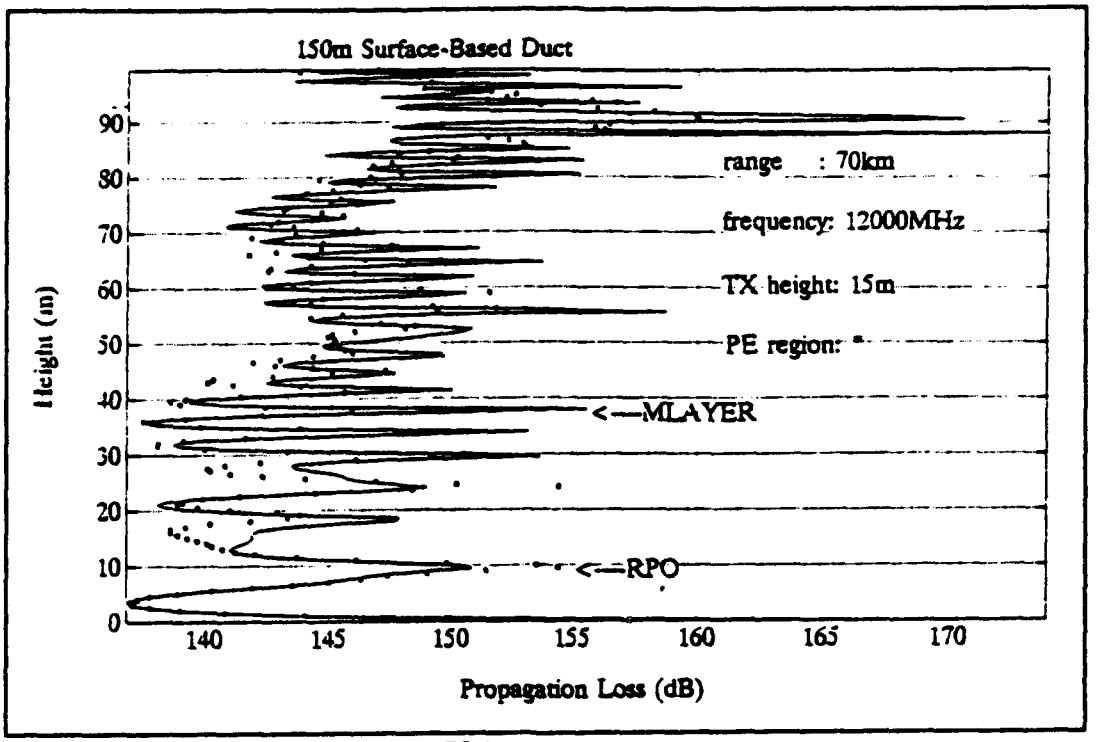

Figure E.35. Propagation loss at 70 km.

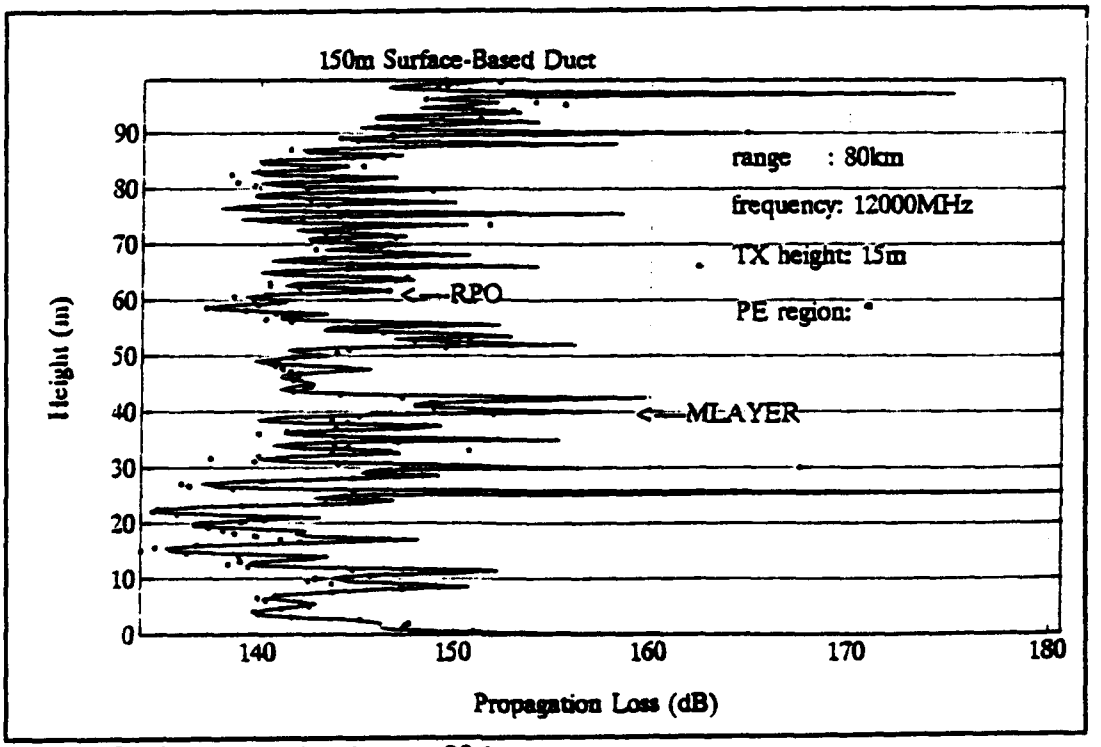

Figure E.36. Propagation loss at 80 km.

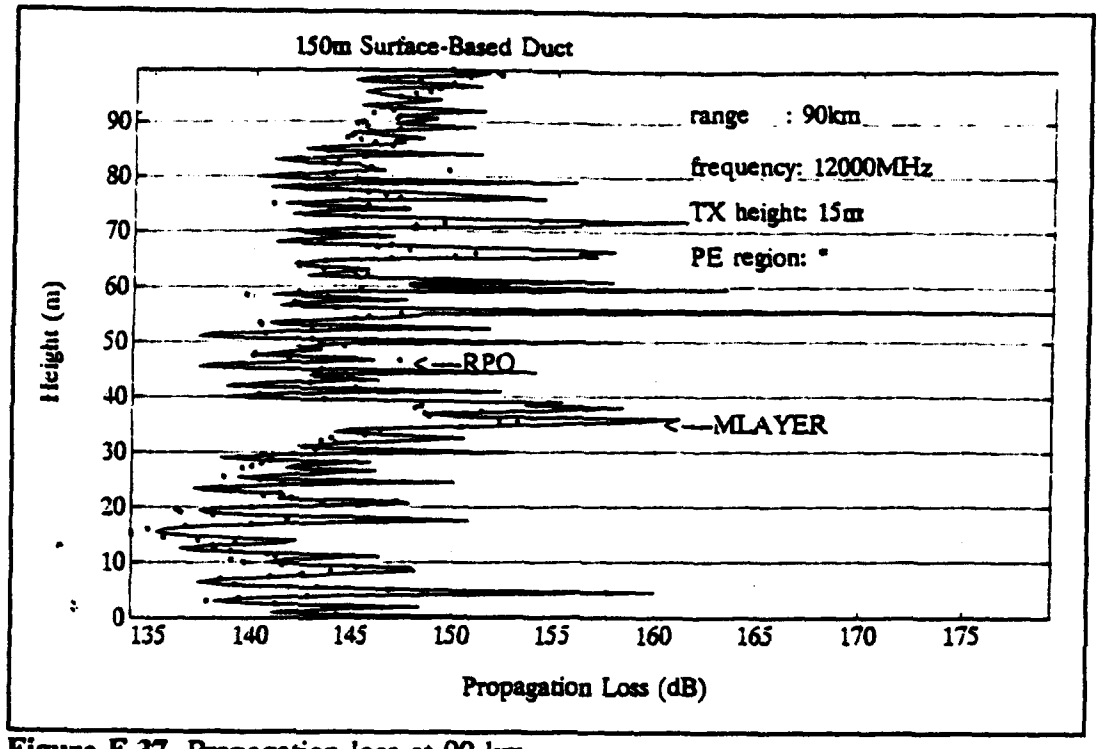

Figure E.37. Propagation loss at 90 km.

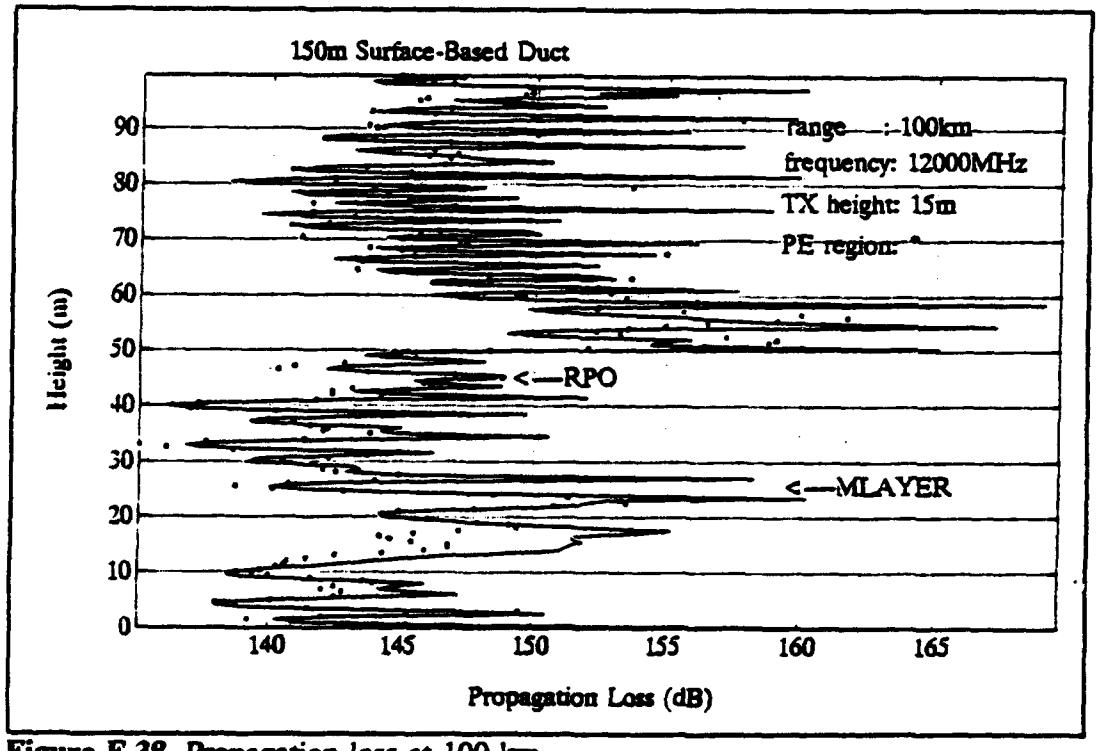

Figure E.38. Propagation loss at 100 km.

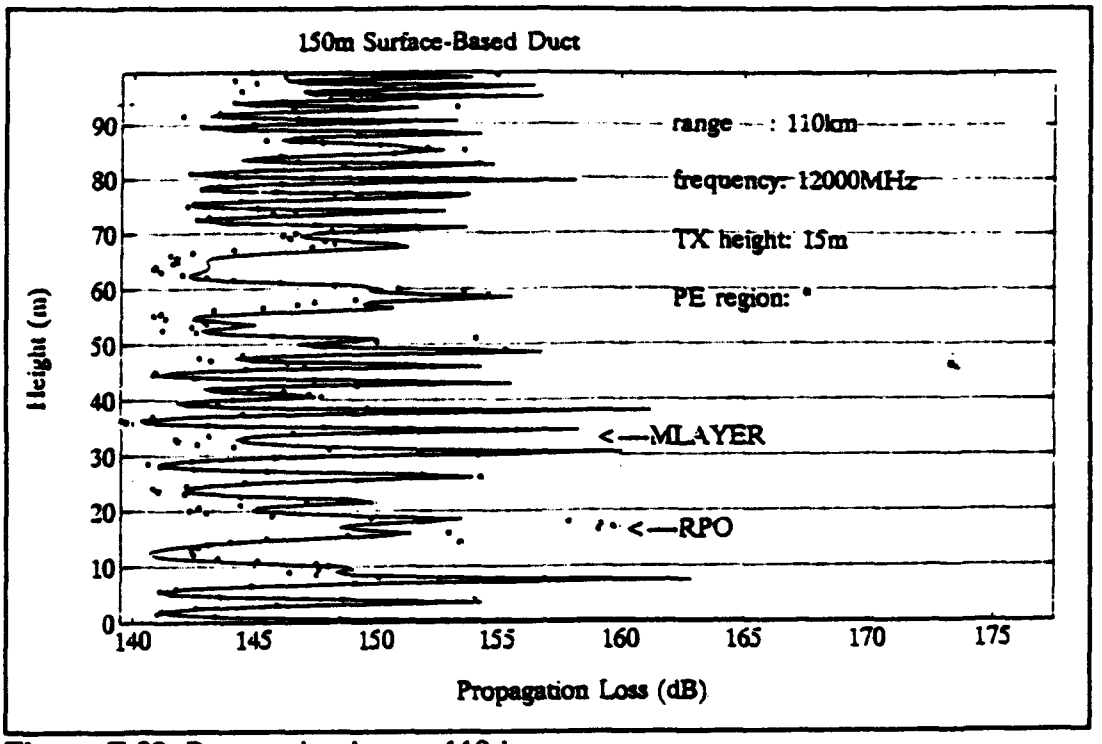

Figure E.39. Propagation loss at 110 km.

APPENDIX F: PROPAGATION LOSS UNDER THE INFLUENCE OF A 100 M SURFACE-BASED DUCT

This Appendix displays the propagation loss computed by RPO and M-Layer under the influence of a 100 m surface-based duct at 3 GHz, 6 GHz and 12 GHz at ranges of 15, 20, 25, 30, 35, 40, 50, 60, 70, 80, 90, 100 and 110 km. The modified refractivity profile is given in Table F.1.

Table F.1. A 100 m surface-based duct.

i	Z_i meters	M_i
0	0.0	339.0
1	50.0	344.9
2	100.0	295.4
3	1000.0	401.6

1. Propagation loss at 3 GHz

Figures F.1 through F.13 displays the propagation loss at 3 GHz computed by RPO and M-Layer.

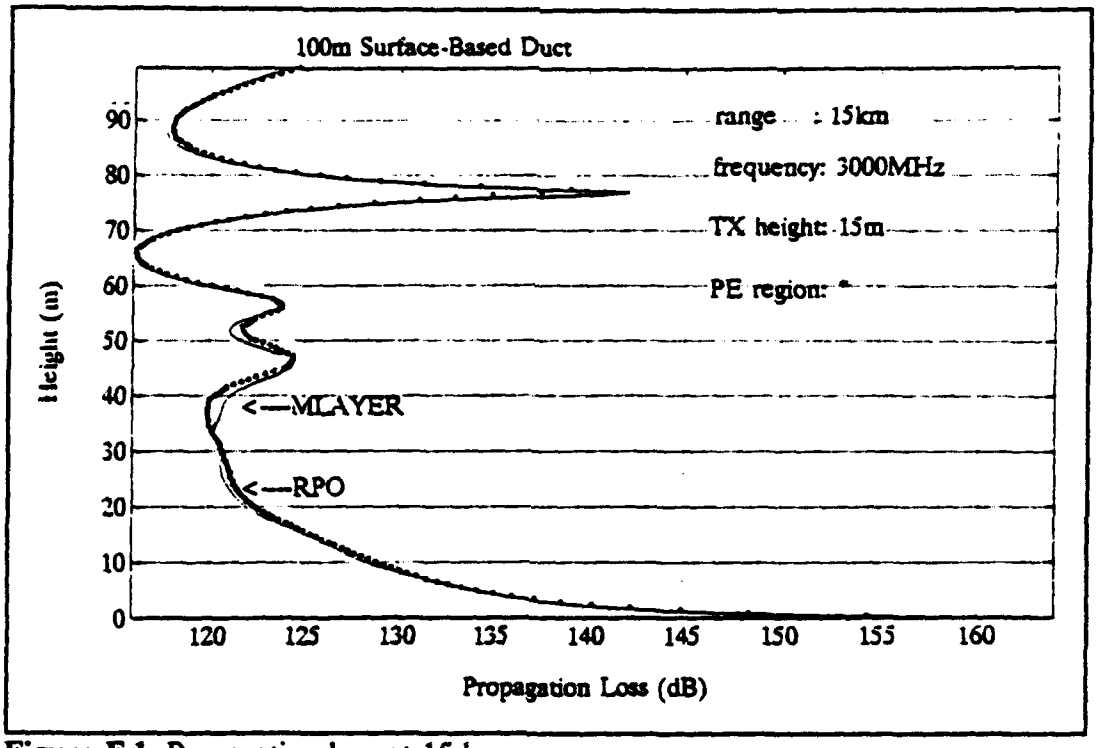

Figure F.1. Propagation loss at 15 km.

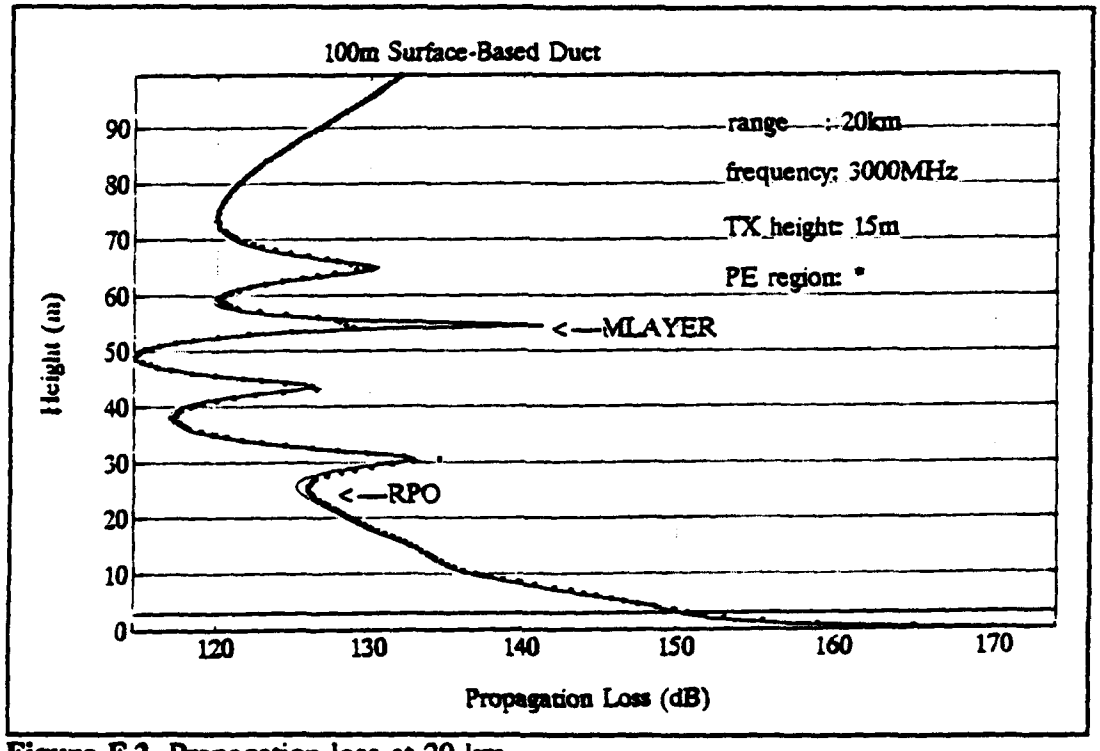

Figure F.2. Propagation loss at 20 km.

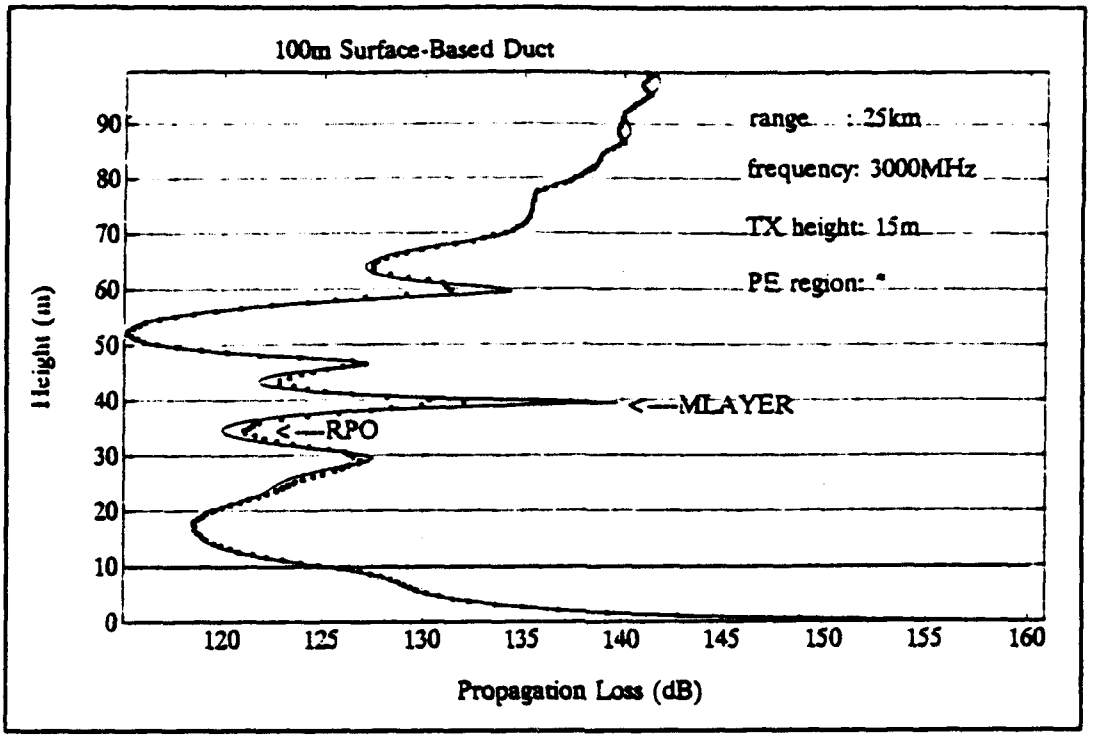

Figure F.3. Propagation loss at 25 km.

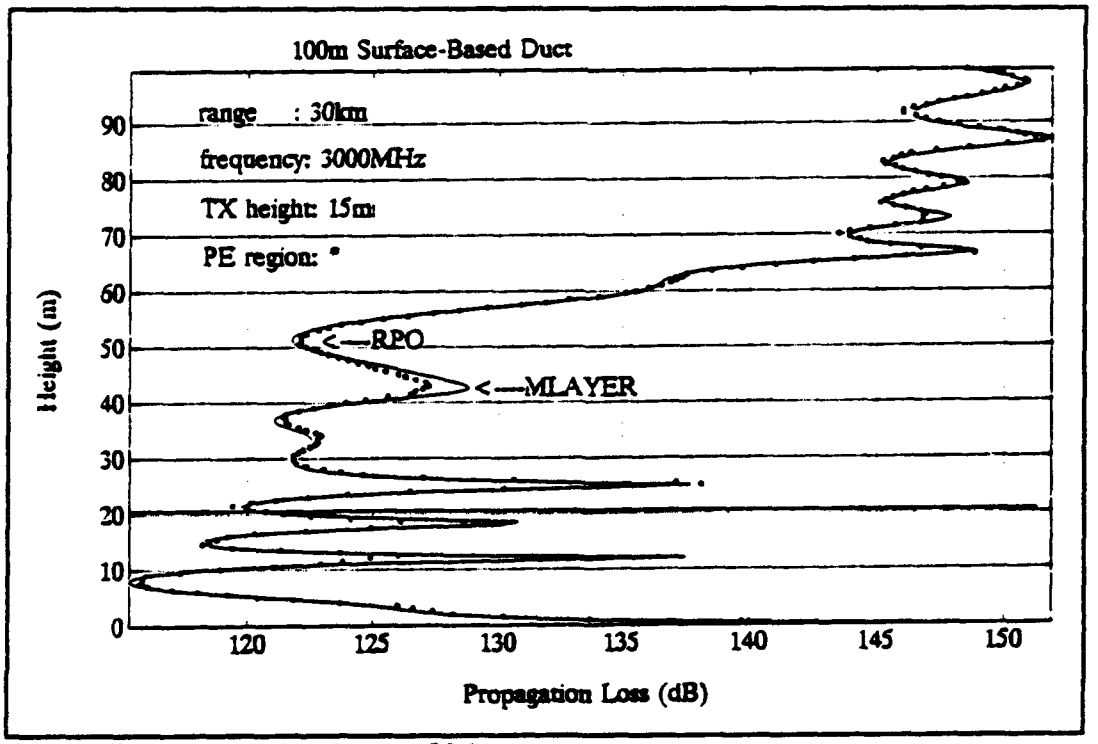

Figure F.4. Propagation loss at 30 km.

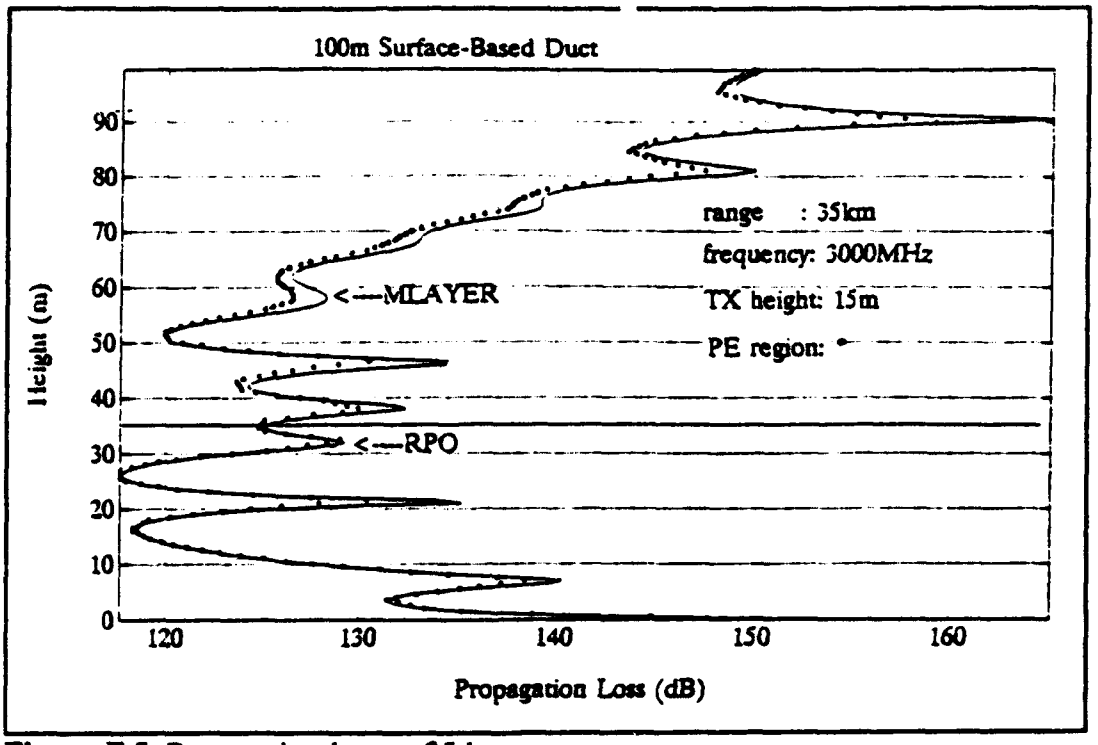

Figure F.5. Propagation loss at 35 km.

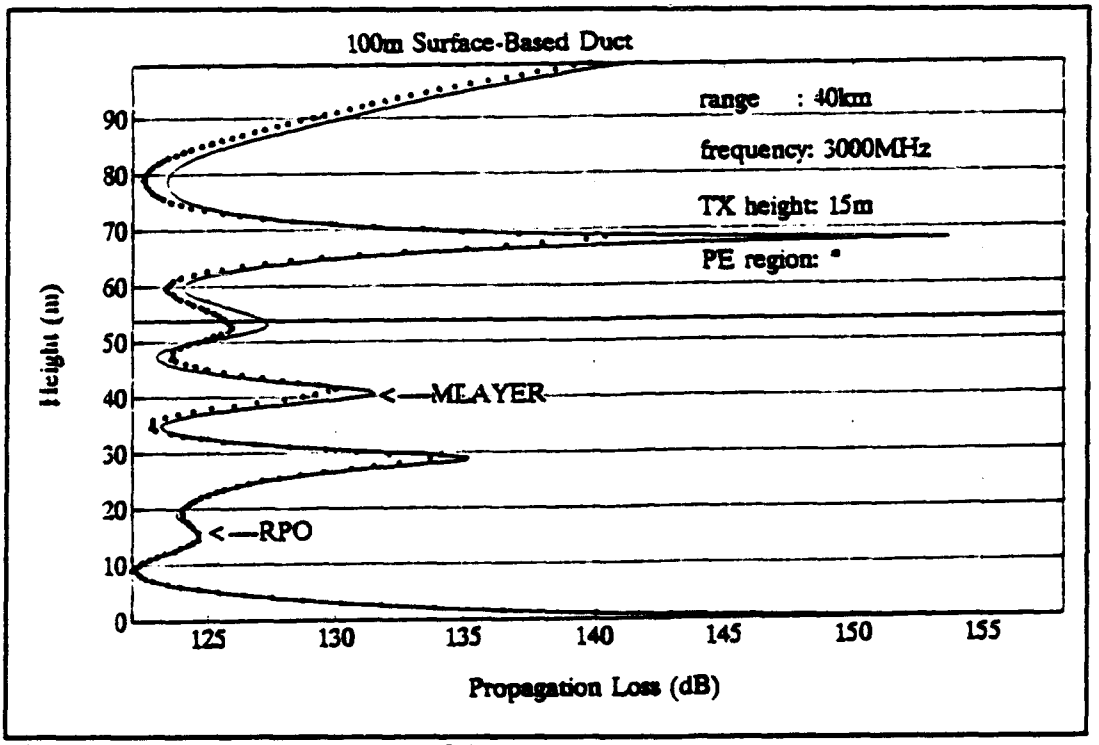

Figure F.6. Propagation loss at 40 km.

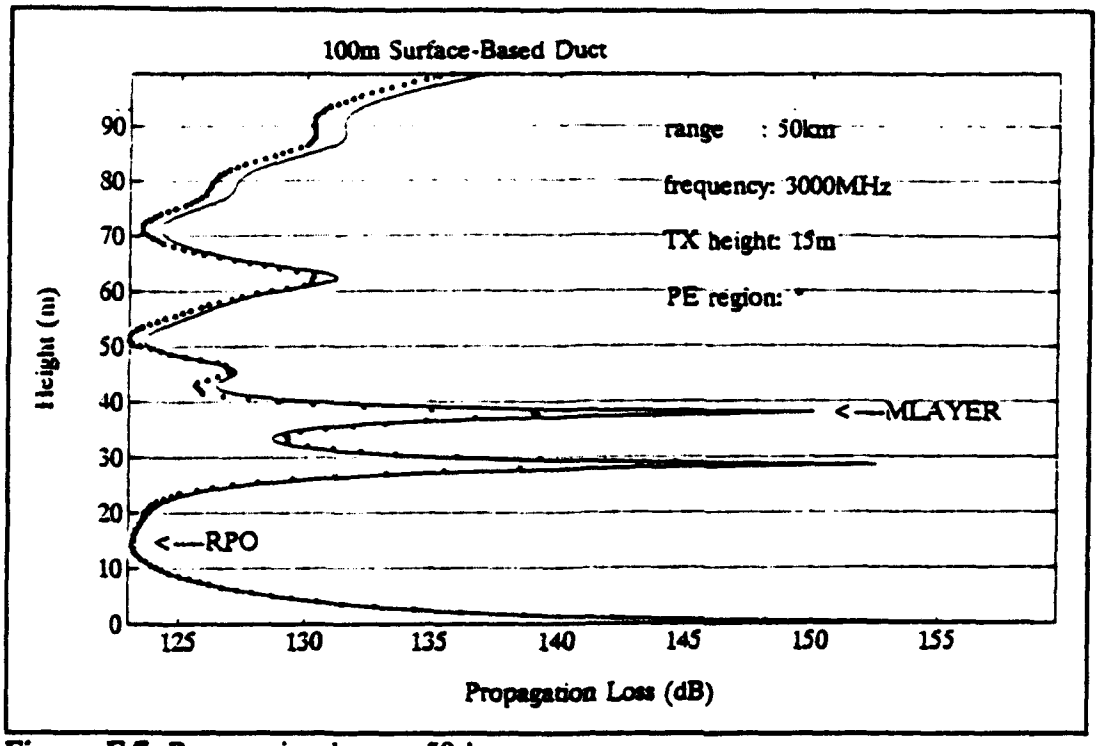

Figure F.7. Propagation loss at 50 km.

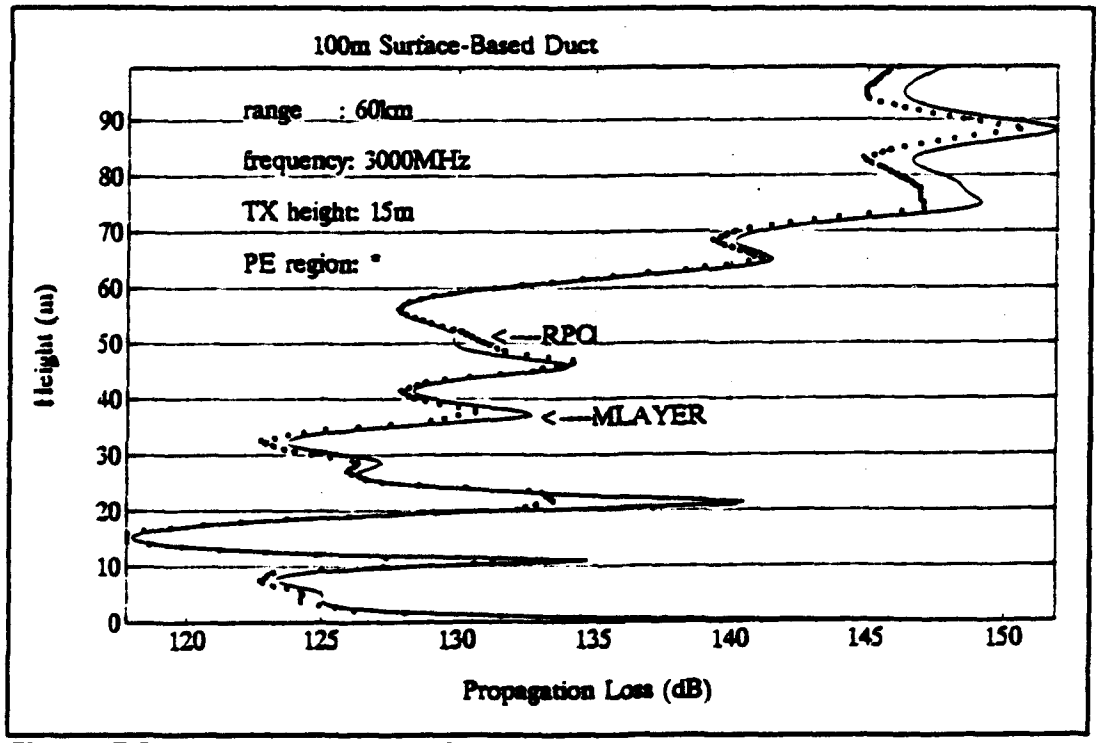

Figure F.8. Propagation loss at 60 km.

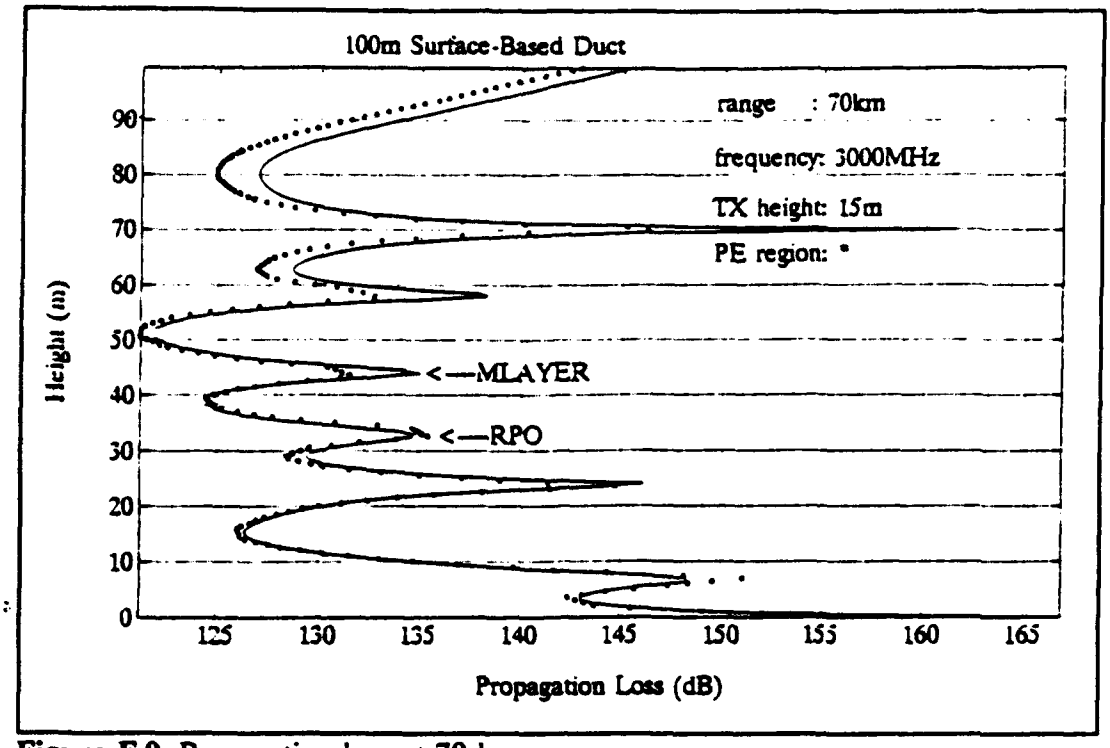

Figure F.9. Propagation loss at 70 km.

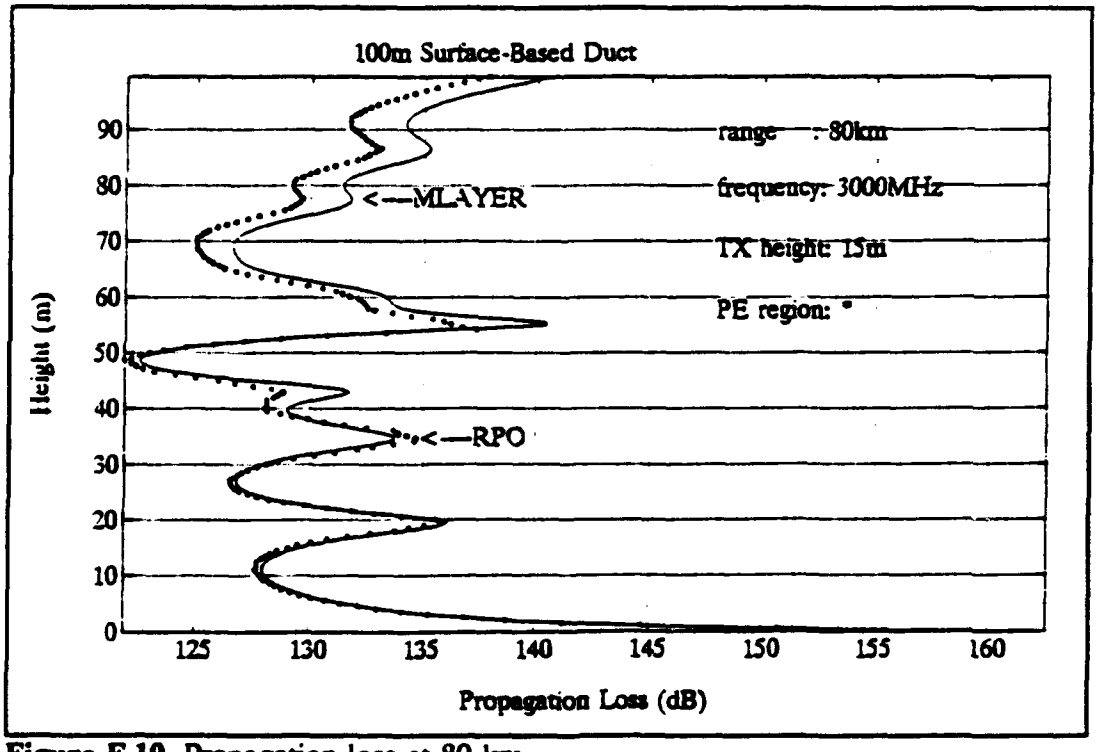

Figure F.10. Propagation loss at 80 km.

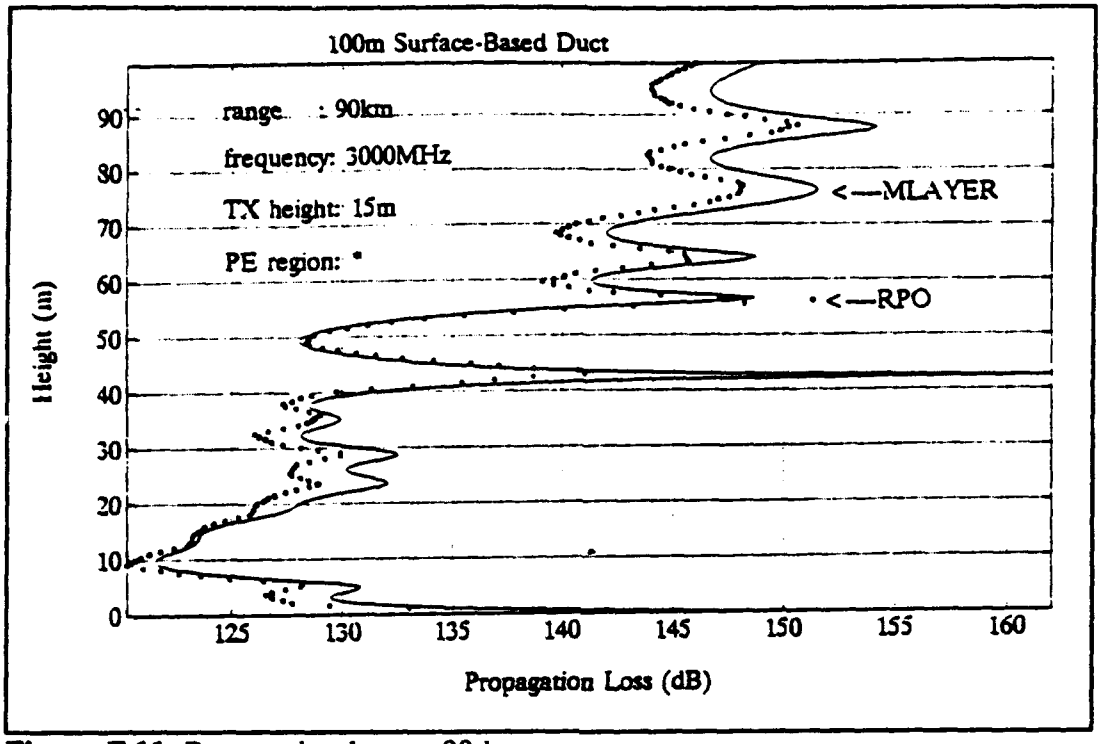

Figure F.11. Propagation loss at 90 km.

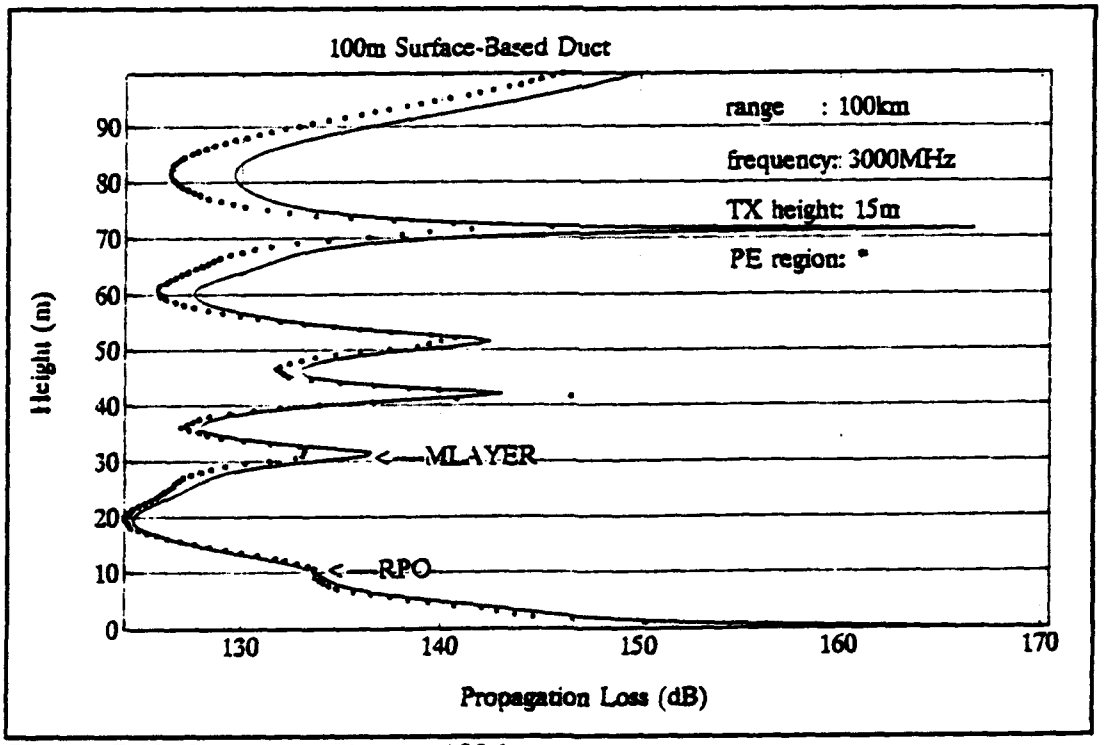

Figure F.12. Propagation loss at 100 km.

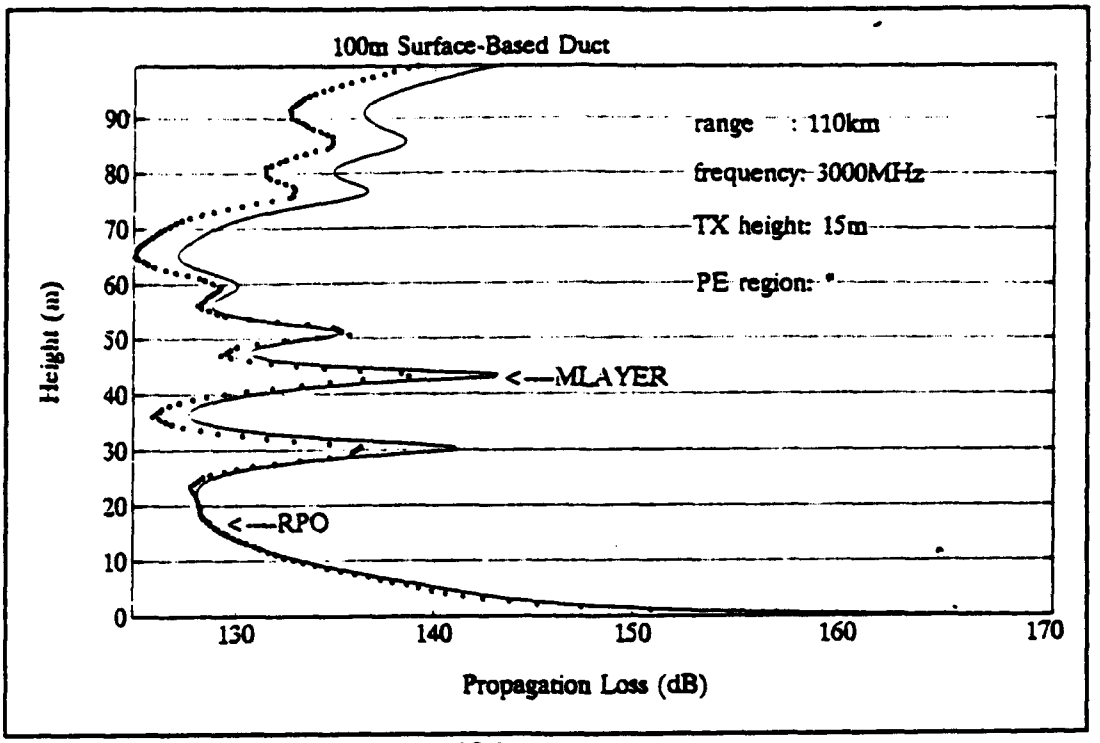

Figure F.13. Propagation loss at 110 km.

2. Propagation loss at 6 GHz

Figures F.14 through F.26 displays the propagation loss at 6 GHz computed by RPO and M-Layer.

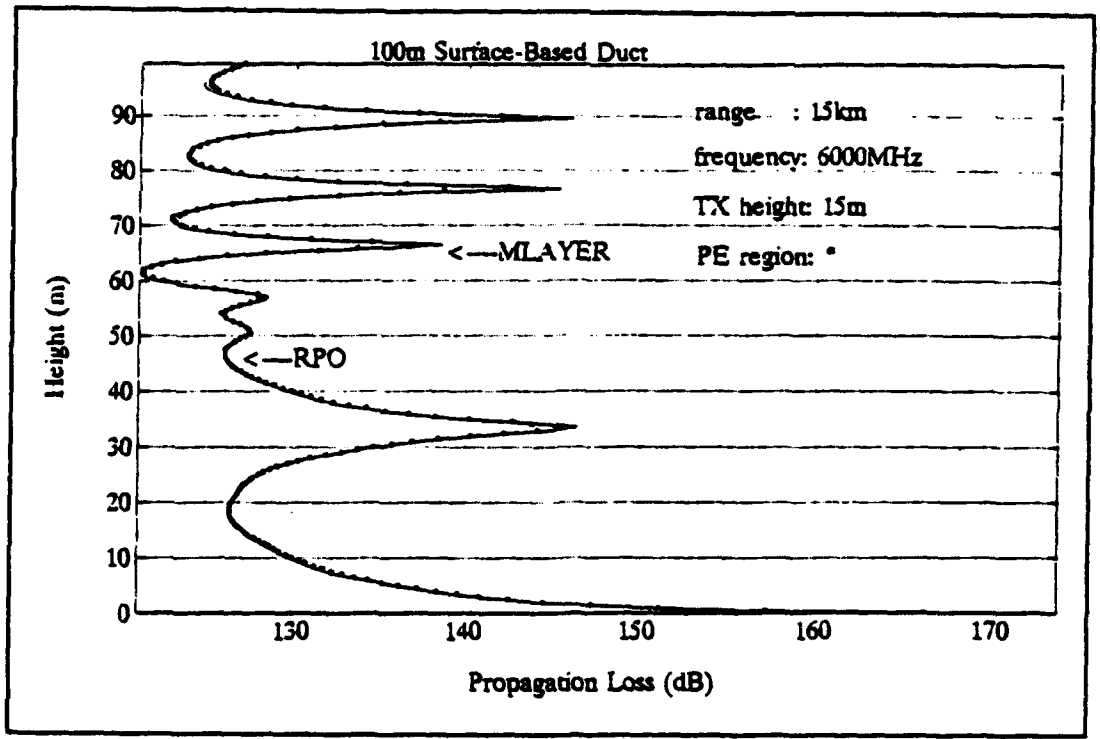

Figure F.14. Propagation loss at 15 km.

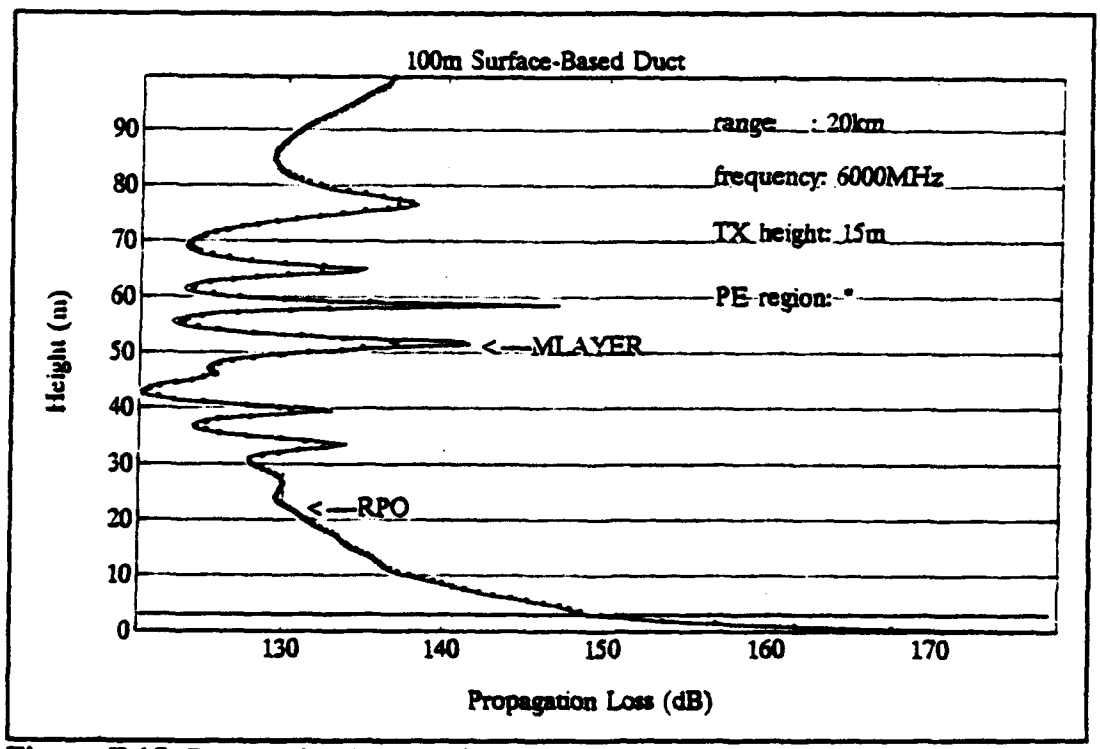

Figure F.15. Propagation loss at 20 km.

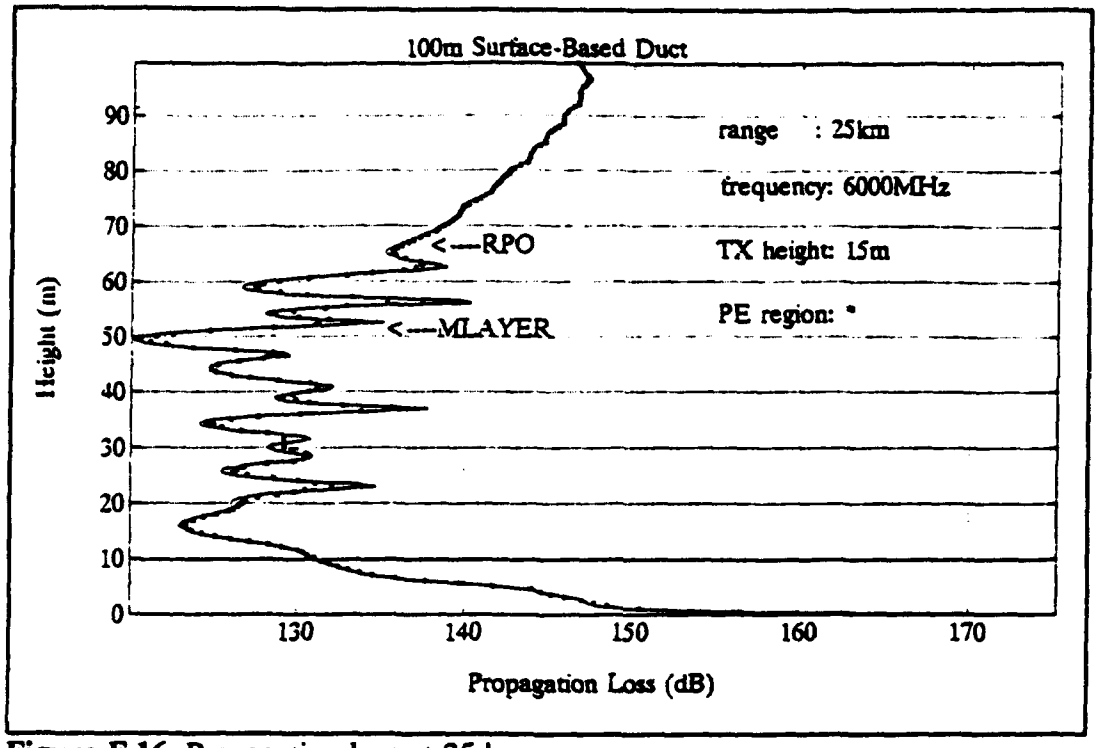

Figure F.16. Propagation loss at 25 km.

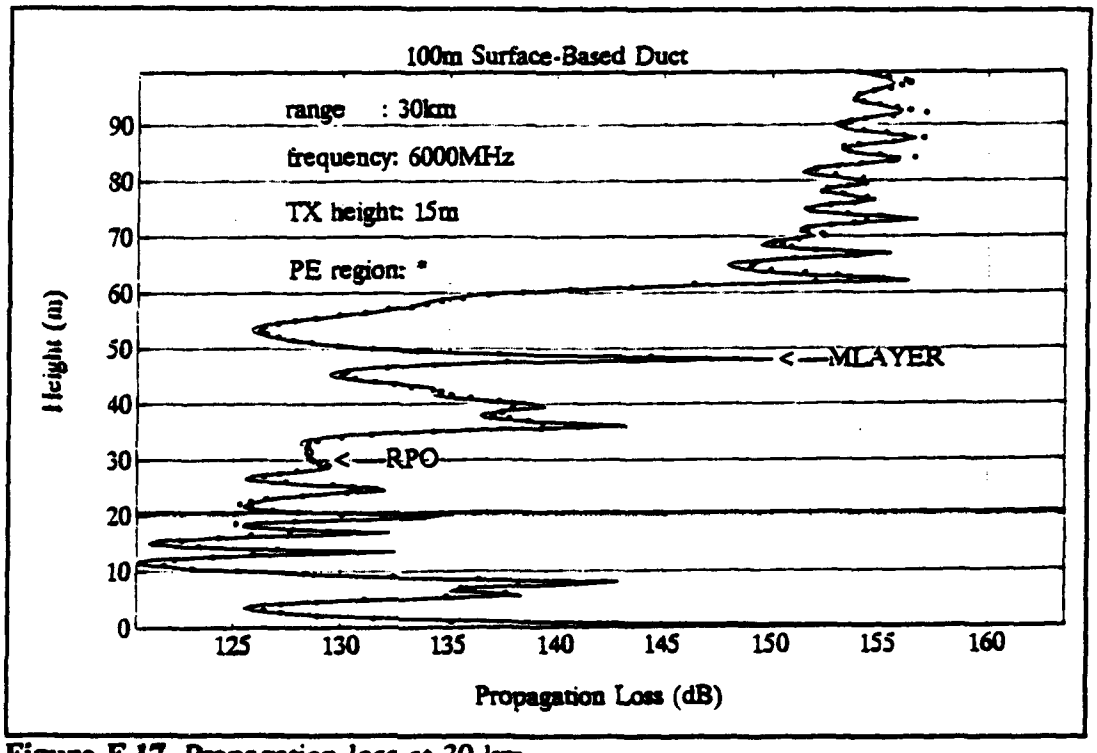

Figure F.17. Propagation loss at 30 km.

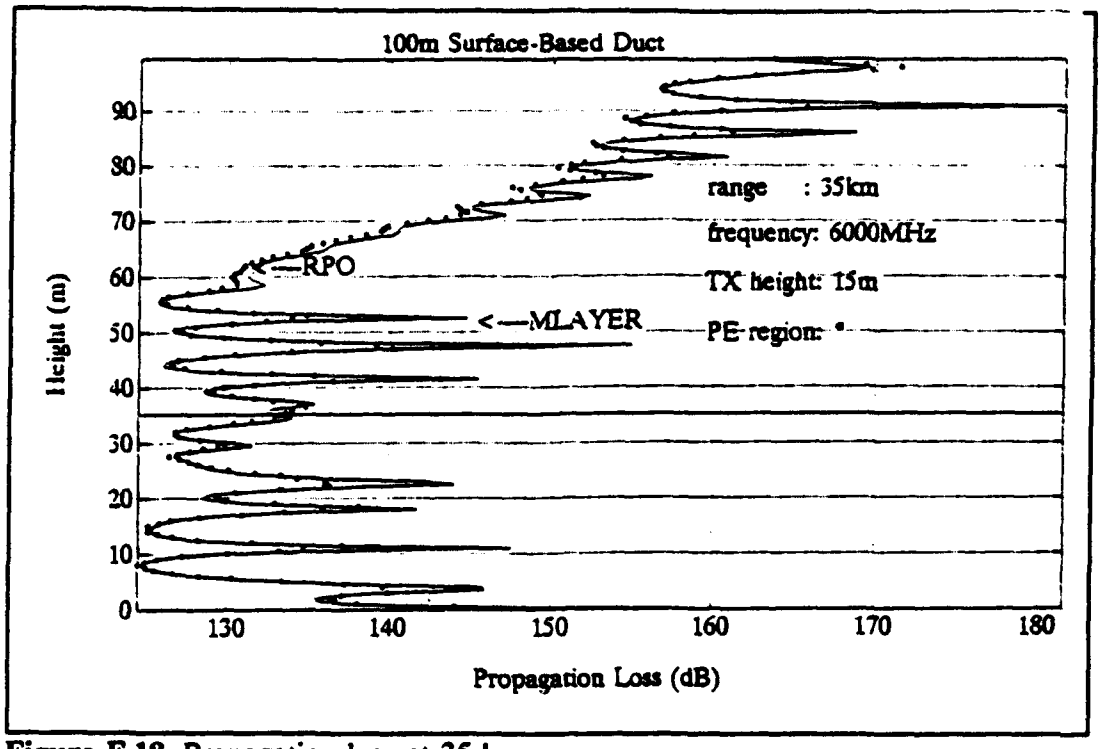

Figure F.18. Propagation loss at 35 km.

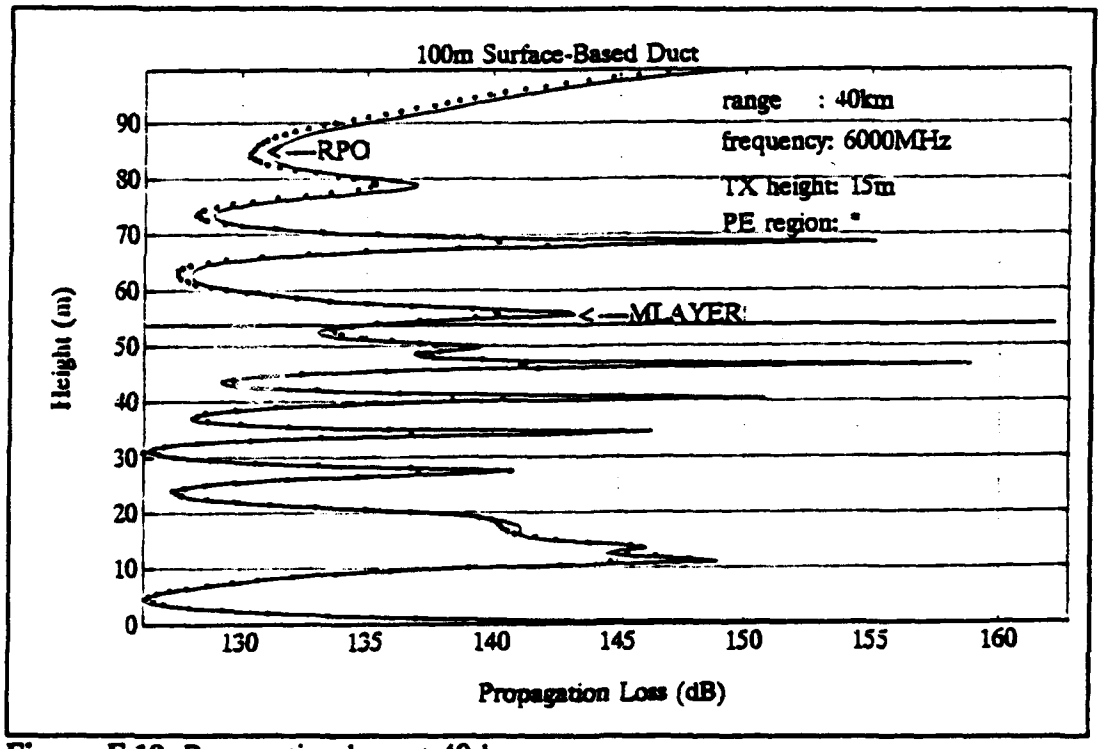

Figure F.19. Propagation loss at 40 km.

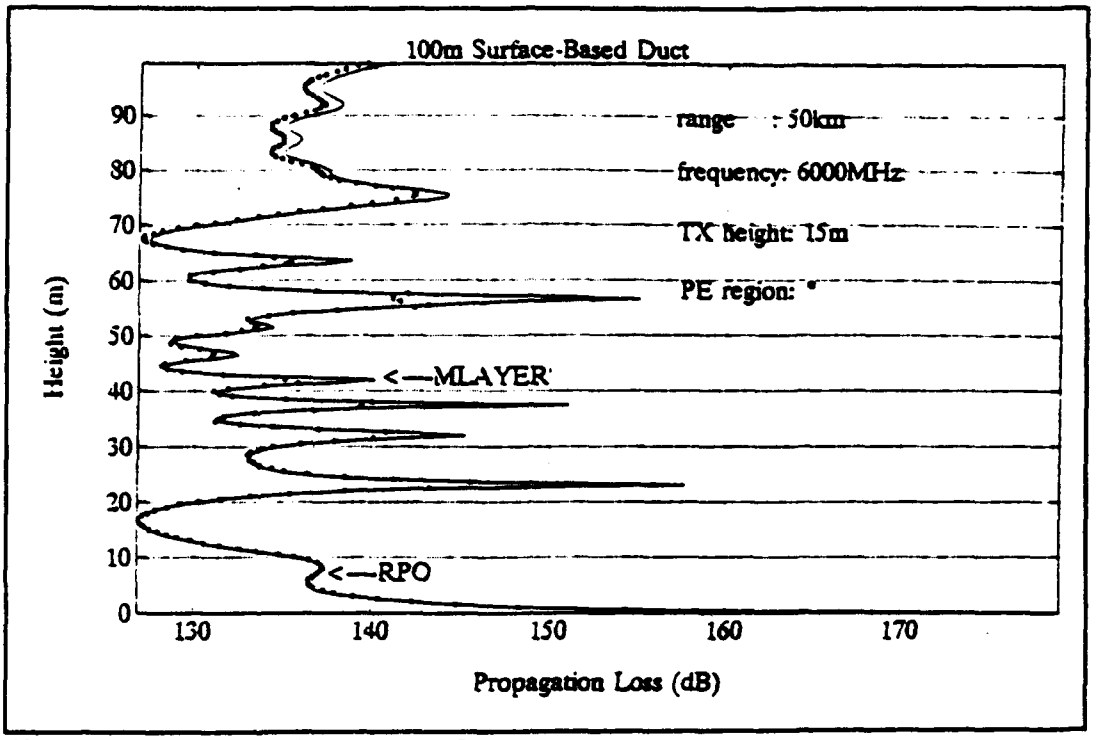

Figure F.20. Propagation loss at 50 km.

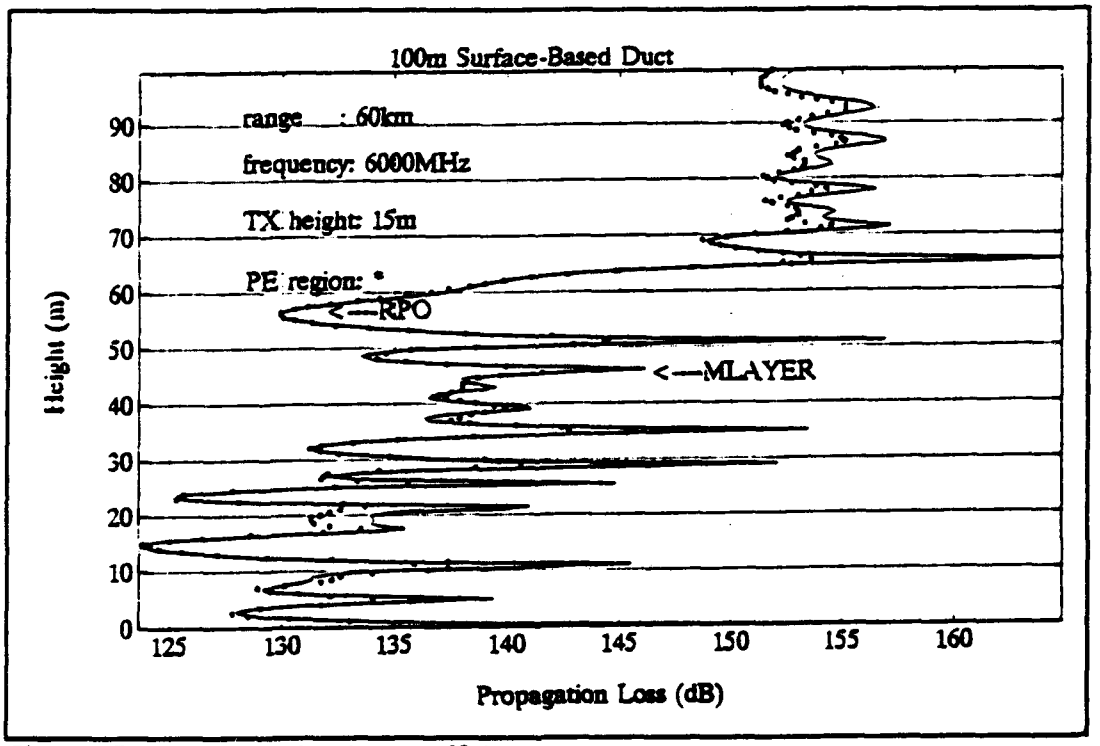

Figure F.21. Propagation loss at 60 km.

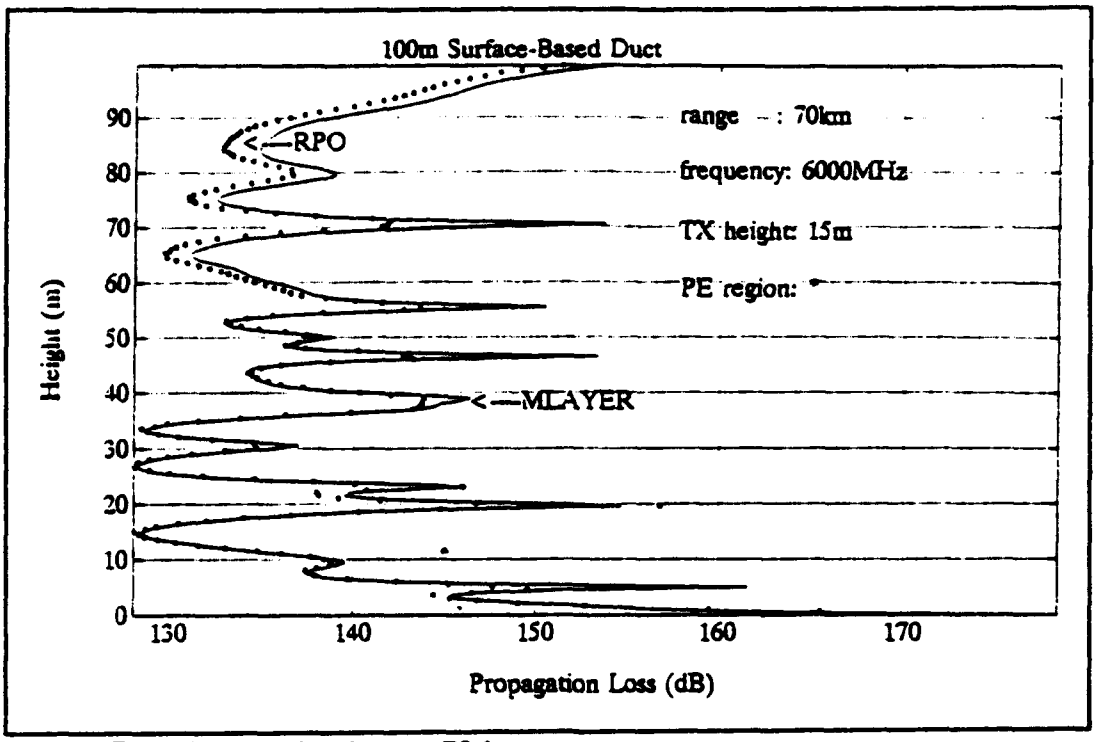

Figure F.22. Propagation loss at 70 km.

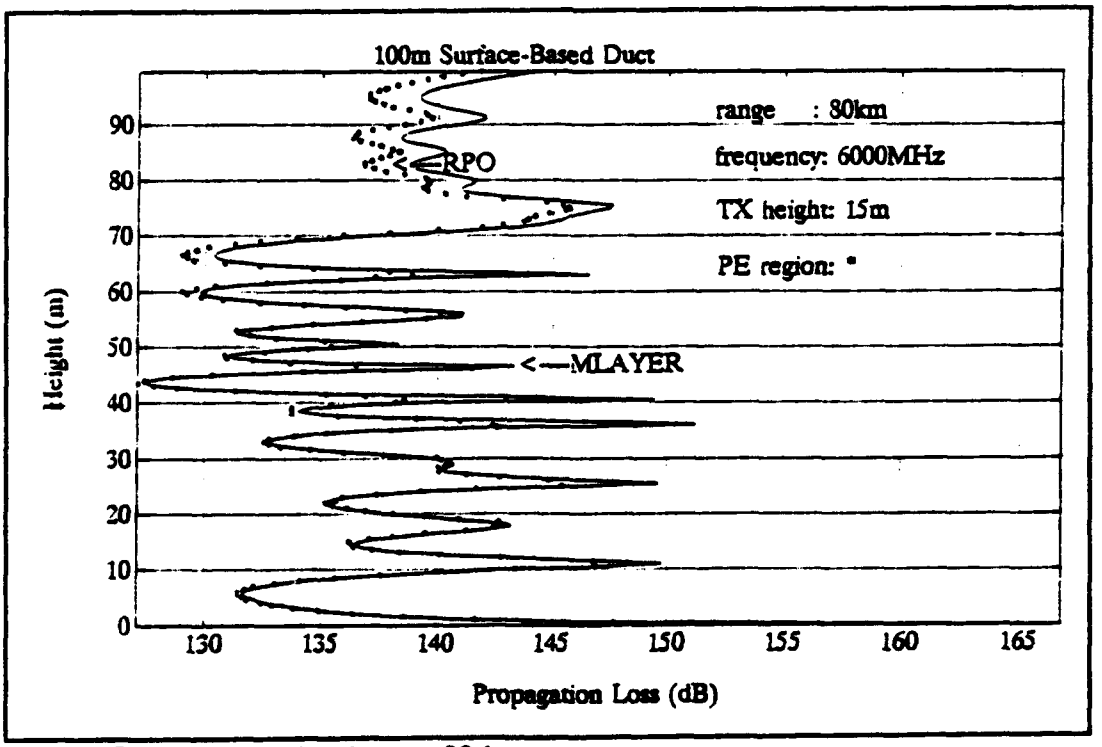

Figure F.23. Propagation loss at 80 km.

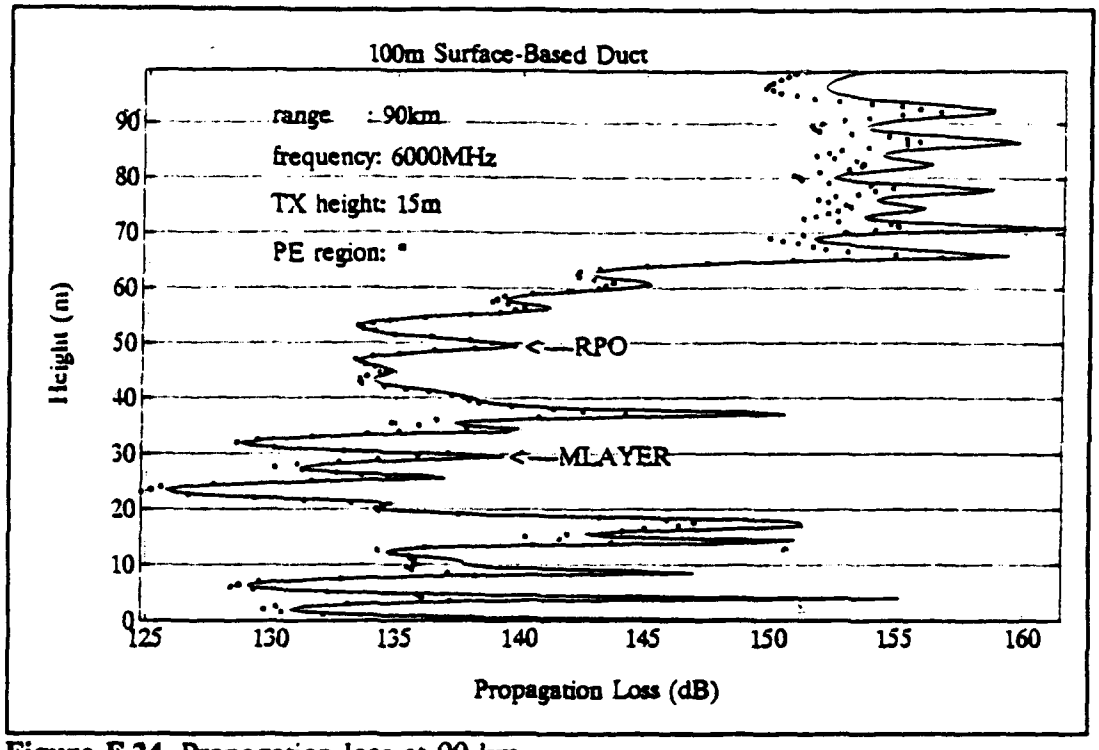

Figure F.24. Propagation loss at 90 km.

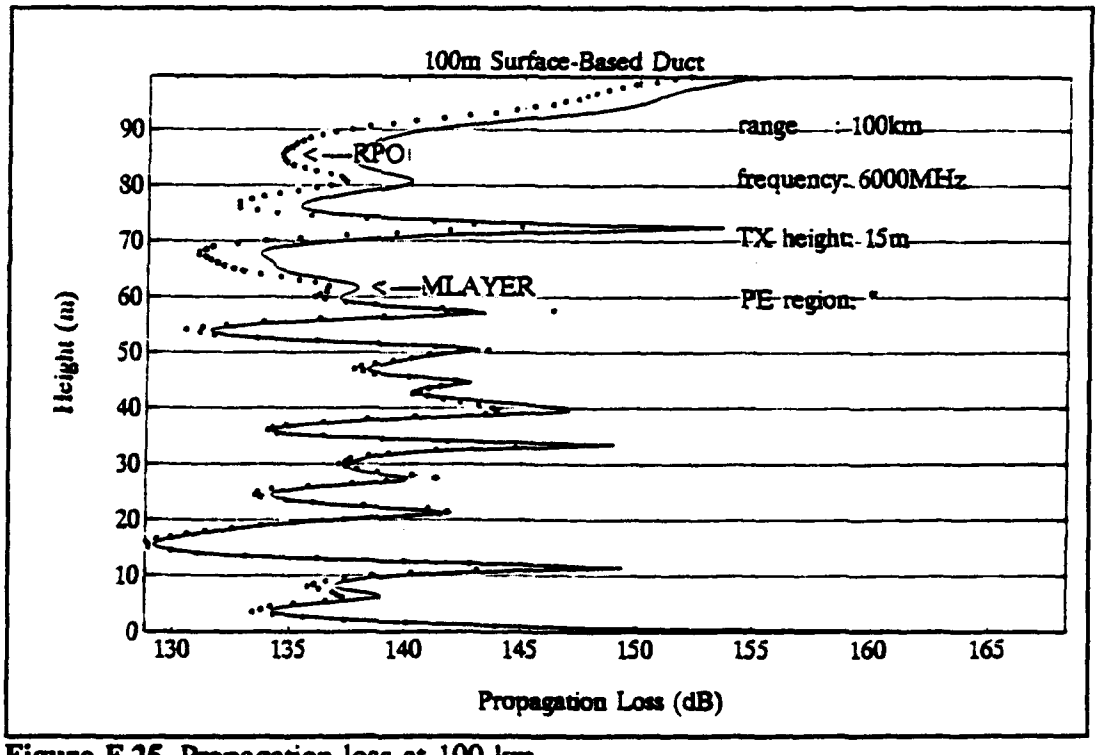

Figure F.25. Propagation loss at 100 km.

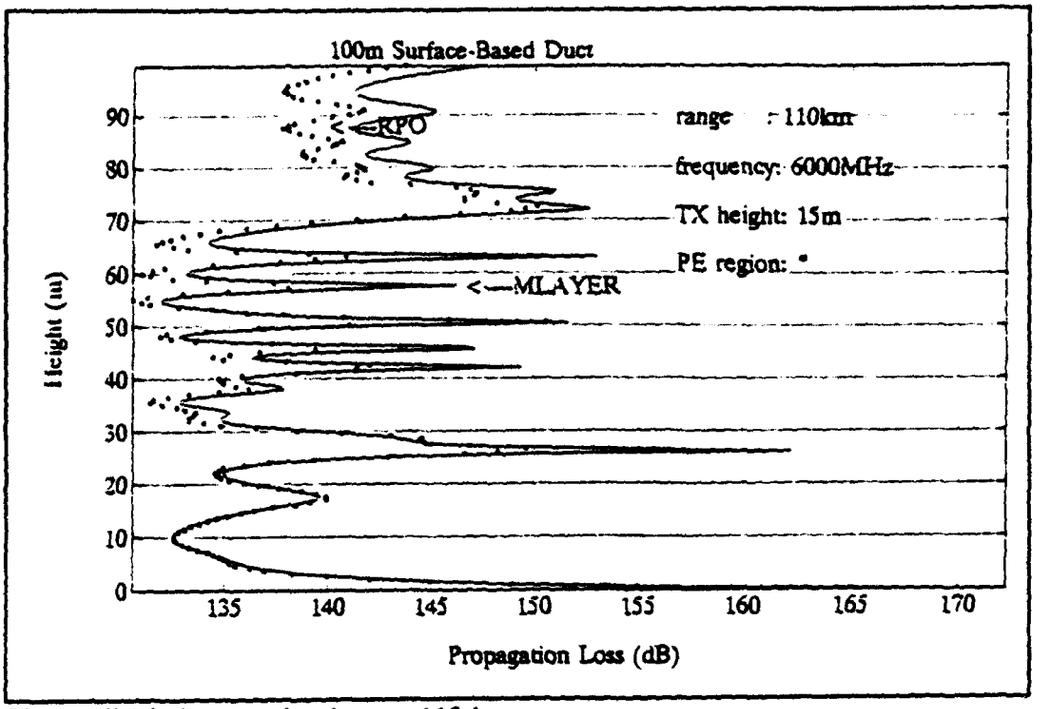

Figure F.26. Propagation loss at 110 km.

3. Propagation loss at 12 GHz

Figures F.27 through F.39 displays the propagation loss at 12 GHz computed by RPO and M-Layer.

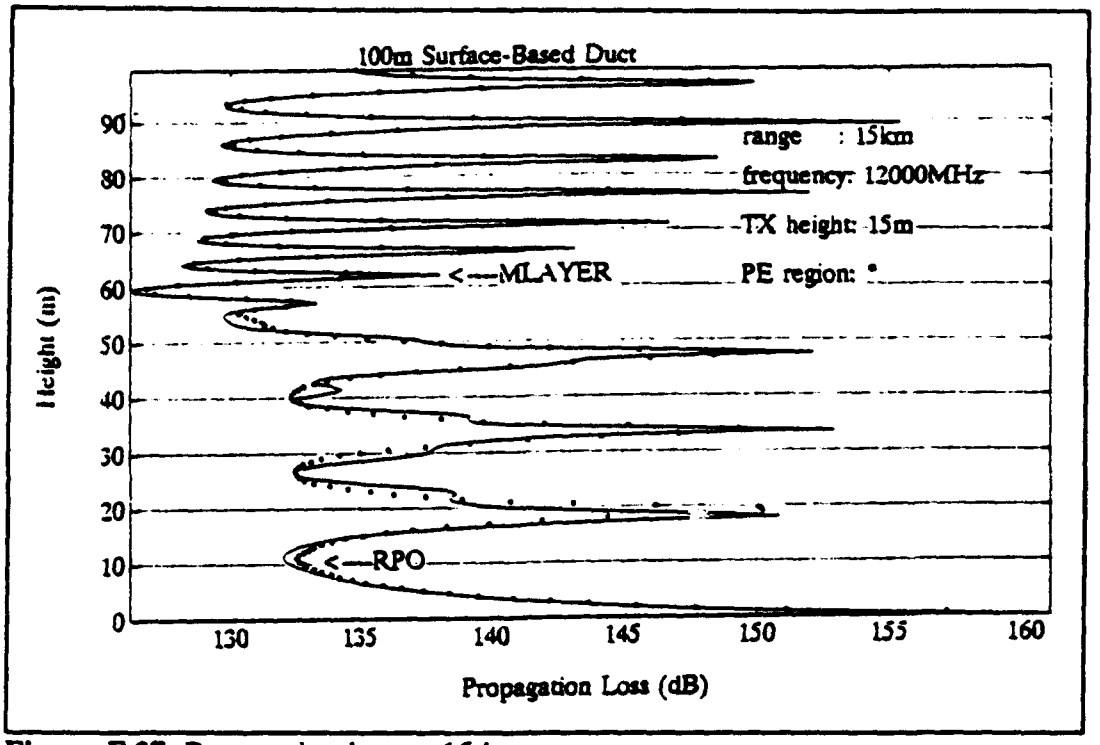

Figure F.27. Propagation loss at 15 km.

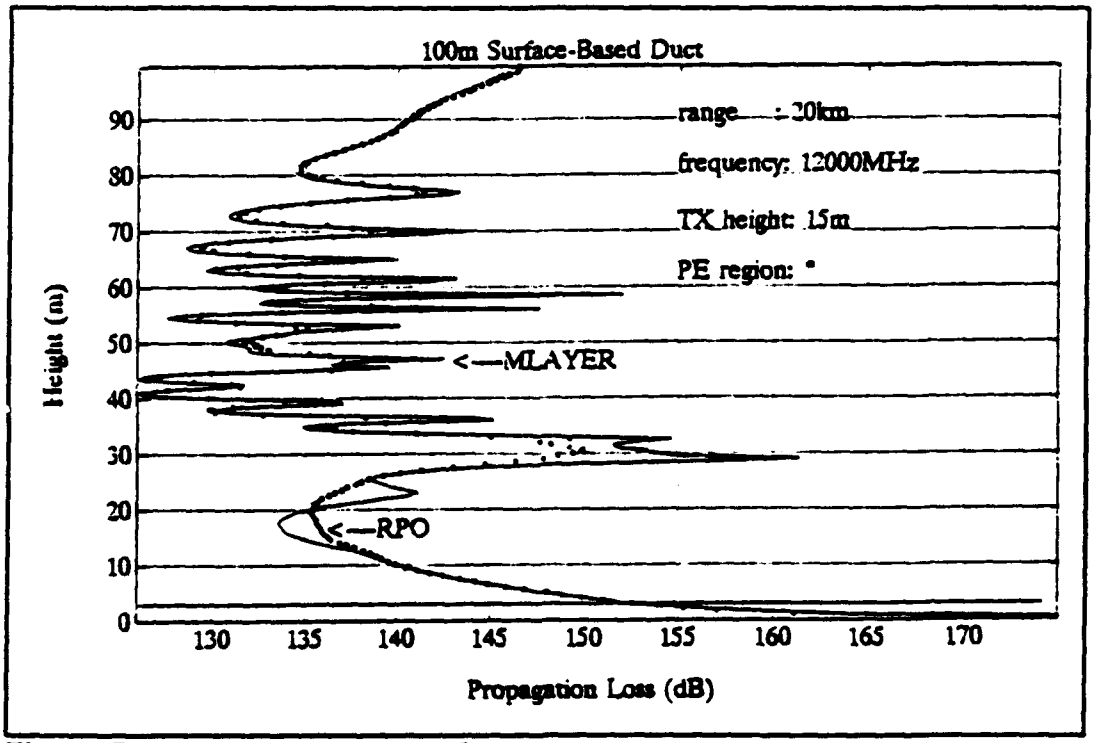

Figure F.28. Propagation loss at 20 km.

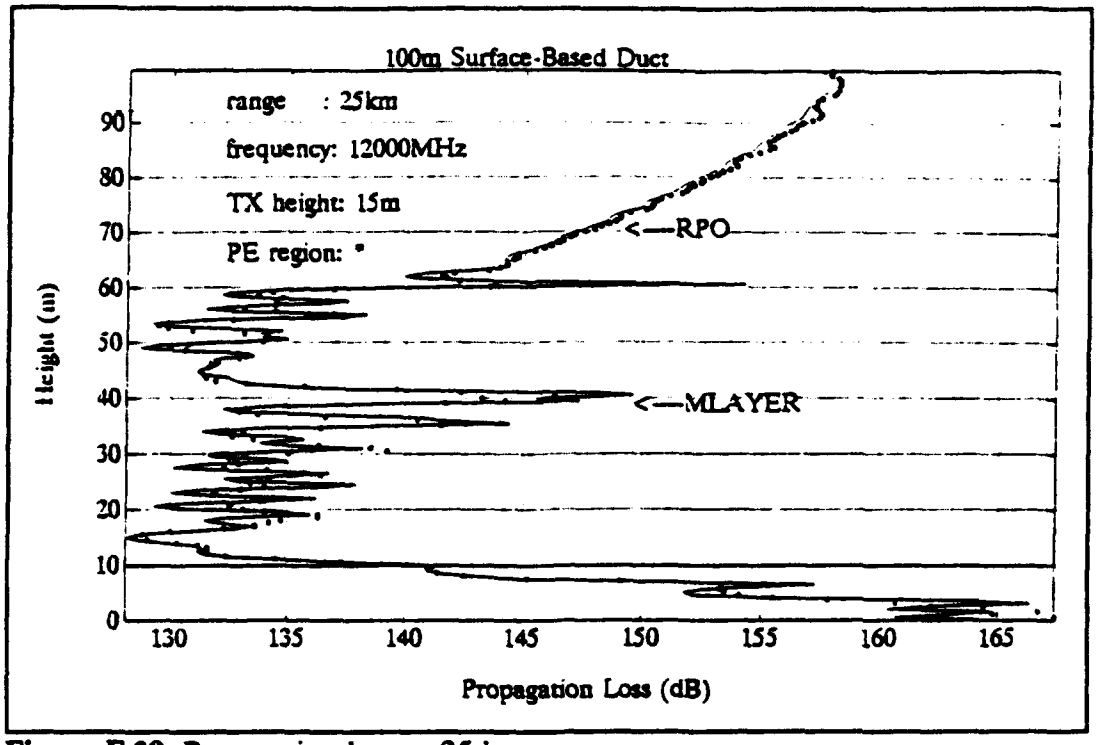

Figure F.29. Propagation loss at 25 km.

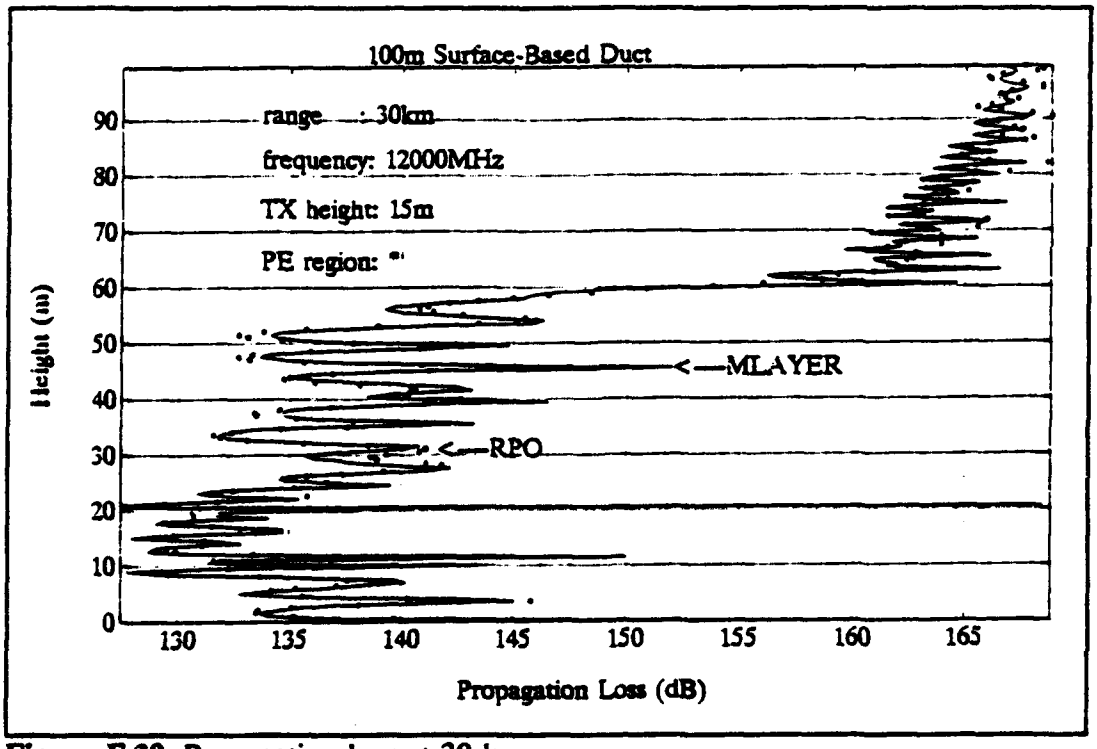

Figure F.30. Propagation loss at 30 km.

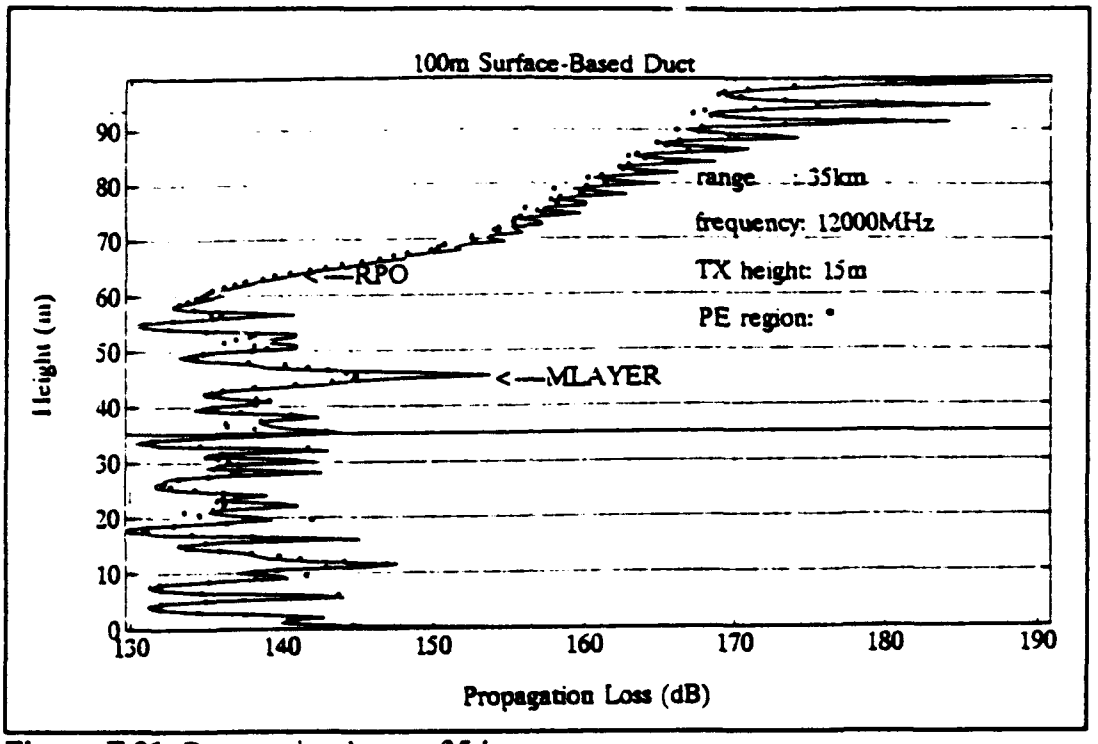

Figure F.31. Propagation loss at 35 km.

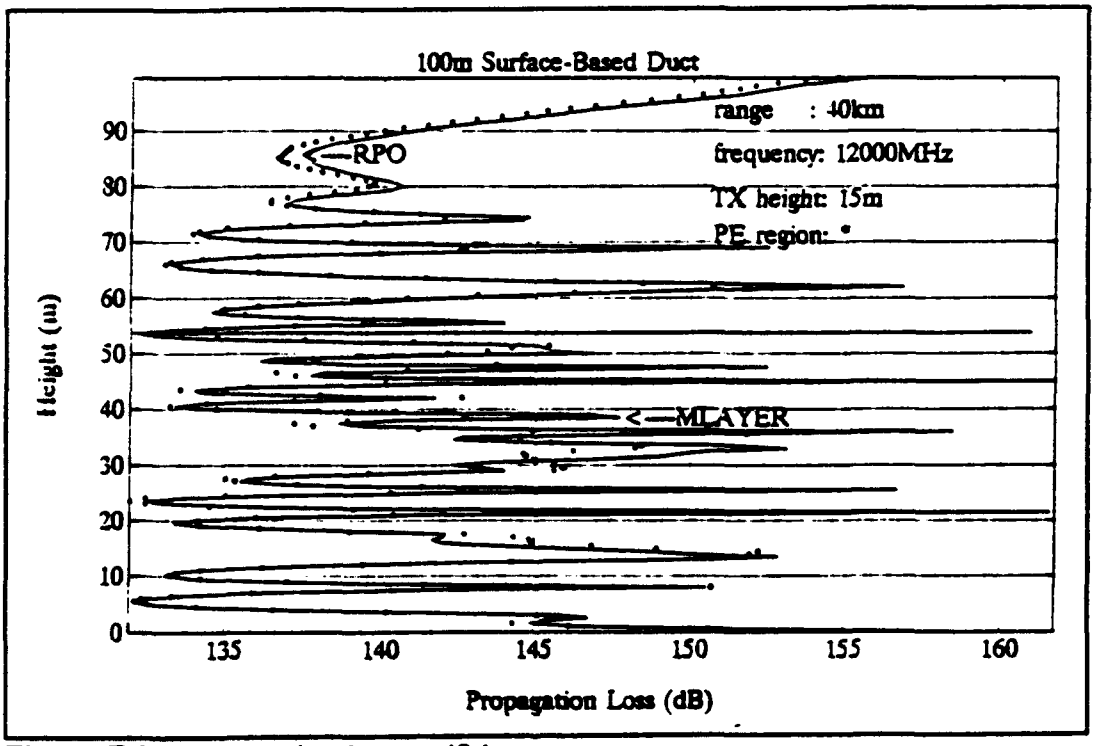

Figure F.32. Propagation loss at 40 km.

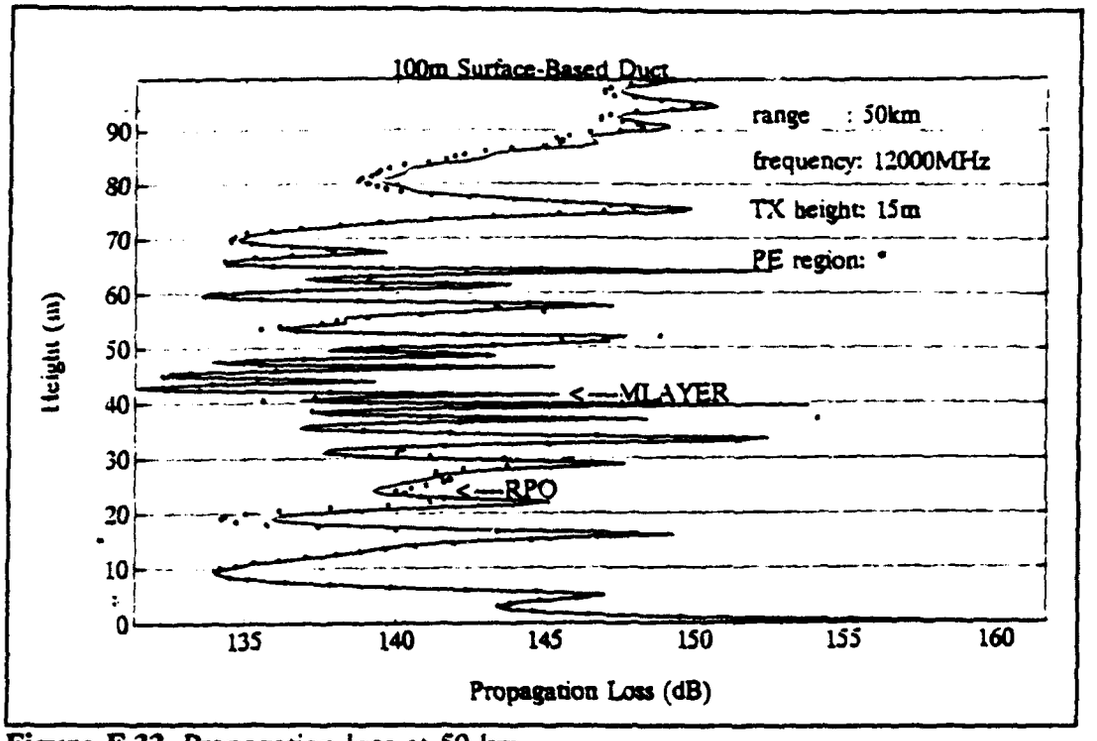

Figure F.33. Propagation loss at 50 km.

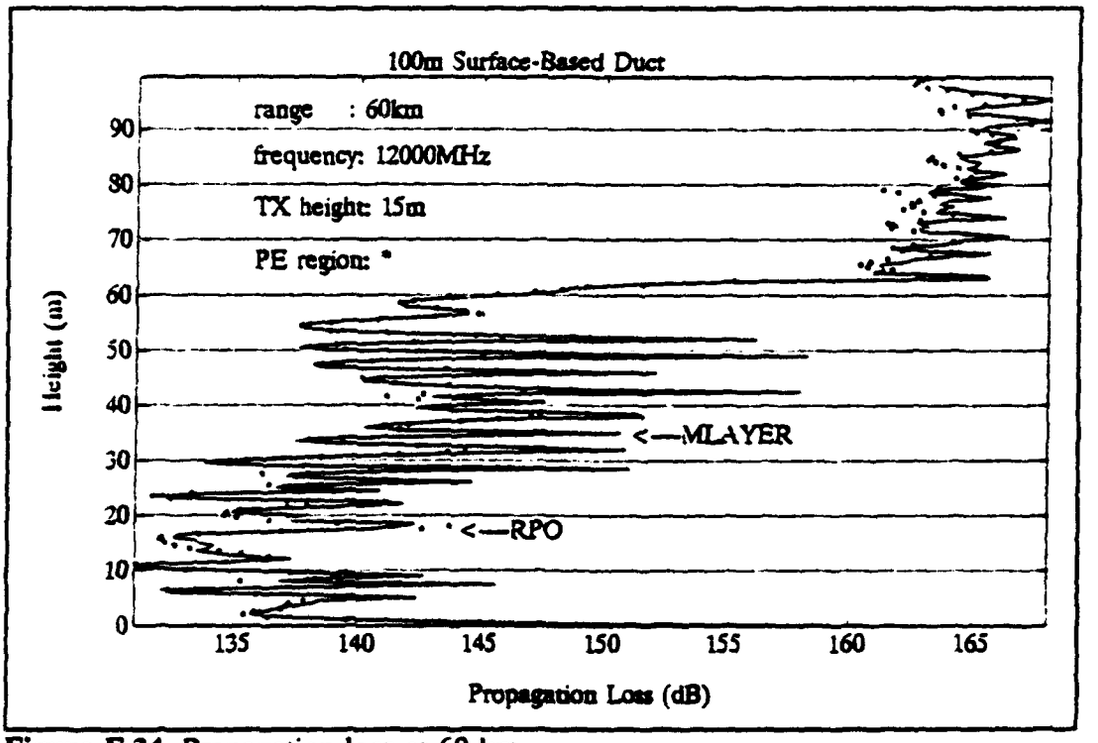

Figure F.34. Propagation loss at 60 km.

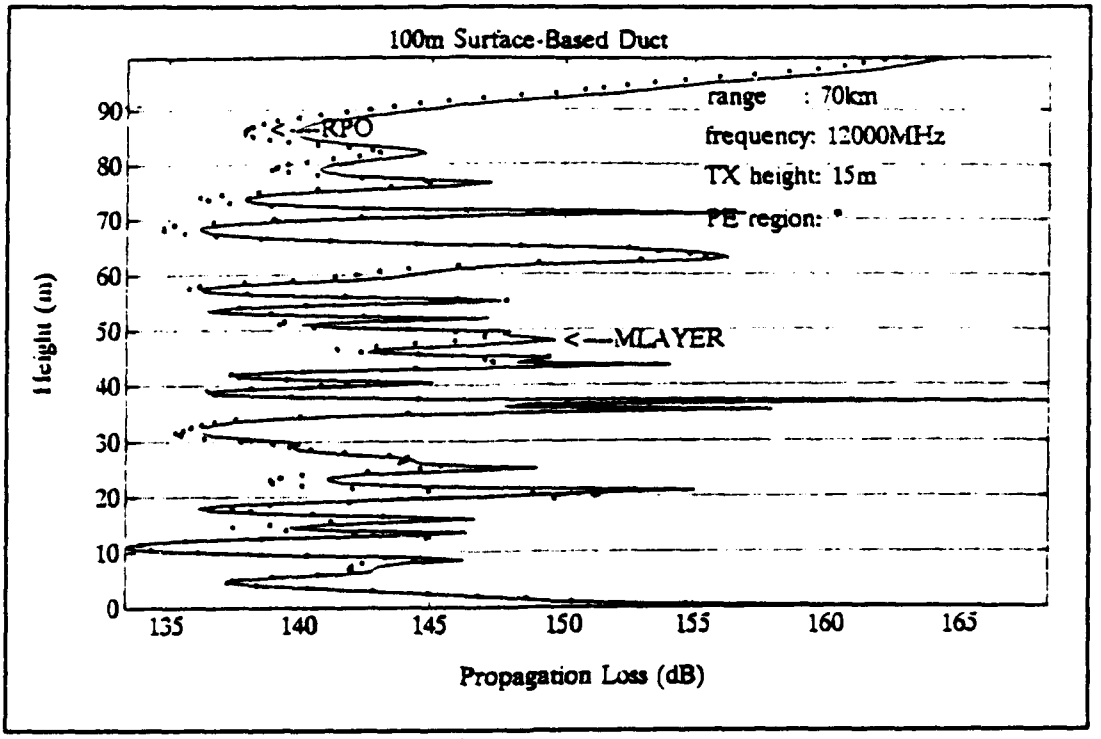

Figure F.35. Propagation loss at 70 km.

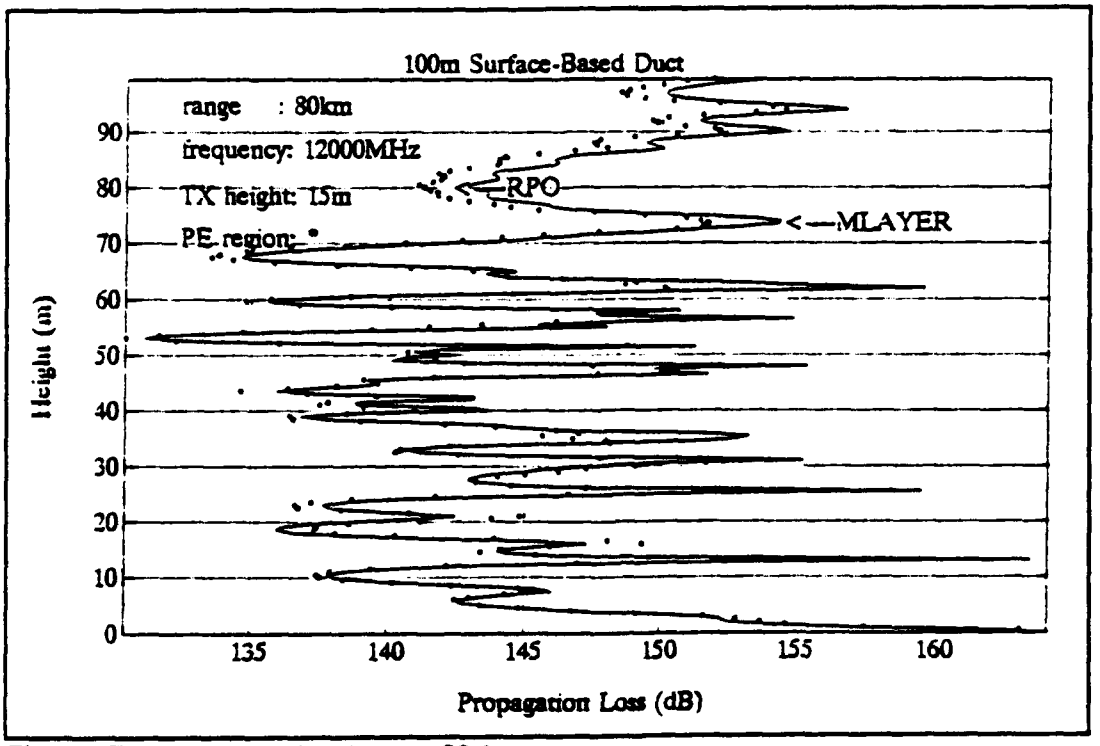

Figure F.36. Propagation loss at 80 km.

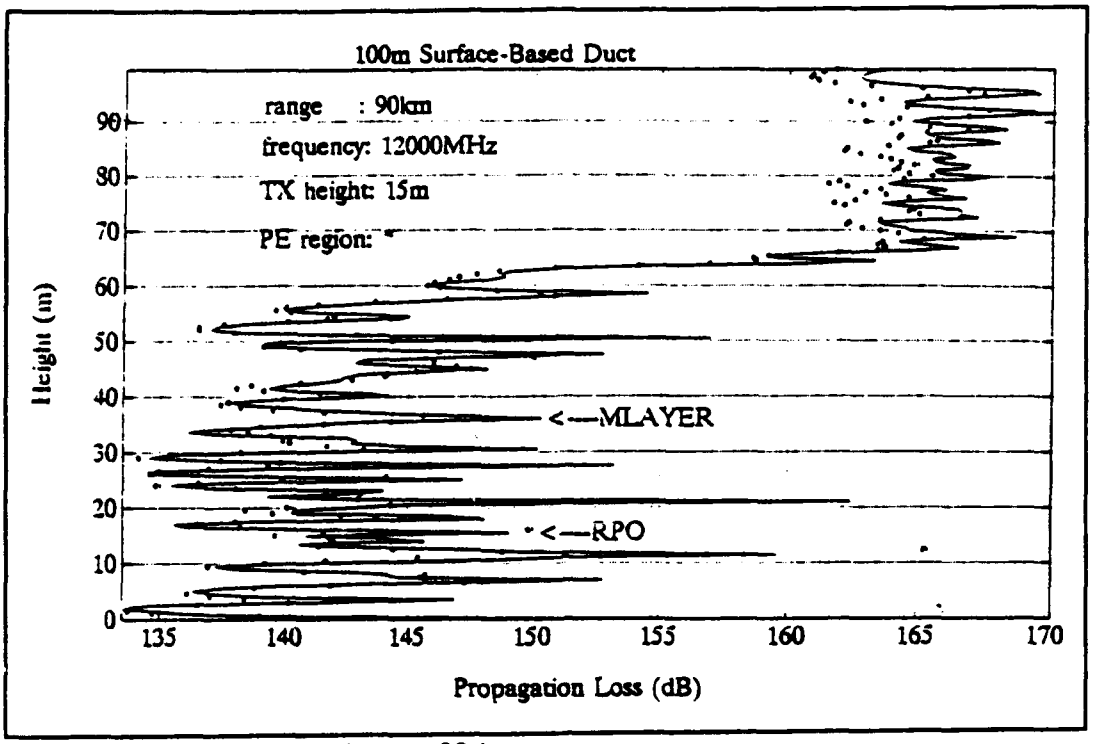

Figure F.37. Propagation loss at 90 km.

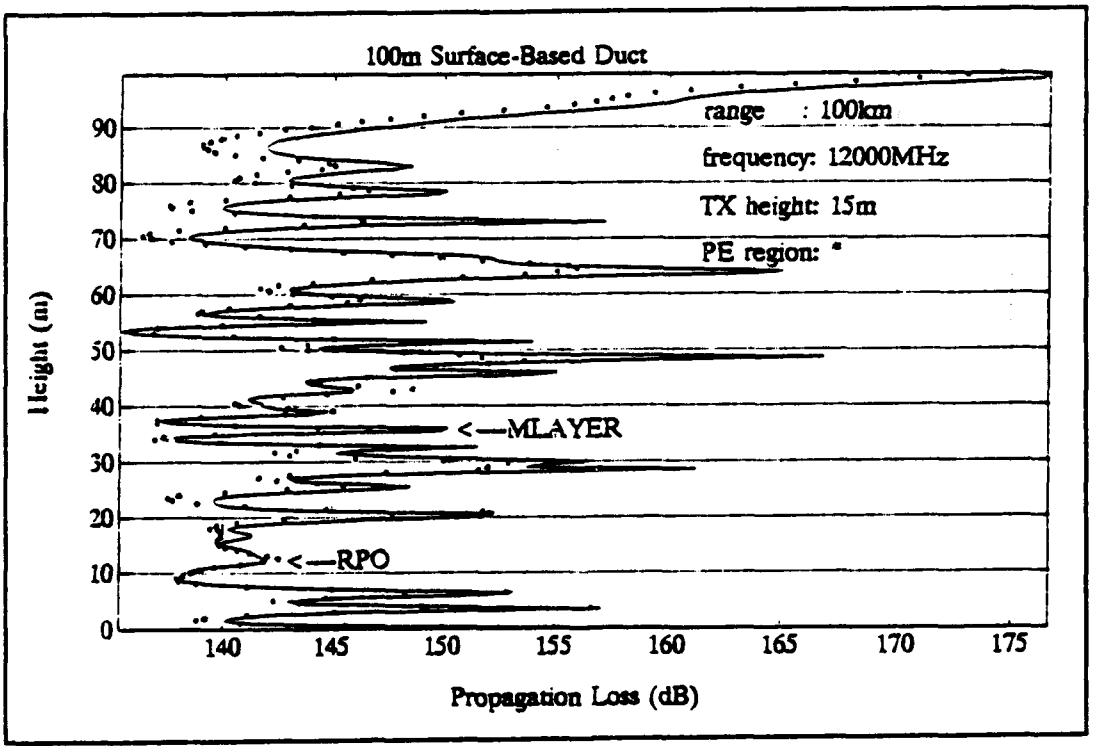

Figure F.38. Propagation loss at 100 km.

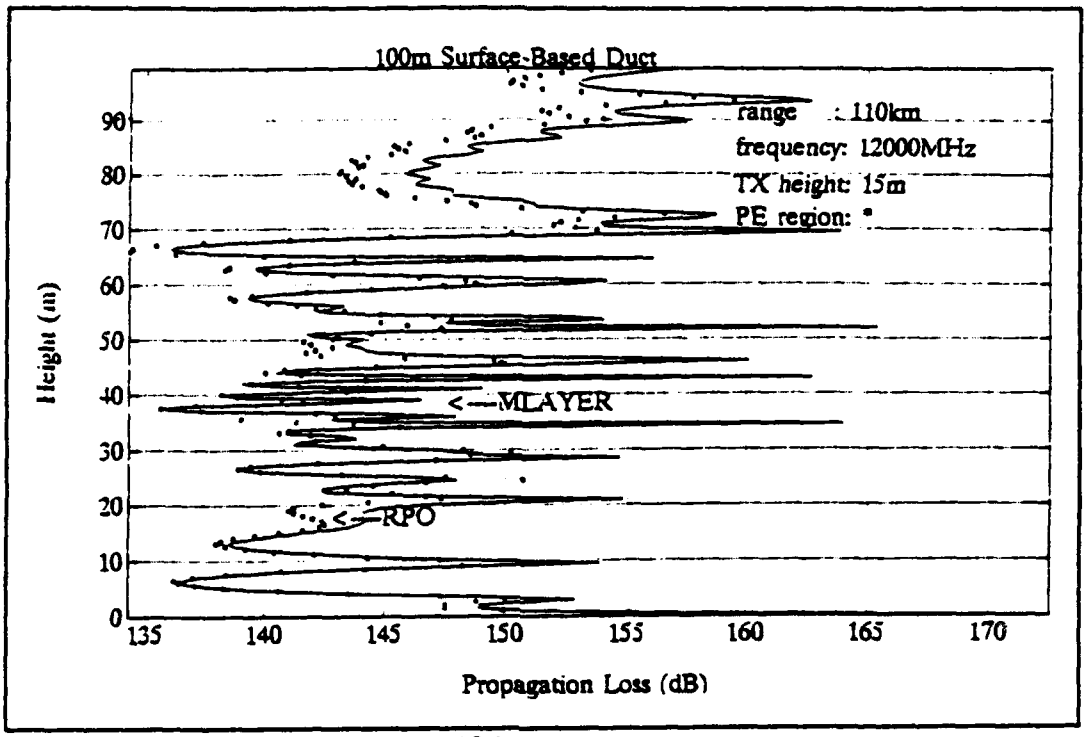

Figure F.39. Propagation loss at 110 km.

LIST OF REFERENCES

1. H.V. Hitney and J.H. Richter, "Integrated refraction effects prediction system (IREPS)," *Naval Engineers Journal*, 257-262, 1976.

2. W.L. Patterson, et. al., "Engineer's Refractive Effects Prediction System (EREPS) Revision 2.0," *Technical Document 1342*, revision 2.0, Naval Ocean Systems Center, San Diego, CA 92152-5000, February 1990.

3. H.V. Hitney, "Engineer's refractive effects prediction system (EREPS), Discussion Summary," in "Proceedings: conference on microwave propagation in the marine boundary layer," *Technical Report TR 89-02*, p. 3-71, Naval Environmental Prediction Research Facility, Monterey, CA 93943-5006, January 1989.

4. L.W. Yeoh, "An analysis of M-Layer: a multilayer tropospheric propagation program," *Technical Report NPS-62-90-009*, Naval Postgraduate School, Monterey, CA 93943, June 1990.

5. H.-M. Lee and Y.Y. Han, "M-Layer: NPS Version," *IEEE Transactions on Magnetics*, *29*(2), 1363-1367, 1993.

6. D.E. Kerr, ed., *Propagation of Short Radio Waves*, Peregrinus, London, 1987; original edition 1951.

7. W.L. Patterson and H.V. Hitney, "Radio physical optics CSCI software documents," *Technical Document 2403*, Naval Command, Control and Ocean Surveillance Center, RDT&E Division, San Diego, CA 92152, December 1992.

8. F.D. Tappert, "The parabolic approximation method," in J.B. Keller and J.S. Papadakis, ed., *Wave Propagation and Underwater Acoustics*, 224-287, Springer-Verlag, 1977.

9. J.R. Kuttler and G.D. Dockery, "Theoretical description of the parabolic approximation/Fourier split-step method of representing electromagnetic propagation in the troposphere," *Radio Science*, *26*(2), 381-393, 1991.

INITIAL DISTRIBUTION LIST

1.	Defense Technical Information Center Cameron Station Alexandria, VA 22304-6145	2
2.	Dudley Knox Library, Code 52 Naval Postgraduate School Monterey, CA 93943-5002	2
3.	Chairman, Code EC Department of Electrical and Computer Engineering Naval Postgraduate School Monterey, CA 93943-5121	1
4.	Professor Kenneth L. Davidson (MR/Ds) Department of Meteorology Naval Postgraduate School Monterey, CA 93943-5100	1
5.	Professor Lawrence J. Ziomek (EC/Zm) Department of Electrical and Computer Engineering Naval Postgraduate School Monterey, CA 93943-5121	1
6.	Professor Hung-Mou Lee (EC/Lh) Department of Electrical and Computer Engineering Naval Postgraduate School Monterey, CA 93943-5121	2
7.	Mr. Yeoh, Lean Weng 833 Dyer Road, Room 537C Department of Electrical and Computer Engineering Naval Postgraduate School Monterey, CA 93943-5121	1
8.	Mr. Wu, Chi-Wei No. 22, Lane 35, Wu-Hwa Street, San-Chung City, Taipei County, Taiwan, R.O.C.	1

9. Mr. Ting, Chueh — 1
Department of Electrical Engineering
Chung Cheng Institute of Technology
Tao-Yuan, Tai-Hsi
Taiwan, R.O.C.

10. Program Executive Office, Theater Air Defense (D-21) — 1
Attn: Mr. George Hamilton, NC 2, Room 11N06
2531 Jefferson Davis Highway
Arlington, VA 22242-5170

11. NATO Seasparrow Surface Missile System Project Office (N-US) — 1
Attn: LCDR Scott J. Smith, 4 Crytal Park, Room 210
2531 Jefferson Davis Highway
Arlington, VA 22242-5170

12. Naval Command, Control and Ocean Surveillance Center — 1
RDT&E Division
Ocean and Atmospheric Sciences (Code 54)
San Diego, CA 92152-5000